




2019

## NEUROPROTECTIVE STRATEGIES FOLLOWING EXPERIMENTAL TRAUMATIC BRAIN INJURY: LIPID PEROXIDATION-DERIVED ALDEHYDE SCAVENGING AND INHIBITION OF MITOCHONDRIAL PERMEABILITY TRANSITION

Jacqueline Renee Kulbe

University of Kentucky, j\_kulbe@yahoo.com

Author ORCID Identifier:

 <https://orcid.org/0000-0002-7070-9264>

Digital Object Identifier: <https://doi.org/10.13023/etd.2019.228>

[Right click to open a feedback form in a new tab to let us know how this document benefits you.](#)

---

### Recommended Citation

Kulbe, Jacqueline Renee, "NEUROPROTECTIVE STRATEGIES FOLLOWING EXPERIMENTAL TRAUMATIC BRAIN INJURY: LIPID PEROXIDATION-DERIVED ALDEHYDE SCAVENGING AND INHIBITION OF MITOCHONDRIAL PERMEABILITY TRANSITION" (2019). *Theses and Dissertations--Neuroscience*. 22. [https://uknowledge.uky.edu/neurobio\\_etds/22](https://uknowledge.uky.edu/neurobio_etds/22)

This Doctoral Dissertation is brought to you for free and open access by the Neuroscience at UKnowledge. It has been accepted for inclusion in Theses and Dissertations--Neuroscience by an authorized administrator of UKnowledge. For more information, please contact [UKnowledge@lsv.uky.edu](mailto:UKnowledge@lsv.uky.edu).

## **STUDENT AGREEMENT:**

I represent that my thesis or dissertation and abstract are my original work. Proper attribution has been given to all outside sources. I understand that I am solely responsible for obtaining any needed copyright permissions. I have obtained needed written permission statement(s) from the owner(s) of each third-party copyrighted matter to be included in my work, allowing electronic distribution (if such use is not permitted by the fair use doctrine) which will be submitted to UKnowledge as Additional File.

I hereby grant to The University of Kentucky and its agents the irrevocable, non-exclusive, and royalty-free license to archive and make accessible my work in whole or in part in all forms of media, now or hereafter known. I agree that the document mentioned above may be made available immediately for worldwide access unless an embargo applies.

I retain all other ownership rights to the copyright of my work. I also retain the right to use in future works (such as articles or books) all or part of my work. I understand that I am free to register the copyright to my work.

## **REVIEW, APPROVAL AND ACCEPTANCE**

The document mentioned above has been reviewed and accepted by the student's advisor, on behalf of the advisory committee, and by the Director of Graduate Studies (DGS), on behalf of the program; we verify that this is the final, approved version of the student's thesis including all changes required by the advisory committee. The undersigned agree to abide by the statements above.

Jacqueline Renee Kulbe, Student

Dr. Edward D. Hall, Major Professor

Dr. Wayne A. Cass, Director of Graduate Studies

NEUROPROTECTIVE STRATEGIES FOLLOWING EXPERIMENTAL  
TRAUMATIC BRAIN INJURY: LIPID PEROXIDATION-DERIVED ALDEHYDE  
SCAVENGING AND INHIBITION OF MITOCHONDRIAL PERMEABILITY  
TRANSITION

---

DISSERTATION

---

A dissertation submitted in partial fulfillment of the  
requirements for the degree of Doctor of Philosophy in the  
College of Medicine  
at the University of Kentucky

By

Jacqueline Renee Kulbe

Lexington, Kentucky

Director: Dr. Edward D. Hall, Professor of Neuroscience, Neurology, Neurosurgery and  
Physical Medicine & Rehabilitation

Lexington, Kentucky

2019

Copyright © Jacqueline Renee Kulbe 2019

## ABSTRACT OF DISSERTATION

### NEUROPROTECTIVE STRATEGIES FOLLOWING EXPERIMENTAL TRAUMATIC BRAIN INJURY: LIPID PEROXIDATION-DERIVED ALDEHYDE SCAVENGING AND INHIBITION OF MITOCHONDRIAL PERMEABILITY TRANSITION

Traumatic brain injury (TBI) represents a significant health crisis. To date there are no FDA-approved pharmacotherapies available to prevent the neurologic deficits caused by TBI. Following TBI, dysfunctional mitochondria generate reactive oxygen and nitrogen species, initiating lipid peroxidation (LP) and the formation of LP-derived neurotoxic aldehydes, which bind mitochondrial proteins, exacerbating dysfunction and opening of the mitochondrial permeability pore (mPTP), resulting in extrusion of mitochondrial sequestered calcium into the cytosol, and initiating a downstream cascade of calpain activation, spectrin degradation, neurodegeneration and neurologic impairment.

As central mediators of the TBI secondary injury cascade, mitochondria and LP-derived neurotoxic aldehydes make promising therapeutic targets. In fact, Cyclosporine A (CsA), an FDA-approved immunosuppressant capable of inhibiting mPTP has been shown to be neuroprotective in experimental TBI. Additionally, phenelzine (PZ), an FDA-approved non-selective irreversible monoamine oxidase inhibitor (MAOI) class antidepressant has also been shown to be neuroprotective in experimental TBI due to the presence of a hydrazine (-NH-NH<sub>2</sub>) moiety allowing for the scavenging of LP-derived neurotoxic aldehydes.

The overall goal of this dissertation is to further examine the neuroprotective effects of the mPTP inhibitor, CsA, and the LP-derived neurotoxic aldehyde scavenger, PZ, using a severe controlled cortical impact injury (CCI) model in 3-month old male Sprague-Dawley rats.

First, the effects of CsA on cortical synaptic and non-synaptic mitochondria, two heterogeneous populations, are examined. Our results indicate that compared to non-synaptic mitochondria, synaptic mitochondria sustain greater damage 24h following CCI and are protected to a greater degree by CsA.

Second, the neuroprotective effects of a novel 72h continuous subcutaneous infusion of CsA combined with PZ are compared to monotherapy. Following CCI, our results indicate that individually both CsA and PZ attenuate modification of mitochondrial proteins by LP-derived neurotoxic aldehydes, PZ is able to maintain mitochondrial respiratory control ratio and cytoskeletal integrity, but together, PZ and CsA, are unable to improve and in some cases negate monotherapy neuroprotective effects.

Finally, the effects of PZ (MAOI, aldehyde scavenger), pargyline (PG, MAOI, non-aldehyde scavenger) and hydralazine (HZ, non-MAOI, aldehyde scavenger) are compared. Our results indicate that PZ, PG, and HZ are unable to improve CCI-induced deficits to learning and memory as measured by Morris water maze (post-CCI D3-7). Of concern, PZ animals lost a significant amount of weight compared to all other group, possibly due to MAOI effects. In fact, in uninjured cortical tissue, PZ administration leads to a significant increase in norepinephrine and serotonin. Additionally, although PZ, PG, and HZ did not lead to a statistically significant improvement in cortical tissue sparing 8 days following CCI, the HZ group saw a 10% improvement over vehicle.

Overall, these results indicate that pharmacotherapies which improve mitochondrial function and decrease lipid peroxidation should continue to be pursued as neuroprotective approaches to TBI. However, further pursuit of LP-derived aldehyde scavengers for clinical use in TBI may require the development of hydrazine (-NH-NH<sub>2</sub>)-compounds which lack additional confounding mechanisms of action.

**KEYWORDS:** combinational therapy, cyclosporine A, lipid peroxidation-derived aldehyde scavenging, mitochondria, phenelzine, traumatic brain injury

---

Jacqueline Renee Kulbe

---

05/16/2019

---

Date

NEUROPROTECTIVE STRATEGIES FOLLOWING EXPERIMENTAL  
TRAUMATIC BRAIN INJURY: LIPID PEROXIDATION-DERIVED ALDEHYDE  
SCAVENGING AND INHIBITION OF MITOCHONDRIAL PERMEABILITY  
TRANSITION

By

Jacqueline Renee Kulbe

Edward D. Hall, Ph.D.

---

Director of Dissertation

Wayne A. Cass, Ph.D.

---

Director of Graduate Studies

05/16/2019

---

Date

## ACKNOWLEDGMENTS

First and foremost, I would like to thank my mentor, Dr. Edward Hall, Ph.D. Without his expertise, generosity, extreme patience, and guidance this dissertation would not have been possible. I would also like to thank current members of the Hall lab. Dr. Jeff Bosken, Ph.D. for being an excellent lab manager and for offering advice in navigating the graduate school process. Mr. Jacob Dunkerson for all his assistance with behavior and for being a friend. Dr. Rachel Hill, Ph.D. for her collaboration and help with learning mitochondrial and surgical techniques. Dr. Amy Wang, M.D. for always being available to assist me with surgeries and Western blots and being instrumental in making those processes run smoothly. I would also like to thank previous members of the Hall lab. Dr. Rebecca Smith, Ph.D. for assistance with perfusions and tissue processing. Dr. Johnny Cebak, Ph.D. for being a friend, introducing me to Dr. Hall, and helping me get started in the lab. A special thanks to Dr. Indrapal Singh, Ph.D. who I worked closely with on a daily basis. Thank you for teaching me all about mitochondria, being always willing to lend a hand, listening to me complain about everyone and everything, making everyday fun, and being my best lab buddy.

Thank you to all of my committee members for sharing their time, guidance, and expertise in regards to science, career, and life. Dr. John Gensel, Ph.D. for all of your advice, both scientific and personal, our informal chats, and your scientific enthusiasm. Dr. Greg Gerhardt, Ph.D. for always being willing to listen and your advocacy and support through trying times. In conjunction with Dr. Gerhardt, I would also like to thank CenMeT and Mr. Peter Heuttl for conducting the HPLC analysis. Dr. James Pauly, Ph.D. and his lab member Deann Hopkins, who were instrumental in my ability to undertake behavioral experiments. Dr. Patrick Sullivan, Ph.D. for all your mitochondrial knowledge and for guiding me through my first lab rotation at UK. A special thank you to Dr. John Yanneilli, Ph.D. for offering his time and expertise to serve as my outside examiner.

I would like to thank all of the students, staff and faculty of the Spinal Cord and Brain Injury Research Center (SCoBIRC) and the Department of Neuroscience. Particularly Ms. Linda Simmerman for her assistance in scanning of my histology slides and her advice in regards to analysis. As well as Ms. Zel Madison and Ms. Avalon Sandoval for all of their administrative assistance and the Director of Graduate Studies, Dr. Wayne Cass, Ph.D. I would also like to thank Dr. James Geddes, Ph.D. for serving as my mentor when I initially entered the program and for his assistance and collaboration in writing my first graduate school manuscript.

Thank you to all of the current and past students of the UK MD-Ph.D. program for their advice and support. Thank you to the program director, Dr. Susan Smyth, MD-Ph.D. and the program administrator, Ms. Therese Stearns. Therese, your assistance, friendship, and support are unparalleled and I do not think I would have made it this far without your help.

Thank you to my parents and my brother for always offering me support and standing by me even when I made it difficult to do so. I wouldn't be where I am today without you. Thank you to my husband for all his love, unwavering support, and for making life enjoyable. I also do not think I would have made it to this point without you. Thank you to my best friends, Nips and Niobe.

I am also thankful for all of my funding support including the MD-PhD program, UK College of Medicine, Kentucky Spinal Cord and Head Injury Research Trust (KSCHIRT), and National Institute of Neurologic Disorders and Stroke (NINDS).



## Table of Contents

<b>ACKNOWLEDGMENTS</b> .....	<b>III</b>
<b>LIST OF TABLES</b> .....	<b>XII</b>
<b>LIST OF FIGURES</b> .....	<b>XIII</b>
<b>CHAPTER ONE: INTRODUCTION</b> .....	<b>1</b>
<b>EPIDEMIOLOGY OF TRAUMATIC BRAIN INJURY</b> .....	<b>1</b>
<b>ANIMAL MODELS OF TBI</b> .....	<b>3</b>
<b>TRAUMATIC BRAIN INJURY PATHOPHYSIOLOGY</b> .....	<b>4</b>
<b>Primary Injury Mechanisms</b> .....	<b>4</b>
<b>Secondary Injury Mechanisms</b> .....	<b>5</b>
<b>TBI-Induced Calcium Influx</b> .....	<b>7</b>
<b>MITOCHONDRIA: AN INTRODUCTION</b> .....	<b>7</b>
<b>Mitochondria and Physiologic Calcium</b> .....	<b>7</b>
<b>Mitochondria and Energy Production</b> .....	<b>8</b>
<b>Analysis of Mitochondrial Respiration (i.e. Bioenergetics)</b> .....	<b>10</b>
<b>Heterogeneity of Mitochondria</b> .....	<b>13</b>
<b>THE ROLE OF MITOCHONDRIA, OXIDATIVE STRESS, LIPID PEROXIDATION, AND NEUROTOXIC ALDEHYDES IN TBI</b> .....	<b>15</b>
<b>Reactive Oxygen Species, Reactive Nitrogen Species, and Peroxynitrite</b> .....	<b>15</b>
<b>Does Calcium Always Increase Generation of Mitochondria-Derived Reactive Species?</b> .....	<b>17</b>
<b>Non-Mitochondrial Sources of Oxidative Stress</b> .....	<b>18</b>
<b>Endogenous Mitochondrial Antioxidants</b> .....	<b>19</b>
<b>Lipid Peroxidation</b> .....	<b>20</b>
<i>Lipid Peroxidation: Initiation</i> .....	<i>20</i>
<i>Lipid Peroxidation: Propagation</i> .....	<i>22</i>
<i>Lipid Peroxidation: Termination</i> .....	<i>22</i>
<b>Lipid Peroxidation-Derived Aldehydes: 4-HNE and Acrolein</b> .....	<b>22</b>
<b>MITOCHONDRIAL PERMEABILITY TRANSITION PORE</b> .....	<b>27</b>
<b>DOWNSTREAM CONSEQUENCES OF MITOCHONDRIAL DYSFUNCTION</b> .....	<b>29</b>
<b>ATP Depletion</b> .....	<b>29</b>
<b>Calpain Activation &amp; Necrosis</b> .....	<b>30</b>
<b>Caspase Activation &amp; Apoptosis</b> .....	<b>30</b>
<b>Neurodegeneration</b> .....	<b>31</b>
<b>TIME COURSE OF OXIDATIVE STRESS, MITOCHONDRIAL DYSFUNCTION, AND NEURODEGENERATION FOLLOWING TBI</b> .....	<b>32</b>
<b>TIME COURSE OF ANTIOXIDANT DEPLETION FOLLOWING TBI</b> .....	<b>34</b>

<b>Behavioral Impairment .....</b>	<b>34</b>
<b>AN INTRODUCTION TO BIOGENIC AMINES .....</b>	<b>38</b>
<b>Biogenic Amines .....</b>	<b>38</b>
<b>Biogenic Amine Anatomic Pathways and Physiologic Functions.....</b>	<b>40</b>
<i>Dopamine .....</i>	<i>40</i>
<i>Norepinephrine .....</i>	<i>40</i>
<i>Serotonin .....</i>	<i>41</i>
<b>TBI AND ACUTE MONOAMINE DYSREGULATION .....</b>	<b>41</b>
<b>MONOAMINE METABOLISM.....</b>	<b>42</b>
<b>Monoamine Oxidase: An Outer Mitochondrial Membrane Protein .....</b>	<b>44</b>
<b>Monoamine Oxidase Inhibitors.....</b>	<b>45</b>
<i>MAOI Properties of Phenelzine.....</i>	<i>47</i>
<i>MAOI Properties of Pargyline .....</i>	<i>49</i>
<i>Comparison of Phenelzine and Pargyline MAO Inhibitory Effects on Drug-Induced Behavioral Changes .....</i>	<i>49</i>
<b>TBI AND NEUROPROTECTIVE DRUG DEVELOPMENT .....</b>	<b>50</b>
<b>Failure of Clinical TBI Drug Trials .....</b>	<b>50</b>
<b>Review of Selected Neuroprotective Strategies .....</b>	<b>51</b>
<b>Targeting of Mitochondrial Dysfunction .....</b>	<b>51</b>
<i>Inhibition of mPTP: Cyclosporine A and NIM811 .....</i>	<i>52</i>
<i>Mild Uncoupling .....</i>	<i>54</i>
<i>Ketones .....</i>	<i>55</i>
<b>Targeting of ROS/RNS, LP, and LP-Derived Neurotoxic Aldehydes .....</b>	<b>55</b>
<i>Select Antioxidant Therapies .....</i>	<i>55</i>
<i>Superoxide Dismutase.....</i>	<i>56</i>
<i>Lazaroids .....</i>	<i>56</i>
<i>Spin-Trapping Agents .....</i>	<i>57</i>
<i>Induction of Endogenous Antioxidant Pathways.....</i>	<i>57</i>
<i>Nrf2 .....</i>	<i>57</i>
<i>Glutathione Precursors.....</i>	<i>58</i>
<i>Carbonyl Scavenging.....</i>	<i>58</i>
<i>Additional Properties of Phenelzine.....</i>	<i>62</i>
<i>Properties of Hydralazine .....</i>	<i>63</i>
<b>Use of Monoamine Agonists, Antagonists, and Monoamine Oxidase Inhibitors in TBI .....</b>	<b>64</b>
<b>Combinational Therapies .....</b>	<b>65</b>
<b>OVERALL DISSERTATION OBJECTIVE AND SPECIFIC AIMS .....</b>	<b>67</b>
<b>Specific Aim 1 .....</b>	<b>68</b>
<b>Specific Aim 2.....</b>	<b>68</b>

Specific Aim 3.....	68
<b>CHAPTER TWO: SYNAPTIC MITOCHONDRIA SUSTAIN MORE DAMAGE THAN NON-SYNAPTIC MITOCHONDRIA AFTER TRAUMATIC BRAIN INJURY AND ARE PROTECTED BY CYCLOSPORINE A.....</b>	<b>70</b>
PREFACE .....	70
INTRODUCTION .....	71
METHODS .....	75
Animals .....	75
CCI TBI .....	75
Cyclosporine A Administration .....	76
Tissue Extraction .....	76
Mitochondrial Isolation .....	76
Measurement of Mitochondrial Respiratory Function .....	77
Statistical analysis .....	78
RESULTS .....	79
State II: Addition of Pyruvate + Malate to Activate Mitochondrial Complex I .....	79
State III: Addition of ADP to Activate Complex V ATP Production .....	81
State IV: Addition of Oligomycin to Inhibit Complex V ATP Production .....	83
RCR (State III / State IV): Difference in Oxygen Utilization Between Activation and Inhibition of ATP Production .....	85
State V(I): Maximal Complex I-Driven Respiration After Addition of the Protonophore FCCP.....	87
State V(II): Succinate-Activated Complex II-Driven Respiration after Inhibition of Complex I with Rotenone .....	89
DISCUSSION.....	91
CONCLUSION .....	99
ACKNOWLEDGMENTS .....	100
<b>CHAPTER THREE: CONTINUOUS INFUSION OF PHENELZINE, CYCLOSPORINE A, OR THEIR COMBINATION: EVALUATION OF MITOCHONDRIAL BIOENERGETICS, OXIDATIVE DAMAGE, AND CYTOSKELETAL DEGRADATION FOLLOWING SEVERE CONTROLLED CORTICAL IMPACT TRAUMATIC BRAIN INJURY IN RATS .....</b>	<b>101</b>
PREFACE .....	101
INTRODUCTION .....	102
METHODS .....	108
Animals .....	108
Experimental Design.....	108
Controlled Cortical Impact Traumatic Brain Injury.....	112

Loading Dose Drug Administration .....	112
Osmotic Pump Preparation.....	113
Implantation of Osmotic Pumps .....	113
Phenelzine 12hr Intermittent Dosing Protocol .....	114
Tissue Extraction and Pump Removal.....	114
Isolation of Ficoll-Purified Cortical Mitochondria.....	114
Mitochondrial Bioenergetics Analysis.....	115
Western Blot Analysis: Cortical $\alpha$ -Spectrin Degradation & Lipid Peroxidation-Induced Cortical Mitochondrial Oxidative Damage .....	116
Statistical Analysis .....	117
<b>RESULTS .....</b>	<b>119</b>
<b>CCI-TBI Induced Mitochondrial Bioenergetics Dysfunction.....</b>	<b>119</b>
<i>State III: ADP Activation of ATP Synthase and Coupling of Electron Transport with Oxidative     Phosphorylation .....</i>	<i>119</i>
<i>State IV: Oligomycin Inhibition of ATP Synthase .....</i>	<i>119</i>
<i>Respiratory Control Ratio (RCR): State III Respiration / State IV Respiration .....</i>	<i>121</i>
<i>State V(I): FCCP Protonophore Addition and Initiation of Maximal Complex-I Respiration .....</i>	<i>121</i>
<i>State V(II): Rotenone Inhibition of Complex-I and Succinate Activation of Maximal Complex-II     Respiration.....</i>	<i>123</i>
<b>CCI-TBI Modification of Mitochondrial Proteins by 4-HNE and Acrolein .....</b>	<b>123</b>
4-HNE.....	123
Acrolein.....	125
<b>CCI-TBI Induced <math>\alpha</math>-Spectrin Degradation: Continuous Infusion Dosing Paradigm ....</b>	<b>125</b>
145 kD – Calpain-Dependent $\alpha$ -Spectrin Breakdown Product .....	125
150 kD – Calpain/Caspase 3-Dependent $\alpha$ -Spectrin Breakdown Product .....	126
<b>CCI-TBI Induced <math>\alpha</math>-Spectrin Degradation: Phenelzine 12hr Intermittent Dosing   Paradigm .....</b>	<b>128</b>
145 kD – Calpain-Dependent $\alpha$ -Spectrin Breakdown Products .....	128
150 kD – Calpain/Caspase 3-Dependent $\alpha$ -Spectrin Breakdown Product .....	128
<b>DISCUSSION.....</b>	<b>130</b>
<b>TBI Induction of Mitochondrial Dysfunction and Lipid Peroxidation-Derived Aldehyde   Generation .....</b>	<b>130</b>
<b>Cyclosporine A and Inhibition of the Mitochondrial Permeability Transition Pore ....</b>	<b>130</b>
<b>Phenelzine Scavenging of Lipid Peroxidation-Derived Aldehydes 4-HNE and Acrolein   .....</b>	<b>136</b>
<b>Phenelzine + Cyclosporine A: A multi-mechanistic Combinatory Pharmacotherapy   Approach.....</b>	<b>142</b>
<b>CONCLUSION .....</b>	<b>146</b>
<b>ACKNOWLEDGMENTS .....</b>	<b>148</b>

<b>CHAPTER FOUR: COMPARATIVE EFFECTS OF PHENELZINE, HYDRALAZINE, AND PARGYLINE ON LEARNING AND MEMORY AND CORTICAL TISSUE SPARING FOLLOWING EXPERIMENTAL TRAUMATIC BRAIN INJURY .....</b>	<b>149</b>
<b>PREFACE .....</b>	<b>149</b>
<b>INTRODUCTION .....</b>	<b>150</b>
<b>METHODS .....</b>	<b>155</b>
<b>Animals .....</b>	<b>155</b>
<b>Experimental Design: High Performance Liquid Chromatography (HPLC) Monoamine and Metabolite Analysis .....</b>	<b>155</b>
<b>High Performance Liquid Chromatography with Electrical Detection (HPLC-EC) for Monoamine and Metabolite Tissue Levels .....</b>	<b>157</b>
<b>Controlled Cortical Impact Traumatic Brain Injury (CCI) .....</b>	<b>157</b>
<b>CCI Dosing Paradigm .....</b>	<b>158</b>
<b>Morris Water Maze .....</b>	<b>160</b>
<b>Tissue Processing for Histology .....</b>	<b>161</b>
<b>Statistical Analysis .....</b>	<b>162</b>
<b>RESULTS .....</b>	<b>164</b>
<b>PG, PZ, or HZ: HPLC Monoamine and Metabolite Tissue Levels and Turnover Ratios in Uninjured Cortical Tissue.....</b>	<b>164</b>
<b>Morris Water Maze Latency to Platform (MWM D1-D4, Post CCI D3-D6).....</b>	<b>171</b>
<b>Morris Water Maze Distance to Platform (MWM D1-D4, Post CCI D3-D6) .....</b>	<b>173</b>
<b>Morris Water Maze Swim Speed (MWM D1-D4, Post CCI D3-D6) .....</b>	<b>174</b>
<b>Morris Water Maze Reference Memory .....</b>	<b>174</b>
<b>Percentage Weight Loss Following CCI-MWM.....</b>	<b>174</b>
<b>Total Percentage Cortical Tissue Sparing .....</b>	<b>178</b>
<b>Individual Coronal Section Percent Cortical Tissue Sparing .....</b>	<b>182</b>
<b>Qualitative Behavioral Observations of PZ group .....</b>	<b>182</b>
<b>DISCUSSION.....</b>	<b>184</b>
<b>Lipid Peroxidation and TBI Secondary Injury .....</b>	<b>184</b>
<b>Aldehyde Scavengers and Neuroprotection .....</b>	<b>186</b>
<b>Monoamines and Monoamine Oxidase (MAO).....</b>	<b>187</b>
<i>Dopamine .....</i>	<i>187</i>
<i>Norepinephrine .....</i>	<i>188</i>
<i>Serotonin .....</i>	<i>188</i>
<i>Monoamine Oxidase (MAO) .....</i>	<i>189</i>
<b>Choice of Experimental Design: Dosing Paradigms .....</b>	<b>190</b>
<b>Choice of Experimental Design: Morris Water Maze.....</b>	<b>191</b>
<b>Phenelzine: A Comparison to Previous Neuroprotective CCI Studies.....</b>	<b>195</b>

Phenelzine as a Monoamine Oxidase Inhibitor .....	198
The Effects of Phenelzine on Weight .....	199
The Effects of Phenelzine on Behavior .....	200
Phenelzine: A Comparison to Previous Neuroprotective SCI and Ischemic- Reperfusion Injury Studies .....	203
Monoamines and TBI .....	205
Phenelzine: Other Possible Confounding Mechanisms of Action .....	207
Pargyline .....	208
Hydralazine .....	213
Clinical Translation of PZ, HZ, and Other Aldehyde Scavengers .....	216
CONCLUSION .....	219
ACKNOWLEDGMENTS .....	220
<b>CHAPTER FIVE: SUPPLEMENTARY DATA: COMPARATIVE EFFECTS OF PHENELZINE, HYDRALAZINE, AND PARGYLINE ON LEARNING AND MEMORY AND CORTICAL TISSUE SPARING FOLLOWING EXPERIMENTAL TRAUMATIC BRAIN INJURY .....</b>	<b>221</b>
INTRODUCTION .....	221
METHODS .....	222
Experimental Design: 24h HPLC Monoamine and Metabolite Analysis .....	222
Experimental Design: CCI Time Course HPLC Monoamine and Metabolite Analysis .....	224
Percent Weight Loss in Uninjured Rats Following PG, PZ, or HZ Administration .....	224
RESULTS .....	226
24h Single Dose PG, PZ, or HZ: HPLC Monoamine and Metabolite Tissue Levels and Turnover Ratios in Uninjured Cortical Tissue .....	226
CCI Time Course HPLC Monoamine and Metabolite Tissue Levels and Turnover Ratios in Penumbral Cortical Tissue .....	232
Percent Weight Loss in Uninjured Rats Following PG, PZ, or HZ Administration (HPLC Experiments) .....	238
DISCUSSION AND CONCLUSION .....	240
24h Single Dose PG, PZ, or HZ: HPLC Monoamine and Metabolite Tissue Levels and Turnover Ratios in Uninjured Cortical Tissue .....	240
CCI Time Course HPLC Monoamine and Metabolite Tissue Levels and Turnover Ratios in Penumbral Cortical Tissue .....	242
Percent Weight Loss in Uninjured Rats Following PG, PZ, or HZ Administration (HPLC Experiments) .....	244
<b>CHAPTER SIX: FINAL DISCUSSION AND CONCLUDING REMARKS .....</b>	<b>245</b>
SUMMARY OF RESULTS AND CONCLUSIONS .....	245

<b>Synaptic Mitochondria Sustain More Damage than Non-Synaptic Mitochondria after Traumatic Brain Injury and are Protected by Cyclosporine A.....</b>	<b>246</b>
<b>Continuous Infusion of Phenzelzine, Cyclosporine A, or Their Combination: Evaluation of Mitochondrial Bioenergetics, Oxidative Damage, and Cytoskeletal Degradation Following Severe Controlled Cortical Impact Traumatic Brain Injury in Rats .....</b>	<b>249</b>
<b>Comparative Effects of Phenzelzine, Hydralazine, and Pargyline on Learning and Memory and Cortical Tissue Sparing Following Experimental Traumatic Brain Injury .....</b>	<b>254</b>
<b>APPENDIX: ABBREVIATIONS.....</b>	<b>259</b>
<b>REFERENCES.....</b>	<b>264</b>
<b>VITA.....</b>	<b>292</b>

## LIST OF TABLES

Table 3.1 Subcutaneous Continuous Infusion Dosing Paradigm.....	110
Table 3.2 Phenzelzine 12hr Intermittent Dosing Paradigm .....	111
Table 3.3 Summary of Result: Subcutaneous Continuous Infusion Dosing Paradigm..	132
Table 3.4 $\alpha$ -Spectrin Degradation: Phenzelzine Continuous Infusion Versus Phenzelzine Intermittent Dosing .....	138
Table 4.1 Mean Percent Cortical Tissue Sparing for Vehicle, Pargyline, Phenzelzine, and Hydralazine on Post-CCI D8.....	181



## LIST OF FIGURES

Figure 1.1 Glasgow Coma Scale .....	2
Figure 1.2 Simplified schematic of the TBI secondary injury cascade.....	6
Figure 1.3 Mitochondria electron transport chain.....	9
Figure 1.4 Mitochondria states of respiration.....	11
Figure 1.5 Schematic of synaptic mitochondria.....	16
Figure 1.6 Phases of lipid peroxidation.....	21
Figure 1.7 Acrolein and 4-HNE reactions.....	24
Figure 1.8 Downstream effects of mitochondrial dysfunction.....	26
Figure 1.9 Schematic of the mitochondrial permeability transition pore (mPTP).....	28
Figure 1.10 Synthesis of the monoamines.....	39
Figure 1.11 Simplified monoamine metabolism pathways.....	43
Figure 1.12 Chemical structures of phenelzine and pargyline.....	48
Figure 1.13 Chemical structure of cyclosporine A.....	53
Figure 1.14 Phenelzine scavenging of lipid peroxidation-derived aldehydes.....	60
Figure 1.15 Chemical structures of phenelzine and hydralazine.....	61
Figure 2.1 State II: Effect of CsA on synaptic and non-synaptic mitochondria.....	80
Figure 2.2 State III: Effect of CsA on synaptic and non-synaptic mitochondria.....	82
Figure 2.3 State IV: Effect of CsA on synaptic and non-synaptic mitochondria.....	84
Figure 2.4 RCR: Effect of CsA on synaptic and non-synaptic mitochondria.....	86
Figure 2.5 State V(I): Effect of CsA on synaptic and non-synaptic mitochondria.....	88
Figure 2.6 State V(II): Effect of CsA on synaptic and non-synaptic mitochondria.....	90
Figure 2.7 Representative oxymetric traces.....	92
Figure 3.1 Simplified schematic of TBI pathophysiology and phenelzine and cyclosporine A mechanisms of action.....	104
Figure 3.2 State III – State V(II): PZ, CsA, and PZ + CsA.....	120

Figure 3.3 RCR: PZ, CsA, and PZ + CsA .....	122
Figure 3.4 4-HNE and Acrolein: Effect of PZ, CsA, and PZ + CsA.....	124
Figure 3.5 Spectrin: Effect of PZ, CsA, and PZ + CsA. ....	127
Figure 3.6 Spectrin: Intermittent PZ dosing.....	129
Figure 3.7 Schematic illustration of CsA monotherapy results. ....	134
Figure 3.8 Schematic illustration of PZ monotherapy results. ....	140
Figure 3.9 Schematic demonstrating a mitochondrion extensively bound to CsA and PZ. .....	145
Figure 4.1 Simplified schematic of traumatic brain injury (TBI) pathophysiology and pargyline (PG), phenelzine (PZ) and hydralazine (HZ) mechanisms of action. ....	151
Figure 4.2 Chemical structures of pargyline, phenelzine and hydralazine.....	154
Figure 4.3 Monoamine and metabolite HPLC experimental design.....	156
Figure 4.4 Controlled cortical impact and Morris water maze experimental design. ....	159
Figure 4.5 Tissue Level (ng/g) of norepinephrine (NE) in 72h uninjured cortex.....	165
Figure 4.6 Tissue Level (ng/g) of serotonin (5-HT) and metabolites in 72h uninjured cortex. ....	166
Figure 4.7 Tissue Level (ng/g) of dopamine (DA) and metabolites in 72h uninjured cortex. ....	167
Figure 4.8 Morris water maze latency and distance to platform. ....	172
Figure 4.9 Overall Morris water maze swim speed. ....	175
Figure 4.10 Morris water maze reference memory.....	176
Figure 4.11 Percent weight loss between D0 (CCI) and D7 (MWM probe trial).....	177
Figure 4.12 Total percent cortical tissue sparing (ipsilateral/contralateral) D8 post-CCI. .....	179
Figure 4.13 Representative cortical tissue sparing on post-CCI day 8. ....	180
Figure 4.14 Individual coronal section percent cortical tissue sparing post-CCI day 8.	183

Figure 5.1 Monoamine and metabolite 24h HPLC experimental design.....	223
Figure 5.2 Monoamine and metabolite CCI time course experimental design.....	225
Figure 5.3 Tissue Level (ng/g) of norepinephrine (NE) in 24h uninjured cortex.....	227
Figure 5.4 Tissue Level (ng/g) of serotonin (5-HT) and metabolites in 24h uninjured cortex. ....	228
Figure 5.5 Tissue Level (ng/g) of dopamine (DA) and metabolites in 24h uninjured cortex. ....	229
Figure 5.6 Tissue Level (ng/g) of norepinephrine (NE) in penumbral cortical tissue.....	233
Figure 5.7 Tissue Level (ng/g) of serotonin (5-HT) and metabolites in penumbral cortical tissue.....	234
Figure 5.8 Tissue Level (ng/g) of dopamine (DA) and metabolites in penumbral cortical tissue.....	235
Figure 5.9 Percent weight loss in uninjured animals for 72h HPLC experiment. ....	239

## **CHAPTER ONE:**

### **Introduction**

#### **Epidemiology of Traumatic Brain Injury**

Traumatic brain injury (TBI) represents a significant health crisis in the United States and worldwide. Currently there are no FDA-approved pharmacological agents capable of attenuating the devastating neurologic consequences that can occur following TBI [1]. TBIs range from mild to severe, with at least two and a half million documented cases occurring in the United States annually [2]. However, these numbers are underestimates because the majority of TBIs are classified as mild [3], and often go unreported, especially in sports and military communities [4, 5]. In fact, it is estimated that sports-related TBIs alone occur at a rate of 3.8 million annually [6]. Young children (0-4 years), older teenagers (15-19 years), the elderly (>65 years), and males across all ages groups are at the highest risk of sustaining a TBI [7]. In the US, falls and motor vehicle accidents are the leading causes of TBI [7].

Clinically, TBIs are classified using the Glasgow Coma Scale (GCS: mild 13-15, moderate 9-12, severe 3-8) an injury scale which relies on assessments of eye, motor, and verbal responses [8] (**Fig. 1.1**). However, it must be noted that although GCS can give a clinical assessment of brain injury, it is unable to characterize injury pathology [9], but clinical utilization of imaging can be useful in this regard. For example, amongst TBI patients categorized as having a severe TBI by GCS score, CT or MRI scans can distinguish between injury pathologies such as epidural hematoma, subdural hematoma, subarachnoid hemorrhage, etc. [9].

<b>Glasgow Coma Scale</b>		
<b>Response</b>	<b>Scale</b>	<b>Score</b>
<b>Eye Opening Response</b>	Eyes open spontaneously	4
	Eyes open to verbal command	3
	Eyes open to pain	2
	No eye opening	1
<b>Verbal Response</b>	Oriented	5
	Confused conversation; able to answer questions	4
	Inappropriate responses; words discernable	3
	Incomprehensible speech or sounds	2
	No verbal response	1
<b>Motor Response</b>	Obeys movement commands	6
	Purposeful movement to painful stimuli	5
	Withdraws from pain	4
	Spastic flexion; decorticate posture	3
	Rigid extensor response; decerabrate posture	2
	No Motor Response	1
<b>Mild = 13 - 15, Moderate = 9 - 12, Severe = 3 - 8</b>		

**Figure 1.1 Glasgow Coma Scale** indicating the specific eye opening, verbal and motor responses and the corresponding scores utilized for clinical assessment of brain injury severity.

Although the majority of diagnosed TBIs are classified as mild on the GCS, the most severe injuries, those resulting in hospitalization and death, account for ninety percent of TBI-associated costs, a staggering amount considering that in 2010 both direct and indirect TBI medical costs were estimated to be seventy-five billion dollars [10, 11].

Additionally, there are over five million people in the United States living with a TBI-related disability [12]. In fact, over fifty percent of persons hospitalized due to TBI, will continue to suffer from a TBI-associated disability more than a year following injury [13]. Such disabilities can include cognitive, physical, and emotional impairments [12].

### **Animal Models of TBI**

Animal models have been used extensively to model TBI and are able to recapitulate several aspects of human TBI neuropathology and behavioral impairment [167]. Although large animal (e.g. swine) models of TBI exist, the majority of TBI studies utilize rodents [167]. However, there are several anatomic and physiologic differences between humans and rodents which must be taken into consideration [168]. For example, compared to rodents, human brains contain higher ratios of white to grey matter, higher ratios of glia to neurons, sulci, gyri, longer myelinated axons, and a denser vascular supply [168].

In humans, TBI injury pathology is heterogeneous and as such, several animal models of TBI have been developed, including controlled cortical impact injury (CCI), fluid percussion injury (FPI), and the Marmarou weight drop (WD) model. In recent years, with the growing interest in military and sports-related injuries, models of blast injury, mild closed head injury (CHI) and rotational injury have also been developed [167]. Due to the clinical heterogeneity of TBI, as well as the failure of TBI clinical trials,

many recent pre-clinical TBI studies, such as “Operation Brain Trauma Therapy” are screening drugs across multiple animal models of TBI [384]. These studies aim to identify drugs that have robust neuroprotective effects across multiple experimental injury paradigms, with the hope that such drugs will be clinically translationally for use in multiple types of human TBI. On the other hand, these types of studies have the ability to identify drugs that only have neuroprotective effects in certain experimental models, a finding that can improve future clinical trial designs by limiting the type of human TBI such drugs are evaluated in.

The majority of severe injury studies have utilized the CCI, FPI and WD models, all of which have aspects of focal contusion, diffuse axonal injury, and hemorrhage. However, WD is often identified as being diffuse, FPI as mixed (focal/diffuse), and CCI as focal [167]. Although each model has its advantages and disadvantages, CCI, the model utilized in this dissertation, is considered to be more reproducible and have a lower mortality rate than both the WD and FPI models [167].

## **Traumatic Brain Injury Pathophysiology**

### **Primary Injury Mechanisms**

TBI consists of a primary injury followed by a secondary injury cascade. The primary injury occurs immediately and is caused by external forces, such as a direct impact, rapid acceleration/deceleration, or a blast wave. Primary injury can result in contusion, hemorrhage, ischemia, shearing and straining of axons and blood vessels, and diffuse axonal injury from the mechanical insult [14-16].

## **Secondary Injury Mechanisms**

Cellular strain and deformation caused by the primary injury results in membrane depolarization, mechanoporation of membranes, ionic imbalances, and neurotransmitter release, resulting in initiation of the secondary injury cascade, a process which occurs hours to weeks following injury [14, 15], and is heavily influenced by alterations in calcium homeostasis [16], mitochondrial function [17], and the process of lipid peroxidation (LP) [17], but includes additional processes such as neuroinflammation [14, 18] (**Fig. 1.2**). The following sections present a simplified description of TBI secondary injury mechanisms and focuses on specific aspects of mitochondrial function and LP. Although not the main focus of this dissertation, because the drug of interest phenelzine (PZ) is classified as a monoamine oxidase inhibitor, dysfunction of monoamine neurotransmitter systems following TBI will also be briefly discussed.



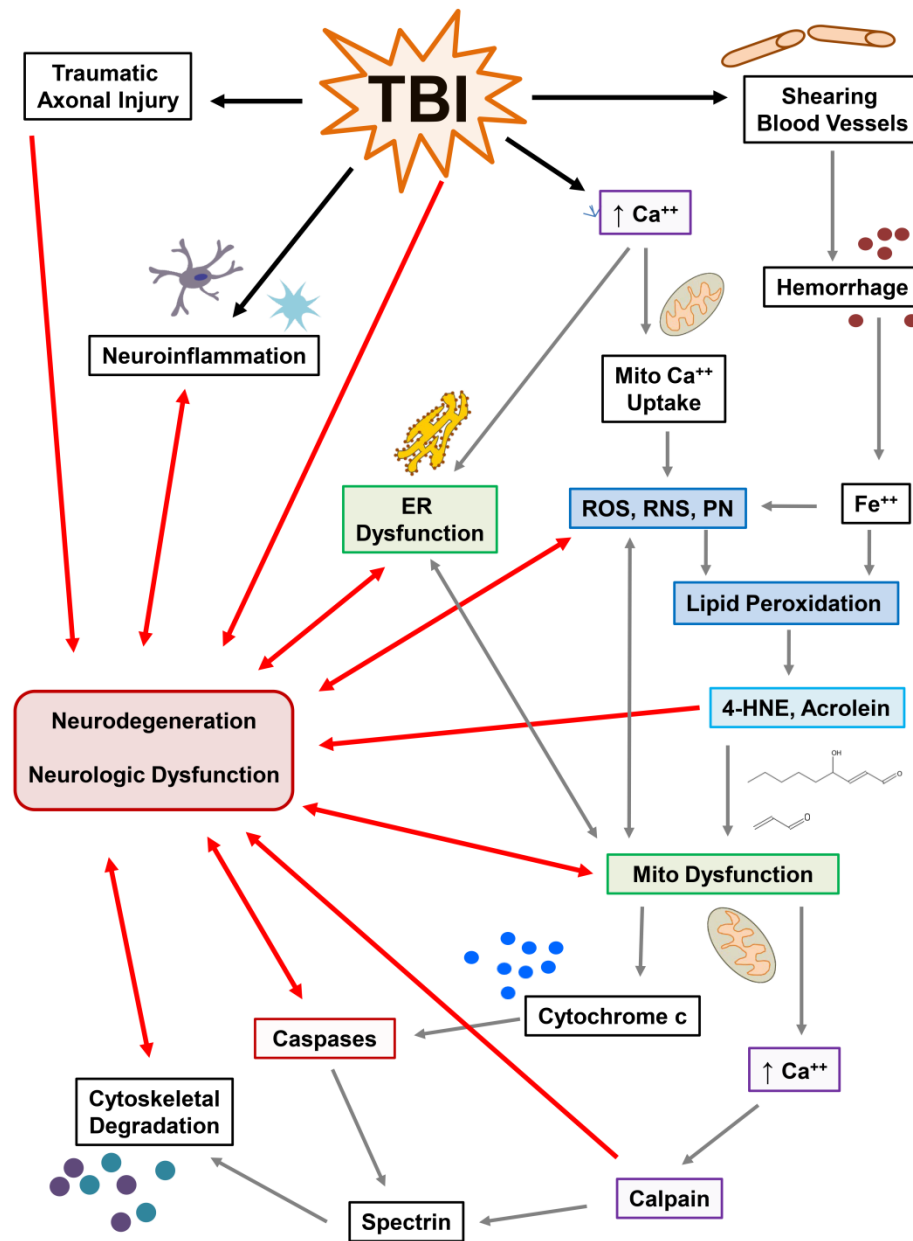


**Figure 1.2 Simplified schematic of the TBI secondary injury cascade.** ROS = reactive oxygen species, RNS = reactive nitrogen species, PN = peroxynitrite, Mito = mitochondria, 4-HNE = 4-hydroxynoneal, ER = endoplasmic reticulum. Adapted from Kulbe et al. 2017 [19].

## **TBI-Induced Calcium Influx**

Activation of calcium channels by high levels of extracellular glutamate following injury, along with activation of voltage-gated calcium channels, failure of energy-dependent calcium efflux pumps, and membrane leakage leads to large increases in intracellular calcium [16]. As essential regulators of calcium [20, 21], mitochondria attempt to maintain calcium homeostasis by taking up excess intracellular calcium, a process dependent upon the presence of the mitochondrial calcium uniporter, a calcium concentration gradient, and a negative mitochondrial membrane potential [22-24]. Additionally, calcium-binding proteins and the endoplasmic reticulum (ER) function to sequester calcium following injury [16].

## **Mitochondria: An Introduction**

### **Mitochondria and Physiologic Calcium**

In addition to being able to sequester calcium under pathologically high intracellular calcium concentrations, mitochondria can regulate calcium homeostasis under physiologic conditions as well. Calcium is an activator of the citric acid cycle (TCA) enzymes, including pyruvate dehydrogenase, NAD<sup>+</sup> dependent isocitrate dehydrogenase, and  $\alpha$ -ketoglutarate dehydrogenase, therefore increases in calcium can induce increases in mitochondrial respiratory rates [21, 25]. Furthermore, the ability of mitochondria to cycle calcium allows for fine tuning of calcium concentrations in subcellular compartments such as the presynaptic terminal, allowing for tight regulation of processes such as neurotransmitter release [21, 25, 26].

### **Mitochondria and Energy Production (Fig. 1.3)**

Although mitochondria serve an important role in maintenance of calcium homeostasis under both physiologic and pathologic conditions, mitochondria are generally known for their role in adenosine triphosphate (ATP, i.e. energy) production. The brain primarily utilizes glucose as its energy source [27], a process which begins with cytosolic glycolysis, in which one molecule of glucose, a product of carbohydrate metabolism, is catabolized to form two molecules of pyruvate, two molecules of ATP, and two molecules of nicotinamide adenine dinucleotide (NADH). Fortunately, mitochondria can utilize pyruvate to significantly increase the amount of ATP that can be generated from each glucose molecule, through the process of oxidative phosphorylation.

Pyruvate is transported across both the outer and inner mitochondrial membranes, into the mitochondrial matrix where it is converted into acetyl-coA before entering into the citric acid cycle (TCA). Through a series of oxidation (loss of electrons) and reduction (gain of electrons) reactions NADH and flavin adenine diculeotide (FADH<sub>2</sub>) are produced. NADH and FADH<sub>2</sub> provide the electrons and protons utilized by the electron transport chain (ETC) complexes, located in the inner mitochondrial membrane, during the process of oxidative phosphorylation. Complex I (NADH dehydrogenase) receives electrons from NADH, while complex II (succinate dehydrogenase) receives electrons from FADH<sub>2</sub>. Complex I and II both pass these electrons on to complex III (coenzyme Q-cytochrome c oxidoreductase) through the electron-carrier coenzyme Q (ubiquinone).

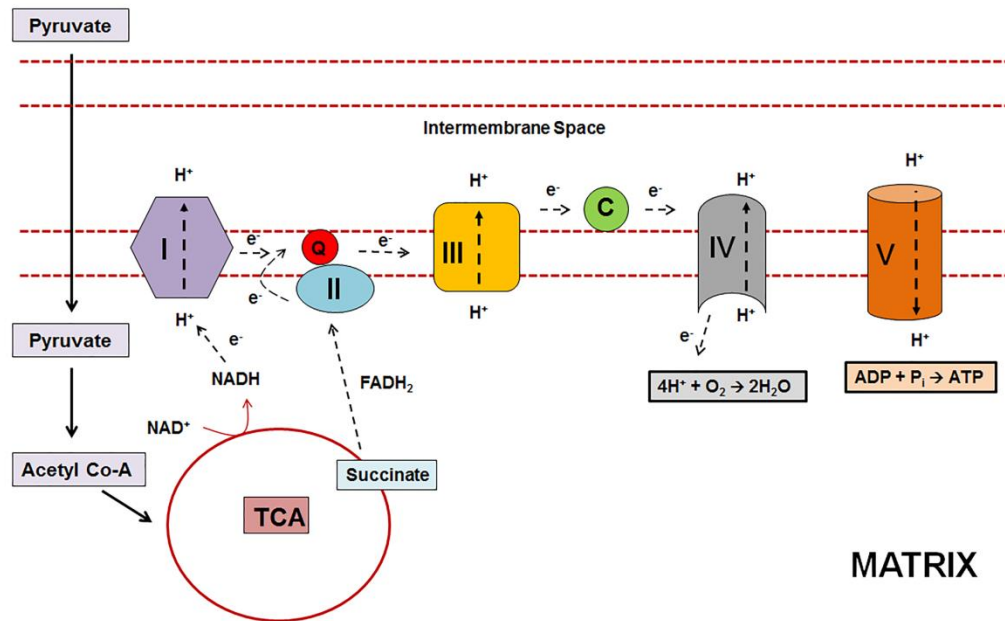


**Figure 1.3 Mitochondria electron transport chain.** Following glycolysis pyruvate is transported into the mitochondrial matrix where it is converted into acetyl-coA before entering into the citric acid cycle (TCA). Electrons and protons are passed from NADH to complex I and from succinate /  $FADH_2$  to complex II. From there electrons are passed through coenzyme Q (Q) to complex III and onto complex IV through cytochrome c (C). At complex IV the electrons are passed onto the final electron acceptor  $O_2$  to generate water. As electrons are passed through the electron transport chain  $H^+$  are pumped from the matrix to the intermembrane space through complex I, III, and IV. Protons flow down their gradient at complex V to generate ATP from ADP.

From complex III electrons are transferred to cytochrome c before reaching complex IV (cytochrome c oxidase) where they are transferred to the ETC's final electron acceptor, O<sub>2</sub>, resulting in the formation of H<sub>2</sub>O.

Importantly, as the initially high energy electrons are passed through the redox centers of the ETC, this energy is used to pump protons (H<sup>+</sup>) from the mitochondrial matrix, across the inner mitochondrial membrane at complexes I, III, and IV, into the mitochondrial intermembrane space, producing the mitochondrial membrane potential, which under physiologic conditions is approximately -150 mV to -180mV [25, 28]. Generation of the mitochondrial membrane potential allows for H<sup>+</sup> to re-enter the relatively negative mitochondrial matrix from the relatively positive mitochondrial intermembrane space, through the transmembrane protein ATP synthase, utilizing the energy generated as protons flow down their gradient to phosphorylate ADP and generate ATP, thus linking the electron transport chain with ATP production (i.e. oxidative-phosphorylation).

### **Analysis of Mitochondrial Respiration (i.e. Bioenergetics)**

One method of evaluating mitochondrial bioenergetics is through the use of a Clark-type oxygen electrode, a device which measures oxygen concentration. Mitochondria are added to a 37°C continuously stirred chamber. As O<sub>2</sub> is the final electron acceptor of the ETC, following addition of ETC substrates, O<sub>2</sub> is consumed and drops in O<sub>2</sub> concentration can be measured to assess respiratory rates. Upon addition of several compounds, information can be obtained regarding various individual states of mitochondrial respiration (**Fig. 1.4**).

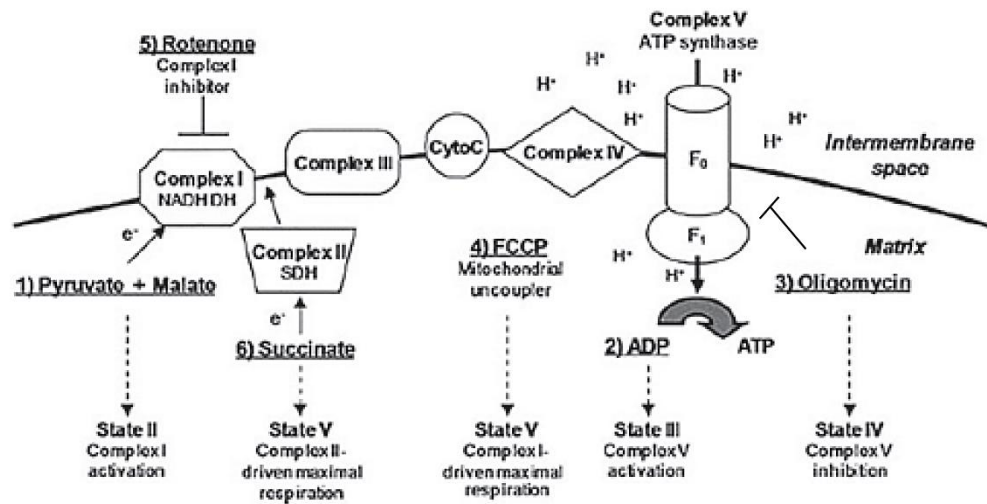


**Figure 1.4 Mitochondria states of respiration.** (1) The complex I substrates pyruvate and malate are added to initiate state II respiration. (2) Next, boluses of ADP are added to initiate state III respiration. (3) Following addition of ADP, oligomycin is added to inhibit complex V (i.e. ATP synthase), inducing state IV respiration. (4) Next, the mitochondrial uncoupler FCCP is added to induce state V(I) respiration. (5) Rotenone is added to inhibit complex I, (6) followed by the complex II substrate succinate, initiating state V(II). Adapted from Vaishnav et al. 2010 [29].

State II respiration occurs after addition of the complex-I substrates pyruvate and malate, but before ADP addition, and represents a slow/basal state of respiration.

State III respiration occurs following the addition of the complex-I substrates pyruvate and malate along with ADP, allowing for the formation of ATP ( $\text{ADP} + \text{P}_i$ ) as protons pumped out of the mitochondrial matrix during electron transport flow back down their proton gradient via ATP synthase, thus coupling electron transport with oxidative phosphorylation. State III is considered one of the most important states of respiration, as decreases in State III respiration can be indicative of both impairments in complex-I driven substrate oxidation and/or ATP turnover [30].

State IV respiration is measured following addition of the ATP synthase inhibitor oligomycin, preventing the flow of protons down their proton gradient through ATP synthase. Therefore, the oxygen consumption which occurs following ATP synthase inhibition is due to proton leak across the membrane. Consequently, in healthy mitochondria state IV respiration should be low, representative of a basal state of respiration similar to state II [30, 31]. Intuitively, damaged mitochondria with leaky membranes would result in an increase in state IV. However, when damaged mitochondria show decreases in state IV, it may represent initial impairments in electron flow either due to damage to complex-I or upstream processes, such as to the citric acid cycle (TCA) enzymes. For example, damage to complex-I would impair electron flow to downstream ETC complexes (**Fig. 1.3**), resulting in a decrease in all complex-I-dependent respiration states, including that of state IV. Similarly, damage to TCA proteins would impair electron flow into complex-I (and complex-II) (**Fig. 1.3**), resulting in a decrease in all individual respiratory states, including that of state IV.

Respiratory control ratio (RCR), the difference in oxygen utilization between activation of ATP production (state III) and inhibition of ATP production (state IV), is a general measure of mitochondrial health and function. Healthy mitochondria are able to generate ATP under minimal proton leak and therefore have high RCR values, whereas damaged mitochondria can have relatively lower RCR values, however, there is not a single RCR value which can be considered diagnostic of dysfunction [30]. However, as RCR is a ratio, equal drops in state III and state IV respiration would result in an unchanging RCR value.

State V(I) is measured following addition of the protonophore, FCCP (carbonyl cyanide p-trifluoromethoxyphenylhydrazone), which allows for free flow of protons across the inner mitochondrial membrane down their gradient, uncoupling oxidative phosphorylation and allowing for complex-I driven maximal respiration, with decreases in state V(I) being indicative of deficits in complex-I initiated substrate oxidation [30].

State V(II) respiration is measured following addition of the complex-I inhibitor, rotenone, and the complex-II substrate, succinate, and is a measure of complex-II driven maximal respiration. Therefore, decreases in state V(II) represent defects in complex-II driven substrate oxidation.

### **Heterogeneity of Mitochondria**

Mitochondria are heterogeneous. Brain mitochondria have distinct properties compared to mitochondria derived from other organ systems as well as other regions of the CNS, such as the spinal cord [32, 33]. Additionally, there exists much heterogeneity within brain mitochondria themselves depending on brain region, cell type, and subcellular compartment.



For example, the activities of respiratory chain complex enzymes vary between brain regions (e.g. cortex, hippocampus, striatum), with high enzyme activities being seen in the cortex. ETC enzyme activities also vary between synaptic and non-synaptic mitochondria [34, 35]. Additionally, mitochondrial sensitivity to calcium-induced permeability transition varies between brain regions and between synaptic and non-synaptic mitochondria, with striatal mitochondria being more sensitive to calcium than cortical mitochondria [36], and synaptic mitochondria being more sensitive to calcium than non-synaptic mitochondria [37, 38]. It has been proposed that differences in calcium sensitivities are in part due to concentrations of cyclophilin D (CyD), a protein which interacts with the mitochondrial permeability transition pore (mPTP). In fact, higher concentrations of CyD are found in both striatum and synaptic mitochondria [36, 38]. Additionally, high concentrations of CyD have been found within the interneurons of several brain regions and certain subpopulations of astrocytes [39]. Furthermore, heterogeneity in calcium responses have also been reported within non-synaptic populations, possibly due to differences in phosphate uptake [40].

Previous studies have revealed that synaptic mitochondria are more susceptible to dysfunction than non-synaptic mitochondria [41-43]. In fact, non-synaptic mitochondria can tolerate larger impairments to respiratory complex activity before ATP production is significantly decreased [35]. Although the role non-synaptic neuronal mitochondria and mitochondria derived from glial subtypes have in brain function should not be dismissed, synaptic mitochondria are considered essential for proper neurotransmission and synaptic plasticity, [44-46] processes which are impaired following TBI [47]. Synaptic mitochondrial dysfunction has been implicated in neurodegeneration, as well as degeneration of synapses and neurons absent overt cell death [37, 48, 49]. However, specifically protecting synaptic mitochondria against injury may prove challenging as

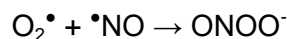
synaptic and non-synaptic mitochondria have been shown to have differential responses to pharmacotherapy [50].

Currently, in order to examine the differences between synaptic mitochondria and non-synaptic mitochondria the populations must be isolated and examined *ex-vivo*. In the isolated mitochondrial preparations utilized in this dissertation, synaptic mitochondria consist of pre-synaptic mitochondria located within the synaptosome, whereas non-synaptic mitochondria consist of neuronal (axonal, somal, dendritic) and non-neuronal (glial, vascular, etc.) mitochondria (**Fig. 1.5**).

### **The Role of Mitochondria, Oxidative Stress, Lipid Peroxidation, and Neurotoxic Aldehydes in TBI**

#### **Reactive Oxygen Species, Reactive Nitrogen Species, and Peroxynitrite**

Increases in intra-mitochondrial calcium following TBI lead to decreased mitochondrial membrane potential, decreased mitochondrial bioenergetics/respiration, and increased production of mitochondrial-derived reactive oxygen and nitrogen species (ROS/RNS) [23, 51]. Although calcium-induced decreases in the membrane potential may initially speed up the ETC in an attempt to maintain membrane potential [25], eventually, exceedingly high levels of calcium [52], along with injury-induced damage to electron transport complexes and upstream metabolic proteins, leads to ETC impairment, and as respiration slows, single electrons leak from complex I (and to a lesser degree complex III), and combine with O<sub>2</sub>, generating superoxide radicals (O<sub>2</sub><sup>•-</sup>), which rapidly react with the nitric oxide (<sup>•</sup>NO) generated by calcium-activated mitochondrial nitric oxide synthase (mtNOS), forming peroxynitrite (PN) anion (ONOO<sup>-</sup>) [53, 54].



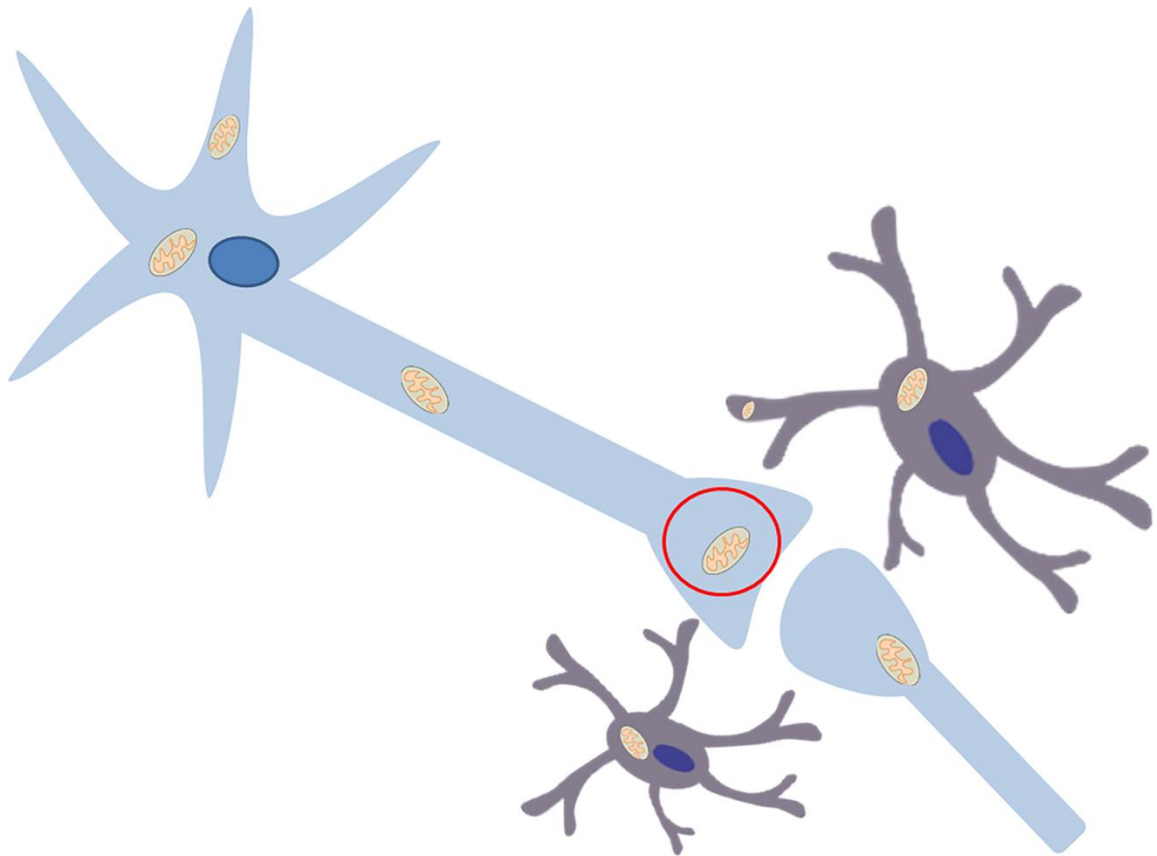


**Figure 1.5 Schematic of synaptic mitochondria.** Synaptic mitochondria are isolated from the presynaptic nerve terminal and represent a purely neuronal population. Non-synaptic mitochondria are isolated from neuronal (e.g. axonal, somal, dendritic) and non-neuronal sources such as astrocytes (shown above) and endothelial cells (not shown).

Protonation of  $\text{ONOO}^-$  results in peroxynitrous acid ( $\text{ONOOH}$ ) which decomposes into nitrogen dioxide ( $\bullet\text{NO}_2$ ) and hydroxyl ( $\bullet\text{OH}$ ) radicals. Alternatively,  $\text{ONOO}^-$  can react with  $\text{CO}_2$  to form nitrosoperoxocarbonate ( $\text{ONOOCO}_2^-$ ) which decomposes into the radicals  $\bullet\text{NO}_2$  and ( $\text{CO}\bullet_3$ ) [1, 55].



PN is demonstratively increased following brain and spinal cord injury [56-59] and because of its unique diffusion radius, mitochondrial-derived PN and its products are capable of damaging multiple cellular structures including proteins, lipids and nucleic acids [1, 55]. In addition to reactive species derived from the ETC and mtNOS, the outer mitochondrial membrane enzyme, monoamine oxidase, which is responsible for oxidation of monoamines such as dopamine (DA), serotonin (5-HT), norepinephrine (NE), and epinephrine (EPI) can also serve as a source of mitochondrial generated reactive species.

### **Does Calcium Always Increase Generation of Mitochondria-Derived Reactive Species?**

Although increases in intra-mitochondrial calcium have been presented to lead to increased production of ROS/RNS, there is some controversy surrounding this topic depending on experimental conditions. For example, in naïve mitochondria calcium decreases respiration [52] and decreases production of mitochondrial-generated ROS/RNS, suggesting that because increases in calcium can immediately induce decreases in respiration, increases in mitochondrial generation of ROS/RNS may be a secondary event [52].

In fact, calcium-induced increases in mitochondrial generated ROS/RNS may require induction of additional pathologies. For example, mitochondrial permeability transition (mPT) has been shown to be required for calcium-induced mitochondrial production of ROS, possibly because mPT decreases the ability of endogenous mitochondria antioxidants, such as glutathione (GSH) and NADH to attenuate ROS production [60]. Additionally, inhibition of complex I (NADH dehydrogenase) [61-63] or the presence of pro-apoptotic proteins [62] have been shown to be required for calcium to induce increases in mitochondrial derived ROS/RNS.

However, it is difficult to extrapolate the findings of studies which utilized isolated mitochondria *ex-vivo* to *in-vivo* pathologies, particularly because *in-vivo* calcium regulation is complex and includes additional organelles, such as the endoplasmic reticulum [52, 63]. If, in fact, respiratory dysfunction does precede calcium-induced increases in mitochondrial ROS/RNS, it is possible that non-mitochondrial sources of oxidative stress (*see below*) may contribute to the initial respiratory deficits. For example, PN is capable of inactivating several mitochondria enzymes such as Complex I and II, creatine kinase, ATP synthase, aconitase, voltage-dependent anion channel (VDAC), and Mn-SOD (mitochondrial superoxide dismutase 2) [52, 54]. Although it is likely that mitochondrial generated ROS/RNS exacerbates dysfunction of these enzymes, it is possible that their initial dysfunction could be caused by non-mitochondrial sources of PN.

### **Non-Mitochondrial Sources of Oxidative Stress**

In addition to the  $O_2^{\bullet-}$  produced by the mitochondria during oxidative phosphorylation,  $O_2^{\bullet-}$  is produced during several other processes, including metabolism of purines by xanthine oxidase, autoxidation of biogenic amines, metabolism of biogenic

amines by monoamine oxidase, and nicotinamide adenine dinucleotide phosphate (NAD(P)H) oxidase generation of inflammatory cell oxidative bursts [1, 64]. In fact, in addition to mitochondria, glial cells represent a significant source of ROS [64].

The metabolism of arachidonic acid, a polyunsaturated fatty acid abundant in cellular membranes, also accounts for generation of ROS [1, 64]. Following brain injury, phospholipases are activated resulting in the release of arachidonic acid. Arachidonic acid is metabolized by cyclooxygenases and lipoxygenases in order to produce a variety of signaling molecules, resulting in formation of ROS in the process [64].

•NO, which reacts with  $O_2^{\bullet-}$  to form PN, can also be generated from several non-mitochondrial sources. For example, calcium-activated endothelial NOS (eNOS) neuronal NOS (nNOS), and calcium-insensitive inducible NOS (iNOS) all lead to generation of NO• [59]. In fact, increases in NOS expression following experimental TBI coincide with PN-induced protein damage [59].

### **Endogenous Mitochondrial Antioxidants**

As a major site of ROS/RNS generation under both pathologic and physiologic conditions, mitochondria require endogenous antioxidant systems. Although the  $O_2^{\bullet-}$  generated through mitochondrial respiration can go onto react with NO• to form PN, this is not always its fate.  $O_2^{\bullet-}$  can spontaneously dismutate to form  $H_2O_2$ , a reaction that is catalyzed by superoxide dismutase (SOD) [1, 65]. Mitochondria contain a specific form of SOD within their matrix, termed MnSOD or SOD2 [65] as well as the cytosolic Cu,Zn-SOD or SOD1, within their intermembrane space [66]. Additionally, cytochrome c can act as an antioxidant in the removal of  $O_2^{\bullet-}$  and  $H_2O_2$  [66]. Another electron carrier within the electron transport chain, ubiquinone, similarly has antioxidant properties [66, 67].

Although  $\text{H}_2\text{O}_2$  is less reactive than its  $\text{O}_2^{\bullet-}$  predecessor, it can itself be damaging, particularly in the presence of iron, which catalyzes the Fenton reaction, resulting in the highly reactive  $\text{OH}^{\bullet}$ .



Fortunately, as glutathione peroxidases (GPx) are present within the mitochondria,  $\text{H}_2\text{O}_2$  can be reduced to  $\text{H}_2\text{O}$  by the glutathione (GSH)/GPx system, which is itself also capable of scavenging  $\bullet\text{OH}$  [66]. Additionally, the reduction of  $\text{H}_2\text{O}_2$  to  $\text{H}_2\text{O}$  can be catalyzed by peroxiredoxins and thioredoxins, enzymes present within brain mitochondria, as well as catalase which is present in brain mitochondria, albeit in small quantities [66]. Furthermore, NAD(P)H, a hydrogen donor, can participate in the regeneration of GSH, as well as directly scavenge both  $\bullet\text{NO}_2$  and  $\text{CO}^{\bullet-}_3$  [66]. Additional antioxidants located in brain mitochondria include ascorbic acid (i.e. vitamin C) and  $\alpha$ -tocopherol (vitamin E), which is capable of scavenging lipid peroxy radicals present within the mitochondrial membranes [66].

### **Lipid Peroxidation (Fig. 1.6)**

#### *Lipid Peroxidation: Initiation*

The highly reactive PN-derived radicals,  $\bullet\text{NO}_2$ ,  $\bullet\text{OH}$ ,  $\text{CO}^{\bullet-}_3$ , initiate lipid peroxidation (LP) by extracting a hydrogen atom and its electron from a polyunsaturated fatty acid, such as arachidonic acid, which is highly enriched in neurons and cellular and organelle membranes, forming a lipid radical ( $\text{L}^{\bullet}$ ) [1, 55].

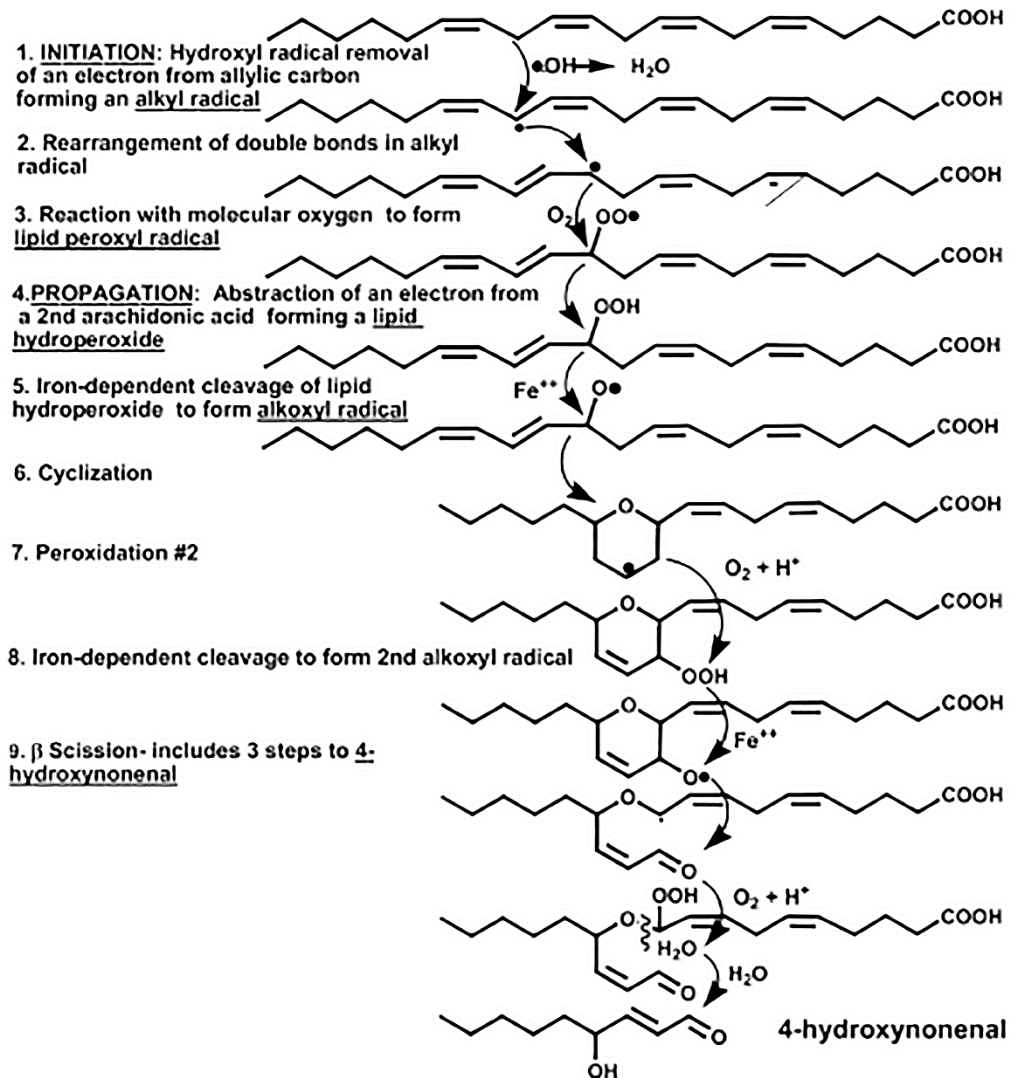


**Figure 1.6 Phases of lipid peroxidation.** Initiation, propagation and termination of lipid peroxidation of arachidonic acid, including catalysis of propagation by  $\text{Fe}^{++}$ , and the resulting formation of the lipid peroxidation-derived neurotoxic aldehyde 4-hydroxynonenal (4-HNE). Adapted from Hall et al. 2010 [1].



### Lipid Peroxidation: Propagation

The lipid radical ( $L^{\bullet}$ ) allows for self-propagation of lipid peroxidation (LP) to occur throughout adjacent polyunsaturated acids, as it first reacts with  $O_2$  to form a lipid peroxy radical ( $LOO^{\bullet}$ ) capable of extracting a hydrogen atom and its electron from neighboring polyunsaturated acids, generating another lipid radical ( $L^{\bullet}$ ) able to participate in further propagation reactions [1, 55]. Although LP is considered to be a self-propagating process, it is also catalyzed by the presence of iron, particularly in the acidic tissues of TBI [1]. Following TBI, decreases in pH cause iron to be released from the iron storage proteins, ferritin and transferritin, with additional iron being released from the hemoglobin deposited during hemorrhages and microbleeds [1].

### Lipid Peroxidation: Termination

LP terminates upon breakdown of the peroxidized polyunsaturated fatty acids to form neurotoxic aldehydic end products, such as 4-hydroxynonenal (4-HNE) and 2-propenal (acrolein) [1, 55]. It is well-established that oxidative stress, LP, and the LP-derived aldehydes are increased in several CNS pathologies including TBI [57, 68-73], spinal cord injury (SCI) [74, 75], ischemic-reperfusion injury and stroke [64, 76], multiple sclerosis [64, 77], neurodegenerative disease [64], epilepsy [64], and psychiatric disorders [64], as well as other conditions which involve oxidative stress such as atherosclerosis, diabetes, and obesity [78].

### **Lipid Peroxidation-Derived Aldehydes: 4-HNE and Acrolein**

Although the breakdown of polyunsaturated fatty acids can result in multiple classes of aldehydic end products including  $\alpha,\beta$ -unsaturated aldehydes, di-aldehydes, and keto-aldehydes, the  $\alpha,\beta$ -unsaturated aldehydes, namely 4-HNE and acrolein, are the most abundant and toxic products of LP [79]. Additionally, as 4-HNE and acrolein

were assessed as part of this dissertation work, 4-HNE and acrolein will be the two products discussed here by name.

The neurotoxic aldehydes, 4-HNE and acrolein, are stable, diffusible end-products, with acrolein being the more reactive of the two [79]. In addition to being a product of LP, acrolein is a well-known environmental pollutant and can also be formed by other physiologic processes such as the metabolism of spermine or hydroxyl-amino acids [79]. 4-HNE and acrolein covalently bind lysine, histidine, arginine and cysteine protein residues through both Schiff base and Michael addition reactions (**Fig 1.7**), and have multiple reactive sites which allows for formation of cross-linkage reactions [1, 79-81]. Neurotoxic aldehydes can be metabolized through conjugation with the endogenous antioxidant GSH or through oxidation/reduction of their carbonyl groups by enzymes such as alcohol and aldehyde dehydrogenase [79, 82]. However, once neurotoxic aldehydes bind proteins, the protein-aldehyde conjugates are often targeted for degradation by the proteasome [83]. Additionally, once covalently bound to proteins, such as occurs following TBI, LP-derived aldehydes induce protein dysfunction and enzyme inactivation, neurotoxicity and cellular death [77, 84-89].

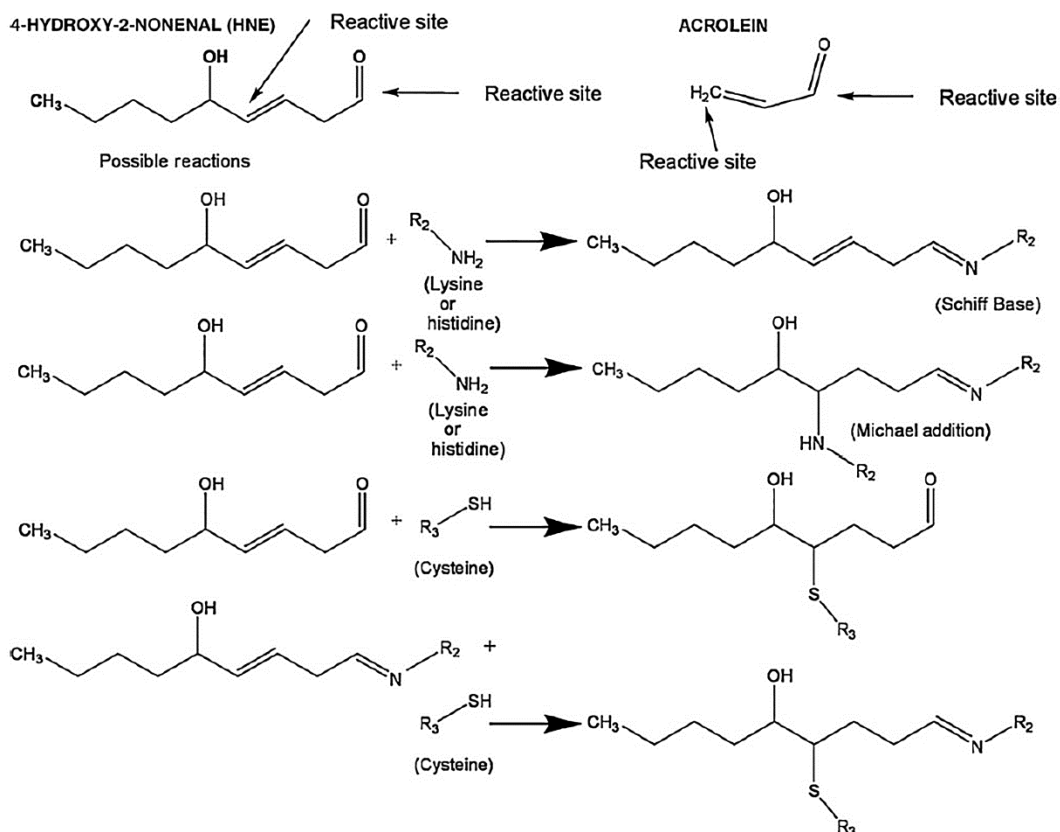


**Figure 1.7 Acrolein and 4-HNE reactions.** The multiple reactive sites of 4-hydroxynonenal (4-HNE) and 2-propenal (acrolein) can react with various amino acids including lysine, histidine, and cysteine through both Schiff base and Michael addition reactions. Adapted from Vaishnav et al. 2010 [29].

Although LP-derived aldehydes have been shown to bind and inactivate a vast array of cellular proteins [79, 81, 90-96], due to their polyunsaturated fatty acid composition and as a major site of PN formation, mitochondria are particularly susceptible to attack by LP-derived neurotoxic aldehydes [17, 68, 90, 91]. Binding of 4-HNE and acrolein to mitochondria results in extensive mitochondrial dysfunction through impairment of mitochondrial respiration and enhanced generation of ROS/RNS [29, 71-73, 97-99]. Following TBI, binding of LP-derived neurotoxic aldehydes to mitochondrial proteins further exacerbates TBI-induced impairment of mitochondrial bioenergetics and the initial ROS/RNS-LP-aldehyde cascade (**Fig 1.8**), which combined with high levels of intra-mitochondrial calcium concentrations can lead to opening of the mitochondrial permeability transition pore (mPTP) [29, 51, 53, 60, 72, 93, 100-102].

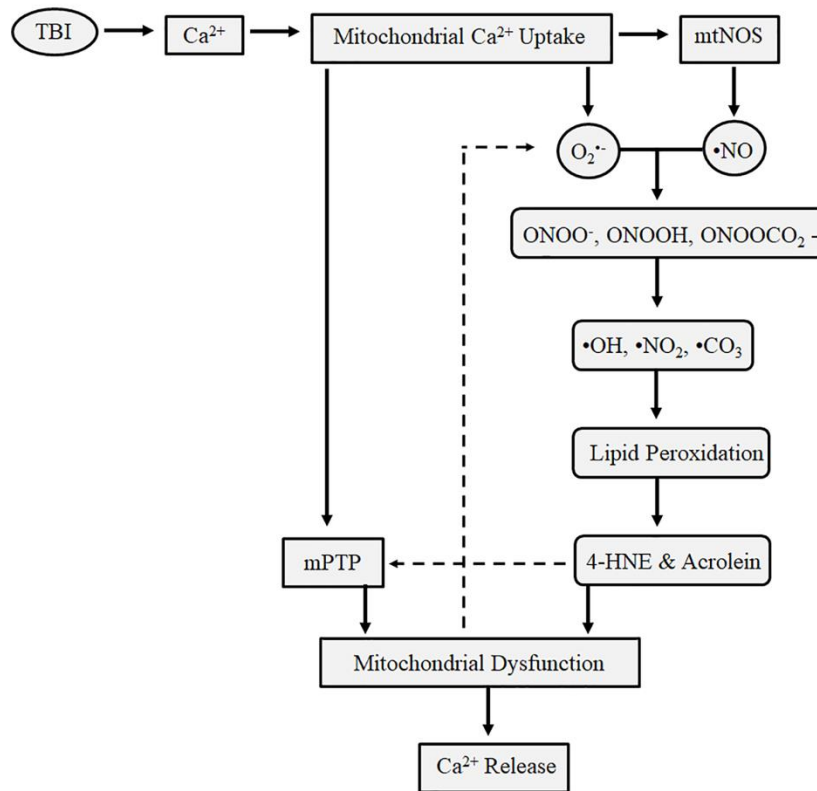


**Figure 1.8 Downstream effects of mitochondrial dysfunction.** Mitochondria generated ROS/RNS initiate LP and the formation of the LP-derived neurotoxic aldehydes 4-HNE and acrolein. 4-HNE and acrolein exacerbate mitochondrial dysfunction and opening of the mPTP. Additionally, 4-HNE and acrolein-induced mitochondrial dysfunction increases generation of ROS/RNS, creating a ROS/RNS-LP-neurotoxic aldehyde-mitochondrial dysfunction-ROS/RNS feedback loop. ROS/RNS = reactive oxygen species/reactive nitrogen species, LP = lipid peroxidation, 4-HNE = 4-hydroxynonenal, mPTP = mitochondrial permeability transition pore.

### **Mitochondrial Permeability Transition Pore**

The mPTP is a non-selective mega channel. Upon formation it forms a pore between the inner and outer mitochondrial membranes that is permeable to solutes <1.5kDa [51]. Although the structure of the mPTP is not entirely elucidated it has been proposed to contain the inner mitochondrial membrane protein adenine nucleotide translocase (ANT) and the outer mitochondrial membrane protein VDAC [51]. Additionally, more recent studies suggest ATP Synthase is involved in pore formation [25]. Although the matrix protein cyclophilin D (CypD) is not a structural component of the mPTP, it can induce mPTP formation through interactions or ANT (or possibly with ATP Synthase [25]) which results in conformational changes [103]. However, CypD is not considered essential for mPTP formation as CypD knock-out mice can still undergo permeability transitions when subjected to high concentrations of substrates capable of inducing mPTP [103]. Additionally, some forms of permeability transition are considered to be insensitive to cyclosporine A (CsA), a compound that inhibits mPTP formation by binding CypD and inhibiting its ability to translocate to ANT to induce pore formation [103] (**Fig. 1.9**). Calcium, oxidative stress, a decrease in membrane potential, and inorganic phosphate ( $P_i$ ) can induce mPTP opening, while opening of the channel can be inhibited by magnesium ( $Mg^{2+}$ ), high membrane potential, ADP, or through pharmacological means (e.g. CsA) [51].

## ***The Mitochondrial Permeability Transition Pore (mPTP) and its Inhibition with Cyclosporine A (CsA)***

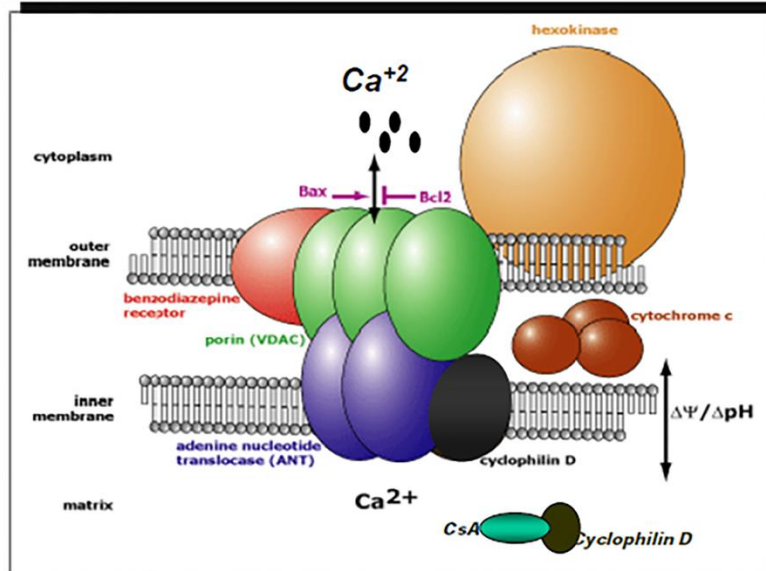


**Figure 1.9 Schematic of the mitochondrial permeability transition pore (mPTP).** CsA binds to the matrix protein cyclophilin D, which prevents cyclophilin D from translocating to the inner mitochondrial membrane and binding the mPTP protein ANT, thus preventing induction of the conformation change required for mPTP opening. Figure originally adapted from [www.mitosciences.com](http://www.mitosciences.com).

Under pathologic conditions, opening of the mPTP leads to extrusion of calcium back into the cytosol, collapse of the membrane potential, cessation of ATP generation, mitochondrial swelling, rupture of the outer mitochondrial membrane, and release of cytochrome c and other apoptotic proteins [51, 104]. However, under physiologic conditions mPTP functions to produce ROS signaling molecules, as well as to regulate calcium concentrations in the microenvironment through transient openings and closings [105].

### **Downstream Consequences of Mitochondrial Dysfunction**

#### **ATP Depletion**

Following TBI, neurons are in a state of high energy demand. Upon massive depolarization and ionic influx, cellular membrane pumps, such as  $\text{Na}^+/\text{K}^+$  ATPase and  $\text{Ca}^{2+}$  ATPase must utilize ATP in an attempt to restore ionic balance [16]. Neurons primarily utilize glucose as an energy source and the initial demand for ATP following TBI is met by acute increases in glucose uptake. However, this acute increase is followed by a severity-dependent decrease. There are several possibilities for this decrease in glucose uptake including decreased cerebral blood flow, impairment of glucose transporters, and impairment of glucose metabolic processes upstream of the citric acid cycle (TCA), decreasing the overall pool of pyruvate available to the mitochondria for ATP generation [27]. Additionally, as calcium influx decreases the mitochondrial membrane potential, ATP synthase begins to slow and has the potential to run in reverse [25]. With limited substrate available to begin with, calcium-overloaded, aldehyde-modified, low membrane potential, dysfunctional mitochondria are unable to produce the amount of ATP required to meet the high energy demands of the injured brain.



## **Calpain Activation & Necrosis**

Calpain is a calcium-activated protease capable of breaking down a variety of cytoskeletal proteins including  $\alpha$ -spectrin [106], a scaffolding protein associated with the inner surface of the plasma membrane [107]. As stated previously, following TBI the induction of the secondary injury cascade relies heavily on increased intracellular calcium levels. Although calpain can be activated by early increases in intracellular calcium, calcium homeostatic mechanisms, including sequestration of calcium by the mitochondria prevent much of the initial activation. However, once the mPTP opens intra-mitochondrial calcium is extruded back into the cytosol where it can again activate calpain [51]. Calpain cleavage of the 250kD  $\alpha$ -spectrin protein results in 145kD (calpain-only) and 150kD (calpain/caspase 3) spectrin breakdown products (SBDP) [106]. Formation of SBDP proceeds neurodegeneration, and SBDP have been used extensively to assess post-TBI axonal damage and the efficacy of neuroprotective agents [56, 70, 108-112]. In fact, prevention of mPT, inhibition of the ROS/RNS-LP-aldehyde cascade, and induction of endogenous antioxidant pathways have all been shown to attenuate  $\alpha$ -spectrin degradation [70, 109, 110, 113]. In TBI, calpain activation is thought to be predominately associated with necrosis [70, 106]. In fact, in the rat model of severe controlled cortical impact traumatic brain injury (CCI) utilized throughout this dissertation, the 120kD SBDP (caspase/apoptosis-dependent) has been shown to not increase with injury [73].

## **Caspase Activation & Apoptosis**

Following opening of the mPTP or increases in mitochondria outer membrane permeability, mitochondria can release pro-apoptotic proteins such as cytochrome c, apoptosis inducing factor (AIF) and Smac/Diablo, leading to a cascade of caspase

activation, including activation of the executioner caspase, caspase-3 [51, 106]. In addition to DNA-fragmentation, caspase-3 can cleave  $\alpha$ -spectrin, resulting in 150kD (calpain/caspase-3) and 120kD fragments [106]. As stated previously, cell death in TBI is thought to be predominately necrotic. However, TBI-associated apoptosis has been documented, particularly in pathologies involving ischemic injury [106, 114], and caspase-3-dependent SBDP have been found to occur in the CSF of rats following moderate CCI, albeit inconsistently and to a lesser degree than calpain-dependent products [115].

### **Neurodegeneration**

In addition to  $\alpha$ -spectrin, calcium-activated calpain can cleave a variety of other cytoskeletal proteins including MAP2 (microtubule-associated protein 2) and tau [51, 104, 106, 116]. One of the consequences of cytoskeletal degradation following TBI is impairment of axonal conductance and axonal transport [117]. Impairment of axonal transport can result in the accumulation of proteins, such as amyloid precursor protein (APP) in axonal varicosities and bulbs of damaged neurons [51, 104, 106, 116]. Additionally, cytoskeletal degradation and impairment of axonal transport interfere with the transport of organelles, such as the transport of healthy mitochondrion from the cell body to the synapse [118], where loss of synaptic mitochondria can result in synaptic degeneration [37, 48, 49] and impairment of synaptic plasticity [119]. The degradation of the cytoskeleton can further impair mitochondria by interfering with normal mitochondrial quality control measures such as fission and fusion, processes essential to maintaining mitochondrial health and function, particularly under times of stress such as occurs following TBI [120].

Sensitive methods for assessing neurodegeneration, such as de Olmos aminocupric silver staining, which specifically stains degenerating neurons and neuronal processes have revealed that following experimental TBI neurodegeneration often occurs to a much greater than that of overt neuronal loss or cavitation, even in primarily focal injury models such unilateral CCI [121]. In fact, following unilateral CCI, neurodegeneration has been demonstrated to occur throughout the ipsilateral cortex, hippocampus and thalamus, as well as to extend into the contralateral hemisphere [121].

Previous studies have demonstrated that both mitochondrial dysfunction and LP contribute to the neurodegenerative process, as pharmacologic interventions aimed at attenuating mitochondrial dysfunction and inhibiting the ROS/RNS-LP-aldehyde cascade have been shown to decrease neurodegeneration following injury. For example, compounds which target these processes such as CsA and NIM811 [110, 122-124], PZ [71, 72], tempol [109], mitochondrial uncouplers [125], and N-acetylcysteine (NAC) [126] are all able to attenuate neurodegeneration or neuronal cell death following TBI.

### **Time Course of Oxidative Stress, Mitochondrial Dysfunction, and Neurodegeneration Following TBI**

Formation of  $\text{OH}\cdot$  occurs as early as five minutes following experimental TBI [161, 162]. Within 30min, there is a significant decrease in cortical and hippocampal mitochondrial respiration, an effect which dissipates 1h post-injury [163]. However, because the ability of mitochondria to buffer calcium 30min post-injury remains intact, it is speculated that this initial burst of oxidative stress [161, 162] induces mitochondrial respiratory dysfunction without inducing permeability transition, allowing mitochondria the ability to functionally recover from early incidences of oxidative stress [163]. However, by 3h post-injury, decreases in mitochondrial respiration reappear and

coincide with a decrease in calcium buffering capacity [163]. Although there is some evidence to suggest a slight recovery between 3h and 24h, this possibility can be explained by the most damaged mitochondria being processed out prior to the 24h time point [73, 163]. Beyond 24h, mitochondrial respiratory dysfunction continues to deteriorate, reaching peak impairment 72h following severe CCI [73]. By five days post-CCI, mitochondrial respiration has begun to recover, likely due to further removal of impaired mitochondria as damaged tissue continues to degenerate [73]. However, it must be noted that decreases in mitochondria respiratory function and membrane potential have been documented as far out as two weeks following experimental TBI [22, 134].

Increases in cortical or hippocampal 3-nitrotyrosine (3-NT, marker of PN damage), 4-HNE, and SBDP have been identified as early as 30-60 min following TBI in mice [56, 57]. However, this time course seems to be slightly delayed in the rat [73, 121], with small increases in cortical or hippocampal 3-NT, 4-HNE, acrolein and SBDP beginning as early as 8h and peaking between 48h and 72h in severe CCI before returning to baseline levels 5d to 7d following injury [73]. Regardless of species, these processes do precede cortical and hippocampal neurodegeneration, as well as increases in cortical lesion volume [121, 164] because although levels of mitochondrial dysfunction, LP, and spectrin degradation have returned to baseline by 5-7days following severe CCI [73], neurodegeneration and cortical lesion volumes continue to progress [56, 121, 164]. In fact, although cortical contusions can be seen early following experimental TBI, volumes continue to increase until at least 28 days post-injury [164].

Up until this point the process of mitochondrial dysfunction, LP, LP-derived aldehyde formation, and spectrin degradation have been presented to occur in a linear fashion for simplicities sake. However, time course studies are an important reminder

that many of these processes can occur simultaneously. Although significant impairments to mitochondrial respiration do appear to occur prior to these other processes, the observation that peak dysfunction for many of these processes occurs between 48h and 72h following severe CCI [73], reinforces the idea that these processes often work synergistically to exacerbate each other's dysfunction.

### **Time Course of Antioxidant Depletion Following TBI**

Following TBI, increases in ROS/RN, LP, and neurotoxic aldehydes result in the depletion of endogenous antioxidants. However, the temporal decrease in antioxidant activities is variable across experimental TBI studies [165, 166]. Following unilateral CCI decreases in a wide range of antioxidants (e.g. GSH, SOD, catalase, GPx, etc.) have been reported to occur in both hemispheres and the hippocampus beginning as early as 3-6h following injury, with some enzymes remaining significantly decreased out to 4 days post-TBI [165, 166].

Although the body has mechanisms for upregulating endogenous antioxidant systems during times of oxidative stress, including through binding of the transcription factor, nuclear factor (erythroid-derived 2) (Nrf2), to the antioxidant responsive element (ARE), mRNA expression for several of the Nrf-2-ARE regulated antioxidants, such as heme oxygenase-1 (HO-1), NAD(P)H quinone oxidoreductase 1 (NqO1), and glutathione S-transferase (GST), do not begin to increase until 24h to 72h following injury [111], much later than 3-6h post-injury timeframe in which antioxidants begin to deplete following TBI [165, 166].

### **Behavioral Impairment**

In human patients, TBI often results in long-term neurobehavioral dysfunction, including cognitive deficits (e.g. attention, memory), aggression, and psychiatric, mood,

and anxiety disorders [127], sequelae that can be recapitulated in animal models, although most behavioral outcome assessments in experimental TBI have focused on motor and sensory dysfunction and impairments to learning and memory.

It is unsurprising that TBI would have neurobehavioral consequences given the widespread neurodegeneration and neuronal dysfunction that is seen in both animal models of injury [56, 57, 121, 128] and in human TBI patients [129-131]. Although the behavioral impairments that occur following TBI will vary depending on the specific neurons, pathways and networks affected by injury, mitochondria dysfunction contributes to development of TBI-induced behavioral deficits, and pharmacologic protection of mitochondria and inhibition of downstream consequences of mitochondrial dysfunction such as LP and spectrin cytoskeletal degradation are able to attenuate behavioral deficits following experimental TBI [109, 110, 123, 125, 126, 132, 133]. Although mitochondrial dysfunction has been shown to precede behavioral impairment [134], behavioral deficits can be seen as early as one day following injury, particularly in regards to motor dysfunction [109, 135-137]. Similarly, although the majority of experimental TBI studies begin assessments of cognitive function at least one week following injury [135, 138-140], early cognitive deficits have also been reported [141-144].

The experimental model of TBI utilized here, a unilateral CCI onto the motor and sensory parietal cortex, although not assessed as part of this dissertation work, expectedly can produce motor and sensory deficits [109, 110, 145]. However, this type of CCI also can induce cognitive impairment. For example, severe unilateral CCI produces widespread degeneration throughout the hippocampus [121, 128], a brain region involved in forming new memories and in spatial memory [146, 147], and throughout the thalamus [121, 128], a subcortical structure through which a variety of

important neuronal tracts pass [148, 149]. Additionally, although the prefrontal cortex is responsible for the majority of executive functions, neuronal projections involved in executive function extend throughout the cortex beyond the pre-frontal region [150, 151]. Therefore, injuries sustained in anatomic regions distinct from the pre-frontal cortex, such as a CCI onto the sensory-motor cortex, additionally put these projections at risk due to Wallerian/anterograde and retrograde degeneration [121]. In fact, unilateral CCI to the sensory-motor cortex has been shown to result in executive function (e.g. motivation, planning, problem-solving, working memory) related behavioral deficits [152].

Although there are several behavioral tests available to assess cognitive function following experimental TBI, the work in this dissertation utilized the Morris water maze (MWM), a task which evaluates spatial, working and reference memory. Briefly, in MWM animals are placed into a circular, featureless pool, filled with opaque water, and surrounded by visual cues. During the acquisition phase, which assesses working memory, animals are allowed 60s to find a submerged platform after which they are allowed to remain on the platform for approximately 20s. Animals which do not find the platform are manually guided and placed onto the platform. Animals are given several trials per day over the course of multiple days, and as the animals learn the location of the platform, the time and distance it take to find the platform should decrease [146, 147]. Following the acquisition phase a probe trial is utilized to test [reference memory](#) [147]. In the probe trial, the platform is removed and animals are given 30s to search for the previously learned platform location [147].

Overt damage to several distinct brain regions have been shown to impair MWM performance, including damage to the hippocampus, cortex, thalamus, raphe nuclei, and striatum [146]. However, overt damage to specific anatomical regions is not required to induce MWM impairment per se, as dysfunction in the neural communication networks

between regions also result in impairments to spatial learning and memory [146]. For example, although the hippocampus is necessary for consolidation, storage, acquisition and retrieval of spatial memory, spatial navigation is complex and requires coordination of several brain regions, including the cortex, as cortical input is required for the planning and execution of the task [146].

In addition to distinct anatomic regions, specific neurotransmitters, such as norepinephrine (NE), serotonin (5-HT), and dopamine (DA) have an important role in cognitive and motor function [150, 151, 153-155]. Although not addressed as part of this study, the neurotransmitter acetylcholine also plays an important role in cognition [385]. In fact, acetylcholinesterase inhibitors, such as donepezil, are often used clinically to treat memory disorders, as are NMDA antagonists, such as memantine [385]. In regards to the monoaminergic system, stimulants, which modulate the DA system, also are clinically used to improve cognition and attention [385]. However, the role each monoamine has in spatial learning in memory remains controversial. For example, drugs which can modulate these systems (e.g. monoamine oxidase inhibitors (MAOI), selective serotonin reuptake inhibitors (SSRI), amphetamines, DA agonists, 5-HT agonists) have variously been reported to improve, decrease, or have no effect on spatial learning and memory performance [146, 156-159].

There are several caveats to utilizing MWM in the assessment of spatial learning and memory. For example, although the intent of MWM is to evaluate spatial learning and working memory by requiring animals to utilize distal cues to locate the platform, animals can utilize other strategies such as a learned set of movement sequences or use of proximal cues [146]. However, varying the start position of trials each day and using featureless pools with opaque surfaces, as was done in the current dissertation work, should help to control for these factors. Furthermore, MWM performance is often



considered independent of locomotor deficits [147] and probe trial performances have been reported to be insensitive to swim speed deficits [147]. However, that assumption is not entirely true as sensorimotor deficits can indeed interfere with MWM performance [147]. For example, animals with sensorimotor deficits often continually follow the pool perimeter without initiating a search pattern, jump off or swim over the platform [147], thus reducing the ability of the animal to associate the platform with a means of escape, which make it more difficult to accurately assess memory impairments [147]. Additionally, visual acuity is required for use of the distal MWM cues, which can be concerning considering that visual pathways run through the thalamus [148] and have been demonstrably damaged following experimental TBI, although this is more commonly seen in closed head injury models [160]. Visual acuity can be assessed through use of visual platform cues, such as a platform flag. However, such visual acuity assessments were not conducted as part of this dissertation work [386].

## **An Introduction to Biogenic Amines**

### **Biogenic Amines**

Biogenic amines consist of polyamines (e.g. putrescine), trace amines, such as phenethylamine (PEA), which exists endogenously as a metabolite of the amino acid phenylalanine and as a metabolite of the drug PZ, and the monoamine neurotransmitters [151, 169]. The monoamine neurotransmitters include the catecholamines DA, NE, and epinephrine (EPI), as well as the non-catecholamines histamine and 5-HT [151, 169]. DA, NE, and EPI are synthesized sequentially from the amino acid tyrosine, while histamine is derived from the amino acid histidine and 5-HT is derived from the essential amino acid tryptophan [151](**Fig. 1.10**).

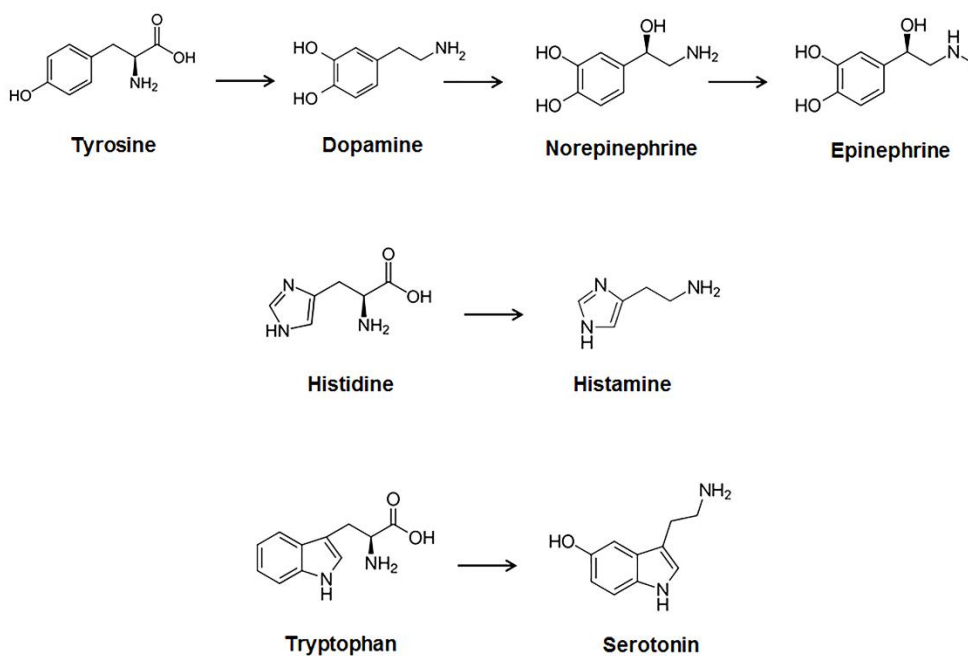


**Figure 1.10 Synthesis of the monoamines.** Dopamine, norepinephrine, and epinephrine are sequentially synthesized from the amino acid tyrosine. Histamine is synthesized from the amino acid histidine, and serotonin (i.e. 5-HT) is synthesized from the amino acid tryptophan.

## **Biogenic Amine Anatomic Pathways and Physiologic Functions**

### *Dopamine*

Within the nervous system DA is involved in a wide range of processes including movement, motivation, reward, addiction, memory, stress and mood [154]. Although the majority of DA is found within the striatum, DA is found throughout the brain [154]. For example, within the mesocorticolimbic system, DA neurons from the ventral tegmental area project directly to the hippocampus and prefrontal cortex [153, 170]. Further, although the nigrostriatal pathway, predominately involved in movement regulation, consists of dopaminergic neurons projecting directly from the substantia nigra to the striatum, it is part of complex circuitry that includes input and output to the motor cortex, along tracts that pass through the thalamus [153]. As a catecholamine, in addition to binding DA receptors, DA can bind adrenergic receptors [154]. Clinically, DA can be used as a vasopressor to elevate cerebral perfusion pressure and mean arterial blood pressure following severe TBI [154].

### *Norepinephrine*

Within the brain NE neurons are concentrated in the locus coeruleus with widespread connections to areas including the cortex, limbic system, and thalamus, and it is involved in modulation of arousal, attention, mood, cognition and memory [150, 151]. As a catecholamine, NE, also known as the “flight or fight” neurotransmitter can bind adrenergic receptors and induce sympathetic responses such as vasoconstriction [154, 171]. As such, similar to DA, NE can be used as vasopressor in clinical TBI [154].

## Serotonin

Within the CNS, 5-HT neurons arise from the raphe nuclei and project extensively throughout most of the brain including the cortex, limbic system, and thalamus [151], modulating arousal, mood, cognition and memory [155]. Interestingly, the majority of 5-HT is found outside the CNS, within the gastrointestinal tract [155]. Additionally, 5-HT plays a role in platelet activation, vasodilation, and vasoconstriction [172].

## **TBI and Acute Monoamine Dysregulation**

Neurobehavioral sequelae following TBI are common and include dysregulation of cognition (e.g. attention, memory), mood (e.g. depression, anxiety), and emotion (e.g. aggression) [127]. Given the role the monoamines DA, NE, and 5-HT have in modulating these domains, sustained neurobehavioral impairments following TBI points to chronic dysregulation of monoamine neurotransmitter systems. However, as the goal of this dissertation is to evaluate acute neuroprotective pharmacologic strategies, the following brief discussion only includes acute changes in the monoamine systems following TBI.

In general, less is understood about acute effects to monoamine systems following TBI, with the majority of work being focused on DA systems [154, 170]. Although DA is known to be acutely altered following experimental TBI [154, 170], some studies indicate increased DA levels, whereas others report decreased DA levels depending on brain region and time point [173, 174]. Additionally, other aspects of the dopaminergic system such as DA synthesis, metabolism, and DA transporter protein expression, have also been reported to be altered following TBI [175-177].

Similarly, NE levels and turnover rates have been demonstrated to be acutely altered following experimental TBI, with variations again been seen across distinct brain

regions [174, 178, 179]. Further, high NE levels have been shown to be associated with worse outcomes and/or mortality rates in TBI patients [180, 181]. However, because catecholamine levels increase with activation of the sympathetic nervous system, as would occur following trauma, it is difficult to determine whether high catecholamine levels following TBI are an actual cause or rather an effect of injury severity [181].

Less data are available regarding acute levels of 5-HT following TBI. However, increases in extracellular 5-HT levels have been demonstrated to occur [182]. Similarly, at subacute time points 5-HT expression has been shown to be increased [183]. On the other hand, at subacute time points 5-HT transport protein expression has been reported to decrease [184] and degeneration of 5-HT neurons has been seen following multiple types of experimental TBI [185], unsurprising given the widespread projections of 5-HT pathways throughout the brain.

### **Monoamine Metabolism**

Monoamines are removed from the synaptic cleft by reuptake into pre-synaptic nerve terminals and glial cells [151]. DA has two major metabolites, 3,4 dihydroxyphenylacetic acid (DOPAC) and homovanillic acid (HVA), both of which are measured in this dissertation. The metabolism of DA involves three enzymes, monoamine oxidase (MAO), catechol-O-methyl transferase (COMT), and aldehyde dehydrogenase (ALDH), and the additional intermediate metabolite 3-methoxytyramine (3-MT) [186] (**Fig. 1.11**).

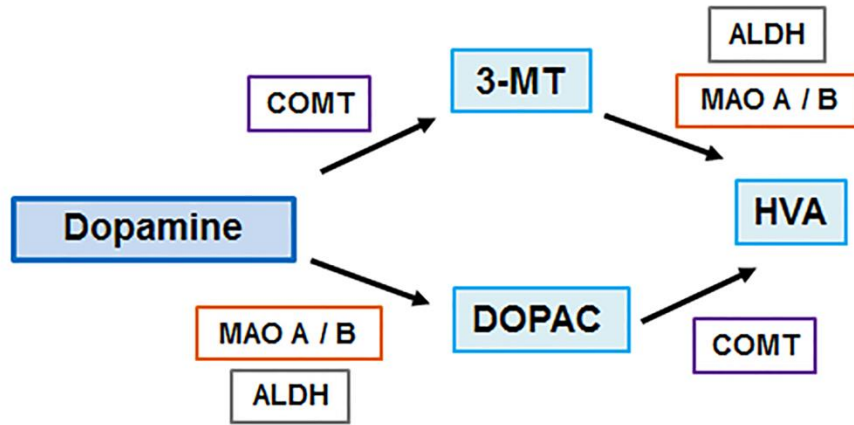


**Figure 1.11 Simplified monoamine metabolism pathways.** Dopamine is metabolized by monoamine oxidase (MAO-A/B), catechol-O-methyl transferase (COMT), and aldehyde dehydrogenase (ALDH) to form the metabolites 3,4 dihydroxyphenylacetic acid (DOPAC) and homovanillic acid (HVA), and the intermediate metabolite 3-methoxytyramine (3-MT). Norepinephrine (NE) is metabolized by MAO-A and COMT. Serotonin (5-HT) is metabolized by MOA-A and ALDH to form 5-hydroxyindolacetic acid (5-HIAA).

MAO is located in the outer mitochondria membrane. MAO requires the presence of the cofactor  $FAD^+/FADH_2$  and oxygen to function [186]. ALDH is also a mitochondrial protein, located within the matrix and requires the cofactors  $NAD^+/NADH$ . COMT is a cytosolic enzyme [186]. DA is metabolized by MAO-A/B and ALDH to form DOPAC which can be further metabolized to HVA by COMT. Additionally, DA can first be metabolized by COMT to form 3-MT before being further metabolized to HVA by MAO-A/B and ALDH [186]. The metabolism of NE also involves MAO-A and COMT, as well as a variety of other enzymes, and results in the formation of metabolites such vanillylmandelic acid (VMA) and 3-methoxy-4-hydroxyphenylglycol (MHPG) [186]. However, NE metabolites were not measured as part of this study due to their low cortical tissue levels. 5-HT is metabolized to 5-hydroxyindoleacetic acid (5-HIAA) by MOA-A and ALDH [186], and is measured as part of this dissertation.

As part of this dissertation work the cortical tissue levels of NE, DA, 5-HT and the metabolites DOPAC, HVA, 5-HIAA were measured using HPLC [187]. The turnover of DA to DOPAC/HVA and the turnover of 5-HT to 5-HIAA were used a surrogate measure of MAO inhibition [188].

### **Monoamine Oxidase: An Outer Mitochondrial Membrane Protein**

The MAO enzyme exists as two subtypes, MAO-A and MAO-B, both of which are located in the outer mitochondrial membrane. MAO contains a flavin group allowing it to participate in oxidative deamination reactions [186]. MAO is responsible for the metabolism of the monoamine neurotransmitters NE, 5-HT, and DA, measured within this dissertation, but additionally participates in the metabolism of EPI, several amino acids, and PEA, a trace amine under physiologic conditions, but which is also an active metabolite of PZ [186, 189]. MAO-A and MAO-B have differing substrate affinities. For

example, MAO-A is selective for NE, 5-HT, and EPI, whereas MAO-B is selective for PEA [186]. DA, on the other hand, is metabolized by both MAO-A and MAO-B [186]. However, the metabolism of DA by MAO differs between rodents and humans, with DA being predominately metabolized by MAO-A in rats and MAO-B in humans [186]. In the brain, monoamines are removed from the synaptic cleft by reuptake into pre-synaptic nerve terminals and glial cells [151]. In fact, the majority of MAO in the brain is located within the glia [190], with the MAO-B isoform predominating in glia as well as in serotonergic neurons and platelets [190].

### **Monoamine Oxidase Inhibitors**

Clinically, MAOIs have been used as anti-depressants, as MAO inhibition leads to increases in neurotransmitters that are dysregulated in mood and other psychiatric disorders. However, MAOIs, particularly irreversible inhibitors, have numerous side effects, including several food interactions that can lead to a dangerous tyramine toxicity syndrome and hypertensive crisis. With the development of newer class anti-depressants, MAOIs are no longer considered a first-line therapy for depression [191].

Multiple classes of MAOIs exist, including irreversible MAO-A selective inhibitors, irreversible MOA-B selective inhibitors (e.g. selegiline, rasagiline), irreversible non-selective inhibitors (e.g. PZ, isocarboxazide, tranylcypromine, pargyline), and several reversible inhibitors, including methamphetamine (MAO-A selective) [191]. PZ, isocarboxazide, and tranylcypromine have all been used clinically in the treatment of anxiety and depression, while selegiline and rasagiline are currently used clinically to treat the symptoms associated with Parkinson's disease [191].

Given their use for the symptomatic treatment of neurodegenerative disease, there has been increasing interest in studying the neuroprotective properties of MAOs



[192]. However, in theory MAOIs could have both neuroprotective and neurotoxic effects. For example, oxidative deamination of monoamine neurotransmitters by MAO, generates ROS [193], suggesting that MAO inhibition could reduce ROS and provide a therapeutic benefit. However, inhibition of MAO also leads to increases in biogenic amines, such as DA, which is capable of directly inhibiting mitochondrial respiration [194], and undergoing non-enzymatic autoxidative formation of toxic H<sub>2</sub>O<sub>2</sub> and quinones [194], suggesting that MAO inhibition could also lead to increases in neurotoxicity and oxidative stress.

Although the plasma half-lives of the MAOIs vary, irreversible MAOIs have longer lasting effects than their plasma half-lives suggest due to the rate of MAO turnover. In fact, the half-life of MAO in the rat brain is 10-13 days [195], increasing to 30 days in humans [196]. However, it must be noted that because effects on neurotransmitter levels and behavior can require 65-80% MAO inhibition, the effective recovery time for MAO in the rat brain may be as low as 4 days [186]. However, multiple doses of an MAOI may prolong MAO inhibitory effects, as might TBI given the fact that regeneration of MAO within presynaptic nerve terminals requires trafficking of MAO and mitochondrion to the synapse [191].

### MAOI Properties of Phenzelzine

Although PZ is classified as a non-selective MAOI, it is slightly more preferential to MAO-A [197]. The structure of PZ contains a hydrazine moiety (-NH-NH<sub>2</sub>), which confers it the ability to scavenge LP-derived neurotoxic aldehydes [72, 198] (**Fig. 1.12**). However, this moiety is also purported to contribute to its ability to act as an irreversible MAO inhibitor [199]. As a MAOI, PZ has both anti-depressant and anxiolytic properties [169]. However, similar to other MAOIs, PZ is not clinically utilized as a first line therapy to treat psychiatric disorders, although it is a choice for the treatment of atypical or intractable depression [191].

In humans, following oral administration the plasma half-life of PZ is approximately 11.5 hours [74], although following intraperitoneal administration in rats, the half-life could be as short as 30min [74]. However, in regards to PZ's MAOI properties, the plasma half-life is of minimal importance, as the effects of irreversible MAO inhibitors are prolonged and based on MAO turnover rates. In rats, the ED<sub>50</sub> for oral administration of PZ has been reported to be 6 mg/kg for MAO-A and 12 mg/kg for MAO-B, resulting in a 2:1 selectivity ratio of MAO-A to MAO-B [197].

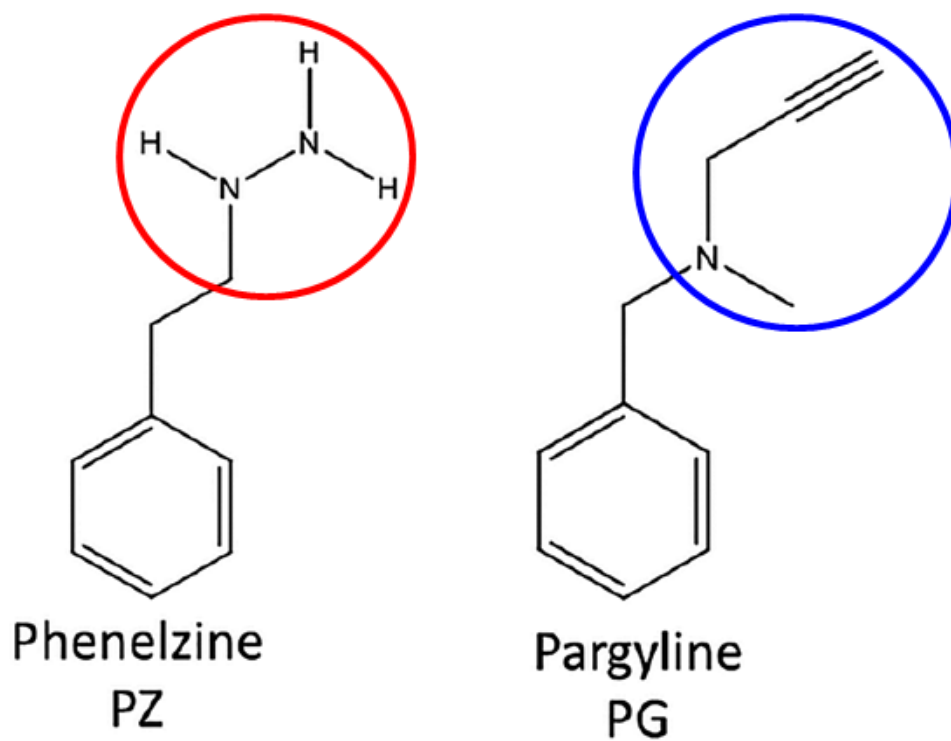


**Figure 1.12 Chemical structures of phenzelzine and pargyline.** Phenzelzine contains an aldehyde-scavenging hydrazine moiety (-NH-NH<sub>2</sub>, circled in red), while pargyline does not. However, PG contains an *N*-propargyl moiety (circled in blue)

### MAOI Properties of Pargyline

Pargyline (PG) is similarly structured to PZ, but does not contain the hydrazine moiety (-NH-NH<sub>2</sub>) which gives PZ its aldehyde-scavenging capabilities (**Fig. 1.12**). Instead, PG contains an *N*-propargyl moiety, which confers its MAOI effects [200]. Interestingly, the *N*-propargyl moiety, itself, has also been suggested to be neuroprotective [201]. PG has been both referred to as a non-selective irreversible MAOI [191], as well as a MAO-B specific irreversible inhibitor [197], likely based on IC<sub>50</sub> values of 0.011522 μmol/L for MAO-A and 0.00820 μmol/L for MAO-B [202]. However, in rats, the ED<sub>50</sub> for oral administration of PG has been reported to be 9.3 mg/kg for MAO-A and 1.4 mg/kg for MAO-B, resulting in a 6.6:1 selectivity ratio of MAO-B to MAO-A [197].

Although PG is classified as a MAOI, clinically it was used more frequently as an anti-hypertensive than as an anti-depressant [203]. This is somewhat paradoxical as the interaction between MAOIs and tyramine-containing foods can induce a hypertensive crisis [191]. However, its anti-hypertensive properties are thought to be due to increased NE levels acting on inhibitory α<sub>2</sub>-adrenergic receptors, such as those found in the brainstem and periphery [204]. Therefore, it is possible that several other irreversible MAOIs may also have anti-hypertensive effects.

### Comparison of Phenelzine and Pargyline MAO Inhibitory Effects on Drug-Induced Behavioral Changes

The MAOI drug class was developed decades ago. Therefore, recent comparisons between PZ and PG are sparse. However, both drugs have been utilized within single studies to assess the effects of MAOIs on drug (e.g. nicotine, cocaine, ethanol) administration. Whereas it has been shown that PZ, but not PG is able to enhance the discriminatory effects of nicotine [205] and nicotine-induced locomotor

activity [206], both PZ and PG are able to decrease cocaine [207] and ethanol self-administration, with PZ requiring lower doses and producing prolonged effects compared to PG [208].

## **TBI and Neuroprotective Drug Development**

### **Failure of Clinical TBI Drug Trials**

Guidelines for acute management of severe TBI do exist. However, these guidelines contain supportive measures such as monitoring and management of intracranial pressure, cerebral perfusion pressure, and systolic blood pressure [209]. Although there are interventions available, for example, utilization of decompressive craniotomy, CSF drainage, and hyperosmolar therapy for the control of intracranial pressure [209], as stated previously, to date there are no FDA-approved pharmacological agents capable of attenuating the devastating neurologic consequences that can occur following TBI [1]. However, this is not for lack of effort.

Recently, large scale clinical trials for progesterone failed to improve outcome following TBI [210]. Similarly, glutamate antagonists, steroids, antioxidants, anti-epileptics, and erythropoietin clinical TBI trials have all failed [211, 212]. Numerous reasons have been cited for the failure of neuroprotective compounds in clinical TBI studies, such as heterogeneity of injury, lack of consideration for pre-injury and post-injury factors, reliance on clinical assessments of injury insensitive to injury pathology such as GCS score, lack of sensitivity in outcome measures or use of inappropriate outcome measures, lack of appropriate subgroup analyses, inadequate pre-clinical experimental design, and lack of understanding of secondary injury mechanisms [9, 211, 213, 214]. However, within the context of pre-clinical experimental design and the complexity of the secondary injury cascade, it is conceivable that investigation into

innovative pre-clinical neuroprotective pharmacological strategies, such as combinational therapies or single drugs with multiple neuroprotective mechanisms of action, may improve the success of future clinical trials.

### **Review of Selected Neuroprotective Strategies**

A multitude of neuroprotective strategies have been investigated in experimental TBI models, including but not limited to NMDA antagonists, calpain inhibitors, hormonal therapy, attenuation of neuroinflammation, stem cell administration, induction of neurogenesis, hypothermia, environmental enrichment, and post-injury rehabilitation, [215, 216]. Although all have led to a greater understanding of TBI pathophysiology, the following discussion will focus on a selection of therapies directed toward attenuation of mitochondrial dysfunction and oxidative stress. Use of monoamine modulators will also be briefly discussed.

### **Targeting of Mitochondrial Dysfunction**

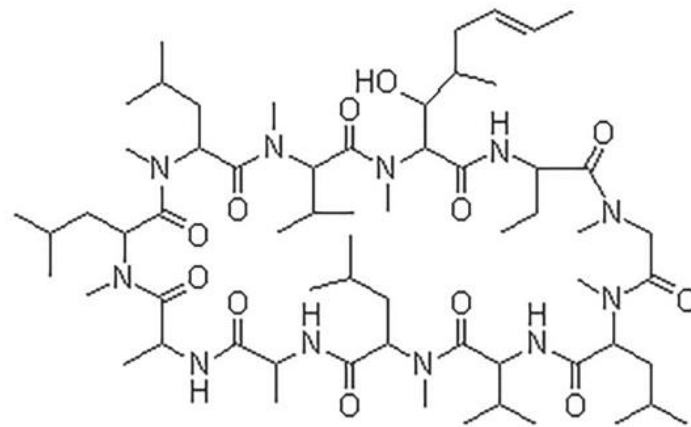
Due to the significant role mitochondria serve in secondary injury processes, they have been and continue to be therapeutic targets for neuroprotection following TBI. Several strategies have been utilized in attempts to improve mitochondrial function and prevent downstream consequences of dysfunction following TBI, including but not limited to inhibition of the mPTP, mild uncoupling, and use of alternative energy sources such as ketones.

### *Inhibition of mPTP: Cyclosporine A and NIM811*

CsA (**Fig. 1.13**) is an FDA-approved immunosuppressant, used clinically to prevent organ rejection after transplant through a mechanism that involves inhibition of calcineurin and T-cell activation [217]. However, CsA also has the ability to bind the mitochondrial matrix protein cyclophilin D (CyD) [218, 219], which inhibits its interaction with ANT, an inner mitochondrial membrane protein, thus preventing formation of the mPTP [220]. Although under normal physiologic conditions CsA is minimally blood brain barrier (BBB) penetrable [221], CsA is able to enter the CNS following TBI due to increases in BBB permeability following injury [222].

In experimental TBI, CsA and NIM811, an mPTP inhibitor but non-immunosuppressive analog of CsA, have been shown to protect against mitochondrial dysfunction, decrease production of reactive species and their termination products, decrease cytoskeletal degradation, attenuate axonal pathology and neurodegeneration, improve cortical tissue sparing, and improve motor and cognitive function [110, 122-124, 135, 136, 223-227].

Although there are studies to suggest that the immunosuppressive properties of calcineurin inhibitors (e.g. CsA, tacrolimus) have neuroprotective effects [228-233], the ability of NIM811 to recapitulate the neuroprotective effects of CsA, confirms mPTP inhibition as a means of neuroprotection.



Cyclosporine A

**Figure 1.13 Chemical structure of cyclosporine A**



To date, large scale clinical trials utilizing CsA have not been conducted, however, small phase II trials have shown CsA to be safe for use clinically in severe TBI patients [234, 235], with the possibility of improved outcomes being seen with a continuous infusion dosing paradigm. However, CsA does have some concerning properties that could make clinical dosing in the TBI patient population challenging, such as a biphasic dose-response curve, [227] and the fact that it is both a substrate and an inhibitor of ATP-dependent p-glycoprotein drug efflux pumps [236]. Additionally, depending on the concentration and length of dosing, CsA and its vehicle, cremophor, have associated toxicities, including neurotoxicities [237-245]. Furthermore, CsA is metabolized by Cyp3A4 and therefore has several adverse drug interactions [246].

#### Mild Uncoupling

Although mitochondria serve an important role in maintaining calcium homeostasis following TBI, high concentrations of intra-mitochondrial calcium can lead to increased production of ROS, collapse of mitochondrial membrane potential, and induction of mPT [125]. Therefore, it is important for mitochondria to maintain an optimal balance between the two scenarios, particularly under the stressful conditions that occur following TBI. Hence, somewhat counterintuitively, decreasing the mitochondrial membrane potential (i.e. a more positive membrane potential) should result in decreased uptake of positively charged calcium ions, resulting in decreases in ROS production and improved mitochondrial function [125]. One way to decrease mitochondria membrane potential is to mildly uncouple the ETC from ATP synthesis, allowing protons to bypass ATP synthase, and freely flow down their gradient through the inner mitochondrial membrane into the mitochondrial matrix [125]. Although mitochondria endogenously express uncoupling proteins [247], uncoupling can also be induced through pharmacologic means through use of chemical uncouplers such as 2,4-dinitrophenol

(2,4-DNP) and FCCP [125]. In fact, following TBI mild uncoupling can improve mitochondrial respiration, decrease ROS production, improve cortical tissue sparing and improve motor and cognitive function [125, 248].

### Ketones

Although the brain relies on glucose as its primary energy source [27], alternative energy substrates, such as ketone bodies do exist. Upon depletion of glucose the body can shift to catabolism of fatty acids, generating ketones in the process, such as  $\beta$ -hydroxybutyrate. During the conversion of  $\beta$ -hydroxybutyrate to acetyl-coA, the complex II substrate succinate is formed, bypassing the citric acid cycle (TCA). From there, acetyl-coA can enter the citric acid cycle (TCA), producing complex I and II substrates, while bypassing the need for glycolysis [139]. Ketones can be provided either directly through administration of  $\beta$ -hydroxybutyrate, or through ketogenic diets and fasting. In TBI, ketones have been shown to improve cortical tissue sparing, decrease cognitive impairment, decrease oxidative stress, and improve mitochondrial function [139]. In addition to being utilized as an alternative substrate, it is possible ketones also provide their neuroprotective effects through direct antioxidant mechanisms and through activation of uncoupling proteins [249, 250]. However, the utility of ketones as neuroprotectants may be limited to juveniles, as juvenile brains are better able to utilize non-glucose energy substrates and use of ketones in TBI seems to be more effective in this population [27, 249].

### **Targeting of ROS/RNS, LP, and LP-Derived Neurotoxic Aldehydes**

#### Select Antioxidant Therapies

A multitude of antioxidants have been utilized over the decades in an attempt to attenuate oxidative stress following TBI [1, 55]. In this context, “antioxidant” will refer to

compounds with the ability to scavenge ROS, RNS, lipid peroxy radicals, alkoxy radicals, or inhibit LP propagation. Presented here are selections of antioxidant agents that have been evaluated in TBI.

### Superoxide Dismutase

As SOD is an endogenous  $O_2^{\bullet-}$  scavenger, it follows that administration of SOD following injury should result in neuroprotective effects by reducing oxidative stress. Although experimental TBI models were able to show that administration of SOD decreases  $O_2^{\bullet-}$  induced microvascular dysfunction and that overexpression of SOD1 or SOD2 prevents mitochondrial dysfunction and attenuates TBI pathophysiology [1, 55, 251], clinical trials with PEG-SOD (a more stable form of SOD) failed, possibly due to the short half-life of  $O_2^{\bullet-}$  and brain penetrability issues [1, 55].

### Lazaroids

Lazaroids are compounds structurally related to steroids without having any glucocorticoid activity. Examples of lazarooids include tirilazad and the compound U-83836E. These compounds function to scavenge lipid peroxy radicals while also preventing LP propagation through phospholipid membrane stabilization. U-83836E has the added benefit of being structurally comprised of a portion of  $\alpha$ -tocopherol (i.e. vitamin E) allowing for regeneration of its antioxidant properties through redox reactions with ascorbic acid and GSH. Although both compounds showed neuroprotective effects in experimental TBI, tirilazad failed clinical trials in the United States. Although, post-hoc analysis revealed that tirilazad was able to decrease mortality in a subset of male patients with subarachnoid hemorrhage, the design of these trials has been heavily criticized, underscoring the importance of appropriate clinical trial design [1, 55].

### Spin-Trapping Agents

Spin-trapping agents refer to a group of antioxidants which contain a nitroxide group, and include agents such as tempol. Tempol is capable of scavenging PN-derived radicals such as  $\text{NO}^{\bullet}_2$  and  $\text{CO}^{\bullet}_3$ , as well as other reactive species such as  $\text{O}_2^{\bullet-}$  and  $\text{H}_2\text{O}_2$ . Tempol has shown to be neuroprotective in experimental TBI, decreasing oxidative damage, cytoskeletal and neuronal degeneration, and improving mitochondrial function. However, its limited therapeutic window of 1hr makes clinical translation unlikely [1, 55].

### Induction of Endogenous Antioxidant Pathways

#### *Nrf2*

Neurons contain endogenous antioxidant systems which are activated in times of increased oxidative stress, such as occurs in TBI. Many of these systems are regulated by binding of the transcription factor Nrf2, which is able to translocate to the nucleus under stressful conditions, to ARE, which results in the induction and expression of antioxidants such as HO-1, NqO1, and GST. Compounds such as sulforaphane (found in broccoli and other cruciferous vegetables) and carnosic acid (found in rosemary and sage) are considered Nrf2 activators and have been shown to be neuroprotective in experimental TBI, reducing LP-derived aldehyde formation, improving mitochondrial bioenergetics, decreasing cytoskeletal and neuronal degeneration, decreasing edema, and attenuating motor and cognitive deficits [55, 97, 113, 138, 252].

### *Glutathione Precursors*

In addition to induction of endogenous antioxidant transcription pathways, another approach at enhancing endogenous antioxidant activity is through utilization of glutathione precursors, such as gamma-glutamylcysteine ethyl ester (GCEE) or NAC [126, 253-255]. Following TBI, GCEE is able to attenuate increases in PN and carbonyl protein damage and decrease BBB permeability [255]. More impressively, NAC and the more membrane permeable, N-acetylcysteine amide (NACA) have been shown to reduce PN and 4-HNE protein damage, increase mitochondrial glutathione concentration, improve mitochondrial respiration, and attenuate cortical lesion volume and cognitive impairment [126, 254].

### *Carbonyl Scavenging*

Although LP, itself, is known to directly affect membrane fluidity and destabilize membrane integrity [256], the LP-derived aldehydes, including 4-HNE and acrolein are known to have directly toxic effects [29, 72, 76, 77, 85-89, 93, 101, 102, 257, 258], with a notably devastating effect on mitochondrial function.

Therefore, scavenging of LP-derived aldehydes, such as 4-HNE and acrolein, the stable final breakdown products of LP represents a practical neuroprotective approach to TBI [1, 79]. In fact, scavenging of LP-derived aldehydes is more clinically feasible than the use of conventional antioxidants, as LP-derived aldehydes are longer lived than their highly reactive free radical predecessors [79, 81, 259].

LP-derived aldehydes, such as 4-HNE and acrolein, are considered strong electrophiles [260]. Therefore, strong nucleophiles can be used as scavengers [260]. Several classes of compounds have been shown capable of scavenging LP-derived aldehydes such as thiol compounds (e.g. NAC, D-penicillamine), histidine containing

compounds (e.g. carnosine), and guanidine derivatives (e.g. metformin) [79]. However, hydrazine (-NH-NH<sub>2</sub>) compounds, which react with LP-derived aldehydes to form hydrazone derivatives, represent one of the most potent aldehyde scavenging groups available (**Fig. 1.14**) [258, 261].

Further, hydrazine (-NH-NH<sub>2</sub>) compounds are able to scavenge both free aldehydes and aldehyde-protein conjugates to prevent further cross-linking [79, 262]. There are several FDA-approved drugs in current clinical use which contain a hydrazine moiety (-NH-NH<sub>2</sub>) capable of scavenging aldehydes, including the anti-tuberculosis agent isoniazid, the anti-hypertensive hydralazine (HZ), and the MAOI PZ [198] (**Fig. 1.15**). Of these FDA-approved hydrazine containing (-NH-NH<sub>2</sub>) compounds, HZ and PZ have been the most extensively studied in experimental models of brain and spinal cord injury.

Following brain or spinal cord injury, HZ, clinically used as an anti-hypertensive, or PZ, an irreversible non-selective MAOI-class anti-depressant, are able to attenuate formation of aldehyde-protein conjugates, enhance tissue sparing and neuronal survival, attenuate mitochondrial respiratory dysfunction, and improve behavioral outcomes [71, 72, 74-76]. Although PZ contains both aldehyde-scavenging and MAOI capabilities, *in-vitro* experiments comparing PZ to the similarly structured MAOI pargyline (PG), which lacks a hydrazine moiety (-NH-NH<sub>2</sub>), confirm that the presence of the hydrazine moiety (-NH-NH<sub>2</sub>) and not steric hindrance confers PZ's aldehyde scavenging abilities [72]. However, due to the absence of MAO substrate, the cited *in-vitro* study by Cebak et al. did not allow for rigorous assessment of MAOI effects [72]. However, in further support of the hydrazine moiety (-NH-NH<sub>2</sub>) being protective, *in-vivo* studies show that PZ but not PG decrease carbonyl and atherosclerotic plaque formation in experimental models of atherosclerosis [198].

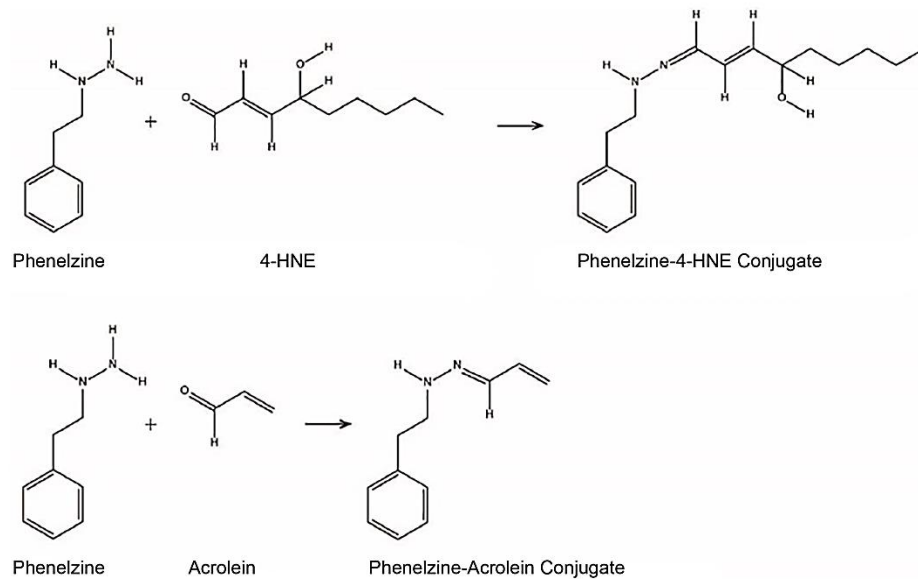
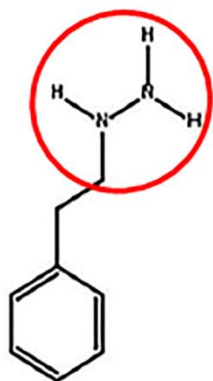
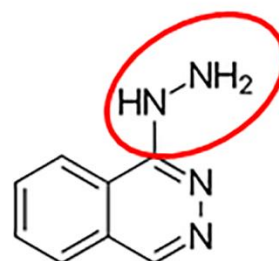


**Figure 1.14 Phenelzine scavenging of lipid peroxidation-derived aldehydes.** Phenelzine covalently binds 4-HNE (4-hydroxynonenal) and acrolein, leading to the formation of phenelzine-aldehyde conjugates.



**Phenelzine**



**Hydralazine**

**Figure 1.15 Chemical structures of phenelzine and hydralazine.** Phenelzine is a monoamine oxidase inhibitor class anti-depressant and hydralazine is an anti-hypertensive. However, both compounds contain hydrazine moieties (-NH-NH<sub>2</sub>), circled in red, which are capable of scavenging lipid peroxidation-derived aldehydes.



However, there are some concerns regarding the use of carbonyl scavengers as neuroprotective compounds. For example, hydrazine (-NH-NH<sub>2</sub>) drugs can react with physiologically important molecules and enzymes that contain carbonyl groups, such as pyridoxal phosphate, a cofactor required for several enzymes involved in the biosynthesis of neurotransmitters such as DA, 5-HT, and gamma-aminobutyric acid (GABA) [78]. Additionally, it is currently unknown how drug-aldehyde-protein conjugates are metabolized or what, if any, the long-term consequences of drug-aldehyde-protein conjugate formation are [78]. In fact, there is evidence to suggest that drug-aldehyde-protein complexes can induce an immune response [258]. For example, the use of hydralazine has been linked to development of systemic lupus erythematosus [258].

#### *Additional Properties of Phenzelzine*

As stated previously PZ is an irreversible non-selective MAOI which contains an aldehyde-scavenging hydrazine moiety (-NH-NH<sub>2</sub>), and although the plasma half-life of PZ, which is 11.5h in humans and possibly as short as 30min in rats [74], is not as clinically relevant to its MAOI properties, it likely does have an effect on its role as an aldehyde scavenger.

In general PZ has complex pharmacokinetics which must be considered in regards to developing it for clinical use in TBI patients. For example, in addition to being a MAO inhibitor, PZ is also a MAO substrate, being metabolized to PEA and phenylethyldenehydrazine (PEH). Both PEH and PEA are considered to be active metabolites [263]. For example, PEA, is similar to amphetamine and can produce stimulatory effects [207], whereas PEH inhibits several transaminases, including GABA transaminase (GABA-T), alanine transaminase (ALA-T), and ornithine transaminase (ORN-T) [169]. These transaminases serve important physiologic functions. For example, GABA-T is responsible for the conversion of the inhibitory neurotransmitter

GABA, to succinic semi-aldehyde, which can be further oxidized to succinate [169], a substrate of the Krebs cycle and complex II of the ETC. Therefore, inhibition of GABA-T could lead to increases in GABA, which can paradoxically cause excitotoxicity following neuronal injury through reversal of chloride channels [264], as well as decreases in ETC substrates during a time in which there is ongoing mitochondrial dysfunction and ATP depletion [22, 25, 51, 73]. Similarly, inhibiting ALA-T, the enzyme which catalyzes the reaction of alanine +  $\alpha$ -ketoglutarate to form glutamate + pyruvate, could also lead to decreased formation of Krebs cycle substrates. Further, ORN-T catalyzes the formation of glutamate, from the urea cycle product, ORN. However, inhibition of ORN-T could alternately lead to decarboxylation of ORN by ornithine decarboxylase (OCD), the result of which is formation of neurotoxic polyamines [169].

Of additional concern in regards to clinical translation of PZ is that anti-depressants can lower seizure threshold [265], a complication for which TBI patients are already at increased risk [209], although of all the anti-depressant drug classes, MAOIs are at the least risk to do so [265]. Therefore, use of PZ could increase the risk of post-traumatic seizure in TBI patients. Additionally, it must be noted that although PZ is not technically classified as a CYP3A4 inhibitor, there is data to suggest that PZ is capable of inhibiting CYP3A4 [266, 267], which could lead to several adverse drug interactions.

#### *Properties of Hydralazine*

Although HZ's hydrazine (-NH-NH<sub>2</sub>) moiety can act as an aldehyde scavenger, HZ is an anti-hypertensive, used clinically to treat emergent and essential hypertension, eclampsia, and congestive heart failure in African-Americans [268]. In humans, HZ has a short plasma half-life of 30-60 minutes, similar to the 60min half-life seen in rats [74, 78]. The anti-hypertensive properties of HZ are due to its ability to act as an arteriolar

vasodilator. Although the exact mechanism of action remains unknown, it has been hypothesized to be due to activation of guanylate cyclase, inhibition of sarcoplasmic reticulum calcium release, or increased conductance of calcium-dependent K<sup>+</sup> channels [258]. Interestingly, in relation to the properties of PZ, there is evidence to suggest that HZ may also be able to act as a reversible non-selective MAOI, with a slight preference to MAO-A [258, 269].

Although HZ's anti-hypertensive effects could be a barrier to using it clinically in TBI patients, in experimental SCI intraperitoneal doses of HZ ranging from 5mg/kg-25mg/kg, do not induce changes in systolic blood pressure [270]. However, HZ does undergo polymorphic acetylation within the liver, which means even an optimized dose of HZ could lead to elevated concentrations in patients with slow acetylator phenotypes [268].

### **Use of Monoamine Agonists, Antagonists, and Monoamine Oxidase Inhibitors in TBI**

Although there is a need for more established guidelines for the pharmacological treatment of TBI-induced chronic neurobehavioral sequelae, several options do exist which work by modulating monoamine neurotransmitter systems, such as antidepressants for the treatment of depression and aggression, dopamine enhancers and stimulants for the treatment of attention deficits and enhancement of learning and memory, and beta blockers for the treatment of aggression [127].

In the context of acute TBI, drugs that modulate monoaminergic systems such as DA and 5-HT agonists have shown promise as neuroprotective agents [154, 170, 271]. However, these drugs often have additional purportedly protective mechanisms of action. For example, amantadine, in addition to being a DA agonist is an NMDA

glutamate receptor antagonist. Additionally these drugs are often receptor subtype specific, such as the D2 agonist bromocriptine and the 5-HT<sub>1A</sub> agonist buspirone [154, 170, 271], and therefore would have more specific effects than an overall increase in monoamine levels, as would be induced through use of an MAOI.

Specifically in regards to MAOIs, they have been demonstrated to be neuroprotective in both models of stroke and closed head injury [272, 273]. Although some studies suggest that inhibition of MAO itself is protective [193], others have shown MAOIs can be neuroprotective at concentrations which are too low to inhibit MAO [274, 275]. Therefore, it is possible that the neuroprotective effects of several similarly structured MAOIs such as PG, deprenyl (selegiline), clorgyline, and rasagiline [192, 201, 276-278] are due to another property such as the presence of an *N*-propargyl moiety [201], which, itself, has been proposed capable of exerting neuroprotective effects through a variety of mechanisms ranging from modulation of apoptotic proteins to direct targeting of the mPTP [192, 274-276, 278, 279].

### **Combinational Therapies**

To date, all single agent pharmacotherapy clinical trials for TBI have failed. Although there have been numerous reasons cited for these failures, due to the heterogeneity of injury and the complexity of the secondary injury cascade, there is interest in developing multi-mechanistic combinational therapies for the treatment of TBI [213]. Indeed, the need for combinational approaches can be seen in experimental TBI models where agents, such as CsA and PZ, are unable to completely restore pre-injury function [71, 72, 76, 110, 136].

In 2008, NIH funded six multi-drug combinational experimental TBI studies. Of the six studies, only the combination progesterone and nicotinamide (NAD<sup>+</sup> precursor,

antioxidant, anti-inflammatory) was able to significantly improve cognitive and motor deficits over monotherapy [280]. On the other end of the spectrum, despite studies showing that creatine (maintenance of ATP levels)[281] or choline (various mechanisms of action, precursor to neurotransmitter synthesis)[140] were protective in experimental TBI, combining the two worsened outcomes [280].

However, a recent comprehensive review by Kline and colleagues detailing experimental TBI combinational therapy studies is more optimistic [215]. Of the 35 studies reviewed, all of which included behavioral outcomes, 46% resulted in additive or synergistic effects, 35% had neutral outcomes, and only 19% resulted in negative interactions [215]. Unlike the six studies that were funded under the NIH “multi-drug combinational therapy” funding announcement, several of these studies included non-drug therapies such as hypothermia, environmental enrichment, exercise, and stem cell administration. Although the Kline review focused on distinct categories (inflammation, oxidative stress, neurotransmitter dysregulation, neurotrophins, stem cells, and rehabilitative therapies), environmental enrichment combinations were utilized the most, and the majority of successes were either achieved through a combination of stem cell implantation and environmental enrichment [282], or through attenuation of neuroinflammation [215]. Of important note here is that one study, which utilized CsA and minocycline (antibiotic, anti-inflammatory), saw a 100% lethality rate in the combination group [215, 283].

In general both reviews highlight some of the challenges in developing combinational therapies for TBI including optimization of combined dosing paradigms, consideration of sub-optimal doses, consideration of altered pharmacokinetics, pharmacodynamics, toxicities, and side effects, choice of time point, choice and

sensitivity of outcome measures, inclusion of behavioral assessments, use of appropriate statistics, and variations in efficacy across outcome measures [215, 280].

### **Overall Dissertation Objective and Specific Aims**

Traumatic brain injury (TBI) represents a significant health crisis in the United States. To date there are no FDA-approved pharmacotherapies available to prevent the devastating neurologic deficits caused by TBI. Due to the complex pathophysiology which occurs following TBI, more robust pharmacological approaches must be developed. As central mediators of the TBI secondary injury cascade, mitochondria and LP-derived neurotoxic aldehydes make promising therapeutic targets. In fact, Cyclosporine A (CsA), an FDA-approved immunosuppressant capable of inhibiting the mitochondria permeability transition pore (mPTP) has been shown to be neuroprotective in experimental TBI. Additionally, phenelzine (PZ), an FDA-approved non-selective irreversible monoamine oxidase inhibitor (MAOI) class antidepressant has also been shown to be neuroprotective in experimental TBI due to the presence of a hydrazine (-NH-NH<sub>2</sub>) moiety allowing for the scavenging of LP-derived neurotoxic aldehydes.

The overall goal of this dissertation is to further examine the neuroprotective capabilities of the mPTP inhibitor, CsA, and the LP-derived neurotoxic aldehyde scavenger, PZ, using a severe controlled cortical impact injury (CCI) model in 3-month old male Sprague-Dawley rats. First, the neuroprotective effects of CsA are examined in isolated synaptic and non-synaptic mitochondria, two heterogeneous populations. Next, the ability of a novel 72h subcutaneous continuous infusion of PZ combined with CsA to improve mitochondrial respiration, attenuate mitochondria-aldehyde conjugate formation, and prevent cytoskeletal spectrin degradation is compared to monotherapy. Finally, the effects of PZ (MAOI, aldehyde scavenger) on learning and memory and cortical tissue

sparing following injury are compared to the effects of pargyline (MAOI, non-aldehyde scavenger) and hydralazine (non-MAOI, aldehyde scavenger).

**Specific Aim 1:** To test the hypothesis that CsA will have a differential neuroprotective effect on isolated synaptic and non-synaptic mitochondrial bioenergetics following experimental traumatic brain injury. Following a severe controlled cortical impact injury (2.2mm) in 3mo male Sprague-Dawley rats, an intraperitoneal dose of CsA (20mg/kg) will be administered 15min following injury. At 24h following injury cortical synaptic and non-synaptic mitochondria will be isolated and respiratory rates will be measured using a Clark-type oxygen electrode.

**Specific Aim 2:** To test the hypothesis that a 72h subcutaneous continuous infusion of PZ combined with CsA will improve mitochondrial respiration, attenuate formation of LP-derived aldehyde mitochondrial protein conjugates, and maintain cytoskeletal integrity following experimental TBI to a greater degree than monotherapy. Following a severe controlled cortical impact injury (2.2mm) in 3mo male Sprague-Dawley rats, subcutaneous osmotic pumps containing PZ (10mg/kg/day/3d) and/or CsA (10mg/kg/day/3d) will be implanted. Loading doses of PZ (10mg/kg) and/or CsA (20mg/kg) will also be administered 15min following injury. At 72h post-injury 1) cortical mitochondria (total) respiratory rates will be assessed using a Clark-type oxygen electrode and 2) cortical mitochondria (total) bound 4-HNE and acrolein will be assessed using Western blot. Additionally, Western blot will be used to assess cortical tissue for 145kD (calpain-only) and 150kD (calpain/caspase 3)  $\alpha$ -spectrin breakdown as a marker for cytoskeletal integrity.

**Specific Aim 3:** To test the hypothesis that PZ, a LP-derived neurotoxic aldehyde scavenger and MAOI, and hydralazine (HZ), an LP-derived neurotoxic

aldehyde scavenger incapable of inhibiting MAO will improve cognitive function and cortical tissue sparing following experimental TBI, whereas pargyline (PG), a MAOI incapable of scavenging LP-derived neurotoxic aldehydes, will not. Following severe controlled cortical impact injury (2.0mm), 3mo male Sprague-Dawley rats will receive an intraperitoneal dose of PZ (15mg/kg), HZ (5mg/kg), or PG (15mg/kg) at 15min, 24h, and 48h following injury. Morris water maze testing will be conducted on day 3 – day 7, and animals will be perfused on day 8 for analysis of cortical tissue sparing. Additionally, the effects of the PZ, HZ, and PG dosing paradigms on MAO inhibition and monoamine neurotransmitter (NE, 5-HT, DA) tissue levels will be evaluated via HPLC in uninjured cortical tissue.



## **CHAPTER TWO:**

### **Synaptic Mitochondria Sustain More Damage than Non-Synaptic Mitochondria after Traumatic Brain Injury and are Protected by Cyclosporine A**

**Preface:** Chapter Two has been adapted from: **Kulbe JR**, Hill RL, Singh IN, Wang JA, Hall ED. Synaptic mitochondria sustain more damage than non-synaptic mitochondria after traumatic brain injury and are protected by cyclosporine A. *Journal of Neurotrauma*. 34(7): 1291-1301 (2017). DOI: 10.1089/neu.2016.4628. (*Mary Ann Leibert, Inc., New York, NY*). Figures have been renumbered and formatted in accordance with University of Kentucky Graduate School requirements.

## **Introduction**

Traumatic brain injury (TBI) represents a significant health crisis. In the United States, there are over 5 million persons currently living with a disability resulting from a TBI [12] with an associated economic burden of 76.5 billion dollars. [10, 11] TBI consists of a primary mechanical injury followed by a secondary injury cascade. [14] Aspects of this cascade include increases in excitotoxic amino acids such as glutamate, increases in intracellular calcium, mitochondrial dysfunction, production of reactive oxygen and nitrogen species (ROS/RNS), initiation and propagation of lipid peroxidation (LP), formation of LP-derived neurotoxic aldehydes, activation of calcium-dependent proteases such as calpain, cytoskeletal degradation, cell death, and neurologic dysfunction. [1, 16, 17, 22, 24, 41, 51, 55, 56, 58, 71, 108, 109, 114, 161-163, 223, 224, 284-288] The secondary injury cascade should be amenable to therapeutic intervention. Currently, there are no Food and Drug Administration (FDA)-approved pharmacotherapies for the treatment of patients with TBI, however. [1]

Mitochondria play a central role in the secondary injury cascade. Mitochondria are essential regulators of calcium homeostasis [20, 21] and buffer increased intracellular calcium after TBI. [22] High levels of mitochondrial calcium, however, lead to mitochondrial dysfunction, including increased generation of ROS/RNS, decreased oxidative phosphorylation and adenosine triphosphate (ATP) production, and induction of the mitochondria permeability transition pore (mPTP). [22, 51, 53, 56, 60, 163, 225, 251, 289, 290]

The mPTP is a non-selective mega channel located in the inner mitochondrial membrane that is permeable to solutes <1.5 kDa. [51] Opening of the mPTP leads to extrusion of calcium back into the cytosol, mitochondrial swelling, and rupture of the

outer mitochondrial membrane. [51, 104] Mitochondrial dysfunction contributes to several aspects of the aforementioned injury cascade, including ROS/RNS induction of LP and formation of the LP-derived neurotoxic aldehydes 4-hydroxynonenal and acrolein, which are capable of covalently binding mitochondrial proteins, further exacerbating mitochondrial dysfunction. [29, 69, 71, 77, 101, 113, 163] Additional downstream consequences of mPTP formation include activation of the calcium-dependent protease calpain, cytoskeletal degradation, cell death, and neurologic dysfunction. [1, 17, 29, 51, 55, 56, 58, 69, 70, 84, 93, 98, 99, 110, 163, 226] Therefore, as central mediators of the secondary injury cascade, mitochondria are promising therapeutic targets for prevention of cellular death and dysfunction after TBI.

Several therapies targeting mitochondria have been shown to be neuroprotective in experimental models of TBI, including mild uncoupling, [125, 248] ketogenic diets, [249, 291] increased antioxidant availability, [113, 126] and scavenging of neurotoxic aldehydes. [71] One of the most promising and extensively studied mitochondrial targeted TBI therapies, however, is inhibition of mPTP by the FDA-approved immunosuppressant, cyclosporine A (CsA). In experimental TBI, CsA or its non-immunosuppressant analog, NIM811, prevent mitochondrial swelling and axonal pathology, [223, 224] maintain mitochondrial membrane potential and decrease production of reactive oxygen species, [225] improve total (synaptic and non-synaptic) mitochondrial respiration, [226] prevent oxidative (synaptic and non-synaptic) mitochondrial damage, [123, 226] improve cortical tissue sparing, [122, 124, 227] decrease calpain-mediated cytoskeletal degradation and neurodegeneration, [110] and improve motor and cognitive function. [110, 123, 135, 136]

Interestingly, despite the fact that CsA directly targets mitochondria, only a limited number of studies have evaluated the effects of CsA on mitochondria after

experimental TBI, [225, 226, 292] with no studies evaluating the effects of CsA on isolated synaptic and non-synaptic mitochondria. Mitochondria are heterogeneous, consisting of both synaptic and non-synaptic populations. Isolated synaptic mitochondria consist of pre-synaptic mitochondria located within the synaptosome, while isolated non-synaptic mitochondria consist of neuronal (axonal, somal, dendritic) and non-neuronal (glial, vascular, etc.) mitochondria.

To our knowledge, there is currently no method available to further separate the non-synaptic mitochondrial population into non-synaptic neuronal and non-synaptic non-neuronal, (e.g., glial) populations. Therefore, whereas synaptic mitochondria consist of pure pre-synaptic neuronal mitochondria, non-synaptic mitochondria are isolated from numerous cell types. Synaptic mitochondria are considered essential for proper neurotransmission and synaptic plasticity, [44-46] processes which are impaired after TBI. [47] Their dysfunction has been implicated in neurodegeneration, as well as degeneration of synapses and neurons absent overt cell death, [37, 48, 49] and studies reveal synaptic mitochondria to be more susceptible to dysfunction. Importantly, these two mitochondrial populations show different characteristics both *in-vitro* [37, 38] and *in-vivo*, [41, 50] including differential responses to pharmacotherapy. [50]

The heterogeneity of the two populations, however, can be masked in total mitochondrial (synaptic and non-synaptic) preparations, especially because of the high glia to neuron ratio of the cerebral cortex. [293] Therefore, it is essential that mitochondria targeted pharmacotherapies, such as CsA, be evaluated in both populations.

This is the first study to examine the effects of CsA on isolated synaptic and non-synaptic mitochondria after experimental TBI. We hypothesized that synaptic mitochondria would sustain more damage than non-synaptic mitochondria 24h after

severe controlled cortical impact injury (CCI), and that intraperitoneal administration of CsA (20 mg/kg) 15 min after injury would differentially attenuate injury-induced synaptic and non-synaptic respiratory impairment.

## **Methods**

### **Animals**

Young adult male Sprague-Dawley rats ( $n=20$ , Harlan, Indianapolis, IN) weighing 300 to 350 g were used for all studies. Animals were allowed food and water *ad libitum* and were housed in the Division of Laboratory Animal Resources of the University of Kentucky Medical Center. All animal and husbandry were conducted in accordance with the University of Kentucky Institutional Animal Care and Use Committee. Animals were randomly assigned to experimental groups: sham ( $n=6$ ), CCI + vehicle ( $n=6$ ), CCI + CsA ( $n=8$ ).

### **CCI TBI**

Animals were initially anesthetized with 4% isoflurane and placed in a stereotaxic frame (David Kopf, Tujunga, CA), where they were maintained at 3% isoflurane for the duration of the procedure. A midline incision was made to expose the skull, and a 6 mm craniotomy was made lateral to the sagittal suture midway between lambda and bregma. The exposed brain with intact dura was injured using a computer controlled pneumatic impactor (TBI 03010; Precision Systems and Instrumentation, Fairfax Station, VA) fitted with a 5 mm beveled tip set to impact at ~3.5 m/sec, 2.2 mm depth and 500 msec dwell time, as described previously. [71] After injury, Surgicel was placed onto the dura, and an 8 mm plastic disk was affixed with tissue adhesive to close the craniotomy site. Body temperature was monitored and maintained at 37°C with a thermo-regulating heating pad. Sham animals underwent all procedures but did not receive an impact injury.

## **Cyclosporine A Administration**

The CsA concentration chosen was based on previously optimized concentrations for CCI. [225, 294] The CCI + CsA group was administered CsA obtained from the University of Kentucky Medical Center Hospital Pharmacy (Perrigo, Minneapolis, MN; 50 mg/mL) 15 min after injury as a single intraperitoneal dose of 20 mg/kg in saline/650 mg cremophor/33.2% (v/v) ethanol diluted in saline to a final concentration of 10 mg/mL. The injection volume was 0.2 mL/100g of body weight. CCI + vehicle-treated animals received an equivalent dose of saline/cremophor/ethanol 15 min after injury.

## **Tissue Extraction**

Animals were euthanized at 24h using CO<sub>2</sub> anesthetization followed by decapitation, and an 8 mm cortical punch centered over the injury site was collected for analysis of mitochondrial respiration.

## **Mitochondrial Isolation**

Mitochondria were isolated as described previously [71, 163] with modifications to isolate synaptic and non-synaptic populations. [41, 50] Cortical tissue was homogenized in ice-cold isolation buffer (215 mmol/L mannitol, 75 mmol/L sucrose, 0.1% bovine serum albumin, 20 mmol/L HEPES, 1 mmol/L EGTA, pH 7.2) using Potter-Elvehjem homogenizers. Samples were then centrifuged twice at 1400 x g for 3 min at 4°C. Supernatants were collected and spun at 13,000 x g for 10 min at 4°C.

The crude mitochondrial pellet was resuspended and layered onto a discontinuous 7.5% and 10% Ficoll gradient and centrifuged at 100,000 x g for 30 min at 4°C. The non-synaptic mitochondria pellet was resuspended in isolation buffer without

EGTA and centrifuged at 10,000 x g for 10 min at 4°C to remove Ficoll and then resuspended to a final concentration of approximately 10 mg/mL in isolation buffer without EGTA.

The synaptosomal layer was removed from the 7.5%-10% Ficoll interface, resuspended in isolation buffer and spun at 13,000 x g for 10 min at 4°C to remove Ficoll. The synaptosome pellet was resuspended in isolation buffer, placed into a nitrogen bomb at 1200 psi for 10 min at 4°C to release synaptic mitochondria, [295, 296] layered onto a second discontinuous 7.5% and 10% Ficoll gradient, and centrifuged at 100,000 x g for 30 min at 4°C. The synaptic mitochondria pellet was resuspended in isolation buffer without EGTA and centrifuged at 10,000 x g for 10 min at 4°C to remove Ficoll and resuspended in isolation buffer without EGTA. Protein concentrations were determined with a BCA protein assay kit and measured at absorbance 562 nm with a BioTek Synergy HT plate reader (Winooski, VT, USA). Mitochondria were immediately used for respiratory analysis.

### **Measurement of Mitochondrial Respiratory Function**

Mitochondria respiratory rates were measured using a Clark-type electrode in a continuously stirred, sealed, thermostatically controlled chamber (Oxytherm System, Hansatech Instruments, Norfolk, UK) that was maintained at 37°C. Mitochondria (>30 µg) were placed into a chamber containing 250 µl of KCl respiration buffer (125 mmol/L, 2 mmol/L MgCl<sub>2</sub>, 2.5 mmol/L KH<sub>2</sub>PO<sub>4</sub>, 0.1% bovine serum albumin, 20 mmol/L HEPES, pH 7.2). Mitochondria equilibrated for 1 min prior to complex-I initiation.

Complex-I respiration was initiated with 5 mmol/L pyruvate and 2.5 mmol/L malate and state II respiration was monitored. Two boluses of 150 µmol/L adenosine diphosphate (ADP) were added to initiate state III respiration. State IV respiration was



monitored following 2  $\mu\text{mol/L}$  addition of the ATP synthase inhibitor oligomycin. Maximal state V(I) respiration was initiated by addition of 2  $\mu\text{mol/L}$  of the protonophore FCCP. Complex I was inhibited by addition of 100  $\text{nmol/L}$  rotenone. Complex II driven respiration was initiated by addition of 10  $\text{mmol/L}$  succinate and state V(II) was monitored. Respiratory control ratio (RCR) was calculated by dividing the state III respiration rate (second bolus ADP rate) by the state IV respiration rate. [163, 248]

### **Statistical analysis**

Statistical analysis was conducted using Prism version 6.0 (Graph Pad, San Diego, CA). Results are reported as mean  $\pm$  standard deviation. Initial statistical analysis was performed using a two-way analysis of variance (ANOVA), followed by a Tukey *post hoc* analysis when appropriate.

## **Results**

The following details the comparative effects of CCI TBI, with and without early CsA treatment, on the respiratory functional status of non-synaptic versus synaptic mitochondria as measured by changes in oxygen utilization during the various respiratory states. Overall, the results show that, in general, synaptic mitochondria are more susceptible to post-traumatic complex I and II-driven dysfunction within the electron transport chain than non-synaptic mitochondria. Nevertheless, early CsA treatment is able to protect respiration that is linked to neuronal ATP production within the more damaged synaptic mitochondria.

### **State II: Addition of Pyruvate + Malate to Activate Mitochondrial Complex I**

A two-way ANOVA (injury x population) revealed a significant main effect for injury [ $F(1, 20) = 23.75, p < 0.0001$ ] and population [ $F(1, 20) = 17.22, p = 0.0005$ ], but not interaction [ $F(1, 20) = 0.2018, p = 0.6581$ ]. *Post-hoc* testing (Tukey's) revealed that state II respiration for non-synaptic CCI + vehicle was significantly impaired compared with non-synaptic sham ( $p < 0.01$ ), synaptic CCI + vehicle was significantly impaired compared with synaptic sham ( $p < 0.05$ ), and that the state II respiration rate for synaptic sham was significantly decreased compared with non-synaptic sham ( $p < 0.05$ ) (**Fig. 2.1A**).

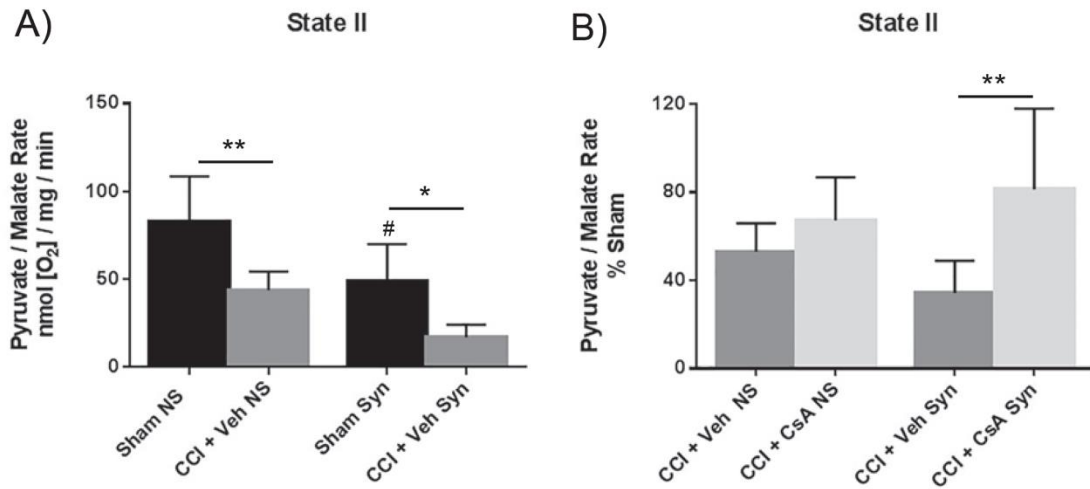


**Figure 2.1 State II: Effect of CsA on synaptic and non-synaptic mitochondria. (A)** Effect of injury on non-synaptic and synaptic mitochondria for state II respiration (pyruvate/malate) 24 h after severe controlled cortical impact (CCI). **(B)** Effect of early post-injury (15 min) intraperitoneal administration of cyclosporine A (CsA) (20 mg/kg) on non-synaptic and synaptic mitochondria for state II respiration (pyruvate/malate) 24h after severe CCI, calculated as % sham. Sham NS, sham non-synaptic ( $n = 6$ ), Sham Syn, sham synaptic ( $n = 6$ ), CCI + Veh NS, CCI + vehicle non-synaptic ( $n = 6$ ), CCI + Veh Syn, CCI + vehicle synaptic ( $n = 6$ ), CCI + CsA NS, CCI + CsA non-synaptic ( $n = 8$ ), CCI + CsA Syn, CCI + CsA synaptic ( $n = 8$ ); values, mean  $\pm$  standard deviation; two-way analysis of variance followed by Tukey *post hoc*; \* $p < 0.05$ , \*\* $p < 0.01$ , # $p < 0.05$  compared with non-synaptic sham.

To assess drug effect, state II respiratory rates for CCI + vehicle and CCI + CsA were calculated as a percentage of the sham respiratory rate. A two-way ANOVA (treatment x population) revealed a significant main effect for treatment [ $F(1, 24) = 11.07, p = 0.0028$ ], but not for population [ $F(1, 24) = 0.06332, p = 0.8035$ ] or interaction [ $F(1, 24) = 3.182, p = 0.0871$ ]. While CsA improved state II respiration in both injured non-synaptic and injured synaptic mitochondria, *post-hoc* testing (Tukey) revealed this effect was only significant in the synaptic population ( $p < 0.01$ ) (**Fig. 2.1B**).

### **State III: Addition of ADP to Activate Complex V ATP Production**

A two-way ANOVA (injury x population) revealed a significant main effect for injury [ $F(1, 20) = 31.10, p < 0.0001$ ] and population [ $F(1, 20) = 12.39, p = .0022$ ], but not interaction [ $F(1, 20) = .0075, p = 0.9318$ ]. *Post-hoc* testing (Tukey's) revealed that state III respiration for non-synaptic CCI + vehicle was significantly impaired compared with non-synaptic sham ( $p < 0.01$ ), and synaptic CCI + vehicle was significantly impaired compared with synaptic sham ( $p < 0.01$ ) (**Fig. 2.2A**).

To assess drug effect, state III respiratory rates for CCI + vehicle and CCI + CsA were calculated as a percentage of the sham respiratory rate. A two-way ANOVA revealed a significant main effect for treatment [ $F(1, 24) = 10.45, p = 0.0036$ ], and population [ $F(1, 24) = 4.847, p = 0.0375$ ], but not interaction [ $F(1, 24) = 0.5409, p = 0.4692$ ]. While CsA improved state III respiration in both injured non-synaptic and injured synaptic mitochondria, *post-hoc* testing (Tukey) revealed this effect was only significant in the synaptic population ( $p < 0.05$ ) (**Fig. 2.2B**).

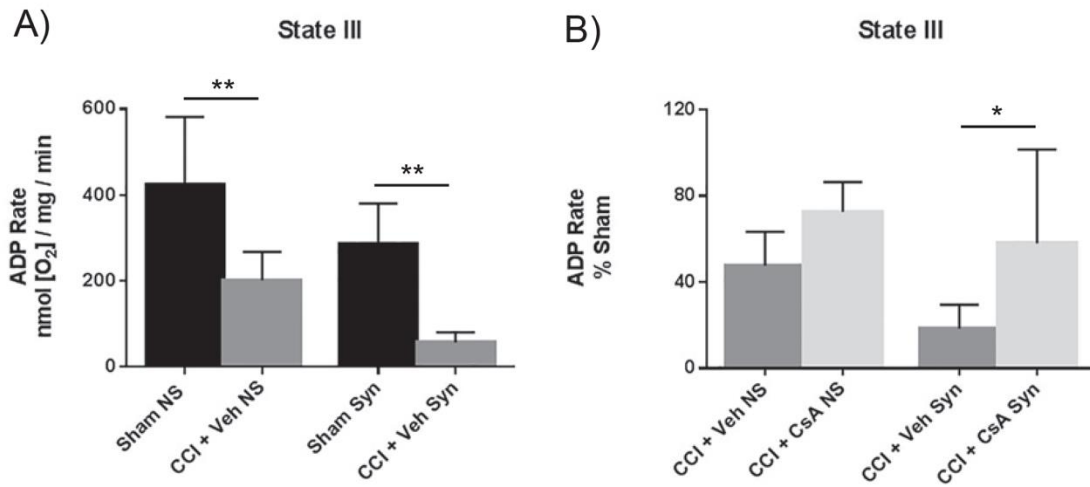


**Figure 2.2 State III: Effect of CsA on synaptic and non-synaptic mitochondria (A)** Effect of injury on non-synaptic and synaptic mitochondria for state III respiration (pyruvate/malate/adenosine diphosphate [ADP]) 24h after severe controlled cortical impact (CCI). **(B)** Effect of early post-injury (15 min) intraperitoneal administration of cyclosporine A (CsA) (20 mg/kg) on non-synaptic and synaptic mitochondria for state III respiration (pyruvate/ malate/ADP) 24h after severe CCI, calculated as % sham. Sham NS, sham non-synaptic ( $n = 6$ ), Sham Syn, sham synaptic ( $n = 6$ ); CCI + Veh NS, CCI + vehicle non-synaptic ( $n = 6$ ); CCI + Veh Syn, CCI + vehicle synaptic ( $n = 6$ ); CCI + CsA NS, CCI + CsA non-synaptic ( $n = 8$ ); CCI + CsA Syn, CCI + CsA synaptic ( $n = 8$ ); values = mean  $\pm$  standard deviation; two-way analysis of variance followed by Tukey *post hoc*; \* $p < 0.05$ , \*\* $p < 0.01$ .

#### **State IV: Addition of Oligomycin to Inhibit Complex V ATP Production**

A two-way ANOVA (injury x population) revealed a significant main effect for injury [ $F(1, 20) = 27.77, p < 0.0001$ ] and population [ $F(1, 20) = 8.680, p = .0080$ ], but not interaction [ $F(1, 20) = .0276, p = 0.8698$ ]. *Post-hoc* testing (Tukey) revealed that state IV respiration for non-synaptic CCI + vehicle was significantly impaired compared with non-synaptic sham ( $p < 0.01$ ), and synaptic CCI + vehicle was significantly impaired compared with synaptic sham ( $p < 0.01$ ) (**Fig. 2.3A**).

To assess drug effect, state IV respiratory rates for CCI + vehicle and CCI + CsA were calculated as a percentage of the sham respiratory rate. A two-way ANOVA revealed a significant main effect for treatment [ $F(1, 24) = 11.91, p = 0.0021$ ], but not population [ $F(1, 24) = 1.964, p = 0.1738$ ] or interaction [ $F(1, 24) = 0.0046, p = 0.9465$ ]. While CsA improved state IV respiration in both injured non-synaptic and injured synaptic mitochondria, *post-hoc* testing (Tukey) revealed these effects were not significant (**Fig. 2.3B**).

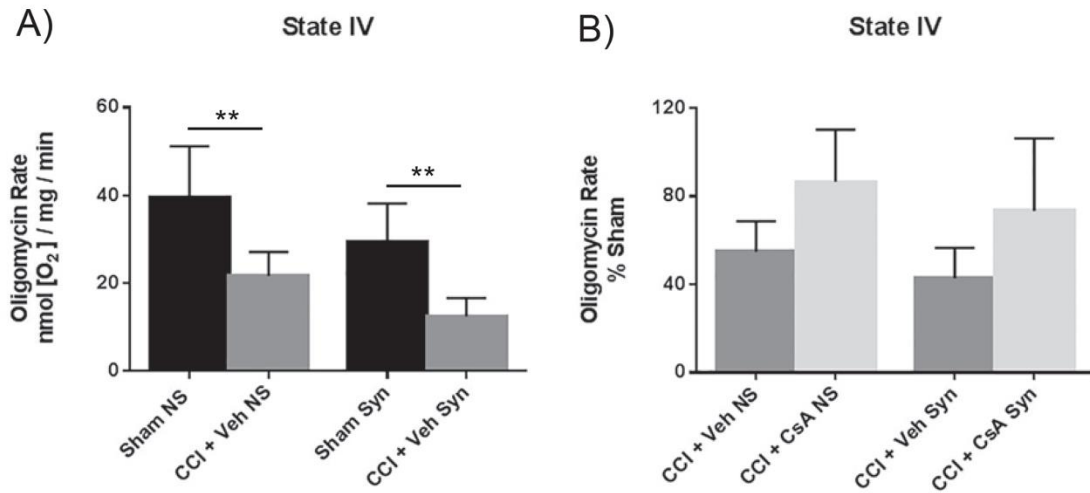


**Figure 2.3 State IV: Effect of CsA on synaptic and non-synaptic mitochondria (A)** Effect of injury on non-synaptic and synaptic mitochondria for state IV respiration (oligomycin) 24h after severe controlled cortical impact (CCI). **(B)** Effect of early post-injury (15 min) intraperitoneal administration of cyclosporine A (CsA) (20 mg/kg), on non-synaptic and synaptic mitochondria for state IV respiration (oligomycin) 24h after severe CCI, calculated as % sham. Sham NS, sham non-synaptic ( $n = 6$ ); Sham Syn, sham synaptic ( $n = 6$ ); CCI + Veh NS, CCI + vehicle non-synaptic ( $n = 6$ ); CCI + Veh Syn, CCI + vehicle synaptic ( $n = 6$ ); CCI + CsA NS, CCI + CsA non-synaptic ( $n = 8$ ); CCI + CsA Syn, CCI + CsA synaptic ( $n = 8$ ); values mean  $\pm$  standard deviation; two-way analysis of variance followed by Tukey *post hoc*; \*\* $p < 0.01$ .

### **RCR (State III / State IV): Difference in Oxygen Utilization Between Activation and Inhibition of ATP Production**

A two-way ANOVA (injury x population) revealed a significant main effect for injury [ $F(1, 20) = 26.02, p < 0.0001$ ], population [ $F(1, 20) = 12.23, p = 0.0023$ ], and interaction [ $F(1, 20) = 5.418, p = 0.0305$ ]. *Post-hoc* testing (Tukey) revealed that RCR for synaptic CCI + vehicle was significantly impaired compared with synaptic sham ( $p < 0.001$ ) and that synaptic CCI + vehicle was significantly impaired compared with non-synaptic CCI + vehicle ( $p < 0.01$ ) (**Fig. 2.4A**).

To assess drug effect, RCR for CCI + vehicle and CCI + CsA were calculated as a percentage of sham RCR. A two-way ANOVA revealed a significant main effect for treatment [ $F(1, 24) = 7.092, p = 0.0136$ ] and population [ $F(1, 24) = 9.680, p = 0.0048$ ], but not interaction [ $F(1, 24) = 3.437, p = 0.0761$ ]. *Post-hoc* testing (Tukey) revealed that CsA treatment significantly improved RCR in the injured synaptic population ( $p < 0.05$ ) and that the RCR for synaptic CCI + vehicle is significantly impaired compared to the RCR for non-synaptic CCI + vehicle ( $p < 0.05$ ) (**Fig. 2.4B**).



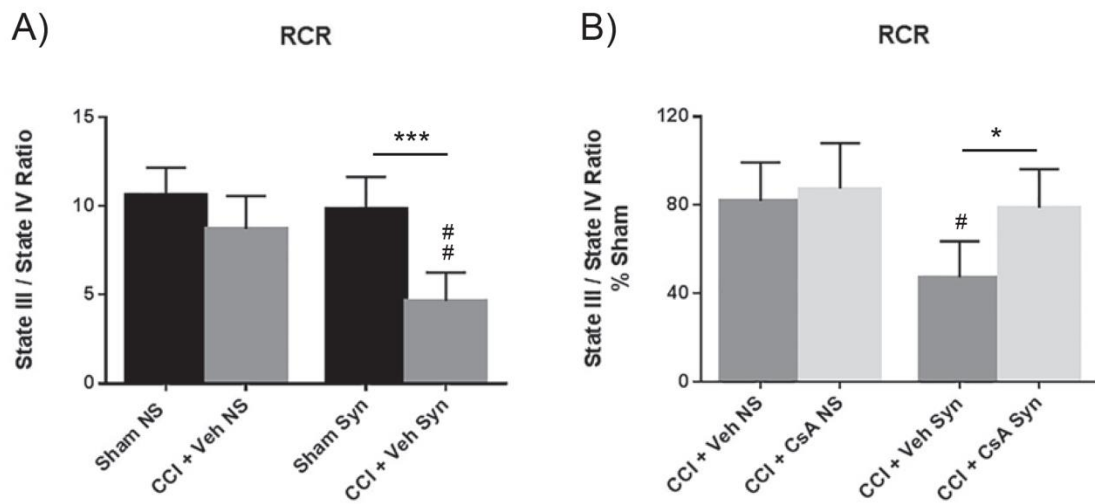


**Figure 2.4 RCR: Effect of CsA on synaptic and non-synaptic mitochondria (A)** Effect of injury on non-synaptic and synaptic mitochondria for respiratory control ratio (RCR) (state III/state IV) 24h after severe controlled cortical impact (CCI). **(B)** Effect of early post-injury (15 min) intraperitoneal administration of cyclosporine A (CsA) (20 mg/kg), on non-synaptic and synaptic mitochondria for RCR (state III/state IV) 24h after severe CCI, calculated as % sham. Sham NS, sham non-synaptic ( $n = 6$ ); Sham Syn, sham synaptic ( $n = 6$ ); CCI + Veh NS, CCI + vehicle non-synaptic ( $n = 6$ ); CCI + Veh Syn, CCI + vehicle synaptic ( $n = 6$ ); CCI + CsA NS, CCI + CsA non-synaptic ( $n = 8$ ); CCI + CsA Syn, CCI + CsA synaptic ( $n = 8$ ); values = mean  $\pm$  standard deviation; two-way analysis of variance followed by Tukey *post hoc*; \* $p < 0.05$ , \*\* $p < 0.001$ , # $p < 0.05$  vs non-synaptic vehicle, ## $p < 0.01$  vs. non-synaptic vehicle.

### **State V(I): Maximal Complex I-Driven Respiration After Addition of the Protonophore FCCP**

A two-way ANOVA (injury x population) revealed a significant main effect for injury [ $F(1, 20) = 37.82, p < 0.0001$ ] and population [ $F(1, 20) = 9.556, p = .0058$ ], but not interaction [ $F(1, 20) = .2492, p = 0.6231$ ]. *Post-hoc* testing (Tukey) revealed that state V(I) respiration for non-synaptic CCI + vehicle was significantly impaired compared with non-synaptic sham ( $p < 0.001$ ), and synaptic CCI + vehicle was significantly impaired compared with synaptic sham ( $p < 0.01$ ) (**Fig. 2.5A**).

To assess drug effect, state V(I) respiratory rates for CCI + vehicle and CCI + CsA were calculated as a percentage of the sham respiratory rate. A two-way ANOVA revealed a significant main effect for treatment [ $F(1, 24) = 14.25, p = 0.0009$ ], but not population [ $F(1, 24) = 3.580, p = 0.0706$ ] or interaction [ $F(1, 24) = 0.0084, p = 0.9276$ ]. While CsA improved state V(I) respiration in both injured non-synaptic and injured synaptic mitochondria, *post-hoc* testing (Tukey) revealed neither effect was statistically significant (**Fig. 2.5B**).

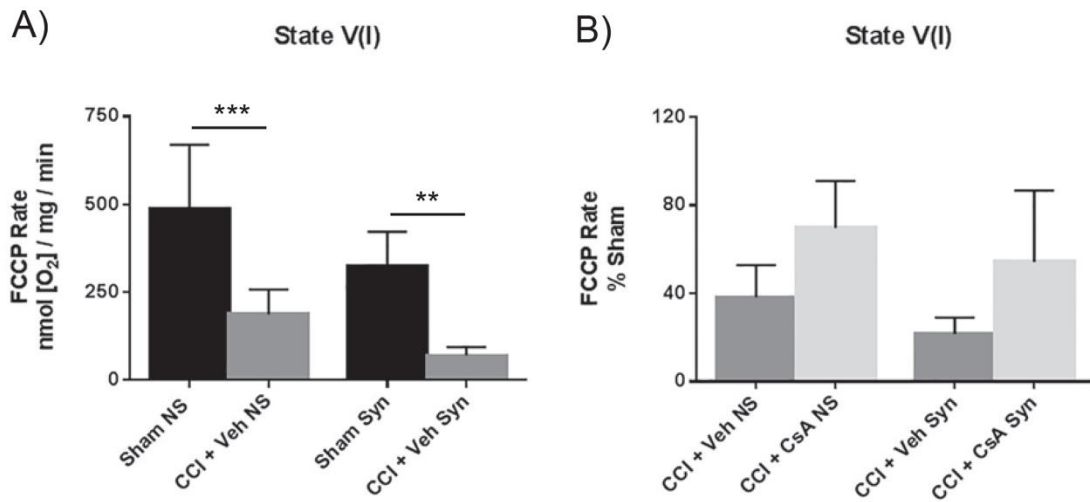


**Figure 2.5 State V(I): Effect of CsA on synaptic and non-synaptic mitochondria (A)** Effect of injury on non-synaptic and synaptic mitochondria for state V(I) respiration (FCCP) 24h after severe controlled cortical impact (CCI). **(B)** Effect of early post-injury (15 min) intraperitoneal administration of cyclosporine A (CsA) (20 mg/kg) on non-synaptic and synaptic mitochondria for state V(I) respiration (FCCP) 24h after severe CCI, calculated as % sham. Sham NS, sham non-synaptic ( $n = 6$ ); Sham Syn, sham synaptic ( $n = 6$ ); CCI + Veh NS, CCI + vehicle non-synaptic ( $n = 6$ ); CCI + Veh Syn, CCI + vehicle synaptic ( $n = 6$ ); CCI + CsA NS, CCI + CsA non-synaptic ( $n = 8$ ); CCI + CsA Syn, CCI + CsA synaptic ( $n = 8$ ); values = mean  $\pm$  standard deviation; two-way analysis of variance followed by Tukey *post hoc*; \*\* $p < 0.01$ , \*\*\* $p < 0.001$ .

### **State V(II): Succinate-Activated Complex II-Driven Respiration after Inhibition of Complex I with Rotenone**

A two-way ANOVA (injury x population) revealed a significant main effect for injury [ $F(1, 20) = 23.97, p < 0.0001$ ] and population [ $F(1, 20) = 15.37, p = 0.0008$ ], but not for interaction [ $F(1, 20) = 0.3787, p = 0.5452$ ]. *Post-hoc* testing (Tukey) revealed that state V(II) respiration for non-synaptic CCI + vehicle was significantly impaired compared with synaptic sham ( $p < 0.05$ ), and that the state V(II) respiration rate for synaptic sham was significantly decreased compared with non-synaptic sham ( $p < 0.05$ ) (**Fig. 2.6A**).

To assess drug effect, state V(II) respiratory rates for CCI + vehicle and CCI + CsA were calculated as a percentage of the sham respiratory rate. A two-way ANOVA revealed a significant main effect for treatment [ $F(1, 24) = 10.45, p = 0.0035$ ], but not for population [ $F(1, 24) = 0.3533, p = 0.5578$ ] or interaction [ $F(1, 24) = 1.272, p = 0.2706$ ]. While CsA improved state V(II) respiration in both injured non-synaptic and injured synaptic mitochondria, *post-hoc* testing (Tukey) revealed this effect was only significant in the synaptic population ( $p < 0.05$ ) (**Fig. 2.6B**).

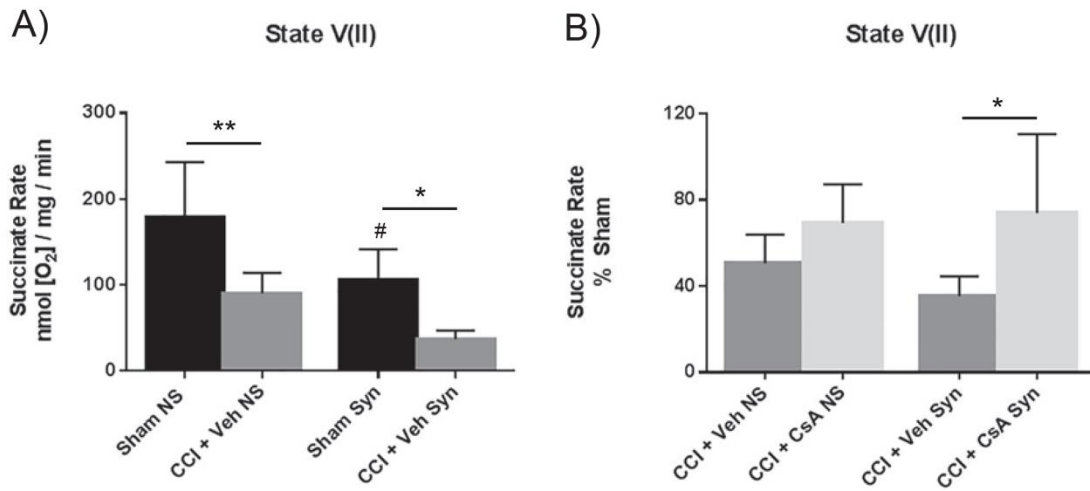


**Figure 2.6 State V(II): Effect of CsA on synaptic and non-synaptic mitochondria (A)** Effect of injury on non-synaptic and synaptic mitochondria for state V(II) respiration (rotenone/succinate) 24h after severe controlled cortical impact (CCI). **(B)** Effect of early post-injury (15 min) intraperitoneal administration of CsA (20 mg/kg) on non-synaptic and synaptic mitochondria for state V(II) respiration (rotenone/succinate) 24h after severe CCI, calculated as % sham. Sham NS, sham non-synaptic ( $n = 6$ ); Sham Syn, sham synaptic ( $n = 6$ ); CCI + Veh NS, CCI + vehicle non-synaptic ( $n = 6$ ); CCI + Veh Syn, CCI + vehicle synaptic ( $n = 6$ ); CCI + CsA NS, CCI + CsA non-synaptic ( $n = 8$ ); CCI + CsA Syn, CCI + CsA synaptic ( $n = 8$ ); values = mean  $\pm$  standard deviation; two-way analysis of variance followed by Tukey *post hoc*; \* $p < 0.05$ , \*\* $p < 0.01$ , # $p < 0.05$  vs. non-synaptic sham.

## **Discussion**

These results indicate that synaptic mitochondria sustain more damage than non-synaptic mitochondria 24h after severe CCI and that intraperitoneal administration of CsA (20 mg/kg) 15 min after injury improves synaptic and non-synaptic respiration (**Fig. 2.7**), with a significant improvement being seen in the more severely impaired synaptic population.

CsA is an FDA-approved immunosuppressant, used clinically to prevent organ rejection after transplant through a mechanism that involves inhibition of calcineurin and T-cell activation. [217] CsA, however, also has the ability to bind the mitochondrial matrix protein cyclophilin D, [218, 219] which inhibits its interaction with the adenine nucleotide transporter, an inner mitochondrial membrane protein, thus preventing formation of mPTP. [220] It is through inhibition of mPTP that CsA exerts its neuroprotective effects after TBI.

NIM811, a non-immunosuppressive analog of CsA unable to bind calcineurin, but capable of binding cyclophilin D and inhibiting mPTP, [297] maintains the neuroprotective effects of CsA, improving mitochondrial respiration, decreasing oxidative damage, decreasing calpain-mediated cytoskeletal degradation and neurodegeneration, and improving motor and cognitive function after experimental TBI. [110, 123, 226]

Under normal physiologic conditions CsA is minimally blood brain barrier penetrable. [221] After TBI, however, CsA is able to enter the CNS because of blood-brain-barrier breakdown, [222] and although concerns have been raised regarding CsA and neurotoxicity, [237-244] two phase II clinical trials show CsA to be safe for use in patients with severe TBI. [234, 235]

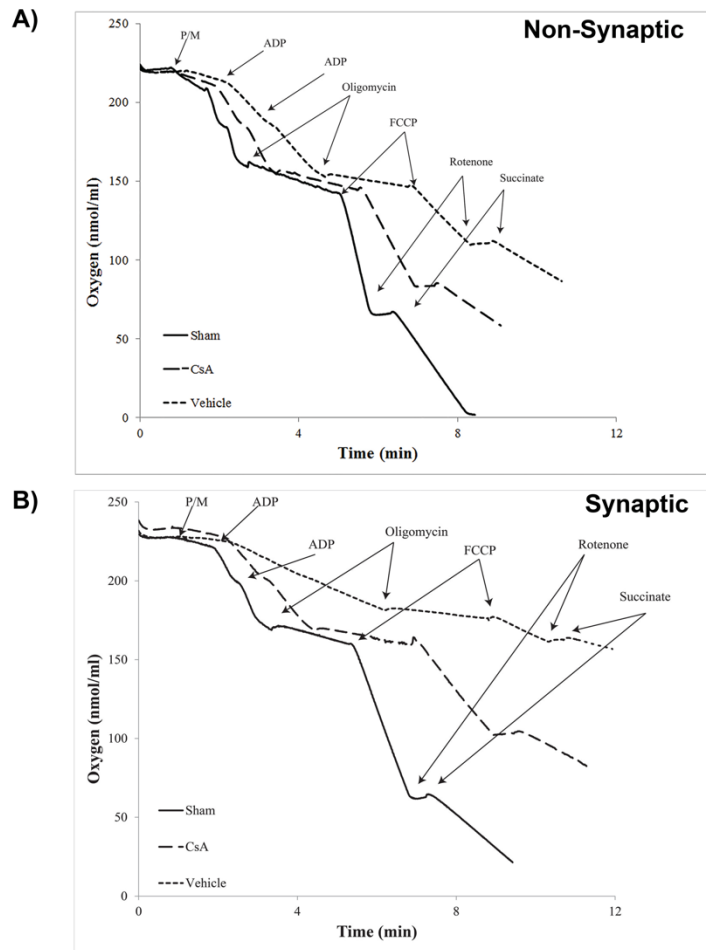


**Figure 2.7 Representative oxymetric traces.** Rates of oxygen consumption of sham, vehicle, and cyclosporine A (CsA) (20 mg/kg, intraperitoneally, 15 min post-injury) for **(A)** non-synaptic and **(B)** synaptic mitochondria isolated from ipsilateral cortex 24h after severe controlled cortical impact (CCI). Purified mitochondrial protein (>30  $\mu$ g) was suspended in respiration buffer (125 mmol/L KCl, 2 mmol/L MgCl<sub>2</sub>, 2.5 mmol/L KH<sub>2</sub>PO<sub>4</sub>, 0.1% BSA, 20 mmol/L HEPES, pH 7.2) in a final volume of 250  $\mu$ l, and oxygen consumption rates were measured using a Clark-type oxygen electrode in the presence of 5 mmol/L pyruvate and 2.5 mmol/L malate (state II), two boluses of 150  $\mu$ mol/L ATP (state III), 2  $\mu$ mol/L oligomycin (state IV), 2  $\mu$ mol/L FCCP (state VI), and 100 nmol/L rotenone and 10 mmol/L succinate (state VII). Sham, sham; CsA, CCI + CsA; vehicle, CCI + vehicle; ADP, adenosine diphosphate.

Despite the fact that the neuroprotective effects of CsA rely on direct protection of mitochondria, [51, 110, 124, 226] many experimental TBI studies using CsA have focused on outcome measures downstream of mitochondrial dysfunction, such as cortical lesion volume, [122, 124, 227, 294] axonal pathology, [110, 117, 223, 224, 298] behavior, [110, 135] and synaptic plasticity. [119] Although important work does confirm the ability of CsA to protect mitochondria after injury, those studies focused on acute injury, [225] microscopic structure analysis, [223] or more indirect measures of mitochondrial function such as brain oxygen consumption [135] and whole brain ATP levels. [299] Only two studies have assessed mitochondrial bioenergetics via oxygen consumption rates, one of which did not extend beyond 12h and was conducted in mice, [226] and one of which utilized juvenile animals. [292] Importantly, none of these mitochondria-focused studies evaluated isolated synaptic and non-synaptic populations.

While it should be noted that Sullivan and coworkers [225] showed that CsA maintains mitochondrial membrane potential in isolated non-synaptic mitochondria and intact synaptosomes acutely (30-60 min) after CCI, this is the first study to examine the effects of CsA on isolated and purified synaptic and non-synaptic mitochondria after experimental TBI. As such, CsA was administered 15 min post-injury. Early administration allows for the greatest chance of neuroprotection, and allows for contextualization of future therapeutic window studies. The 20mg/kg intraperitoneal dosage used is considered optimal and has been used extensively in previously experimental TBI studies. [110, 117, 119, 124, 225-227, 292, 294]

The CsA used in this study is solubilized in a vehicle containing cremophor. Toxicity concerns have been raised in regard to cremophor, and reported side effects include hypersensitivity reactions, hyperlipidemia, erythrocyte aggregation, and peripheral neuropathy, but are usually associated with intravenous infusions or high



cremophor concentrations. [245] Several studies have shown that cremophor has the ability to impair mitochondrial function. These studies, however, were performed in mitochondria isolated from heart muscle, skeletal muscle, and kidney tissue, and cremophor was either administered chronically or *in-vitro*. [300-302]

Interestingly, chronic administration of cremophor or CsA + cremophor impairs heart and skeletal muscle mitochondria similarly, suggesting that any cremophor toxicity is still observable when administered along with CsA. The safety of low doses of CsA + cremophor, such as the dose used in this study (20mg/kg, intraperitoneally), is well supported in the literature, however. For example, administration of CsA + cremophor to sham animals has no effect on long term potentiation, [119] motor or cognitive function, [136] or brain metabolism, [299] although chronic administration can result in weight loss. [136]

Although it is feasible that administration of vehicle or CsA to sham animals could alter basal mitochondrial respiration, evaluating the protective effect of CsA after injury in comparison to sham animals not receiving vehicle or drug is the most clinically appropriate assessment. Therefore, neither vehicle nor CsA were administered to sham animals for this study.

The respiratory function of isolated synaptic and non-synaptic mitochondria was assessed 24h after injury. Total (synaptic and non-synaptic) mitochondrial respiratory dysfunction peaks between 12h and 24h after severe rat CCI, [22] with several studies confirming mitochondrial respiratory dysfunction 24h after injury. [22, 248, 303]

In sham animals, synaptic mitochondria showed decreased respiratory rates compared to non-synaptic mitochondria, decreases that were only significant in state II and state V(II). Previous studies have also shown that healthy synaptic mitochondria

have decreased respiration rates compared with healthy non-synaptic mitochondria, [41, 42] as well as decreased pyruvate dehydrogenase activity, [304] the enzyme responsible for generating the nicotinamide adenine dinucleotide that feeds into complex I of the electron transport chain. Because non-synaptic mitochondria contain mitochondria from both neurons and glia, it is possible the higher respiration rates found in non-synaptic mitochondria are because of astrocytic mitochondria; mitochondria isolated from cultured astrocytes have higher respiration rates than mitochondria isolated from cultured neurons as well as higher levels of electron transport chain subunits. [296]

RCR (state III/state IV) is considered one of the best general measures of mitochondrial function and health and represents the ability of mitochondria to couple oxidation of substrates with generation of ATP via ADP phosphorylation under minimal proton leak. Therefore, healthy mitochondria will have a high RCR, while damaged mitochondria will have a low RCR [30]. In this study, the RCR for synaptic mitochondria was significantly reduced 24h after injury compared with sham, while the RCR for non-synaptic mitochondria was not. The RCR for injured synaptic mitochondria was also significantly reduced compared to the RCR for injured non-synaptic mitochondria. Interestingly, statistical analysis revealed a significant interaction between injury and population for this measure, indicating that synaptic mitochondria are indeed more susceptible to injury.

Importantly, the decrease in synaptic RCR was significantly attenuated by CsA administration. While RCR represents an overall measure of mitochondrial function, its value is affected by multiple aspects of oxidative phosphorylation. [30] Therefore, in addition to RCR we assessed individual states of respiration to identify specific aspects of bioenergetic impairment.

State II respiration is measured after addition of the complex-I substrates pyruvate and malate, but before ADP addition, and represents a slow state of respiration. Severe CCI significantly reduced state II respiration for both synaptic and non-synaptic mitochondria 24h after injury. Decreases in state II respiration are consistent with the fact that pyruvate dehydrogenase, the enzyme linking glycolysis with the citric acid cycle, is known to have decreased activity after TBI. [305, 306] While CsA was able to improve injury induced decreases in state II respiration in both populations, the improvements only reached statistical significance in the synaptic population.

State III respiration is measured following addition of ADP, allowing coupling of oxidative phosphorylation, and is considered one of the most important states of respiration to measure after injury, because decreases in State III respiration are indicative of defects in complex I-driven substrate oxidation and/or ATP turnover. [30] Severe CCI significantly reduced state III respiration for both synaptic and non-synaptic mitochondria 24h after injury. While CsA was able to improve injury-induced decreases in state III respiration in both populations, the improvements only reached statistical significance in the synaptic population. Importantly, the ability of CsA to significantly improve state III synaptic respiration is a major contributory factor to the ability of CsA to also significantly improve synaptic RCR (state III/IV) after injury.

State IV is measured after addition of the ATP synthase inhibitor oligomycin, which returns the mitochondria to a basal state of respiration. Severe CCI significantly reduced state IV respiration for both synaptic and non-synaptic mitochondria 24h after injury. While CsA was able to improve injury induced decreases in state IV respiration in both populations, the improvements were not statistically significant.

State V(I) respiration is measured following addition of the protonophore FCCP, which uncouples substrate oxidation from ATP production, and is used to assess maximal respiration, with decreases in state V(I) respiration being indicative of defects in complex-I driven substrate oxidation. [30] Severe CCI significantly reduced state V(I) respiration for both synaptic and non-synaptic mitochondria 24h after injury. While CsA was able to improve injury-induced decreases in state V(I) respiration in both populations, the improvements were not statistically significant.

State V(II) respiration is assessed following addition of the complex-I inhibitor rotenone, and the complex-II substrate succinate. Therefore, decreases in state V(II) respiration are indicative of defects in complex-II driven respiration. Severe CCI significantly reduced state V(II) respiration for both synaptic and non-synaptic mitochondria 24h after injury. While, CsA improved injury-induced decreases in complex-II driven respiration in both populations, the improvements only reached statistical significance in the synaptic population.

In summary, synaptic mitochondria sustain more damage 24h after severe CCI than non-synaptic mitochondria, as best evidenced by the changes in RCR. This is in agreement with previous work indicating that synaptic mitochondria are more susceptible to dysfunction. For example, synaptic mitochondria are more susceptible to damage 3h after moderate CCI compared with non-synaptic mitochondria, an effect that is compounded by aging. [41] In addition, *in-vitro*, healthy synaptic mitochondria have a decreased ability to buffer calcium before undergoing permeability transition compared with non-synaptic mitochondria. [37]

Several hypotheses have been offered to explain the increased vulnerability of synaptic mitochondria compared with non-synaptic mitochondria, including high

concentrations of cyclophilin D, leading to increased susceptibility toward calcium-induced permeability transition, [38] as well as increased exposure of synaptic mitochondria to oxidative damage. [37, 38] Because non-synaptic mitochondria contain both neuronal and non-neuronal cell types, however, and mitochondria isolated from neurons and glia have differing properties, [38, 296] part of the increased susceptibility of synaptic mitochondria to injury may be because synaptic mitochondria represent a more purely neuronal population, [37-39] rather than their specific subcellular localization to the pre-synaptic terminal. It is likely, however, that both cell type and subcellular localization contribute to synaptic mitochondria vulnerability.

These results also indicate that intraperitoneal administration of CsA (20 mg/kg) 15 min after injury attenuates respiratory dysfunction in both populations 24h after severe CCI, with a statistically significant improvement being seen in the synaptic population. Although there was a significant decrease in each respiration state following injury for the non-synaptic mitochondria, the non-synaptic RCR was unaffected by injury, indicating no overall bioenergetics dysfunction. [30] It is therefore likely that the improvements CsA had on the non-synaptic respiration states were only non-significant due to a lack of robust injury effect in this population, and that CsA would offer significant improvements at time points later than 24h when non-synaptic mitochondria are more significantly impaired.

The fact that CsA is able to significantly protect synaptic mitochondria following injury is impressive, because synaptic mitochondria do not always respond as favorably to pharmaceutical intervention as the non-synaptic population. For example, following spinal cord injury, the catalytic peroxynitrite inhibitor, tempol, is only effective in non-synaptic mitochondria, while the mitochondrial uncoupler 2-4 DNP works in both populations, but has a shorter therapeutic window in the synaptic mitochondria. [50]

Future studies will investigate if there is, indeed, a difference in the therapeutic window for CsA between synaptic and non-synaptic mitochondria. If so, studies may explain the fact that while CsA is able to improve cortical tissue sparing when administration is delayed up to 8h, it is significantly more protective when administered within 3h of injury. [122] Further, the ability of CsA to protect synaptic neuronal mitochondrial respiration is made more impressive by the knowledge that there are higher concentrations of the CsA target protein cyclophilin D in synaptic mitochondria, [37] gamma-aminobutyric acid-ergic interneurons, [39] and cultured neurons when compared to cultured astrocytes. [38]

In fact, *in-vitro* healthy synaptic mitochondria require higher concentrations of CsA to prevent calcium-induced permeability transition. [38] Future studies will therefore evaluate the ability of CsA to attenuate calcium-induced permeability transition in both populations after injury, as well as the ability of CsA to retain its synaptic neuroprotective effect at time points beyond 24h.

## **Conclusion**

This study confirms that synaptic mitochondria are more vulnerable than non-synaptic mitochondria after experimental TBI, and therefore emphasizes the need for further characterization of synaptic and non-synaptic mitochondria after experimental TBI, including the contribution each population makes to TBI pathology, as well as the response each population has to mitochondrial-directed pharmacotherapies.

While the pathology of TBI is complex and factors other than mitochondrial dysfunction contribute to downstream processes such as cytoskeletal degradation, neurodegeneration, and neurologic impairment, it is likely that successful protection of the more vulnerable synaptic population greatly contributes to inhibition of these

downstream processes. Because this study confirms the ability of CsA to significantly improve synaptic respiration following injury, CsA remains a promising neuroprotective candidate for the treatment of TBI.

### **Acknowledgments**

This work was supported by 5R01 NS083405, 5R01 NS084857, 5P30 0NS051220, 1F30 NS096876, and funding from the Kentucky Spinal Cord & Head Injury Research Trust (KSCHIRT).

### **CHAPTER THREE:**

#### **Continuous Infusion of Phenezine, Cyclosporine A, or Their Combination: Evaluation of Mitochondrial Bioenergetics, Oxidative Damage, and Cytoskeletal Degradation Following Severe Controlled Cortical Impact Traumatic Brain Injury in Rats**

**Preface:** Chapter Three has been adapted from: **Kulbe JR**, Singh IN, Wang JA, Cebak JE, Hall ED. Continuous infusion of phenelzine, cyclosporine A, or their combination: evaluation of mitochondrial bioenergetics, oxidative damage, and cytoskeletal degradation following severe controlled cortical impact traumatic brain injury in rats. *Journal of Neurotrauma* 35(11):1280-1293 (2018). DOI: 10.1089/neu.2017.5353. (*Mary Ann Leibert, Inc., New York, NY*). Figures have been renumbered and formatted in accordance with University of Kentucky Graduate School requirements. The figures 3.7-3.9 have been added and portions of the Discussion and Conclusion have been expanded upon. The data which appears in Figure 3.6 was generated by Dr. John E. Cebak, Ph.D. and was first presented in his University of Kentucky Doctoral Dissertation, *“Mitochondrial and neuroprotective effects of phenelzine related to scavenging of neurotoxic lipid peroxidation products”* (2015).



## **Introduction**

In the United States, there are more than 2.5 million documented cases of traumatic brain injury (TBI) annually [2], which resulted in direct and indirect medical costs of over \$75 billion dollars in 2010, with the most severe injuries (those resulting in hospitalization and death) accounting for 90% of these costs [10, 11]. Currently, there are over 5 million people in the U.S. living with a TBI-related disability [12]. Further, over 50% of persons hospitalized due to TBI will continue to suffer from a TBI-associated disability more than a year following injury [13]. Such disabilities can include cognitive, physical, and emotional impairments [12]. To date, there are no FDA-approved pharmacotherapies for neuroprotection following clinical TBI [1].

Although numerous reasons have been cited for the failure of neuroprotective compounds in clinical TBI studies, [9, 213], due to the complex secondary injury cascade which occurs following injury and encompasses a multitude of neurodegenerative processes, single agent therapies may be unlikely to succeed at completely preventing the devastating neurological consequences that occur following injury [213]. In fact, in 2008, the National Institutes of Health (NIH), in conjunction with the Department of Veterans Affairs, convened a workshop focusing on development of combinatorial approaches for the treatment of traumatic brain injury over the first 72h following injury; [213] underscoring the importance of developing multi-mechanistic combinational neuroprotective approaches for acute TBI.

Following injury (**Fig. 3.1**), increases in intracellular calcium are taken up by mitochondria in an attempt to maintain calcium homeostasis [22, 23]. However, high levels of intra-mitochondrial calcium lead to opening of the mitochondrial permeability transition pore (mPTP), resulting in collapse of the mitochondrial membrane potential, cessation of adenosine triphosphate (ATP) production, and release of calcium back into the cytosol [51]. Further, increases in intra-mitochondrial calcium can lead to increased generation of mitochondrial-produced reactive oxygen and nitrogen species (ROS/RNS) [17, 163]. For example, as the levels of mitochondrial calcium increase and the mitochondrial membrane potential depolarizes, electron transport slows, allowing electrons to leak from complex-I to combine with  $O_2$  to form superoxide radical ( $O_2^{\bullet-}$ ) [307], which can go on to react with nitric oxide radicals ( $NO^{\bullet}$ ) generated by the calcium-activated mitochondrial nitric oxide synthase (mtNOS), forming peroxynitrite anion ( $ONOO^-$ ) [17, 53]. Peroxynitrite is unique in the fact that it has quite a large diffusion radius, thus allowing it to cross membranes, expanding its area of devastation [308]. Peroxynitrite is either protonated to form peroxynitrous acid ( $ONOOH$ ) or reacts with  $CO_2$  to form nitrosoperoxy carbonate ( $ONOOCO_2^-$ ), followed by decomposition into the highly reactive radicals, hydroxyl ( $\bullet OH$ ), nitrogen dioxide ( $\bullet NO_2$ ) or carbonate ( $CO_3^{\bullet-}$ ) [17, 55, 308].

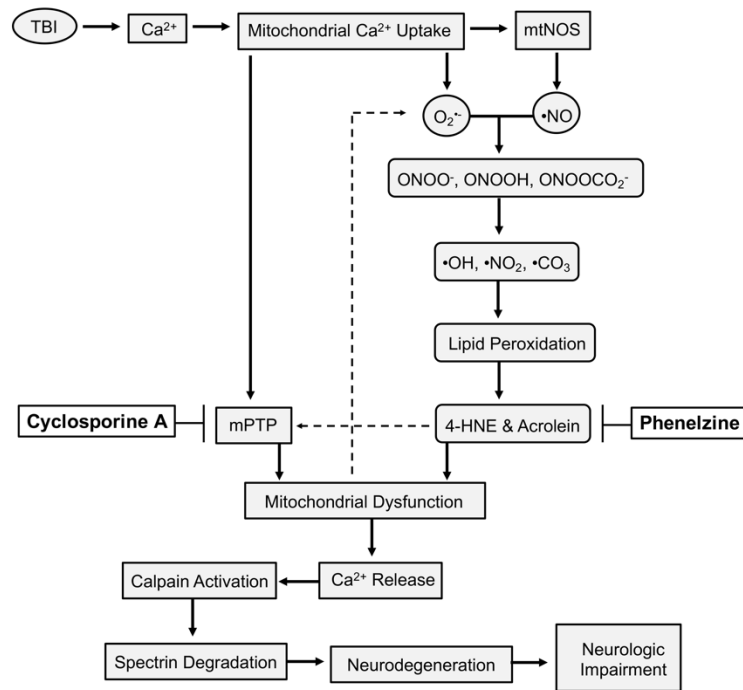


**Figure 3.1 Simplified schematic of TBI pathophysiology and phenelzine and cyclosporine A mechanisms of action.** The role of mitochondrial dysfunction and lipid peroxidation following traumatic brain injury (TBI) and the mechanisms of action of phenelzine (PZ) and cyclosporine A (CsA). Following injury, mitochondria uptake calcium ( $\text{Ca}^{2+}$ ) which leads to opening of the mitochondrial permeability transition pore (mPTP), generation of superoxide ( $\text{O}_2^{\bullet-}$ ) and activation of mitochondrial nitric oxide synthase (mtNOS), which leads to formation of nitric oxide ( $\bullet\text{NO}$ ).  $\text{O}_2^{\bullet-}$  and  $\bullet\text{NO}$  combine to form peroxynitrite anion ( $\text{ONOO}^-$ ), which can be protonated or react with  $\text{CO}_2$  to form peroxynitrous acid ( $\text{ONOOH}$ ) or nitrosoperoxycarbonate ( $\text{ONOOCO}_2^-$ ), followed by degradation into hydroxyl ( $\bullet\text{OH}$ ), nitrogen dioxide ( $\bullet\text{NO}_2$ ) or carbonate ( $\text{CO}_3^{\bullet-}$ ), highly reactive radicals which initiate lipid peroxidation (LP). LP terminates with the formation of the LP-derived aldehydes 4-hydroxynonenal (4-HNE) and acrolein. 4-HNE and acrolein bind mitochondrial proteins causing mitochondrial dysfunction and can exacerbate opening of the mPTP. Mitochondrial dysfunction itself exacerbates the reactive oxygen species/nitrogen species-lipid peroxidation-aldehyde cascade.  $\text{Ca}^{2+}$  is released back into the cytosol upon mPTP opening, activating calpain, which degrades cytoskeletal  $\alpha$ -spectrin, resulting in neurodegeneration and neurologic impairment. CsA inhibits mPTP. PZ scavenges the LP-derived aldehydes 4-HNE and acrolein.

These highly reactive radicals initiate lipid peroxidation (LP) of polyunsaturated fatty acids, which are highly enriched in brain cells and cellular and organelle membranes [1, 55]. As lipid peroxy radicals are formed, they are able to react with neighboring polyunsaturated acids, resulting in a self-propagating process [1, 55]. Lipid peroxidation terminates upon formation of LP-derived aldehydes, such as 4-hydroxynonenal (4-HNE) and acrolein [1, 55]. These LP-derived aldehydes have multiple reactive sites, making it possible for them to covalently bind lysine, histidine, arginine and cysteine protein residues through both Schiff base and Michael addition reactions [1, 79-81]. Once covalently bound to proteins, including mitochondrial proteins, LP-derived aldehydes induce protein dysfunction and enzyme inactivation, neurotoxicity and cellular death [77, 84-89]. In the case of mitochondria, binding of LP-derived aldehydes exacerbates impairment of bioenergetics and generation of the ROS/RNS-lipid peroxidation-aldehyde cascade, as well as opening of mPTP [29, 72, 93, 100-102]. Once permeability transition occurs and calcium has been released back into the cytosol, it can activate calcium-dependent proteases, such as calpain, which can cleave cytoskeletal proteins, such as  $\alpha$ -spectrin, resulting in further downstream consequences, including neurodegeneration and neurologic impairment [1, 51, 55, 56, 70, 109, 110].

As central mediators of the TBI secondary injury cascade, both mitochondria and LP-derived aldehydes make promising neuroprotective targets. In fact, several pre-clinical studies have demonstrated the neuroprotective ability of agents which aim to prevent mitochondrial dysfunction or attenuate lipid peroxidation [58, 69-72, 75, 109, 110, 123, 125, 226, 249, 257, 309, 310]. One of the most extensively investigated mitochondrial protective agents, the FDA-approved immunosuppressant cyclosporine A (CsA), is capable of inhibiting the mPTP [110, 218, 219, 226] (**Fig. 3.1**), and has been shown to be safe for use clinically in severe TBI patients [234, 235]. Another drug,

phenelzine (PZ) (**Fig. 3.1**), which is an FDA-approved irreversible non-selective monoamine oxidase inhibitor, contains a hydrazine moiety (-NH-NH<sub>2</sub>), which is capable of scavenging LP-derived aldehydes [71, 72, 74, 76, 198, 258, 262, 311, 312]. Importantly, scavenging of LP-derived aldehydes is likely to offer a more clinically translational approach in regards to therapeutic window, compared to conventional antioxidants, as LP-derived aldehydes are longer lived than their highly reactive free radical predecessors [79, 81, 259].

Both CsA and PZ have individually been shown capable of attenuating pathophysiologic processes in pre-clinical models of neurotrauma [71, 72, 74, 76, 110, 122-124, 136, 223-227, 292, 294, 298, 309, 313]. Therefore, it follows that the mPTP inhibitor CsA and the LP-derived aldehyde scavenger PZ may together enhance neuroprotection over either agent alone through the combining of distinct but complementary mechanisms. In fact, CsA was one of the agents identified as a candidate for combinational therapy during the NIH combinational therapy TBI workshop [213]. Additionally, as the first 72h represents a critical time period following injury [213], including the peak of mitochondrial dysfunction, lipid peroxidation, and neuronal cytoskeletal ( $\alpha$ -spectrin) degradation [73], it follows that continuous drug infusion over the first 72h following injury may also lead to optimal neuroprotective effects [79].

This is the first study to investigate the neuroprotective effects of the combination CsA and PZ 72h following severe controlled cortical impact injury (CCI), a model combining focal, contusive, hemorrhagic and diffuse injury pathologies [128, 314]. Additionally, this is the first study to investigate the effects of 72h continuous infusion of CsA, PZ, and the combination on mitochondrial dysfunction, aldehydic modification of mitochondrial proteins, and  $\alpha$ -spectrin degradation 72h following severe CCI, using a CsA dosing paradigm that previously has been shown to improve cortical tissue sparing

following CCI [122], and a PZ dosing paradigm based upon a 12hr intermittent dosing protocol which has previously been shown to be neuroprotective following CCI [72].

## **Methods**

### **Animals**

Three-month-old male Sprague-Dawley rats (Harlan, Indianapolis, IN) were housed in the Division of Laboratory Animal Resources of the University of Kentucky Medical Center. All animal and husbandry were conducted in accordance with the University of Kentucky Institutional Animal Care and Use Committee. Animals were housed in a 12hr light and dark cycle and allowed food and water *ad libitum*.

### **Experimental Design**

Two cohorts of animals were randomly assigned to the following subcutaneous continuous infusion dosing paradigm experimental groups: sham, vehicle, PZ, CsA, and phenelzine + cyclosporine A (PZ + CsA), with one cohort of animals being used for all mitochondria experiments and another cohort of animals being used for cortical  $\alpha$ -spectrin analysis. An additional cohort of animals was randomly assigned to the following 12hr intermittent PZ dosing paradigm experimental groups: sham, vehicle, or PZ. Following injury and closing of the craniotomy site, all animals in the subcutaneous continuous infusion dosing paradigm, other than sham, were immediately implanted with two subcutaneous osmotic pumps loaded with either drug or vehicle, and additionally received two bolus doses of either drug or vehicle 15 min following impact. Animals within the subcutaneous continuous infusion dosing paradigm received the following doses: i) sham (no impact injury, no drug administration); ii) vehicle (15 min post-injury bolus dose: intraperitoneal cremophor/ethanol/saline; 15 min post-injury bolus dose: subcutaneous saline; subcutaneous osmotic pump: cremophor/ethanol/saline; subcutaneous osmotic pump: saline); iii) PZ (15 min post-injury bolus dose: intraperitoneal cremophor/ethanol/saline; 15 min post-injury bolus dose: subcutaneous

10mg/kg PZ in saline; subcutaneous osmotic pump: cremophor/ethanol/saline; subcutaneous osmotic pump: 10mg/kg/day/3d saline); iv) CsA (15 min post-injury bolus dose: intraperitoneal 20mg/kg CsA in cremophor/ethanol/saline; 15 min post-injury bolus dose: subcutaneous saline; subcutaneous osmotic pump: 10mg/kg/day/3d CsA in cremophor/ethanol/saline; subcutaneous osmotic pump: saline) v) PZ + CsA (15 min post-injury bolus dose: intraperitoneal 20mg/kg CsA in cremophor/ethanol/saline; 15 min post-injury bolus dose: subcutaneous 10mg/kg PZ in saline; subcutaneous osmotic pump: 10mg/kg/day/3d CsA in cremophor/ethanol/saline, subcutaneous osmotic pump: 10mg/kg/day/3d PZ in saline) **(Table 3.1)**. Following euthanasia one group of the subcutaneous continuous infusion dosing paradigm animals were used for mitochondria experiments while the other group was utilized for analysis of  $\alpha$ -spectrin degradation.

The third cohort of animals was assigned to the 12hr intermittent PZ dosing paradigm. Animals in the 12hr intermittent PZ dosing paradigm received the following dosing schedule: sham (no impact injury, no drug administration); vehicle (15 min post-injury bolus dose of subcutaneous saline, followed by subcutaneous bolus saline every 12h up to and including 60h); PZ (15 min post-injury bolus dose of 10mg/kg PZ in saline, followed by subcutaneous bolus 5mg/kg PZ in saline every 12h up to and including 60h) **(Table 3.2)**.



**Table 3.1 Subcutaneous Continuous Infusion Dosing Paradigm**

<b>Group</b>	<b>Loading Dose (15min post-injury)</b>	<b>Osmotic Pump (Immediate)</b>
Sham	None	None
Vehicle	Saline s.c. Cremophor i.p.	Saline Cremophor
Phenelzine	10mg/kg s.c. PZ Cremophor i.p.	10mg/kg/day/3d PZ Cremophor
Cyclosporine A	Saline s.c. 20mg/kg i.p. CsA	Saline 10mg/kg/day/3d CsA
Phenelzine + Cyclosporine A	10mg/kg s.c. PZ 20mg/kg i.p. CsA	10mg/kg/day/3d PZ 10mg/kg/day/3d CsA

Demonstration of the subcutaneous continuous infusion dosing paradigm followed. Osmotic pumps were placed subcutaneously immediately following impact injury and closure of the craniotomy site. Pumps were removed 72h later at the time of euthanasia. Loading doses were administered 15 min following impact. Cremophor (saline/650mg cremophor/32.9% ethanol/ml) was prepared to deliver an equal amount cremophor as received by CsA animals. Saline was prepared to deliver an equal amount of saline as PZ animals. PZ, phenelzine (in saline); CsA, cyclosporine A (in saline/650mg cremophor/32.9% ethanol/ml); s.c, subcutaneous, i.p., intraperitoneal.

**Table 3.2 Phenezine 12hr Intermittent Dosing Paradigm**

<b>Group</b>	<b>Loading Dose (15min post-injury)</b>	<b>Maintenance dosing: 12h, 24h, 36h, 48h, 60h</b>
Sham	None	None
Vehicle	Saline s.c.	Saline s.c.
Phenezine	10mg/kg s.c. PZ	5mg/kg s.c. PZ

Demonstration of the PZ 12hr intermittent dosing paradigm followed. Loading doses were administered 15 min following impact. Maintenance doses were administered every 12h up to and including 60h. Animals were euthanized 72h post-injury. Saline was prepared to deliver an equal amount of saline as PZ animals. PZ, phenezine (in saline); s.c., subcutaneous.

## **Controlled Cortical Impact Traumatic Brain Injury**

Animals were anesthetized using 4% isoflurane, shaved, and placed into a stereotaxic frame (David Kopf, Tujunga, CA), where isoflurane was maintained at 3% for the duration of the procedure. A midline incision was made to expose the skull, and a 6 mm craniotomy was created lateral to the sagittal suture and midway between lambda and bregma using a Michele Trephine (Miltex, Bethpage, NY). The exposed brain with intact dura received a severe CCI using a computer-controlled pneumatic impact device (TBI 03010; Precision Systems and Instrumentation, Fairfax Station, VA) fitted with a 5 mm beveled tip and set to impact at a depth of 2.2 mm with a 500 ms dwell time and an impact velocity of ~3.5 m/s, as described previously [71]. After injury, Surgicel (Johnson & Johnson, Arlington, TX) was placed onto the dura and an 8 mm plastic disk was affixed to the skull using tissue adhesive (Gesswein, Bridgeport, CT) to close the craniotomy site, and the incision was closed using wound clips. Sham animals underwent the same procedure but did not receive an impact injury.

## **Loading Dose Drug Administration**

Fifteen minutes following injury, animals assigned to the subcutaneous continuous infusion dosing paradigm, received a loading dose of the appropriate drug. CsA (Perrigo; Minneapolis, MN; 50mg/ml in saline/650mg cremophor/32.9% ethanol/ml) was administered intraperitoneal at 20mg/kg [122, 227]. Cremophor (CsA vehicle) was administered intraperitoneal to deliver an equivalent volume of saline/cremophor/ethanol. Phenelzine (MP Biochemicals, Solon, OH) was administered subcutaneously at 10mg/kg in saline [72]. Saline (PZ vehicle) was administered subcutaneously to deliver an equivalent volume of saline. Sham animals did not receive injections.

## **Osmotic Pump Preparation**

The day prior to implantation, osmotic pumps (2ML1, Alzet osmotic pumps, Cupertino, CA) were loaded with appropriate drug concentrations and allowed to prime overnight at 37°C and then maintained at 37°C until the time of implantation. CsA pumps were loaded to deliver 10mg/kg/day/3d of CsA (Perrigo; Minneapolis, MN; 50mg/ml in saline/650mg cremophor/32.9% ethanol/ml) based on a previously optimized CsA dosing protocol [122, 227]. Cremophor pumps (CsA vehicle) were loaded to deliver an equivalent volume of saline/cremophor/ethanol. PZ pumps were loaded to deliver 10mg/kg/day/3d of PZ (MP Biochemicals, Solon, OH) in saline based on an approximate 12h plasma half-life in humans and a previously optimized 12hr intermittent dosing protocol [72]. Saline pumps (PZ vehicle) were loaded to deliver an equivalent amount saline.

## **Implantation of Osmotic Pumps**

Immediately following impact injury and closure of the craniotomy site, a sagittal incision was made approximately half-way down the animal's back. Hemostats were used to create a subcutaneous pocket anterior and posterior to the incision site. Pre-loaded osmotic pumps (2ML1, Alzet osmotic pumps, Cupertino, CA) were inserted into the subcutaneous pockets with the flow moderator positioned away from the incision site. The incision was then closed with wound clips, and animals were allowed to recover while body temperature was maintained at 37°C using a warm water circulating heating pad. Vehicle animals received a saline pump (PZ's vehicle) and a cremophor pump (CsA's vehicle). PZ animals received a PZ pump and a cremophor pump. CsA animals received a CsA pump and a saline pump. PZ + CsA animals received a PZ pump and a CsA pump. Sham animals did not undergo pump implantation.

### **Phenelzine 12hr Intermittent Dosing Protocol**

Fifteen minutes following injury, PZ animals received 10mg/kg PZ (MP Biochemicals, Solon, OH) in saline subcutaneously, followed by 5mg/kg PZ subcutaneously every 12h up to including 60h [72]. Vehicle animals received an equivalent amount of saline at the appropriate time point. Sham animals did not receive injections (**Table 3.2**).

### **Tissue Extraction and Pump Removal**

Animals were euthanized 72h following injury, which represents the peak of mitochondrial dysfunction, LP and  $\alpha$ -spectrin degradation [73], using CO<sub>2</sub>, followed by decapitation. An 8 mm cortical punch centered over the injury was collected in order to collect the epicenter of injury and the penumbral region. Cortical punches were either processed for isolation of mitochondria or cortical protein. Pumps were removed and residual volumes were measured to ensure proper drug delivery. Animals in which pumps did not run properly, as determined by the removed pumps still having most of their drug still in the pumps, were removed from the study.

### **Isolation of Ficoll-Purified Cortical Mitochondria**

Mitochondria were isolated as described previously [71, 163]. Cortical punch tissue was immediately homogenized in ice-cold isolation buffer (215 mmol/L mannitol, 75 mmol/L sucrose, 0.1% bovine serum albumin, 20mmol/L HEPES, 1mmol/L EGTA, pH 7.2) using Potter-Elvehjem homogenizers. Samples were then centrifuged twice at 1300 g for 3 min at 4°C. Supernatants were additionally centrifuged at 13,000 g for 10 min at 4°C. The crude mitochondrial pellet was resuspended in isolation buffer, placed into a nitrogen bomb at 1200 psi for 10 min at 4°C to release synaptic mitochondria, and then layered onto a discontinuous 7.5% and 10% Ficoll gradient and centrifuged for 100,000

g for 30 min at 4°C. The mitochondrial pellet was resuspended in isolation buffer without EGTA, centrifuged at 10,000 g for 10 min at 4°C to remove Ficoll, and then resuspended in isolation buffer without EGTA to a final concentration of ~10mg/kg. Protein concentrations were determined with a BCA protein assay kit (ThermoFisher, Cleveland, OH) and measured at absorbance 562nm with a BioTek Synergy HT plate reader (Winooski, VT).

### **Mitochondrial Bioenergetics Analysis**

Mitochondrial respiratory function was measured using a Clark-type electrode in a continuously stirred, sealed, and thermostatically controlled chamber maintained at 37°C (Oxytherm System; Hansatech Instruments, Norfolk, UK). Mitochondria (60 µg – 80 µg) were placed into the chamber containing 250 µl of KCl respiration buffer (125 mmol/L KCl, 2 mmol/L MgCl<sub>2</sub>, 2.5 mmol/L KH<sub>2</sub>PO<sub>4</sub>, 0.1% bovine serum albumin, 20 mmol/L HEPES, pH 7.2). Following a 1 minute equilibration, complex-I respiration was initiated by addition of 5 mmol/L pyruvate and 2.5 mmol/L malate. Two boluses of 150 µmol/L ADP were added and state III respiration was monitored. The ATP synthase inhibitor, oligomycin (2 µmol/L) was added and state IV respiration was monitored. The protonophore FCCP (2 µmol/L) was added and maximal state V(I) respiration was monitored. Complex-I was inhibited by addition of 100 nmol/L rotenone. Complex-II maximal respiration was initiated by the addition of succinate (10 mmol/L) and state V(II) was monitored. Respiratory rates for individual states were calculated as nmol O<sub>2</sub> per mg of protein per min. Respiratory control ratio (RCR) was calculated by dividing state III respiration rate (second bolus of ADP) by state IV respiration rate [163, 248]. Following bioenergetics analysis, remaining mitochondrial protein was immediately frozen at -80°C for use in Western blot.

## **Western Blot Analysis: Cortical $\alpha$ -Spectrin Degradation & Lipid Peroxidation-Induced Cortical Mitochondrial Oxidative Damage**

Cortical punch tissue collected from the cohorts of animals designated for analysis of  $\alpha$ -spectrin degradation was immediately placed into ice-cold Triton-lysis buffer (1% Triton, 20 mmol/L Tris-HCl, 150 mmol/L NaCl, 5 mmol/L EGTA, 10 mmol/L EDTA, 20 mmol/L HEPES, pH 7.4) containing protease inhibitors (Complete Mini™ Protease Inhibitor Cocktail tablet, Roche). Similarly, mitochondria protein being stored at -80°C following bioenergetics analysis was thawed and resuspended in lysis buffer. All samples were sonicated, vortexed, and then centrifuged at 14,000 rpm for 30 min at 4°C. Protein concentrations were determined with a BCA protein assay kit (ThermoFisher, Cleveland, OH) and measured at absorbance 562nm with a BioTek Synergy HT plate reader (Winooski, VT). Due to the limited yield of mitochondrial protein following Ficoll-purified isolation, bioenergetics analysis and processing for Western blot, only samples containing greater than 100  $\mu$ g of protein, allowing for analysis of both 4-HNE and acrolein, were utilized for Western Blot. For analysis of  $\alpha$ -spectrin, 10  $\mu$ g of protein was run on a 3-8% Tris-Acetate Criterion™ XT polyacrylamide gel (Bio-Rad, Hercules, CA) with XT Tricine Running Buffer (Bio-Rad, Hercules, CA). For analysis of 4-HNE or acrolein, 50  $\mu$ g of protein was run on a 4-12% Tris-Acetate Criterion™ XT polyacrylamide gel (Bio-Rad, Hercules, CA) with MOPS buffer (Bio-Rad, Hercules, CA). Following separation of proteins by polyacrylamide gel, protein was transferred to a nitrocellulose membrane using a semi-dry electro-transferring unit for 15 min ( $\alpha$ -spectrin) or 1hr (4-HNE, acrolein) at 15V. Following transfer, membranes were blocked at room temperature for 1hr in Tris-buffered saline (TBS) containing 5% milk. Membranes were incubated with the following primary antibodies in TBS with Tween (TBST) containing 5% milk overnight at 4°C: mouse monoclonal anti- $\alpha$ -spectrin (Enzo, Farmingdale, NY,

1:5,000), rabbit polyclonal anti- $\beta$ -tubulin (Abcam, Cambridge, CA, 1:5,000-1:10,000), rabbit polyclonal anti-4HNE (Alpha Diagnostics, San Antonio, TX, 1:1,000), rabbit polyclonal anti-acrolein (Abcam, Cambridge, CA, 1:2,000), and rabbit polyclonal anti-VDAC (EMD Millipore, Billerica, MA, 1:30,000). Membranes were washed in TBST following incubation with primary antibody.

Membranes were incubated with the following secondary antibodies in TBST with 5% milk for one 1hr at room temperature: goat anti-rabbit IgG IRdye800CW (Rockland, Limerick, PA, 1:5,000), goat anti-rabbit IgG Alexa Fluor 680 (ThermoFisher, Waltham, MA 1:10,000), and goat anti-mouse IgG IRDye800CW (Rockland, Limerick, PA, 1:5,000). Membranes were washed in TBST, and then imaged and quantified using the Li-Cor Odyssey Infrared Imaging System (Li-Cor Biosciences, Lincoln, NE). For analysis of  $\alpha$ -spectrin degradation,  $\alpha$ -spectrin breakdown products were normalized to tubulin. For analysis of mitochondrial protein, 4-HNE and acrolein were normalized to VDAC. A protein loading control was loaded onto each gel to control for inter-gel variability. For  $\alpha$ -spectrin, bands at 145kD and 150kD were analyzed. Due to broad binding of 4-HNE and acrolein to lysine, histidine, arginine, cysteine protein residues, as well as differential banding patterns between 4-HNE and acrolein [73], mitochondrial 4-HNE was analyzed between 80kD-150kD and mitochondrial acrolein was analyzed between 60kD-100kD.

### **Statistical Analysis**

Statistical analysis was conducted using Prism version 7.0 (Graph Pad, San Diego, CA). Results are reported as mean  $\pm$  standard deviation. Analysis was done by one-way analysis of variance (ANOVA), followed by Student-Newman-Keuls (SNK) *post-*



*hoc* analysis when appropriate. A p-value  $<0.05$  was considered significant. Grubb's test was used to remove statistical outliers.

## **Results**

### **CCI-TBI Induced Mitochondrial Bioenergetics Dysfunction**

#### **State III: ADP Activation of ATP Synthase and Coupling of Electron Transport with Oxidative Phosphorylation**

A one-way ANOVA revealed a statistically significant effect across all groups ( $F_{[4,35]} = 19.45, p < 0.0001$ ). *Post-hoc* testing (SNK) revealed that compared with sham, state III respiration was significantly impaired for vehicle ( $p < 0.0001$ ), PZ ( $p < 0.0001$ ), CsA ( $p < 0.0001$ ), and PZ + CsA ( $p < 0.0001$ ), thus indicating that severe CCI significantly decreased state III respiration compared with sham, and that 72h subcutaneous continuous infusion of neither PZ, CsA, nor PZ + CsA was able to significantly attenuate CCI-induced decreases in state III respiration (**Fig. 3.2A**).

#### **State IV: Oligomycin Inhibition of ATP Synthase**

A one-way ANOVA revealed a statistically significant effect across all groups ( $F_{[4,35]} = 11.44, p < 0.0001$ ). *Post-hoc* testing (SNK) revealed that compared with sham, state IV respiration was significantly impaired for vehicle ( $p < 0.0001$ ), PZ ( $p < 0.0001$ ), CsA ( $p < 0.001$ ), and PZ + CsA ( $p < 0.0001$ ), thus indicating that severe CCI significantly decreased state IV respiration compared with sham, and that 72h subcutaneous continuous infusion of neither PZ, CsA, nor PZ + CsA was able to significantly attenuate CCI-induced decreases in state IV respiration (**Fig. 3.2B**).

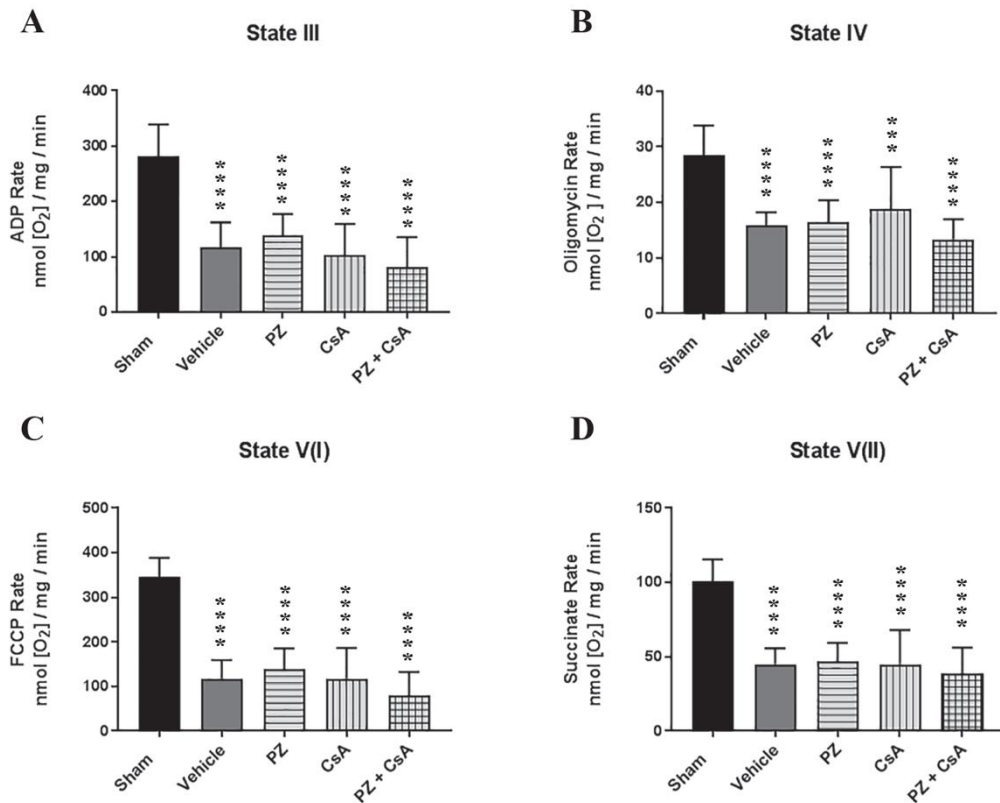


**Figure 3.2 State III – State V(II): PZ, CsA, and PZ + CsA.** Effect of the 15 min post-injury loading dose + 72h subcutaneous continuous infusion dosing paradigm on mitochondrial oxygen consumption 72h following severe cortical impact injury for **(A)** state III (pyruvate/malate/ADP), **(B)** state IV (oligomycin), **(C)** state V(I) (FCCP), and **(D)** state V(II) (rotenone/succinate). Sham (no impact injury, no drug administration). Vehicle (15 min post-injury bolus dose: intraperitoneal cremophor/ethanol/saline; 15 min post-injury bolus dose: subcutaneous saline; subcutaneous osmotic pump: cremophor/ethanol/saline; subcutaneous osmotic pump: saline). PZ = phenelzine (15 min post-injury bolus dose: intraperitoneal cremophor/ethanol/saline; 15 min post-injury bolus dose: subcutaneous 10mg/kg PZ in saline; subcutaneous osmotic pump: cremophor/ethanol/saline; subcutaneous osmotic pump: 10mg/kg/day/3d PZ in saline). CsA = cyclosporine A (15 min post-injury bolus dose: intraperitoneal 20mg/kg CsA in cremophor/ethanol/saline; 15 min post-injury bolus dose: subcutaneous saline; subcutaneous osmotic pump: 10mg/kg/day/3d CsA in cremophor/ethanol/saline; subcutaneous osmotic pump: saline). PZ + CsA + cyclosporine A (15 min post-injury bolus dose: intraperitoneal 20mg/kg CsA in cremophor/ethanol/saline; 15 min post-injury bolus dose: subcutaneous 10mg/kg PZ in saline; subcutaneous osmotic pump: 10mg/kg/day/3d CsA in cremophor/ethanol/saline; subcutaneous osmotic pump: 10mg/kg/day/3d PZ in saline). One-way analysis of variance followed by Student-Newman-Keuls *post-hoc* test. \*\*\* $p < 0.001$ , \*\*\*\* $p < 0.0001$  compared with sham. Error bars represent mean  $\pm$  standard deviation.  $n = 8$  rats per group.

Respiratory Control Ratio (RCR): State III Respiration / State IV Respiration

A one-way ANOVA revealed a statistically significant effect across all groups ( $F_{[4,35]} = 5.961$ ,  $p=0.0009$ ). *Post-hoc* testing (SNK) revealed that compared with sham, RCR was significantly impaired for vehicle ( $p<0.05$ ), CsA ( $p<0.01$ ), and PZ + CsA ( $p<0.01$ ), whereas PZ was not significantly different from either vehicle ( $p>0.05$ ) or sham ( $p>0.05$ ), thus indicating that severe CCI significantly decreased RCR compared with sham, and that 72h subcutaneous continuous infusion of neither CsA, nor PZ + CsA was able to significantly attenuate CCI-induced decreases in RCR. However, PZ was able to maintain RCR, compared with sham (**Fig 3.3**).

State V(I): FCCP Protonophore Addition and Initiation of Maximal Complex-I Respiration

A one-way ANOVA revealed a statistically significant effect across all groups ( $F_{[4,35]} = 33.55$ ,  $p<0.0001$ ). *Post-hoc* testing (SNK) revealed that compared with sham, state V(I) respiration was significantly impaired for vehicle ( $p<0.0001$ ), PZ ( $p<0.0001$ ), CsA ( $p<0.0001$ ), and PZ + CsA ( $p<0.0001$ ), thus indicating that severe CCI significantly decreased state V(I) respiration compared with sham, and that 72h subcutaneous continuous infusion of neither PZ, CsA, nor PZ + CsA was able to significantly attenuate CCI-induced decreases in state V(I) respiration (**Fig. 3.2C**).

## Respiratory Control Ratio (RCR)

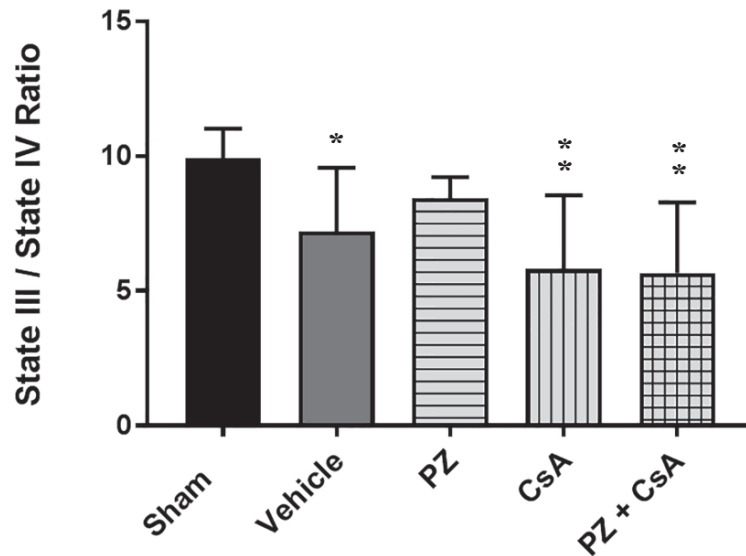


**Figure 3.3 RCR: PZ, CsA, and PZ + CsA** Effect of the 15 min post-injury loading dose + 72h subcutaneous continuous infusion dosing paradigm on mitochondrial respiratory control ratio (state III respiration / state IV respiration) 72h following severe cortical impact injury. Sham (no impact injury, no drug administration). Vehicle (15 min post-injury bolus dose: intraperitoneal cremophor/ethanol/saline; 15 min post-injury bolus dose: subcutaneous saline, subcutaneous osmotic pump: cremophor/ethanol/saline; subcutaneous osmotic pump: saline). PZ = phenelzine (15 min post-injury bolus dose: intraperitoneal cremophor/ethanol/saline; 15 min post-injury bolus dose: subcutaneous 10mg/kg PZ in saline; subcutaneous osmotic pump: cremophor/ethanol/saline; subcutaneous osmotic pump: 10mg/kg/day/3d PZ in saline). CsA = cyclosporine A (15 min post-injury bolus dose: intraperitoneal 20mg/kg CsA in cremophor/ethanol/saline; 15 min post-injury bolus dose: subcutaneous saline; subcutaneous osmotic pump: 10mg/kg/day/3d CsA in cremophor/ethanol/saline; subcutaneous osmotic pump: saline). PZ + CsA (15 min post-injury bolus dose: intraperitoneal 20mg/kg CsA in cremophor/ethanol/saline; 15 min post-injury bolus dose: subcutaneous 10mg/kg PZ in saline; subcutaneous osmotic pump: 10mg/kg/day/3d CsA in cremophor/ethanol/saline; subcutaneous osmotic pump: 10mg/kg/day/3d PZ in saline). One-way analysis of variance followed by Student-Newman-Keuls *post-hoc* test. \* $p < 0.05$ , \*\* $p < 0.01$  compared with sham. Error bars represent mean  $\pm$  standard deviation.  $n = 8$  rats per group.

### State V(II): Rotenone Inhibition of Complex-I and Succinate Activation of Maximal Complex-II Respiration

A one-way ANOVA revealed a statistically significant effect across all groups ( $F_{[4,35]} = 19.55$ ,  $p < 0.0001$ ). *Post-hoc* testing (SNK) revealed that compared with sham, state V(II) respiration was significantly impaired for vehicle ( $p < 0.0001$ ), PZ ( $p < 0.0001$ ), CsA ( $p < 0.0001$ ), and PZ + CsA ( $p < 0.0001$ ), thus indicating that severe CCI significantly decreased state V(II) respiration compared with sham, and that 72h subcutaneous continuous infusion of neither PZ, CsA, nor PZ + CsA was able to significantly attenuate CCI-induced decreases in state V(II) respiration (**Fig. 3.2D**).

### **CCI-TBI Modification of Mitochondrial Proteins by 4-HNE and Acrolein**

#### 4-HNE

A one-way ANOVA revealed a statistically significant effect across all groups ( $F_{[4,30]} = 6.765$ ,  $p = 0.0005$ ). *Post-hoc* testing (SNK) revealed that compared with sham, binding of 4-HNE to mitochondrial proteins was significantly increased for vehicle ( $p < 0.001$ ) and PZ + CsA ( $p < 0.01$ ), and that binding of 4-HNE to mitochondrial proteins was significantly decreased in the PZ group ( $p < 0.05$ ) and the CsA group ( $p < 0.05$ ) compared with vehicle, with neither the PZ group or the CsA group being significantly different from sham ( $p > 0.05$ ), thus indicating that severe CCI significantly increases formation of 4-HNE bound mitochondrial proteins compared with sham, and that 72h subcutaneous continuous infusion of either PZ or CsA, but not PZ + CsA, significantly decreases CCI-induced formation of 4-HNE bound mitochondrial proteins (**Fig. 3.4A**).

Figure 4

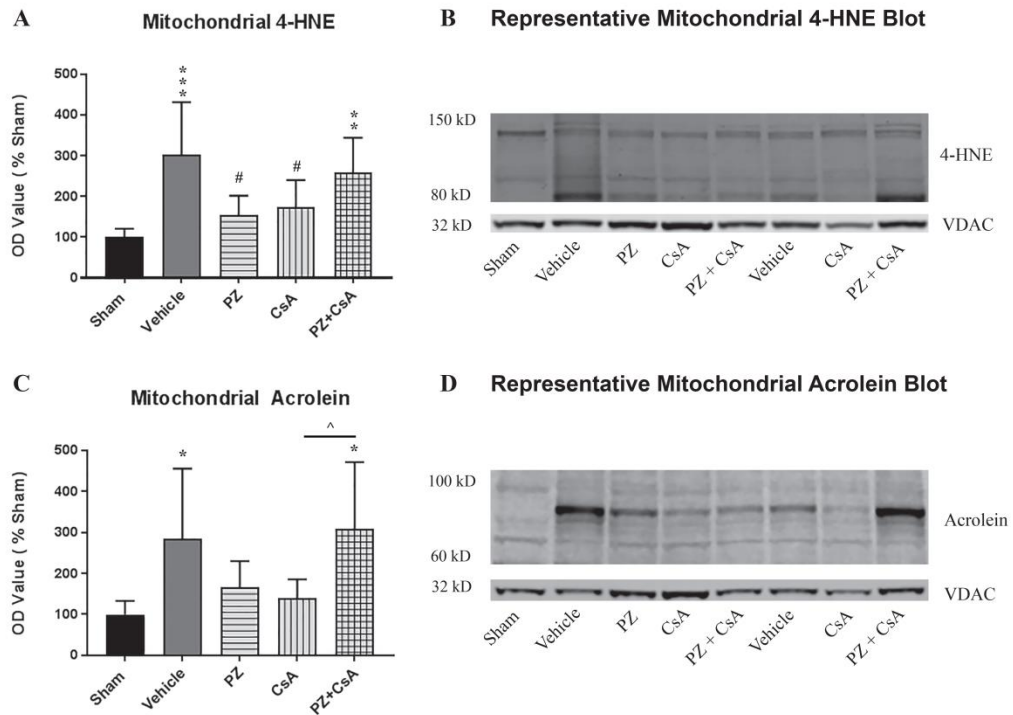


**Figure 3.4 4-HNE and Acrolein: Effect of PZ, CsA, and PZ + CsA.** Effect of the 15 min post-injury loading dose + 72h subcutaneous continuous infusion dosing paradigm on binding of **(A)** 4-HNE (4-hydroxynonenal) or **(C)** acrolein to mitochondrial protein 72h following severe cortical impact injury as assessed by Western blot. Representative Western blot images demonstrating analysis of **(B)** 4-HNE between 150 kD and 80 kD and internal loading control VDAC (voltage-dependent anion channel) and analysis of **(D)** Acrolein between 100 kD and 60 kD and internal loading control VDAC. Sham (no impact injury, no drug administration). Vehicle (15 min post-injury bolus dose: intraperitoneal cremophor/ethanol/saline; 15 min post-injury bolus dose: subcutaneous saline; subcutaneous osmotic pump: cremophor/ethanol/saline; subcutaneous osmotic pump: saline). PZ = phenelzine (15 min post-injury bolus dose: intraperitoneal cremophor/ethanol/saline; 15 min post-injury bolus dose: subcutaneous 10mg/kg PZ in saline; subcutaneous osmotic pump: cremophor/ethanol/saline; subcutaneous osmotic pump: 10mg/kg/day/3d PZ in saline). CsA = cyclosporine A (15 min post-injury bolus dose: intraperitoneal 20mg/kg CsA in cremophor/ethanol/saline; 15 min post-injury bolus dose: subcutaneous saline; subcutaneous osmotic pump: 10mg/kg/day/3d CsA in cremophor/ethanol/saline; subcutaneous osmotic pump: saline). PZ + CsA (15 min post-injury bolus dose: intraperitoneal 20mg/kg CsA in cremophor/ethanol/saline; 15 min post-injury bolus dose: subcutaneous 10mg/kg PZ in saline; subcutaneous osmotic pump: 10mg/kg/day/3d CsA in cremophor/ethanol/saline; subcutaneous osmotic pump: 10mg/kg/day/3d PZ in saline). One-way analysis of variance followed by Student-Newman-Keuls *post-hoc* test. \* $p < 0.05$ , \*\* $p < 0.01$ , \*\*\* $p < 0.001$  compared with sham; # $p < 0.05$  compared with vehicle; ^ $p < 0.05$  compared with CsA. Error bars represent mean  $\pm$  standard deviation.  $n = 6-8$  rats per group.

### Acrolein

A one-way ANOVA revealed a statistically significant effect across all groups ( $F_{[4,32]} = 4.607, p=0.0047$ ). *Post-hoc* testing (SNK) revealed that compared with sham, binding of acrolein to mitochondrial proteins was significantly increased for vehicle ( $p<0.05$ ) and PZ + CsA ( $p<0.05$ ). The PZ + CsA group was also significantly increased as compared with the CsA group ( $p<0.05$ ). Although the PZ group and the CsA group were not significantly different from vehicle ( $p>0.05$ ), there was a 42% and 51% decrease in mean acrolein binding of mitochondrial proteins compared with vehicle for the PZ and CsA group, respectively. Further, the PZ group and the CsA group were not significantly different from sham ( $p>0.05$ ), thus indicating that severe CCI significantly increases formation of acrolein bound mitochondrial proteins compared with sham, and that 72h subcutaneous continuous infusion of either PZ or CsA, but not PZ + CsA, decreases CCI-induced formation of acrolein bound mitochondrial proteins (**Fig. 3.4C**).

### **CCI-TBI Induced $\alpha$ -Spectrin Degradation: Continuous Infusion Dosing Paradigm**

#### 145 kD – Calpain-Dependent $\alpha$ -Spectrin Breakdown Product

A one-way ANOVA revealed a statistically significant effect across all groups ( $F_{[4,34]} = 3.032, p=0.0306$ ). *Post-hoc* testing (SNK) revealed that compared with sham, 145 kD  $\alpha$ -spectrin breakdown products were significantly increased for vehicle ( $p<0.05$ ) and CsA ( $p<0.05$ ). Although the PZ group and the PZ + CsA group were not significantly different from vehicle ( $p>0.05$ ), there was a 53% and a 53% decrease in mean absorbance compared with vehicle for the PZ and PZ + CsA groups, respectively. Further, the PZ group and the PZ + CsA group were not significantly different from sham ( $p>0.05$ ) or from each other ( $p>0.05$ ), thus indicating that severe CCI significantly increases formation of the 145 kD calpain dependent  $\alpha$ -spectrin breakdown product, and



that 72h subcutaneous continuous infusion of either PZ or PZ + CsA maintain cytoskeletal  $\alpha$ -spectrin integrity to a similar degree, as compared with sham (**Fig. 3.5A**).

150 kD – Calpain/Caspase 3-Dependent  $\alpha$ -Spectrin Breakdown Product

A one-way ANOVA revealed a statistically significant effect across all groups ( $F_{[4,34]} = 4.49, p=0.0051$ ). *Post-hoc* testing (SNK) revealed that compared with sham, 150 kD  $\alpha$ -spectrin breakdown products were significantly increased for vehicle ( $p<0.01$ ) and CsA ( $p<0.01$ ). Although the PZ group and the PZ + CsA group were not significantly different from vehicle ( $p>0.05$ ), there was a 47% and 47% decrease in mean absorbance compared with vehicle for the PZ and PZ + CsA groups, respectively. Further, the PZ group and the PZ + CsA group were not significantly different from sham ( $p>0.05$ ) or from each other ( $p>0.05$ ), thus indicating that severe CCI significantly increases formation of the 150 kD calpain/caspase 3-dependent  $\alpha$ -spectrin breakdown product, and that 72h subcutaneous continuous infusion of either PZ or PZ + CsA maintain cytoskeletal  $\alpha$ -spectrin integrity to a similar degree, as compared with sham (**Fig. 3.5B**).

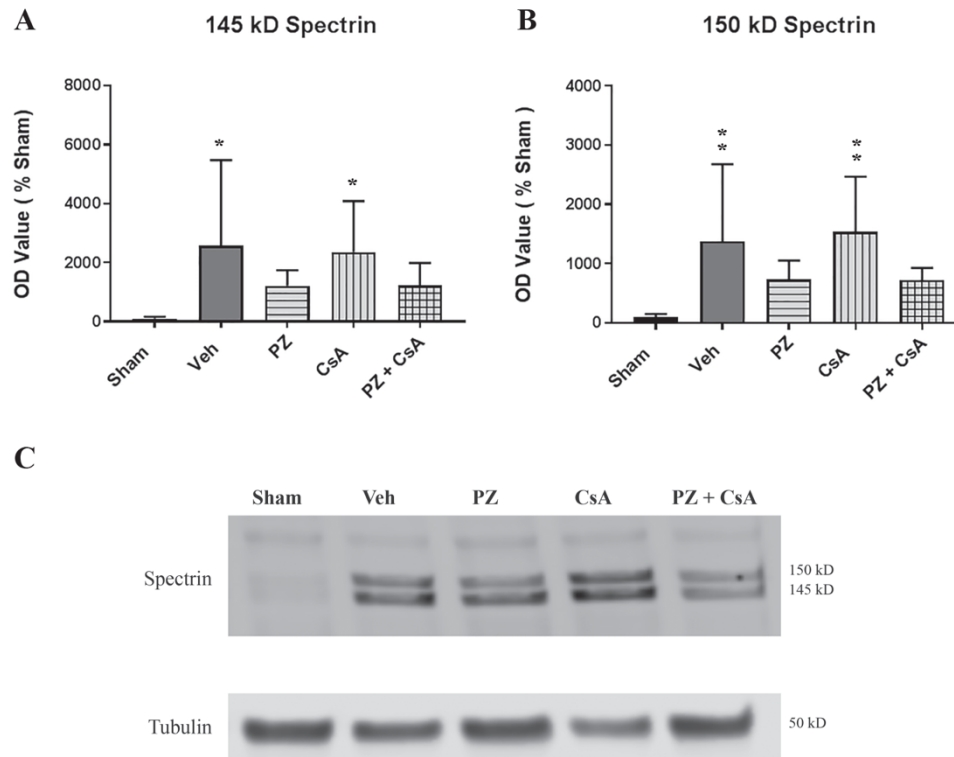


**Figure 3.5 Spectrin: Effect of PZ, CsA, and PZ + CsA.** Effect of the 15 min post-injury loading dose + 72h subcutaneous continuous infusion dosing paradigm on degradation of cytoskeletal protein  $\alpha$ -spectrin into **(A)** 145 kD (calpain dependent) and **(B)** 150 kD (calpain and caspase 3-dependent)  $\alpha$ -spectrin breakdown products 72h following severe cortical impact injury as assessed by Western blot. **(C)** Representative Western blot image demonstrating analysis of 145 kD and 150 kD  $\alpha$ -spectrin bands and the internal loading control tubulin. Sham (no impact injury, no drug administration). Veh = Vehicle (15 min post-injury bolus dose: intraperitoneal cremophor/ethanol/saline; 15 min post-injury bolus dose: subcutaneous saline; subcutaneous osmotic pump: cremophor/ethanol/saline; subcutaneous osmotic pump: saline). PZ = phenelzine (15 min post-injury bolus dose: intraperitoneal cremophor/ethanol/saline; 15 min post-injury bolus dose: subcutaneous 10mg/kg PZ in saline; subcutaneous osmotic pump: cremophor/ethanol/saline; subcutaneous osmotic pump: 10mg/kg/day/3d PZ in saline). CsA = cyclosporine A (15 min post-injury bolus dose: intraperitoneal 20mg/kg CsA in cremophor/ethanol/saline; 15min post-injury bolus dose: subcutaneous saline; subcutaneous osmotic pump: 10mg/kg/day/3d CsA in cremophor/ethanol/saline; subcutaneous osmotic pump: saline). PZ + CsA (15 min post-injury bolus dose: intraperitoneal 20mg/kg CsA in cremophor/ethanol/saline; 15 min post-injury bolus dose: subcutaneous 10mg/kg PZ in saline; subcutaneous osmotic pump: 10mg/kg/day/3d CsA in cremophor/ethanol/saline; subcutaneous osmotic pump: 10mg/kg/day/3d PZ in saline). One-way analysis of variance followed by Student-Newman-Keuls *post-hoc* test. \* $p < 0.05$ , \*\* $p < 0.01$  compared with sham. Error bars represent mean  $\pm$  standard deviation.  $n = 7-9$  rats per group.

## CCI-TBI Induced $\alpha$ -Spectrin Degradation: Phenezine 12hr Intermittent Dosing Paradigm

### 145 kD – Calpain-Dependent $\alpha$ -Spectrin Breakdown Products

A one-way ANOVA revealed a statistically significant effect across all groups ( $F_{[2,21]} = 6.128, p=0.008$ ). *Post-hoc* testing (SNK) revealed that compared with sham, 145 kD  $\alpha$ -spectrin breakdown products were significantly increased for vehicle ( $p<0.05$ ) and PZ ( $p<0.01$ ), thus indicating that severe CCI significantly increases formation of the 145 kD calpain-dependent  $\alpha$ -spectrin breakdown product, and that a subcutaneous bolus dose of PZ (10 mg/kg) 15 min post-injury followed by subcutaneous maintenance doses (5 mg/kg) every 12h up to and including 60h is unable to attenuate degradation (**Fig. 3.6A**).

### 150 kD – Calpain/Caspase 3-Dependent $\alpha$ -Spectrin Breakdown Product

A one-way ANOVA revealed a statistically significant effect across all groups ( $F_{[2,21]} = 5.426, p=0.0126$ ). *Post-hoc* testing (SNK) revealed that compared with sham, 150 kD  $\alpha$ -spectrin breakdown products were significantly increased for vehicle ( $p<0.05$ ) and PZ ( $p<0.05$ ), thus indicating that severe CCI significantly increases formation of the 150 kD calpain/caspase 3-dependent  $\alpha$ -spectrin breakdown product, and that a subcutaneous bolus dose of PZ (10 mg/kg) 15 min post-injury followed by subcutaneous maintenance doses (5 mg/kg) every 12h up to and including 60h is unable to attenuate degradation (**Fig. 3.6B**).

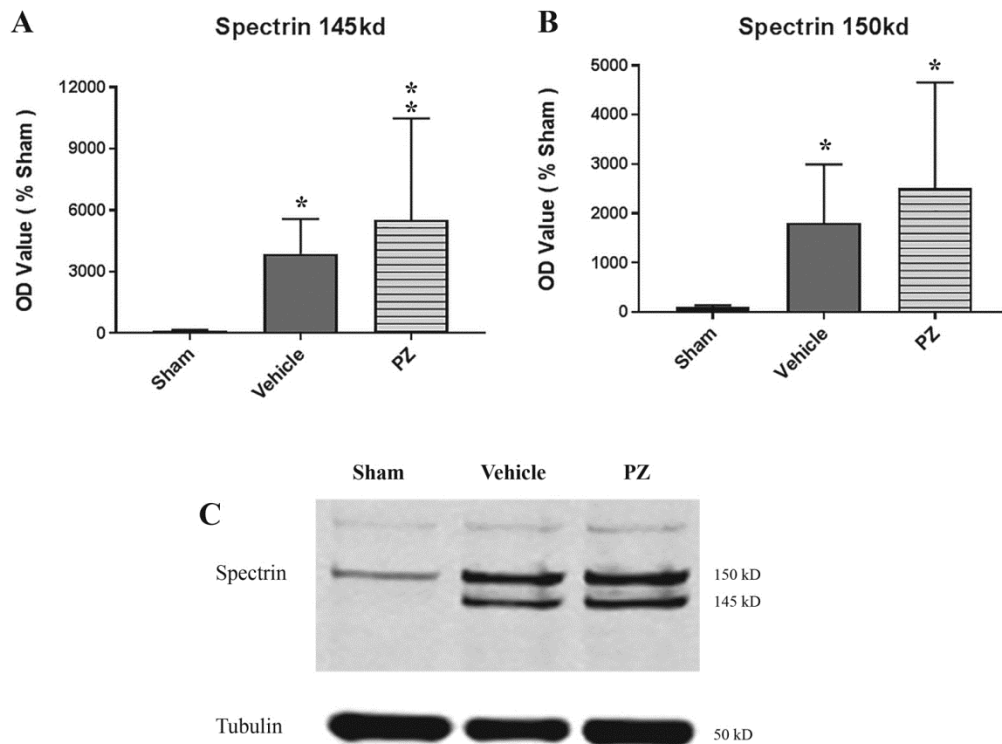


**Figure 3.6 Spectrin: Intermittent PZ dosing.** Effect of the 15 min post-injury loading dose + 12h intermittent phenelzine (PZ) dosing paradigm on degradation of cytoskeletal protein  $\alpha$ -spectrin into **(A)** 145 kD (calpain dependent) and **(B)** 150 kD (calpain and caspase-3 dependent)  $\alpha$ -spectrin breakdown products 72h following severe cortical impact injury as assessed by Western blot. **(C)** Representative Western blot image demonstrating analysis of 145 kD and 150 kD  $\alpha$ -spectrin bands and the internal loading control tubulin. Sham (no impact injury, no drug administration). Vehicle (15 min post-injury bolus dose subcutaneous saline, followed by subcutaneous bolus saline every 12h up to and including 60h). PZ = phenelzine (15 min post-injury bolus dose of 10mg/kg PZ in saline, followed by subcutaneous bolus 5mg/kg PZ in saline every 12h up to and including 60h). One-way analysis of variance followed by Student-Newman-Keuls *post-hoc* test. \* $p < 0.05$ , \*\* $p < 0.01$  compared to sham. Error bars represent mean  $\pm$  standard deviation.  $n = 7-9$  rats per group.

## **Discussion**

### **TBI Induction of Mitochondrial Dysfunction and Lipid Peroxidation-Derived Aldehyde Generation**

It has been firmly established that mitochondrial dysfunction, lipid peroxidation, and production of LP-derived aldehydes occurs following TBI, and that each contributes to TBI pathology [1, 17, 55, 57, 73, 163, 285]. For example, mitochondrial dysfunction can contribute to induction of the ROS/RNS-lipid peroxidation-aldehyde cascade, energy failure, and downstream consequences such as cytoskeletal and neuronal degeneration and neurologic impairment [1, 17, 51, 55, 56, 70, 110, 163], while lipid peroxidation can impair membrane fluidity and destabilize membrane integrity [256], and the LP-derived aldehydes, including 4-HNE and acrolein, can have directly toxic effects on cellular function [29, 72, 77, 85-89, 93, 101, 102, 257, 258], with a notably devastating effect on the mitochondria.

### **Cyclosporine A and Inhibition of the Mitochondrial Permeability Transition Pore**

Several approaches have been utilized to improve mitochondrial function following TBI, including mild uncoupling [125, 248], ketogenic diet [249], induction of endogenous antioxidant pathways [97, 113], and scavenging of lipid peroxyl radicals, peroxynitrite, and LP-derived aldehydes [58, 69, 71, 72, 109, 257, 310, 315]. However, inhibition of the mitochondrial permeability transition pore utilizing the FDA-approved immunosuppressant CsA as a neuroprotective strategy following TBI has remained a focus among the neurotrauma community for the past 20 years. Although the immunosuppressive effects of CsA are attributable to its ability to inhibit calcineurin and, therefore, T-cell activation [316], its neuroprotective effects are purported to be due to inhibition of the mPTP through direct binding of the mPTP component protein, cyclophilin

D [218-220, 317]. In fact, in experimental TBI, CsA or its non-immunosuppressive analog, the mPTP inhibitor NIM811, have been shown to prevent mitochondrial dysfunction, decrease oxidative damage, attenuate axonal pathology and neurodegeneration, and improve behavioral impairments [110, 123, 124, 135, 136, 223-226, 292, 309].

The continuous CsA dosing paradigm utilized here, 20 mg/kg CsA delivered intraperitoneal 15 min post-injury combined with subcutaneous continuous infusion of 10mg/kg/day/3 days CsA, is based on previously optimized dosing paradigms demonstrating that continuous infusion of CsA is more neuroprotective than bolus dosing [122, 227]. Additionally, a 72h continuous infusion CsA dosing protocol has proven safe for clinical use in severe TBI and was suggestive of improved outcomes [234]. However, previous to our study, the effects of continuous infusion of CsA following experimental TBI had not been assessed using outcome measures distinct from cortical tissue sparing. Our results indicate (**Table 3.3**) that while CsA was able to significantly decrease TBI-induced increases in aldehydic-modified mitochondrial proteins (**Fig. 3.4**), it was unable to prevent mitochondrial respiratory dysfunction (**Fig 3.2 and 3.3**) or cytoskeletal  $\alpha$ -spectrin degradation (**Fig. 3.5**).

**Table 3.3 Summary of Result: Subcutaneous Continuous Infusion Dosing**

**Paradigm**

	<b>Vehicle</b>	<b>PZ</b>	<b>CsA</b>	<b>PZ + CsA</b>
<b>Mitochondrial RCR</b>	↓*	↔^	↓*	↓*
<b>Mitochondrial Individual Respiratory States</b>	↓*	↓*	↓*	↓*
<b>Mitochondrial 4-HNE</b>	↑*	↓#	↓#	↑*
<b>Mitochondrial Acrolein</b>	↑*	↔^	↔^	↑*
<b>Spectrin Degradation</b>	↑*	↔^	↑*	↔^

Effect of the 15 min post-injury loading dose + 72h subcutaneous continuous infusion dosing paradigm on the above listed outcome measures 72h following severe cortical impact injury. Vehicle (15 min post-injury bolus dose: intraperitoneal cremophor/ethanol/saline; 15 min post-injury bolus dose: subcutaneous saline; subcutaneous osmotic pump: cremophor/ethanol/saline; subcutaneous osmotic pump: saline). PZ (15 min post-injury bolus dose: intraperitoneal cremophor/ethanol/saline; 15 min post-injury bolus dose: subcutaneous 10mg/kg PZ in saline; subcutaneous osmotic pump: cremophor/ethanol/saline; subcutaneous osmotic pump: 10mg/kg/day/3d PZ in saline). CsA (15 min post-injury bolus dose: intraperitoneal 20mg/kg CsA in cremophor/ethanol/saline; 15 min post-injury bolus dose: subcutaneous saline; subcutaneous osmotic pump: 10mg/kg/day/3d CsA in cremophor/ethanol/saline; subcutaneous osmotic pump: saline). PZ + CsA (15 min post-injury bolus dose: intraperitoneal 20mg/kg CsA in cremophor/ethanol/saline; 15 min post-injury bolus dose: subcutaneous 10mg/kg PZ in saline; subcutaneous osmotic pump: 10mg/kg/day/3d CsA in cremophor/ethanol/saline; subcutaneous osmotic pump: 10mg/kg/day/3d PZ in saline). PZ, phenelzine; CsA, cyclosporine A; RCR, respiratory control ratio (state III/state IV); 4-HNE, 4-hydroxynonenal; ↓\* = significantly decreased from sham, ↑\* = significantly increased from sham, ↓# = significantly decreased from vehicle, ↔^ = not significantly different from sham.

The fact that continuous infusion of CsA is able to decrease TBI-induced increases in mitochondrial bound 4-HNE and acrolein, is consistent with the fact that inhibition of the permeability transition pore in brain mitochondria is able to prevent calcium-induced increases in ROS [60], which would in turn decrease the ROS/RNS-lipid peroxidation-aldehyde cascade. However, this does not seem to be enough to maintain mitochondrial respiratory function or prevent downstream calpain-mediated cytoskeletal degradation, at least at the 72h post-injury time point examined (**Fig. 3.7**). It may be that CsA inhibition of the mPTP and sequestration of calcium has decreased mitochondrial membrane potential and led to a decrease in respiration. Additionally, there are known limitations to the ability of CsA to prevent permeability transition, particularly when mitochondria are in an extremely depolarized state [318], which is likely the case 72h following severe injury, the peak of mitochondrial dysfunction [73]. Similarly, there are types of mitochondrial permeability transition demonstrated to be insensitive to CsA [317, 319]. In fact, thiol-crosslinking agents have been implicated in induction of CsA-insensitive permeability through interaction with adenine nucleotide translocase (ANT), an additional component of the mPTP [320], a significant finding in light of the fact that LP-derived aldehydes are known to bind cysteine residues [1, 79-81]. In fact, acrolein has been specifically shown capable of ANT inhibition [101].

On the other hand, it is possible that continuous infusion of CsA did have a protective effect on mitochondrial respiration that was masked in our total mitochondrial preparations (synaptic and non-synaptic) due to the fact that CsA has a greater neuroprotective effect on synaptic mitochondria than non-synaptic mitochondria following CCI (**Fig. 2.1-2.6**) [309], but at 72h post-injury, synaptic mitochondria make up a minority of the mitochondrial population [121, 128, 321, 322]. However, we consider this explanation unlikely when taken in conjunction with the fact that continuous infusion of CsA was also unable to prevent cytoskeletal  $\alpha$ -spectrin degradation (**Fig. 3.5**).



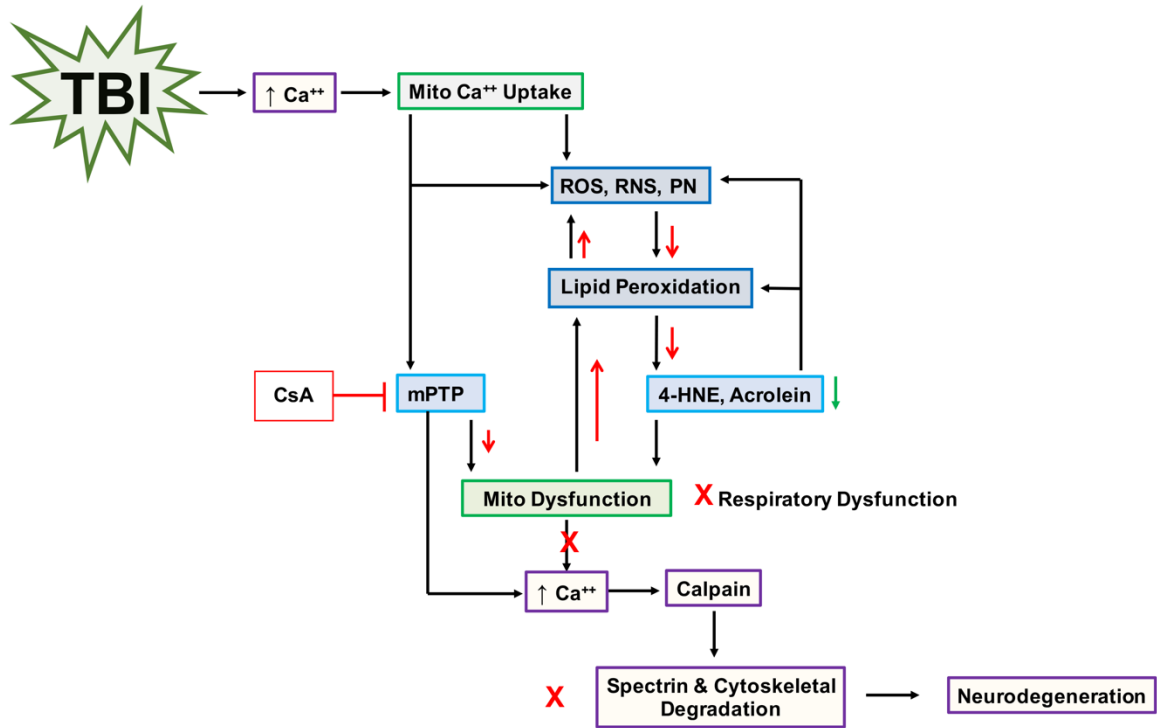


**Figure 3.7 Schematic illustration of CsA monotherapy results.** CsA decreases formation of mitochondrial bound 4-HNE and acrolein without attenuating respiratory dysfunction or cytoskeletal spectrin degradation. CsA inhibits mitochondrial permeability transition (mPTP) leading to attenuation of the mitochondrial dysfunction-ROS/RNS-lipid peroxidation-4-HNE/acrolein cascade (red arrows). Which leads to significant decreases in formation of 4-HNE/acrolein bound mitochondrial conjugates (green arrow). However, inhibition of mPTP and attenuation of 4-HNE and acrolein are not enough to improve overall respiratory dysfunction and downstream effects of mitochondrial calcium release, such as cytoskeletal spectrin degradation (red X's).

An additional caveat to consider is the fact that the CsA dosing paradigm utilized in this study was originally optimized using cortical tissue sparing [122, 227]. It is known that CsA preservation of cortical tissue following experimental TBI has a U-shaped dose-response curve [227]. It is possible that the dose-response for CsA in relation to cortical tissue sparing is not identical to the dose-response for CsA in relation to mitochondrial respiratory protection. This speculation is plausible in light of the fact that CsA has multiple mechanisms of action. For example, although it has been well-established that CsA is able to improve mitochondrial function at early time points and *ex-vivo* through inhibition of mPTP [226, 313, 323], the neuroprotective effects of continuous CsA infusion on cortical tissue sparing at later time points may also be due to its immunosuppressive properties. For example, although FK506 (i.e. tacrolimus), a calcineurin-inhibiting immunosuppressant unable to inhibit mPTP, has been shown unable to attenuate cortical lesion volume following experimental TBI [124], several studies have demonstrated FK506 to be neuroprotective across several other injury paradigms [228-233], and calcineurin signaling is known to have an important role following brain injury [229, 324].

The fact that CsA is known to have a U-shaped dose response curve [227], combined with its multiple mechanisms of action [316, 317], may explain some of the disparities seen between CsA TBI studies, because although there have been a preponderance of studies supporting CsA's neuroprotective capabilities, this is not the first study to demonstrate that CsA is not neuroprotective across all outcome measures [241].

## **Phenelzine Scavenging of Lipid Peroxidation-Derived Aldehydes 4-HNE and Acrolein**

Several approaches have been utilized to attenuate the lipid peroxidation cascade following neurotraumatic injury ranging from the use of antioxidants to the use of iron chelators [1, 55, 109, 325]. However, many of these approaches are limited by a variety of factors including, limited therapeutic window, blood-brain barrier penetrability and elimination rate [1, 55]. Fortunately, scavenging of LP-derived aldehydes, such as 4-HNE and acrolein (the stable final breakdown products of lipid peroxidation) represents a practical therapeutic approach [1, 79].

Phenelzine, a monoamine oxidase inhibitor clinically used for intractable depression contains a hydrazine moiety (-NH-NH<sub>2</sub>) making it capable of covalently binding both free LP-derived neurotoxic aldehydes, such as 4-HNE and acrolein, as well as binding aldehyde-protein conjugates, including mitochondrial protein conjugates, preventing further cross-linking [79, 198, 258, 260-262].

Both *in-vitro* and *in-vivo* studies have shown hydrazine-containing compounds including PZ, to be neuroprotective in models of brain and spinal cord injury, decreasing generation of LP-derived aldehydes, improving mitochondrial bioenergetics, attenuating tissue damage, and improving behavioral outcomes [71, 72, 74-76, 257]. Importantly, *ex-vivo* studies have confirmed that the ability of PZ to protect mitochondria against exogenously administered 4-HNE or acrolein is due to the presence of the hydrazine moiety [72].

The continuous PZ dosing paradigm utilized here, 10 mg/kg PZ delivered subcutaneously 15 min post-injury combined with subcutaneous continuous infusion of 10 mg/kg/day/3 days PZ, was based on previous work showing that 12h intermittent

administration of PZ (10 mg/kg PZ delivered subcutaneously 15 min post-injury followed by 5 mg/kg PZ maintenance dosing every 12 hours) was neuroprotective following severe CCI [72], with the hypothesis being that continuous infusion of PZ should further enhance neuroprotection over the 12h maintenance dosing paradigm.

Our results indicate (**Table 3.3**), that continuous infusion of PZ was able to maintain RCR (**Fig. 3.3**), decrease TBI-induced increases in aldehydic-modified mitochondrial proteins (**Fig. 3.4**), and maintain cytoskeletal  $\alpha$ -spectrin integrity (**Fig. 3.5**), although it was unable to prevent decreases in individual states of mitochondrial respiration (**Fig. 3.2**). Encouragingly, this data parallels the results obtained in the 12h intermittent PZ dosing paradigm studies, in which PZ also demonstrated maintenance of RCR and decreases in 4-HNE and acrolein modification of mitochondrial proteins [72], without being able to attenuate decreases in individual mitochondrial respiratory states (*unpublished data*). However, one important improvement was seen with the continuous infusion PZ dosing paradigm (**Table 3.4**) because whereas continuous infusion of PZ was able to maintain cytoskeletal  $\alpha$ -spectrin integrity (**Fig. 3.5**), 12h intermittent dosing of PZ was not (**Fig 3.6**). Although both of these dosing paradigms were designed based on an approximate 12h plasma half-life of PZ in humans, the fact that the continuous infusion dosing paradigm represented an improvement over intermittent dosing is unsurprising given recent findings that suggest the half-life of PZ in rats may be much shorter than 12h [74].

**Table 3.4  $\alpha$ -Spectrin Degradation: Phenzelzine Continuous Infusion Versus  
Phenzelzine Intermittent Dosing**

	<b>PZ<sub>CI</sub></b>	<b>PZ<sub>ID</sub></b>
<b>Spectrin Degradation</b>	$\leftrightarrow^{\wedge}$	$\uparrow^*$

Comparison of the effect of the PZ continuous infusion dosing paradigm versus the PZ intermittent dosing paradigm on  $\alpha$ -spectrin degradation 72h following severe cortical impact injury. PZ<sub>CI</sub> = phenelzine continuous infusion (15 min post-injury bolus dose: intraperitoneal cremophor/ethanol/saline; 15 min post-injury bolus dose: subcutaneous 10mg/kg PZ in saline; subcutaneous osmotic pump: cremophor/ethanol/saline; subcutaneous osmotic pump: 10mg/kg/day/3d PZ in saline). PZ<sub>ID</sub> = phenelzine intermittent dosing (15 min post-injury subcutaneous bolus dose of 10mg/kg PZ in saline followed by subcutaneous bolus dose of 5mg/kg PZ in saline every 12h up to and including 60h).  $\uparrow^*$  = significantly increased from sham,  $\leftrightarrow^{\wedge}$  = not significantly different from sham. PZ<sub>CI</sub>, phenelzine continuous infusion; PZ<sub>ID</sub> = phenelzine intermittent dosing.

On that note, it is also important to state that the animals receiving continuous PZ infusion were also receiving continuous cremophor infusion (CsA vehicle). Therefore, the fact that the continuous infusion dosing paradigm for PZ was able to perform equally [72] or better than **(Table 3.3 and 3.4)** the 12h intermittent PZ dosing paradigm indicates that continuous infusion of the CsA vehicle, cremophor, which is purportedly toxic [245, 301] is unlikely to be exerting detrimental effects under the current experimental conditions.

Multiple possibilities may explain the ability of continuous infusion of PZ to decrease TBI-induced increases in mitochondrial bound 4-HNE and acrolein and maintain RCR and cytoskeletal  $\alpha$ -spectrin integrity without being able to improve individual mitochondrial respiratory states. First, the ability of PZ to scavenge aldehydes [79, 262] would have a direct effect on decreasing aldehyde binding of mitochondrial proteins, as well as lead to attenuation of the mitochondrial dysfunction-ROS/RNS-lipid peroxidation-aldehyde cascade **(Fig. 3.1)**, further decreasing binding of 4-HNE and acrolein to mitochondrial proteins. This decrease in mitochondrial bound 4-HNE and acrolein would then prevent mitochondrial permeability transition [326], decreasing the release of calcium back into the cytosol and attenuating calpain-dependent  $\alpha$ -spectrin degradation. Further, the decrease in 4-HNE and acrolein mitochondrial binding also may result in a slight improvement in mitochondrial bioenergetics, resulting in maintenance of RCR, a general measure of mitochondrial health, but one which does not have a significant enough effect on mitochondrial bioenergetics to impact individual states of respiration **(Fig. 3.8)**.

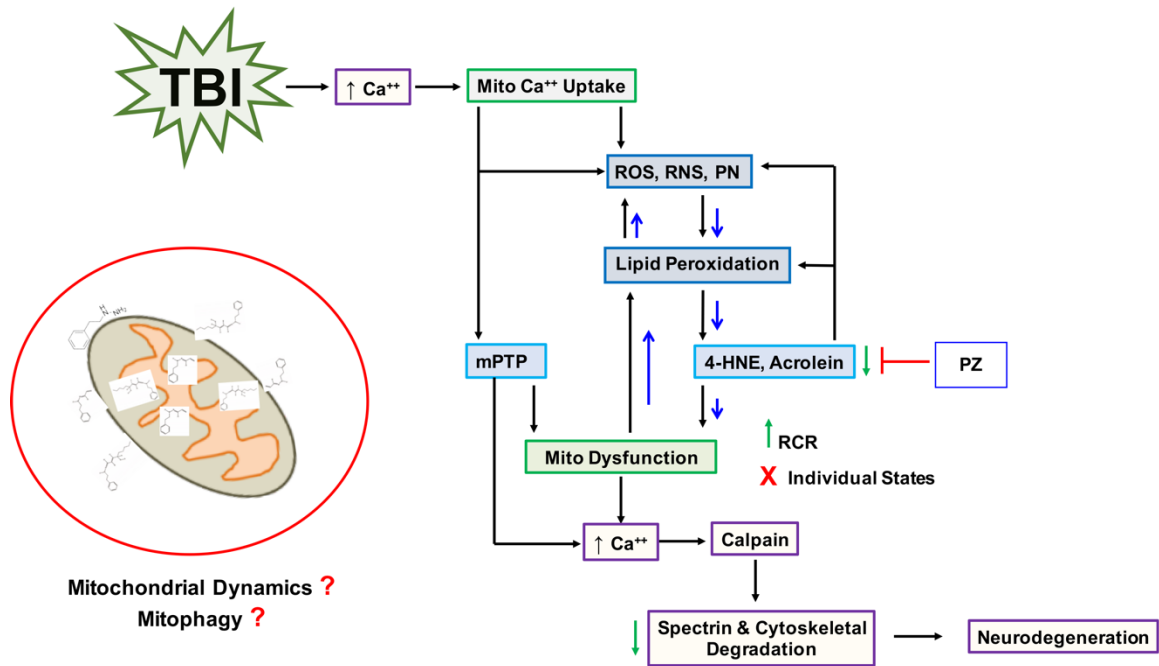


**Figure 3.8 Schematic illustration of PZ monotherapy results.** PZ attenuates mitochondrial bound 4-HNE and acrolein, maintains respiratory control ratio (RCR) and cytoskeletal spectrin integrity, without improving individual states of respiratory dysfunction. PZ scavenges 4-HNE and acrolein directly, decreasing mitochondrial bound 4-HNE and acrolein (green arrow), leading to decreases in the 4-HNE/acrolein-mitochondrial dysfunction-ROS/RNS-lipid peroxidation-4-HNE/acrolein cascade (blue arrows), further decreasing mitochondrial bound 4-HNE and acrolein, and improving respiratory control ratio (green arrows), effects which are able to improve downstream effects of mitochondrial calcium release, such as cytoskeletal spectrin maintenance (green arrow), but not enough to improve individual states of mitochondrial respiration (red X). Bottom left figure demonstrates a single mitochondrion bound to phenelzine and phenelzine-aldehyde conjugates. It is currently unknown what effect these bindings have on mitochondrial dynamics and mitophagy.

Second, it is possibly that we have again masked a significant mitochondrial protective effect. As stated previously, PZ can bind mitochondrial aldehyde-protein conjugates [79, 262]. Additionally, as an irreversible monoamine oxidase inhibitor [278], PZ also associates with the outer mitochondrial membrane enzyme monoamine oxidase [327]. Therefore, it is possible that each individual mitochondrion is bound to a significant amount of PZ, and it is unknown what effect this has on post-injury mitochondrial dynamics and mitophagy (**Fig. 3.8**). In fact, in general, the long-term consequences of drug-aldehyde adduct formation are unknown [258].

It is possible that the binding of PZ to mitochondria which are beyond saving is preventing these mitochondria from being degraded by normal post-injury processes while also significantly improving the bioenergetics of less damaged mitochondria. The unusual presence of these considerably damaged mitochondria in our isolated mitochondria preps could mask improvements to individual states of mitochondrial respiration. Such an explanation would be consistent with an overall mitochondrial protective effect suggested by the  $\alpha$ -spectrin data, as well as the improvement in tissue sparing seen in our previous 12h intermittent PZ dosing studies [72], despite no improvements to individual mitochondrial states of respiration (*unpublished data*).

Last, although *in-vitro* experiments which have compared PZ to the non-hydrazine, non-aldehyde scavenging monoamine oxidase inhibitor pargyline have confirmed that phenelzine's aldehyde scavenging properties are due to the presence of the hydrazine moiety [72, 198], it is unknown what effect monoamine oxidase inhibition has on the bioenergetics of injured mitochondria or in the broader context of TBI pathophysiology. The function of catecholamines and monoamine oxidase following brain injury remains controversial, with some studies suggesting monoamine oxidase inhibition and catecholamine agonists to be protective [154, 193, 278], with others



suggesting them to be pathologic [328]. In fact, for PZ to remain a clinically translatable pharmacotherapy, its role as a monoamine oxidase inhibitor in the context of brain injury must be elucidated. As such, we have planned future experiments aimed at determining the effect of monoamine oxidase inhibition following TBI.

### **Phenelzine + Cyclosporine A: A multi-mechanistic Combinatory Pharmacotherapy Approach**

As pointed out earlier, all monotherapy clinical trials for TBI have failed, and although there have been numerous reasons cited for these failures, due to the heterogeneity of injury and the complexity of the secondary injury cascade, there has been a call for pre-clinical studies to focus on the development of combinational therapies for the acute (first 72h) treatment of TBI [213]. Several strategies have been proposed to aid in the selection of combinatorial agents, including but not limited to therapies that affect multiple targets and therapies that target convergent pathways [213]. This study was aimed at achieving both these goals by combining two drugs that have separate targets, the mPTP inhibitor CsA and the LP-derived aldehyde scavenger PZ both of which should also be capable of attenuating the convergent mitochondria dysfunction-ROS/RNS-lipid peroxidation-aldehyde cascade (**Fig. 3.1**). In fact, CsA was one of the drugs identified by the combinational therapy TBI working group as being a promising combinational candidate [213].

Our results indicate (**Table 3.3**) that continuous infusion of PZ (10 mg/kg PZ subcutaneous 15 min post-injury + 10 mg/kg/day subcutaneous infusion of PZ for 3 days) combined with continuous infusion of CsA (20 mg/kg CsA intraperitoneal 15 min post-injury + 10 mg/kg/day subcutaneous infusion of CsA for 3 days) is unable to improve mitochondrial bioenergetics (either RCR or individual respiratory states; (**Fig.**

**3.2 and 3.3)** or attenuate 4-HNE or acrolein bound to mitochondrial proteins (**Fig. 3.4**). Interestingly, it seems that the combining of PZ and CsA, negates the protective effects that individual administration of PZ or CsA had on formation of 4-HNE and acrolein bound mitochondrial proteins (**Fig. 3.4**). Although the combination of PZ and CsA was able to maintain cytoskeletal  $\alpha$ -spectrin integrity (**Fig. 3.5**), it did so to a degree similar to PZ alone suggesting that this is most likely an effect mainly attributable to PZ.

While these combinatorial results are disappointing, they are not entirely surprising given the fact that individually the continuous infusion CsA dosing paradigm utilized, which had been previously optimized based on cortical tissue sparing [122, 227], did not have a protective effect on all of the neurochemical outcome measures studied.

Moreover, this study combined two dosing paradigms that had been optimized for each drug individually [72, 122]. In fact, this is not the first study to find that utilization of doses optimized for monotherapy did not result in neuroprotection once combined [280]. Indeed, the complex pharmacokinetics and pharmacodynamics that results from the combining of multiple drugs has been identified as one of the most challenging hurdles in the development of combinational therapies for the treatment of TBI [213]. Although utilization of an alternate dosing paradigm following dose-response studies of the combined drugs together could lead to improved results, upon further consideration, the complex pharmacokinetics of each individual drug may make the clinical translation of the combination unfeasible.

For example, CsA is known to be metabolized by cyp3A4 [246], and although PZ is not technically classified as a cyp3A4 inhibitor, there is data to suggest that PZ is capable of inhibiting cyp3A4 [266, 267]. Further, CsA has a U-shaped dose response

curve [294] and has limited blood-brain-barrier penetrability [236], which increases following injury due to blood-brain-barrier disruption [329] and decreases in mitochondrial production of ATP [23, 51] leading to failure of ATP-dependent p-glycoprotein drug efflux pumps, of which CsA is both a substrate and an inhibitor [236]. Taken together, these facts suggest that in a clinical setting maintaining appropriate CsA CSF levels following TBI will be quite challenging even as a monotherapy, while combining CsA with another drug, particularly a drug such as PZ which itself has a complicated pharmacology as it is both a monoamine oxidase inhibitor and a monoamine oxidase substrate which also has several active metabolites [330], would further complicate the matter.

Along similar lines, although the choice of the combination PZ and CsA was aimed at targeting distinct mechanisms which converge on overlapping pathways (**Fig. 3.1**), consistent with stated combinational TBI therapy design goals [213], both of these drugs are capable of physically binding the mitochondria, CsA through binding of the matrix protein cyclophilin D [218-220, 317], and PZ both through binding of 4-HNE and acrolein bound mitochondrial conjugates [79, 258] and through irreversible binding of the outer mitochondrial membrane protein monoamine oxidase [278, 327], which In hindsight may have resulted in too many non-physiologic interactions for the mitochondria to handle (**Fig. 3.9**).

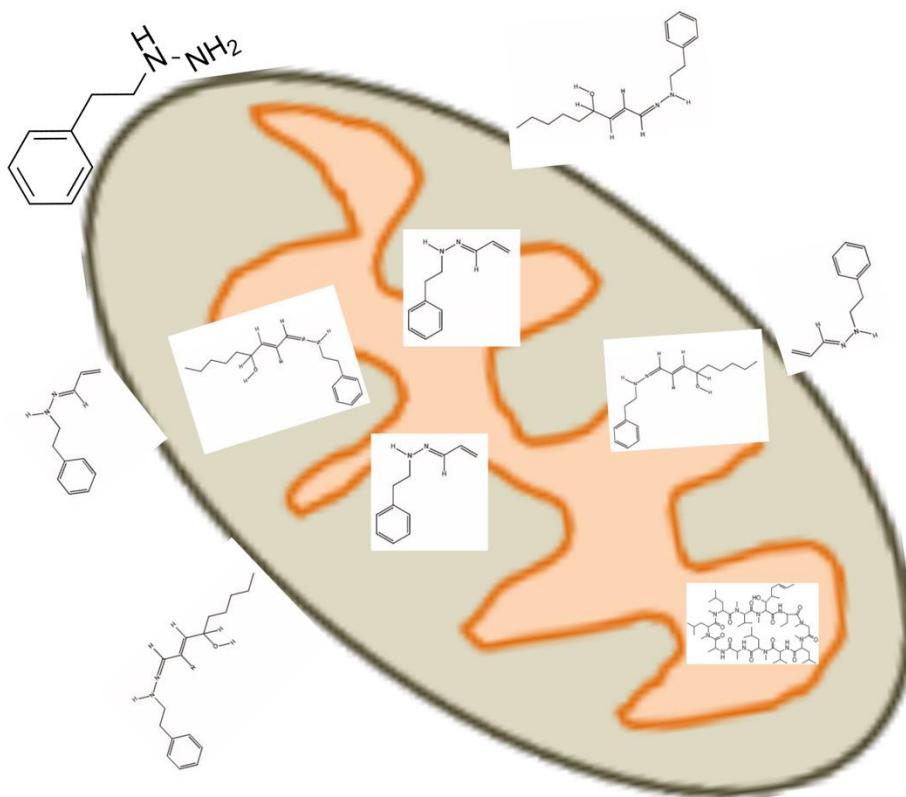


**Figure 3.9 Schematic demonstrating a mitochondrion extensively bound to CsA and PZ.**

CsA binds to the mitochondrial matrix protein cyclophilin D. PZ binds to the outer mitochondrial membrane protein monoamine oxidase. PZ-4-HNE and PZ-acrolein conjugates bind mitochondrial proteins throughout the mitochondrial membranes.

It is possible that assessment of additional outcome measures such as cortical tissue sparing or behavior could have yielded improved results. Indeed, achieving behavioral improvements is the utmost goal in TBI research. However, it must be noted that although a recent summary of NIH-funded pre-clinical combinatorial TBI drug studies reported improvements in non-behavioral outcomes, these positive effects were not maintained in long-term behavioral studies [280]. Therefore, it is unlikely that utilization of our current PZ + CsA combinational dosing paradigm would lead to improvements in more difficult-to-achieve behavioral outcomes.

A better approach may have been to utilize drugs which are mechanistically complementary but are spatially distinct, such as combining either PZ or CsA with a drug such as tirilazad, whose primary effects are localized to the vasculature [1, 256]. In fact, the combination of tirilazad and CsA has been one of the combinations proposed to have beneficial effects [213].

## **Conclusion**

In summary, we found that subcutaneous continuous infusion of PZ (10 mg/kg PZ subcutaneous 15 min post-injury + 10 mg/kg/day subcutaneous infusion of PZ for 3 days) maintained mitochondrial RCR and neuronal cytoskeletal integrity, and decreased binding of 4-HNE and acrolein to mitochondrial proteins 72h following severe controlled cortical impact injury. In fact, continuous infusion of PZ was able to maintain cytoskeletal integrity, whereas 12hr intermittent dosing of PZ was not (10 mg/kg PZ subcutaneous 15 min post-injury + 5 mg/kg PZ subcutaneous every 12h up to and including 60h). Additionally, continuous infusion of CsA (20 mg/kg CsA intraperitoneal 15 min post-injury + 10 mg/kg/day subcutaneous infusion of CsA for 3 days) decreased binding of 4-HNE and acrolein to mitochondrial proteins. Although the combination of PZ + CsA was able

to maintain cytoskeletal integrity, it did so to a similar degree as PZ alone, suggestive of a purely PZ effect, and was unable to attenuate other outcome measures. In fact, once combined the protective effect PZ and CsA individually had on formation of mitochondrial bound 4-HNE and acrolein was lost.

We concede that this study was limited to a single dosing paradigm and time point and a limited number of outcome measures, making it difficult to conclude that the combinational therapy PZ + CsA is unable to enhance neuroprotection under any circumstances. However, upon contemplation of the complicated pharmacokinetics and pharmacodynamics of each drug individually, coupled with the fact that both drugs can physically interact with the mitochondria, in hindsight we believe the combination of CsA and PZ may lack feasible clinical translation and that any further animal studies utilizing the combination may prove unethical. Therefore, for the time being we feel that our future directions are better spent further investigating the less well-characterized drug, PZ, including long-term behavioral studies as well as the effect the non-aldehyde scavenging PZ mechanism of action, monoamine oxidase inhibition, has on mitochondrial function and neuroprotection following TBI. Importantly, we also believe this study highlights some of the challenges in developing combinational therapies for traumatic brain injury including, optimization of combined dosing paradigms, consideration of altered pharmacokinetics and pharmacodynamics, choice of outcome measure and time point, as well as variations in neuroprotective efficacy across distinct outcome measures.

On that note, one reason the combination PZ + CsA was chosen for this study was because both CsA and PZ are FDA-approved drugs, which would make their clinical translation for TBI easier, faster, and cheaper than that of experimental agents. However, combining drugs which are known to have multiple mechanisms of action, CsA

is both a calcineurin inhibitor/immunosuppressant and an inhibitor of mPTP [219, 220, 316, 317], and PZ is both an aldehyde-scavenger and a monoamine oxidase inhibitor [71, 72, 74, 76, 198, 278, 311], may lead to a number of confounding factors. Therefore, although more difficult in regards to clinical translational, it may in fact represent a better approach to limit combinational approaches to compounds with less complicated mechanisms of action, such as the non-immunosuppressive mPTP inhibitor, NIM811, or a pure aldehyde-scavenger, at least in the early proof-of-principle stages of investigation.

### **Acknowledgments**

This work was supported by NIH-NINDS 5R01 NS083405 & 5R01 NS084857. Jacqueline R. Kulbe is currently supported by NIH-NINDS NRSA NS096876.

## **CHAPTER FOUR:**

### **Comparative Effects of Phenezine, Hydralazine, and Pargyline on Learning and Memory and Cortical Tissue Sparing Following Experimental Traumatic Brain Injury**

**Preface:** Portions of Chapter Four to be submitted for publication as: **Kulbe JR**, Dunkerson JA, Huettl PF, Wang JA, Smith R, Gerhardt GA, and Hall ED. Comparative Effects of Phenezine, Hydralazine, and Pargyline on Learning and Memory and Cortical Tissue Sparing Following Experimental Traumatic Brain Injury.



## **Introduction**

Traumatic brain injury (TBI) represents a significant health crisis. Within the United States, 2.8 million TBIs are diagnosed annually [2]. Although the most severe injuries, those resulting in death or requiring hospitalization account for a minority of the TBI diagnoses, they account for 90% of TBI-associated costs [10, 11]. The most severe injuries also result in the highest rates of morbidity. In fact, over fifty percent of TBI patients requiring hospitalization will continue to suffer from TBI-related cognitive, physical or emotional disabilities more than a year following injury [13]. However, to date, no FDA-approved neuroprotective pharmacotherapies exist for acute TBI [1]. Therefore, it is imperative that more robust pharmacological neuroprotective agents be developed.

Lipid peroxidation (LP) is a well-documented pathology that occurs following TBI [1, 17, 55] (**Fig. 4.1**). LP is initiated by reactive oxygen and nitrogen species (ROS/RNS), which extract electrons from the polyunsaturated fatty acids located within neuronal and organelle membranes, generating lipid and lipid peroxyl radicals [1, 55]. Although dysfunctional mitochondria and the electron transport chain serve as a primary source for generation of pathologic ROS/RNS [1, 17, 55], these reactive species are also produced by other sources. Such sources include the metabolism of monoamines by monoamine oxidase (MAO), autoxidation of biogenic amines, inflammatory cell oxidative bursts, and the metabolism of arachidonic acid [1]. LP is a self-propagating process which terminates upon formation of LP-derived neurotoxic aldehydes such as 4-hydroxynonenal (4-HNE) and 2-propenal (i.e. acrolein) [1, 55]. These LP-derived neurotoxic aldehydes covalently bind to proteins, inducing protein dysfunction, cell death and neuronal degeneration [1, 17, 55, 77, 85, 88].

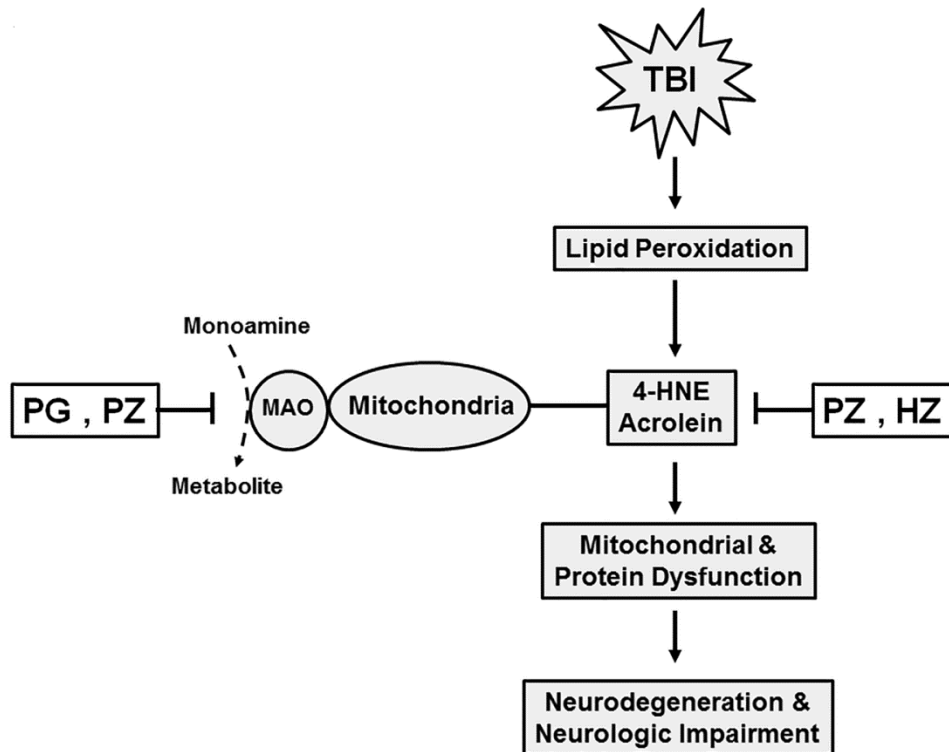


**Figure 4.1 Simplified schematic of traumatic brain injury (TBI) pathophysiology and pargyline (PG), phenelzine (PZ) and hydralazine (HZ) mechanisms of action.** TBI induces generation of reactive oxygen and nitrogen species, leading to lipid peroxidation of polyunsaturated fatty acids. Lipid peroxidation terminates upon formation of neurotoxic aldehydes, such as 4-hydroxynonenal (4-HNE) and 2-propenal (acrolein). 4-HNE and acrolein covalently bind proteins, including mitochondrial proteins, causing dysfunction, neurodegeneration, and neurologic impairment. PZ and HZ are capable of scavenging 4-HNE and acrolein. Additionally, PZ, along with PG, can inhibit monoamine oxidase (MAO), an outer mitochondrial membrane protein responsible for metabolizing monoamine neurotransmitters such as dopamine, serotonin, and norepinephrine.

Importantly, LP-derived neurotoxic aldehydes and their protein-aldehyde derivatives are longer lived than their free radical predecessors [77, 331]. Therefore, scavenging of LP-derived neurotoxic aldehydes offers a practical therapeutic approach [1, 79, 331, 332].

Fortunately, a drug-class exists that is capable of scavenging LP-derived aldehydes. Compounds which contain a hydrazine moiety (-NH-NH<sub>2</sub>), including the FDA-approved drugs phenelzine (PZ) and hydralazine (HZ) [198], can scavenge LP-derived neurotoxic aldehydes through formation of hydrazone derivatives [258, 261]. Clinically PZ, a non-selective irreversible monoamine oxidase inhibitor (MAOI), is used in the treatment of intractable depression and as an anxiolytic [169]. However, PZ has also been shown to be neuroprotective in experimental TBI, especially in regard to biochemical outcome measures such as attenuating TBI-induced mitochondrial respiratory dysfunction [71, 72, 333, 334]. Similar to TBI, PZ and HZ, clinically used as an anti-hypertensive, have been shown to be neuroprotective in models of spinal cord injury (SCI) [74, 75]. Although the neuroprotection PZ and HZ provide is well-established to rely on the presence of their aldehyde-scavenging hydrazine moieties (-NH-NH<sub>2</sub>) [72, 198, 258], it is currently unclear what effect the MAOI properties of PZ may have on TBI pathophysiology.

MAO is an outer mitochondrial membrane enzyme responsible for the metabolism of monoamine neurotransmitters such as norepinephrine (NE), serotonin (5-HT), and dopamine (DA) [197]. Therefore, inhibition of MAO can lead to increases in these neurotransmitters [197]. The effect MAO inhibition and increases in monoamine neurotransmitters would have on TBI pathophysiology remains controversial. For instance, oxidative deamination of monoamine neurotransmitters by MAO generates ROS [193], suggesting that MAO inhibition could reduce ROS and provide an additional

antioxidant neuroprotective mechanism. However, inhibition of MAO also leads to increases in biogenic amines, such as DA, which is capable of directly inhibiting mitochondrial respiration [194], and undergoing non-enzymatic autoxidation formation of toxic H<sub>2</sub>O<sub>2</sub> and quinones [194], suggesting that MAO inhibition could also lead to increases in neurotoxicity and oxidative stress. Additionally, while some studies have shown that acute administration of monoamine agonists can be neuroprotective following TBI; [154] others have shown a correlation between high levels of monoamines, such as NE, and poor outcome [181].

Several pre-clinical studies have indicated that PZ shows promise for use as a neuroprotective agent in brain injury [71, 72, 76, 333, 334]. However, in order for PZ to be further developed for use in clinical TBI, the effect its MAOI properties have on TBI pathophysiology must first be explored. Therefore, the goal of this study was to further investigate PZ's MAOI effects following TBI by comparing PZ, an aldehyde-scavenger and MAOI, to the non-MAOI aldehyde scavenge HZ, and the non-aldehyde-scavenger MAOI pargyline (PG) (**Fig. 4.2**). This is not only the first study to evaluate the effects of PG and HZ in experimental TBI, but also the first study to assess the behavioral effects of PZ in experimental TBI. We evaluate the ability of PZ, HZ, and PG to improve learning and memory and enhance cortical tissue sparing following a severe controlled cortical impact injury (CCI) in 3-month old male Sprague-Dawley rats. Additionally, HPLC is used to measure NE, 5-HT, DA, and their metabolites in uninjured cortical tissue in order to determine the effect of the PZ, HZ, and PG dosing paradigms on MAO inhibition.

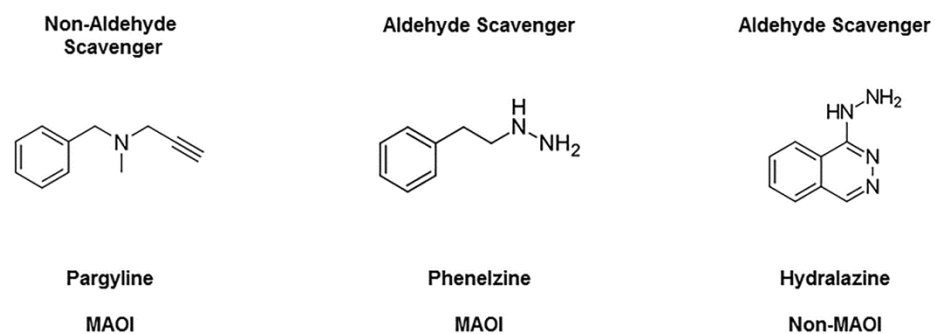


**Figure 4.2 Chemical structures of pargyline, phenelzine and hydralazine.** Both phenelzine and hydralazine are capable of scavenging aldehydes via a hydrazine (-NH-NH<sub>2</sub>) moiety. Pargyline does not contain a hydrazine moiety (-NH-NH<sub>2</sub>) and is unable to scavenge aldehydes. Pargyline and phenelzine are monoamine oxidase inhibitors (MAOI), whereas hydralazine is not.

## **Methods**

### **Animals**

Three-month-old male Sprague-Dawley rats (Harlan, Indianapolis, IN) were housed in the Division of Laboratory Animal Resources of the University of Kentucky Medical Center. All animal and husbandry were conducted in accordance with the University of Kentucky Institutional Animal Care and Use Committee. Animals were housed in a 12hr light and dark cycle and allowed food and water *ad libitum*. Animals were housed in pairs of two in housing containing Enviro-dry enrichment. For behavioral experiments, animals were weighed and handled on a daily basis through the day of euthanasia beginning five days prior to surgery.

### **Experimental Design: High Performance Liquid Chromatography (HPLC) Monoamine and Metabolite Analysis (Fig. 4.3)**

In order to assess MAO inhibition of our dosing paradigm we used HPLC to evaluate monoamine and metabolite tissue levels and turnover ratios in uninjured cortex. Uninjured animals (n = 6 animals per group) were administered an intraperitoneal (i.p.) dose of saline, PZ (Sigma, St. Louis, MO), HZ (Sigma, St. Louis, MO), or PG (Sigma, St. Louis, MO) at time 0h, 24h, and 48h for a total of three injections. Sample size was based upon the University of Kentucky Center for Microelectrode Technology (CenMeT) standard of practice. PZ was administered at 15mg/kg in saline [74], HZ was administered at 5mg/kg in saline [74], and PG was administered at 15mg/kg to parallel *in-vitro* experiments in which equal concentrations of PZ and PG were utilized [72]. Animals were euthanized by CO<sub>2</sub> and decapitation 72h following the first drug administration (24h following third drug administration).

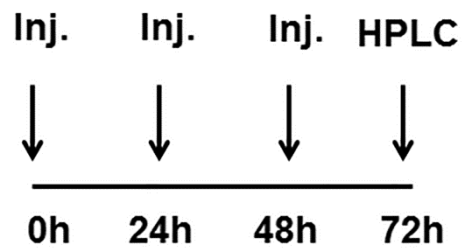


**Figure 4.3 Monoamine and metabolite HPLC experimental design.** Uninjured rats received intraperitoneal injections (Inj.) of vehicle (saline), pargyline (15mg/kg), phenelzine (15mg/kg), or hydralazine (5mg/kg) at 0h, 24h, and 48h for a total of 3 injections, representative of the dosing paradigm utilized in CCI-MWM studies. Animals were euthanized and tissue was collected for HPLC analysis 72h following the first injection.

A sterile biopsy punch (Integra Miltex, Plainsboro, NJ) was used to collect cortical punches 3mm in diameter and 2mm in thickness from the parietal cortex in the same anatomic location to which injured animals would have received a CCI injury. Tissue was immediately placed on dry ice, weighed and stored at -80°C until time of analysis. Tissue was sent to CenMeT for HPLC evaluation of norepinephrine (NE), dopamine (DA), 5-hydroxytryptamine (5-HT), 3,4-dihydroxyphenylacetic acid (DOPAC), homovanillic acid (HVA), and 5-hydroxyindoleacetic acid (5-HIAA).

### **High Performance Liquid Chromatography with Electrical Detection (HPLC-EC) for Monoamine and Metabolite Tissue Levels**

Cortical tissue samples (5mg – 25mg) for HPLC-EC were thawed and immediately processed by CenMeT as previously described [187]. A total of 50µl of filtrate (in mobile phase) was injected onto an HPLC column. Retention times for NE, 5-HT, 5-HIAA, DA, DOPAC, and HVA standards and dihydroxybenzylamine (DHBA), which was used as an internal standard, were used to identify peaks and to determine tissue levels of each neurotransmitter or metabolite found in each brain sample represented as ng/g wet weight of tissue sample [187].

### **Controlled Cortical Impact Traumatic Brain Injury (CCI)**

Animals were anesthetized using 4% isoflurane, shaved, and placed into a stereotaxic frame (David Kopf, Tujunga, CA), where isoflurane was maintained at 3% for the duration of the procedure. Following ethanol and betadine sterilization, a midline incision was made to expose the skull, and a 6mm craniotomy was created lateral to the sagittal suture and midway between lambda and bregma using a Michele Trephine (Miltex, Bethpage, NY). The exposed brain with intact dura received a severe CCI using a computer controlled pneumatic impact device (TBI 03010; Precision Systems and



Instrumentation, Fairfax Station, VA) fitted with a 5mm beveled tip and set to impact at a depth of 2.0mm with a 500ms dwell time and an impact velocity of ~3.5m/s, as described previously [71]. After injury, Surgicel (Johnson & Johnson, Arlington, TX) was placed onto the dura and an 8mm plastic disk was affixed to the skull using tissue adhesive (Gesswein, Bridgeport, CT) to close the craniotomy site and the incision was closed using wound clips. Sham animals (n=13) underwent the same procedure, but did not receive an impact injury and did not receive drug administration. Our previously published PZ experiments which reported the results of biochemical measurements utilized sample sizes = 8 [71, 72, 333]. Therefore, to account for a potential increase in variability the sample size was increased by a factor of 1.5 for the behavioral experiments detailed here. A single experimenter completed all surgeries.

#### **CCI Dosing Paradigm (Fig. 4.4)**

Animals exposed to CCI were randomly assigned to vehicle (n=13), PZ (n=13), HZ (n=13), or PG (n=13). As 48h-72h represents the peak of LP-derived aldehyde formation [73], it follows that drug should be administered throughout this acute time period [72, 333]. Therefore, drug or vehicle was administered 15min, 24h, and 48h post-injury (three injections per animal). PZ was administered at 15mg/kg in saline. HZ was administered at 5mg/kg in saline. As this is the first study to directly compare PZ and HZ in experimental TBI, the dosing paradigms chosen were based on previously optimized doses in which PZ and HZ were compared in SCI [74], and are slightly higher than our previously published PZ dosing paradigms (10mg/kg/day subcutaneous)[72, 333]. Similar to PZ, PG was administered 15mg/kg in saline, to parallel *ex-vivo* mitochondrial studies in which equivalent concentrations of PZ and PG were used [72]. The vehicle group received an equal amount of saline as was administered to drug groups. Drug and vehicle were prepared and coded by a separate experimenter.

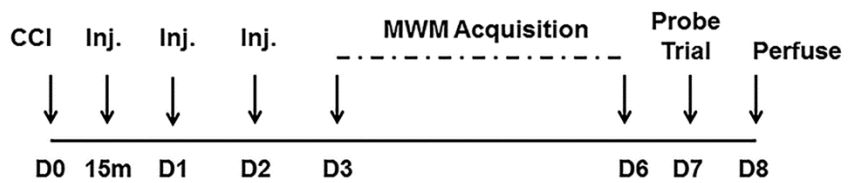


**Figure 4.4 Controlled cortical impact and Morris water maze experimental design.** Beginning on D0 rats were subjected to a severe controlled cortical impact injury (CCI). 15min following injury animals received intraperitoneal injections (Inj.) of vehicle (saline), pargyline (15mg/kg), phenelzine (15mg/kg), or hydralazine (5mg/kg). Sham animals underwent surgical procedures but did not receive an impact or injections. Doses were repeated 24h (D1) and 48h (D2) following injury. On D3-D6 animals underwent Morris water maze (MWM) acquisition, which was followed by a probe trial for reference memory on post-CCI D7. Animals were euthanized, perfused, and whole brains were collected on post-CCI D8.

### **Morris Water Maze (Fig. 4.4)**

Animals began Morris water maze (MWM) testing 72h following injury and 24h following the final drug administration. Animals began MWM testing at this early time point in order to parallel our previous *in-vivo* PZ studies which evaluated mitochondrial bioenergetics, aldehyde-protein modification, and cytoskeletal degradation 72h following injury [72, 333], the peak of mitochondrial dysfunction, lipid peroxidation, and  $\alpha$ -spectrin degradation [73]. The day prior to the start of MWM testing a circular pool (127 cm diameter x 56 cm height) was filled and water was allowed to acclimate to room temperature overnight. A submerged escape platform (13.5 cm diameter) was placed in the center of one quadrant approximately 2cm below the water's surface. Visual cues were placed on curtains surrounding the pool. The pool was filled with black non-toxic paint to ensure opacity. All trials were recorded and analyzed with Noldus Ethovision XT version 12.0 (Cincinnati, OH). MWM acquisition trials were conducted daily from post-CCI D3 through D6 to assess working memory. On post-CCI D3 through D6, animals were given four trials (N, S, E, and W quadrant start) per day. At the beginning of each trial animals were placed into the pool facing the wall. The direction the first trial began from was varied each day. For each trial, animals were allowed 60 seconds to find the platform. Animals that did not find the platform were guided to the platform and manually placed there. Once on the platform, animals were allowed to remain for 20 seconds. A trial was considered successful when an animal reached the platform within 60 seconds and remained there for at least five seconds, which triggered the software to end the trial. Animals were allowed to rest 5min between trials. Software data was confirmed against manual time recordings. To assess reference memory, a probe trial was conducted on post-CCI D7 in which the platform was removed and the animals were given 30 seconds to search the pool for the platform. To prevent hypothermia, all

animals were dried between trials and placed into dry cages sitting on heating pads near a ceramic heat source. At the beginning of the trials, all wound sites were inspected for signs of infection. No signs of infection were seen, but to insure asepsis, betadine was applied to the wound site at the conclusion of the day's trials. Experimenters responsible for behavioral experiments were kept consistent throughout each day and block of testing.

#### **Tissue Processing for Histology (Fig. 4.4)**

On post-CCI D8 (one day following completion of MWM testing) animals were euthanized with an overdose of sodium pentobarbital (150mg/kg). Animals were transcardially perfused with phosphate buffer solution (PBS) followed by 4% paraformaldehyde (PFA) in PBS. Following perfusion, brains were extracted and placed into 4% PFA at 4°C for 48h-72h. Brains were then transferred to a 30% sucrose solution in PBS at 4°C and allowed to sink before being flash frozen in isopentane and stored at -80°C until further processing. Coronal slices 40µm thick were cut on a freezing microtome using a blade angle of 7.5° to the tissue surface. Sections were taken between the septal area and the posterior hippocampus. Every tenth section was collected per series. Sections were store at -20°C in cryoprotectant (30% ethylene glycol, 30% glycerol, Tris-buffered saline (TBS)).

Sections were mounted onto Superfrost Excell microscope slides (ThermoFisher Scientific, Waltham, MA) in TBS and dried. Mounted tissue was soaked in a CHCl<sub>3</sub> (100mL) + EtOH (400ml 95% EtOH) solution for 30min. Slides were then soaked in decreasing concentrations of EtOH (95%, 70%) for 3min each.. Slides were then soaked for 6-8min in a cresyl violet solution (5.64ml 1M acetic acid, 0.816g sodium acetate, 500ml ddH<sub>2</sub>O, 0.2g cresyl violet powder). Slides were then dipped 8x each in the

following solutions: ddH<sub>2</sub>O, 50% EtOH, and 70% EtOH, 95% EtOH + acetic acid, followed by 2min in 95% EtOH, 100% EtOH, and Xylene. Slides were then cover slipped using permount.

Slides were imaged using Axio Scan.Z1 (Zeiss, Thornwood, NY) at 20x magnification and analyzed using HALO version 2.0 (Indica Labs, Corrales, NM). Cortical area was measured from the dorsal aspect of lamina I to the dorsal aspect of the corpus callosum, from the midline to the rhinal sulcus landmark laterally, from interaural level 8.20mm – 3.40mm (12 slices, 400µM apart). For the total percent cortical tissue sparing the area for each coronal section was multiplied by the distance between coronal sections (400µM) and then summed and the ipsilateral total was divided by the contralateral total to give total percent cortical tissue spared  $[\sum(\text{area} \times \text{distance})_{\text{ipsilateral}}] / [\sum(\text{area} \times \text{distance})_{\text{contralateral}}] \times 100\%$  [71, 72]. Sample size (n = 8-9) was based upon previously published histological data indicating that multiple PZ doses can improve cortical tissue sparing at 72h, an early point in tissue degeneration [72], and that single dose PZ can improve cortical tissue sparing at 14d [71]. For histologic analysis, animals were excluded if tissue showed evidence of damage sustained during tissue processing

### **Statistical Analysis**

Statistical analysis was conducted using Prism version 7.0 (Graph Pad, San Diego, CA). All data are reported as mean ± standard deviation or median ± interquartile range as indicated. A p value <0.05 was considered significant. HPLC data were analyzed using a one-way ANOVA, followed by *post-hoc* Tukey's. In cases in which homogeneity of variance was violated (Brown-Forsythe, p < 0.05), data was analyzed using Kruskal-Wallis, followed by *post-hoc* Dunn's. Due to low levels of dopaminergic metabolites in the cortex, some samples showed non-detectable levels of homovanillic

acid (HVA) and were thus excluded as indicated in the results section. Additionally, for HPLC data Grubb's test ( $\alpha = 0.05$ ) was used to remove statistical outliers as indicated in the results section. During the MWM acquisition trials (post-CCI D3 – D6) the four trials per day were averaged for each animal and statistical analysis of latency, distance, and swim speed was conducted using two-way repeated measures ANOVA, followed by *post-hoc* Tukey's. Probe trial, weight, and total cortical tissue sparing were analyzed using a one-way ANOVA, followed by *post-hoc* Tukey's. To determine if there was a difference in % cortical tissue sparing (ipsilateral/contralateral) between groups at the level of individual coronal sections (i.e. intraaural level) a two-way repeated measures ANOVA was utilized to analyze the CCI groups (vehicle, PG, PZ, and HZ).

## Results

### **PG, PZ, or HZ: HPLC Monoamine and Metabolite Tissue Levels and Turnover Ratios in Uninjured Cortical Tissue (Fig. 4.5 – 4.7)**

PG and PZ are classified as monoamine oxidase inhibitors, whereas HZ is not. Saline, PG (15mg/kg), PZ (15mg/kg), or HZ (5mg/kg) were administered intraperitoneally at 0h, 24h, and 48h for a total of three doses and tissue was collected at 72h to parallel CCI-MWM experiments. However, uninjured animals were used in this set of experiments to determine the basal level of MAO inhibition induced by the dosing paradigms. The monoamine neurotransmitters NE, 5-HT, and DA, which are metabolized by MAO into metabolites, were measured along with the 5-HT metabolite 5-HIAA, and the DA metabolites DOPAC and HVA. Monoamine turnover ratios (metabolite/monoamine) are used as a proxy measure of MAO inhibition. Although the metabolism of NE also involves MAO-A, as well as a variety of other enzymes, and results in the formation of metabolites such as VMA and MHPG, NE metabolites were not measured as part of this study due to their low cortical tissue levels. 5-HT is metabolized to 5-hydroxyindoleacetic acid (5-HIAA) by MOA-A and ALDH [186], and is measured as part of this dissertation.

For NE, a single saline sample was identified as an outlier (Grubb's) and excluded ( $G = 1.915$ ,  $Y = 6$ ). For NE, a one-way ANOVA revealed a statistically significant effect across all groups ( $F[3,19] = 10.84$ ,  $p = 0.0002$ ). *Post-hoc* testing (Tukey's) revealed that compared to saline, NE (ng/g) was significantly increased in PZ ( $p < 0.001$ ), and that compared to HZ, NE (ng/g) was significantly increased in PZ ( $p < 0.001$ )(**Fig. 4.5**). Thus, PZ results in an increase in NE.

## Norepinephrine 72h

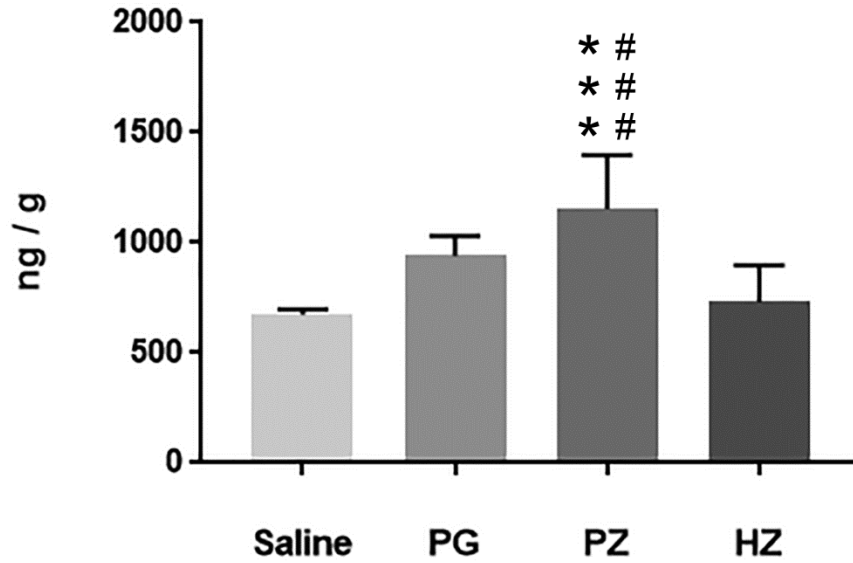


**Figure 4.5 Tissue Level (ng/g) of norepinephrine (NE) in 72h uninjured cortex.** NE measured via HPLC 72h following an initial intraperitoneal injection (0h) of saline, pargyline (PG), phenelzine (PZ), or hydralazine (HZ), with additional doses given at 24h and 48h. Values = mean  $\pm$  standard deviation; one-way analysis of variance followed by Tukey *post hoc*; \*\*\* $p < 0.001$ , compared to saline, ### $p < 0.001$  compared to HZ;  $n = 5-6$  per group.



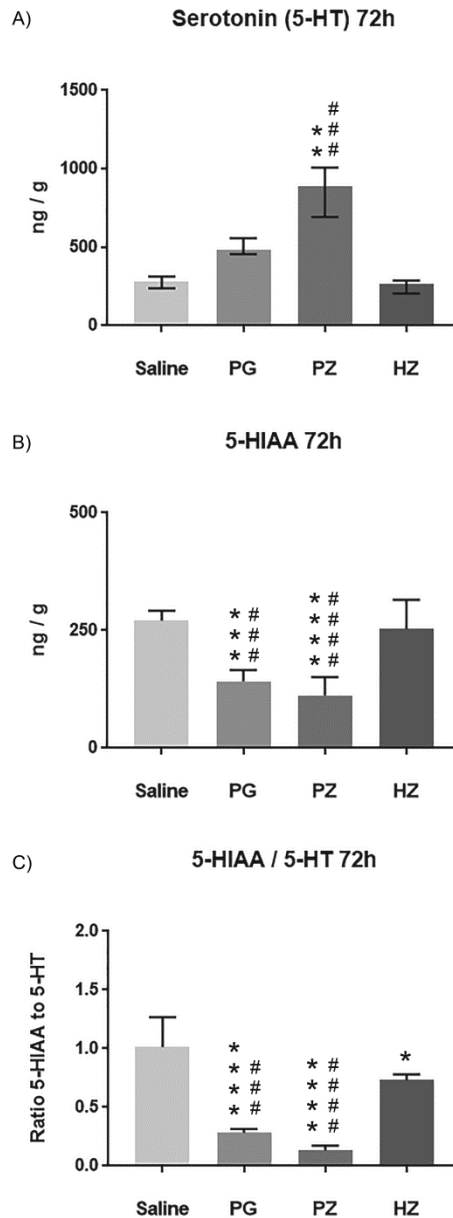


**Figure 4.6 Tissue Level (ng/g) of serotonin (5-HT) and metabolites in 72h uninjured cortex. (A) 5-HT, (B) the 5-HT metabolite 5-hydroxyindoleacetic acid (5-HIAA), (C) and the 5-HT turnover ratio (5-HIAA/5-HT) in uninjured cortex as measured via HPLC 72h following an initial intraperitoneal injection (0h) of saline, pargyline (PG), phenelzine (PZ), or hydralazine (HZ), with additional doses given at 24h and 48h. Values = (A) median  $\pm$  interquartile range, Kruskal- Wallis followed by Dunn *post-hoc* (B,C) mean  $\pm$  standard deviation, one-way analysis of variance followed by Tukey *post hoc*; \* $p$  < 0.05, \*\* $p$  < 0.01, \*\*\* $p$  < 0.001, \*\*\*\* $p$  < 0.0001 compared to saline; ### $p$  < 0.001, #### $p$  < 0.0001 compared to HZ;  $n$  = 5-6 per group.**

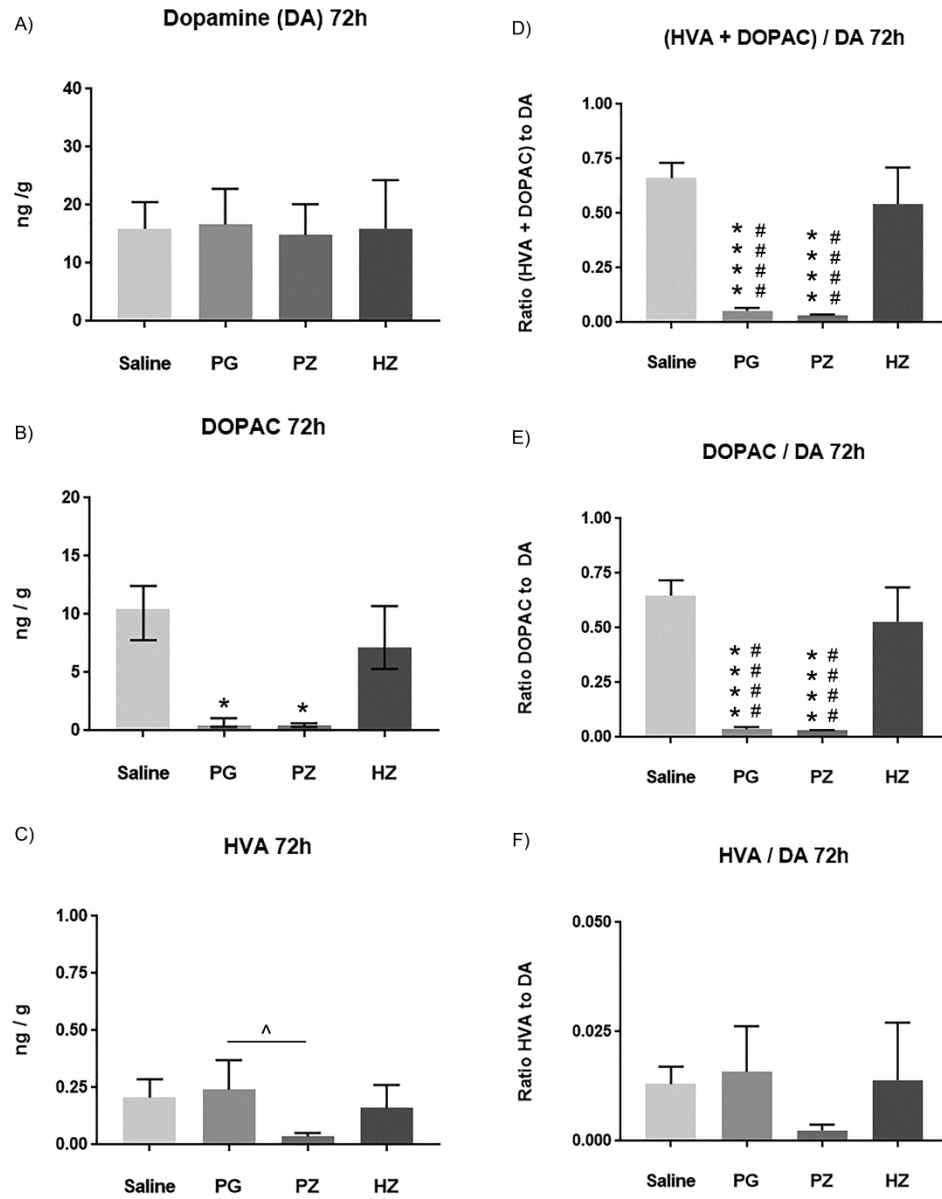


**Figure 4.7 Tissue Level (ng/g) of dopamine (DA) and metabolites in 72h uninjured cortex. (A) DA, (B) the DA metabolite 3,4-dihydroxyphenylacetic acid (DOPAC), (C) the DA metabolite homovanilic acid (HVA), and the DA turnover ratios (D) (DOPAC + HVA) / DA, (E) DOPAC / DA, (F) and HVA / DA in uninjured cortex as measured via HPLC 72h following an initial intraperitoneal injection (0h) of saline, pargyline (PG), phenzelzine (PZ), or hydralazine (HZ), with additional doses given at 24h and 48h. Values = (B) median  $\pm$  interquartile range, Kruskal-Wallis followed by Dunn *post-hoc* (A,C-F) mean  $\pm$  standard deviation, one-way analysis of variance followed by Tukey *post hoc*; \* $p < 0.05$ , \*\*\*\* $p < 0.0001$  compared to saline; ##### $p < 0.0001$  compared to HZ; ^ $p < 0.05$ ; n = 4-5 per group.**

For 5-HT, a one-way ANOVA revealed a statistically significant effect across all groups ( $F[3,20] = 44.81$ ,  $p < 0.0001$ ). However, Brown-Forsythe revealed an inequality of variance ( $p = 0.0075$ ). Therefore, Kruskal-Wallis was used in lieu of a one-way ANOVA. KW revealed a significant effect across all groups ( $H[3, n = 24] = 19.5$ ,  $p = 0.0002$ ). *Post-hoc* testing (Dunn's) revealed that compared to saline, 5-HT (ng/g) was significantly increased in PZ ( $p < 0.01$ ), and that compared to HZ, 5-HT (ng/g) was significantly increased in PZ ( $p < 0.001$ )(**Fig. 4.6A**). Thus, PZ results in an increase in 5-HT.

For the 5-HIAA, a one-way ANOVA revealed a statistically significant effect across all groups ( $F[3,20] = 23.64$ ,  $p < 0.0001$ ). *Post-hoc* testing (Tukey's) revealed that compared to saline, 5-HIAA (ng/g) was significantly decreased in PZ ( $p < 0.0001$ ) and PG ( $p < 0.001$ ), and that compared to HZ, 5-HIAA (ng/g) was significantly decreased in PZ ( $p < 0.0001$ ) and PG ( $p < 0.001$ )(**Fig. 4.6B**). Thus, both PZ and PG result in a decrease in 5-HIAA, a 5-HT metabolite.

For the ratio 5-HIAA / 5-HT, a single HZ sample was identified as an outlier (Grubb's) and excluded ( $G = 2.2024$ ,  $Y = 6$ ). For the ratio 5-HIAA / 5-HT, a one-way ANOVA revealed a statistically significant effect across all groups ( $F[3,19] = 54.29$ ,  $p < 0.0001$ ). *Post-hoc* testing (Tukey's) revealed that compared to saline, the ratio 5-HIAA / 5-HT was significantly decreased in PZ ( $p < 0.0001$ ), PG ( $p < 0.0001$ ), and HZ ( $p < 0.05$ ) and that compared to HZ, the ratio 5-HIAA / 5-HT was significantly decreased in PZ ( $p < 0.0001$ ) and PG ( $p < 0.001$ )(**Fig. 4.6C**). Thus, PZ, PG, and HZ result in a significant decrease in 5-HT turnover to 5-HIAA (i.e. increase in MAO inhibition). However, PZ and PG do so to a significantly greater degree than HZ.

Prior to statistical analysis, due to undetectable HVA levels, one animal was removed from each group (saline, PG, PZ, HZ) for all analysis of DA and DA metabolites. Additionally, during HVA statistical analysis, a single PZ sample was identified as an outlier (Grubb's) and excluded ( $G = 2.2024$ ,  $Y = 6$ ). In order to maintain consistency and be able to calculate DA metabolite/DA turnover ratios, this PZ animal was further excluded from the entire DA data set.

For DA, a one-way ANOVA did not reveal a statistically significant effect across all groups ( $F[3,15] = 0.06434$ ,  $p = 0.9779$  (**Fig. 4.7A**). Thus, PZ, PG, nor HZ affected DA levels.

For DOPAC, a one-way ANOVA revealed a statistically significant effect across all groups ( $F[3,15] = 32.07$ ,  $p < 0.0001$ ). However, Brown-Forsythe revealed an inequality of variance ( $p = 0.0156$ ). Therefore, Kruskal-Wallis was used in lieu of a one-way ANOVA. KW revealed a significant effect across all groups ( $H[3, n = 19] = 14.1$ ,  $p = 0.0028$ ). *Post-hoc* testing (Dunn's) revealed that compared to saline, DOPAC (ng/g) was significantly decreased in PZ ( $p < 0.0001$ ) and PG ( $p < 0.0001$ ) (**Fig. 4.7B**). Thus, both PZ and PG result in a decrease in DOPAC, a DA metabolite.

For HVA, a one-way ANOVA revealed a statistically significant effect across all groups ( $F[3,15] = 3.875$ ,  $p = 0.0310$ ). *Post-hoc* testing (Tukey's) revealed a significant difference between PZ and PG ( $p < 0.05$ ) (**Fig. 4.7C**). Thus, PZ results in a decrease in HVA, a DA metabolite, but only when compared to PG.

For the ratio (HVA + DOPAC) / DA, a one-way ANOVA revealed a statistically significant effect across all groups ( $F[3,15] = 56.69$ ,  $p < 0.0001$ ). *Post-hoc* testing (Tukey's) revealed that compared to saline, the ratio (HVA + DOPAC) / DA is significantly decreased in PZ ( $p < 0.0001$ ) and PG ( $p < 0.0001$ ), and that compared to HZ,

the ratio (HVA + DOPAC) / DA is significantly decreased in PZ ( $p < 0.0001$ ) and PG ( $p < 0.0001$ )(**Fig. 4.7D**). Thus, both PZ and PG result in a decrease in DA turnover to HVA+DOPAC (i.e. increase in MAO inhibition).

For the ratio DOPAC / DA, a one-way ANOVA revealed a statistically significant effect across all groups ( $F[3,15] = 63.42$ ,  $p < 0.0001$ ). *Post-hoc* testing (Tukey's) revealed that compared to saline, the ratio DOPAC / DA was significantly decreased in PZ ( $p < 0.0001$ ) and PG ( $p < 0.0001$ ), and that compared to HZ, the ratio DOPAC / DA was significantly decreased in PZ ( $p < 0.0001$ ) and PG ( $p < 0.0001$ )(**Fig. 4.7E**). Thus, both PZ and PG result in a decrease in DA turnover to DOPAC (i.e. increase in MAO inhibition).

For the ratio HVA / DA, a one-way ANOVA did not reveal a statistically significant effect across all groups ( $F[3,15] = 1.916$ ,  $p = 0.1704$ )(**Fig. 4.7F**). Thus, PZ, PG, nor HZ affected the turnover of DA to HVA.

Overall these results indicate that for the specific dosing paradigms utilized, administration of PG or PZ, the two MAOIs, results in significant MAO inhibition as evidenced by the decrease in both 5-HT (**Fig. 4.6C**) and DA (**Fig. 4.7D-F**) turnover. Interestingly, HZ, which is not classified as an MAOI, also showed some possible MAOI inhibition as HZ administration resulted in a significant decrease to 5-HT turnover (**Fig. 4.6C**). However, HZ did not have the same effect in regards to DA turnover (**Fig. 4.7D-F**). Overall these results also indicate that for the specific dosing paradigms utilized, administration of PZ led to a significant increase in the monoamine neurotransmitters NE and 5-HT (**Fig. 4.5 and 4.6A**).

### **Morris Water Maze Latency to Platform (MWM D1-D4, Post CCI D3-D6) (Fig. 4.8A)**

For latency to platform, a two-way repeated measures ANOVA revealed a statistically significant effect across time ( $F[3,180] = 31.26, p < 0.0001$ ), and treatment ( $F[4,60] = 12.22, p < 0.0001$ ). However, the interaction between time x treatment was not significant ( $F[12,180] = 1.681, p = 0.0743$ ). *Post-hoc* testing (Tukey's) revealed that all groups other than PZ learned to find the platform significantly faster on subsequent trial days. For the sham group, animals found the platform significantly faster on D2 ( $p < 0.01$ ), D3 ( $p < 0.0001$ ), and D4 ( $p < 0.0001$ ) compared to D1. For the vehicle group, animals found the platform significantly faster on D2 ( $p < 0.05$ ), D3 ( $p < 0.01$ ), and D4 ( $p < 0.01$ ) compared to D1. For the PG group, animals found the platform significantly faster on D3 ( $p < 0.01$ ) and D4 ( $p < 0.001$ ) compared to D1. For the HZ group, animals found the platform significantly faster on D2 ( $p < 0.01$ ) and D3 ( $p < 0.0001$ ) compared to D1. However, HZ latency to platform was not significantly different on D4 compared to D1 ( $p > 0.05$ ). Further, on D4 of MWM, vehicle ( $p < .05$ ), PG ( $p < 0.05$ ), PZ ( $p < 0.0001$ ), and HZ ( $p < 0.0001$ ) all took significantly longer to find the platform compared to sham (*not annotated on figure*). Thus, during the first four days of MWM all groups showed a decrease in the time it took to find the submerged platform. However, PZ was the only group in which none of these decreases reached statistical significance, suggesting that the PZ group had the most difficulty in learning to find the platform day to day during the first four days of MWM. Similarly, across the first four days of MWM, *post-hoc* testing (Tukey's) revealed that the overall treatment effect showed a near significant difference between vehicle and PZ ( $p = 0.0706$ ), but not between vehicle and PG ( $p = 0.9191$ ) or vehicle and HZ ( $p = 0.6971$ ) (*not graphically shown*).

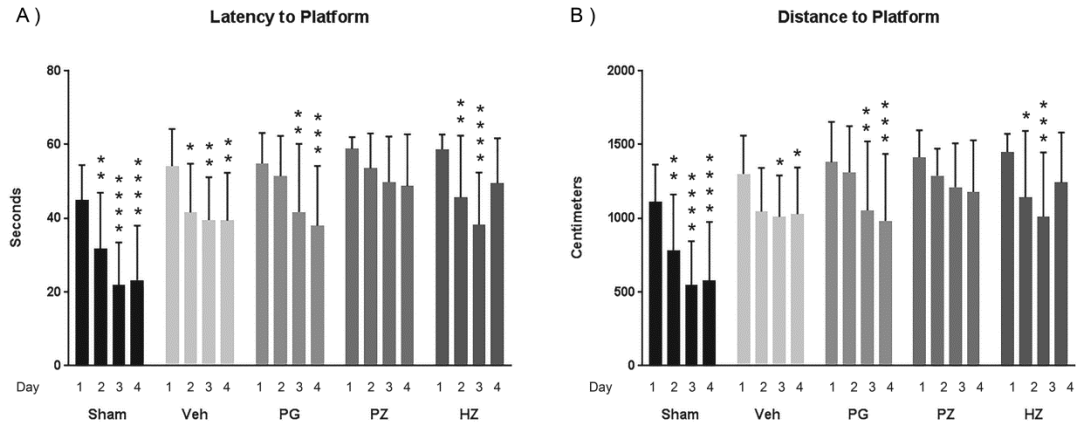


**Figure 4.8 Morris water maze latency and distance to platform.** Rats began the Morris water maze (MWM D1) three days following controlled cortical impact injury (CCI). Animals were given 4x60s trials to find the submerged platform per day for a total of four days (MWM D1 – D4). **(A)** All groups other than PZ were able to find the platform significantly faster (seconds) on subsequent MWM days (D2, D3, D4) when compared to within group MWM D1. **(B)** All groups other than PZ traveled a significantly shorter distance (centimeters) to the platform on subsequent MWM days (D2, D3, D4) when compared to within group MWM D1. Values = mean  $\pm$  standard deviation; repeated measures two-way analysis of variance followed by Tukey *post hoc*; \* $p < 0.05$ , \*\* $p < 0.01$ , \*\*\* $p < 0.001$ , \*\*\*\* $p < 0.0001$  compared to within group MWM D1; Sham, Veh = vehicle + CCI, PG = pargyline + CCI, PZ = phenelzine + CCI, HZ = hydralazine + CCI;  $n = 13$  per group.

### **Morris Water Maze Distance to Platform (MWM D1-D4, Post CCI D3-D6) (Fig. 4.8B)**

For distance to platform, a two-way repeated measures ANOVA revealed a statistically significant effect across time ( $F[3,180] = 25.75$ ,  $p < 0.0001$ ), and treatment ( $F[4,60] = 9.364$ ,  $p < 0.0001$ ). However, the interaction between time x treatment was not significant ( $F[12,180] = 1.611$ ,  $p = 0.0918$ ). *Post-hoc* testing (Tukey's) revealed that all groups other than PZ traveled significantly shorter distances to find the platform on subsequent trial days. For the sham group, animals traveled significantly less distance to the platform on D2 ( $p < 0.01$ ), D3 ( $p < 0.0001$ ) and D4 ( $p < 0.0001$ ) compared to D1. For the vehicle group, animals traveled significantly less distance to the platform on D3 ( $p < 0.05$ ) and D4 ( $p < 0.05$ ) compared to D1. For the PG group, animals traveled significantly less distance to the platform on D3 ( $p < 0.01$ ) and D4 ( $p < 0.001$ ) compared to D1. For the HZ group, animals traveled significantly less distance to the platform on D2 ( $p < 0.05$ ) and D3 ( $p < 0.001$ ) but not D4 ( $p > 0.05$ ) compared to D1. Further, on D4 of MWM, vehicle ( $p < .01$ ), PG ( $p < 0.05$ ), PZ ( $p < 0.0001$ ), and HZ ( $p < 0.0001$ ) all traveled significantly greater distance to the platform compared to sham (*not annotated on figure*). Thus, during the first four days of MWM all groups showed a decrease in the distance traveled to the submerged platform. However, PZ was the only group in which none of these decreases reached statistical significance, suggesting that the PZ group had the most difficulty in learning to find the platform day to day during the first four days of MWM. In regards to overall treatment effect, *post-hoc* testing (Tukey's) revealed that across the first four days of MWM, there is not a significant difference between vehicle and PZ ( $p = 0.3412$ ), vehicle and PG ( $p = 0.8911$ ) or vehicle and HZ ( $p = 0.7387$ ) (*not graphically shown*).



### **Morris Water Maze Swim Speed (MWM D1-D4, Post CCI D3-D6) (Fig. 4.9)**

For swim speed (i.e. velocity), a two-way repeated measures ANOVA revealed a statistically significant effect across time ( $F[3,180] = 12.52, p < 0.0001$ ), and treatment ( $F[4,60] = 3.889, p = 0.007$ ). However, the interaction between time x treatment was not significant ( $F[12,180] = 1.634, p = 0.0858$ ). *Post-hoc* testing (Tukey's) revealed that for the treatment main effect, PG ( $p < 0.05$ ), PZ ( $p < 0.05$ ) and HZ ( $p < 0.05$ ), but not vehicle ( $p > 0.05$ ) had a significantly increased swim speed compared to sham. Thus, during the first four days of MWM, the PZ, PG, and HZ groups had faster mean swim speeds than sham.

### **Morris Water Maze Reference Memory (Fig. 4.10)**

Following removal of the platform (MWM D5, post-CCI D7), a one-way ANOVA revealed a statistically significant effect across all groups ( $F[4,60] = 8.22, p < 0.0001$ ). *Post-hoc* testing (Tukey's) revealed that the number of platform crossings was significantly decreased for vehicle ( $p < 0.01$ ), PG ( $p < 0.01$ ), PZ ( $p < 0.0001$ ), and HZ ( $p < 0.001$ ) compared to sham. Thus, PG, PZ, nor HZ significantly improved CCI-induced decreases in platform crossings, indicating the drugs were unable to improve CCI-induced deficits to reference memory.

### **Percentage Weight Loss Following CCI-MWM (Fig. 4.11)**

For percentage weight loss between D0 (surgery day) and post-injury D7 (last MWM day), a one-way ANOVA revealed a statistically significant effect across all groups ( $F[4,60] = 6.646, p = 0.0002$ ). *Post-hoc* testing (Tukey's) revealed that the PZ group lost a significant amount of weight compared to sham ( $p < 0.001$ ), vehicle ( $p < 0.05$ ), PG ( $p < 0.05$ ), and HZ ( $p < 0.001$ ). Thus, PZ animals lost a significant amount of weight compared to all other groups.

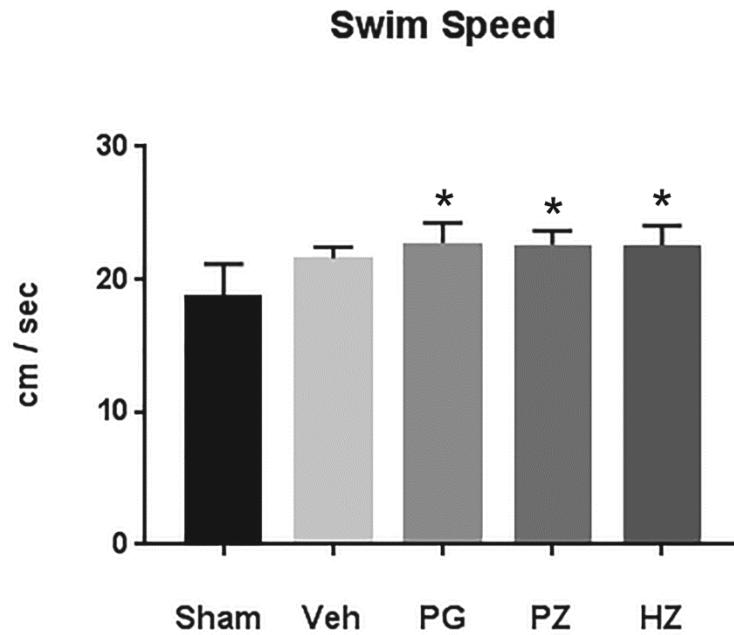


**Figure 4.9 Overall Morris water maze swim speed.** The mean swim speed (velocity, cm/sec) across the first four MWM days was significantly different between groups following controlled cortical impact injury (CCI). The swim speed of the PG, PZ, and HZ groups was significantly increased compared to sham. Values = mean  $\pm$  standard deviation; repeated measures two-way analysis of variance followed by Tukey *post hoc*; \* $p < 0.05$  compared to sham; Sham, Veh = vehicle + CCI, PG = pargyline + CCI, PZ = phenelzine + CCI, HZ = hydralazine + CCI;  $n = 13$  per group.

## Reference Memory - 30s

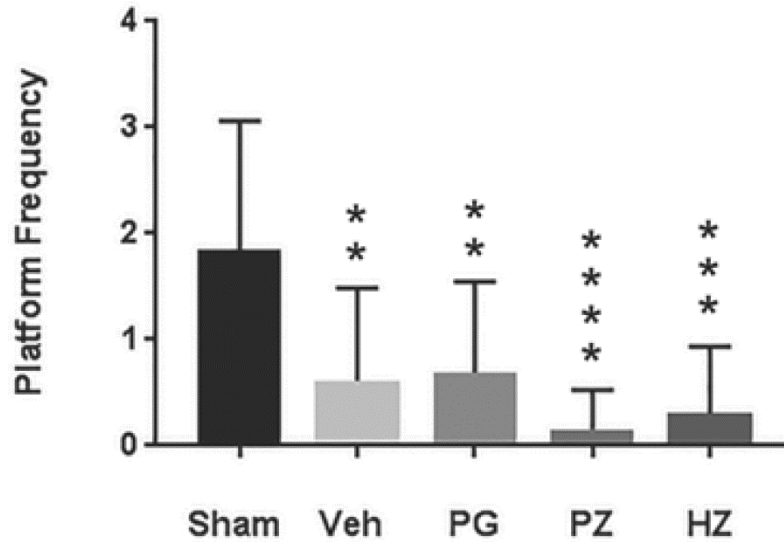


**Figure 4.10 Morris water maze reference memory.** On MWM D5 (post-CCI D7) the platform was removed and the number of platform crossing was counted within the 30s timeframe. Following controlled cortical impact injury (CCI), Veh, PG, PZ, and HZ performed significantly worse than sham. Values = mean  $\pm$  standard deviation; one-way analysis of variance followed by Tukey *post hoc*; \*\* $p < 0.01$ , \*\*\* $p < 0.001$ , \*\*\*\* $p < 0.0001$  compared to sham; Sham, Veh = vehicle + CCI, PG = pargyline + CCI, PZ = phenelzine + CCI, HZ = hydralazine + CCI;  $n = 13$  per group.

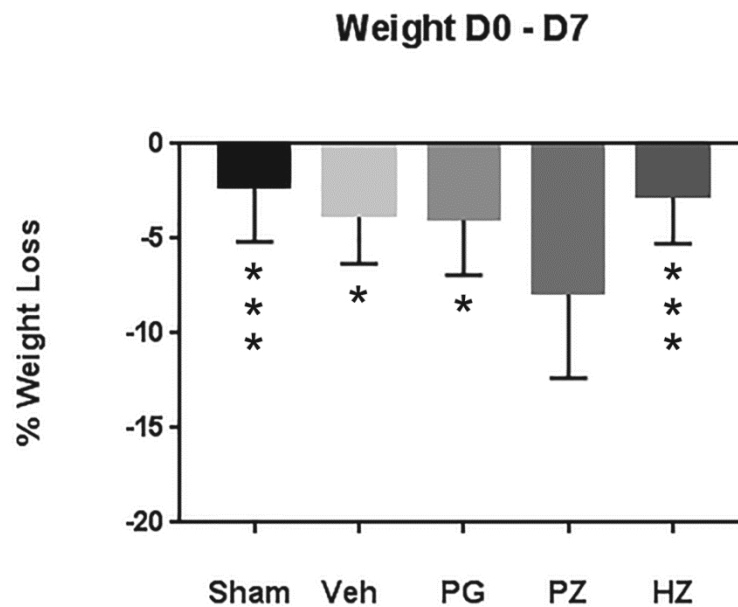


**Figure 4.11 Percent weight loss between D0 (CCI) and D7 (MWM probe trial).** All groups lost significantly less weight compared to PZ. Values = mean  $\pm$  standard deviation; one-way analysis of variance followed by Tukey *post hoc*; \* $p < 0.05$ , \*\*\* $p < 0.001$  compared to PZ; Sham, Veh = vehicle + CCI, PG = pargyline + CCI, PZ = phenelzine + CCI, HZ = hydralazine + CCI;  $n = 13$  per group.

### **Total Percentage Cortical Tissue Sparing (Fig. 4.12 and 4.13)**

For total cortical tissue sparing (ipsilateral / contralateral), a one-way ANOVA revealed a statistically significant effect across all groups ( $F(4,37) = 21.07, p < 0.0001$ ). *Post-hoc* testing (Tukey's) revealed a significant decrease in cortical tissue sparing compared to sham for vehicle ( $p < 0.0001$ ), PG ( $p < 0.0001$ ), PZ ( $p < 0.0001$ ), and HZ ( $p < 0.0001$ ). The mean ( $\pm$  s.d.) cortical tissue sparing (ipsilateral / contralateral) for each group is as follows: sham =  $97.1\% \pm 4.9\%$ , vehicle =  $70.0\% \pm 6.1\%$ , PG =  $74.0\% \pm 6.3\%$ , PZ =  $72.4\% \pm 6.4\%$ , HZ =  $76.9\% \pm 8.9\%$ . Based upon mean values each drug increased cortical tissue sparing compared to vehicle as follows (% treatment / % vehicle): PG = 5.7%, PZ = 3.3%, and HZ = 9.8% (**Table 4.1**). Thus, PG, PZ, nor HZ was able to significantly improve CCI-induced decreases in cortical tissue sparing. However, HZ performed the best with a near 10% improvement compared to vehicle.

### % Cortical Tissue Sparing - Day 8

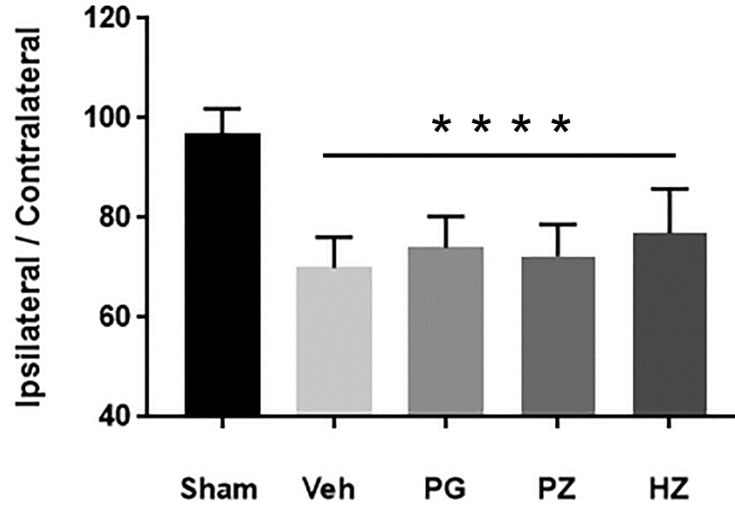


**Figure 4.12 Total percent cortical tissue sparing (ipsilateral/contralateral) D8 post-CCI.** For each individual animal the total percent cortical tissue sparing was calculated as the sum of ipsilateral cortical tissue spared across 12 coronal sections / sum of contralateral cortical tissue across 12 coronal sections. All groups show a significant decrease in cortical tissue sparing compared to sham eight days following controlled cortical impact injury (CCI). Values = mean  $\pm$  standard deviation; one-way analysis of variance followed by Tukey *post hoc*; \*\*\*\* $p < 0.0001$  compared to sham; Sham, Veh = vehicle + CCI, PG = pargyline + CCI, PZ = phenelzine + CCI, HZ = hydralazine + CCI; n = 8-9 per group.

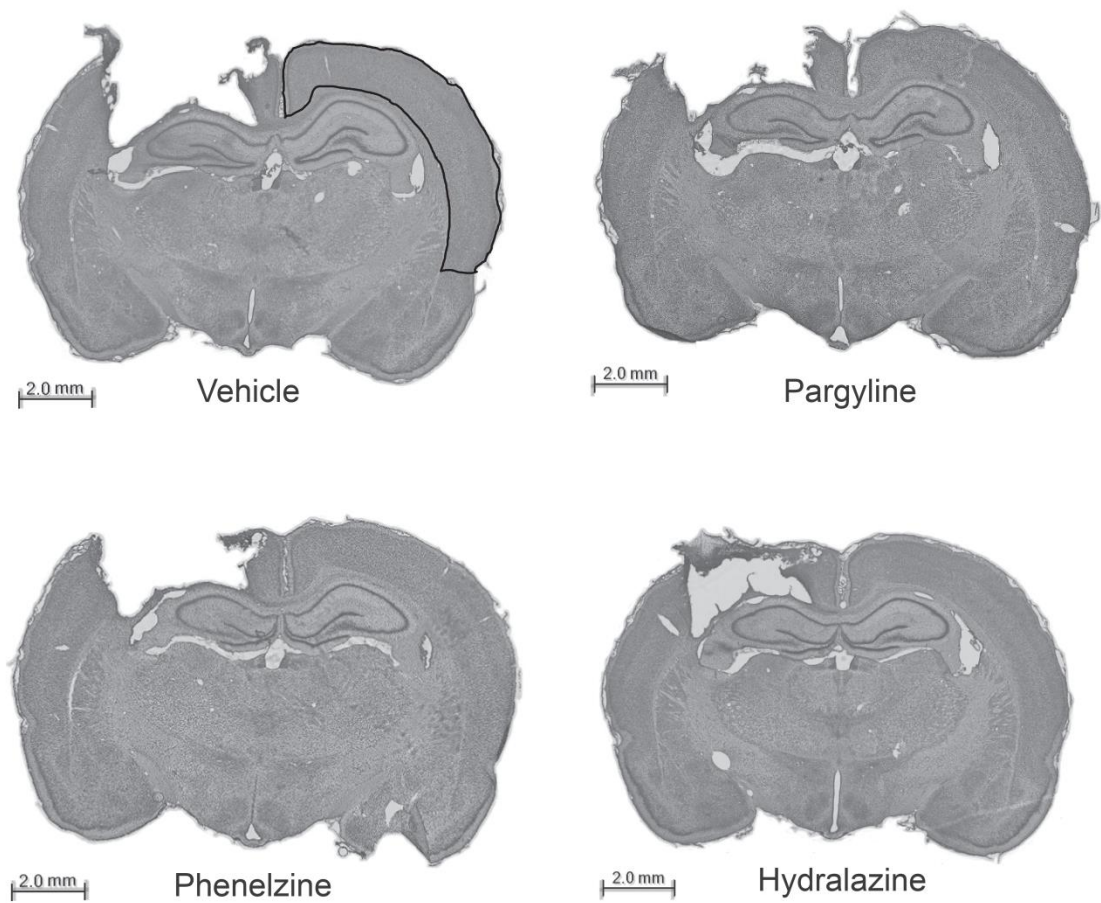


**Figure 4.13 Representative cortical tissue sparing on post-CCI day 8.** Selected coronal sections (40uM) imaged at 20x and stained with cresyl violet for the groups vehicle, pargyline, phenzelzine, and hydralazine. Percent cortical tissue sparing was calculated as ipsilateral / contralateral. The cortical area measure ranges from the dorsal aspect of lamina I to the dorsal aspect of the corpus callosum and the midline to rhinal sulcus, and is demonstrated by the black outline in the contralateral hemisphere of vehicle.

**Table 4.1 Mean Percent Cortical Tissue Sparing for Vehicle, Pargyline, Phenzelzine, and Hydralazine on Post-CCI D8**

<b>Vehicle % Tissue Spared</b>	<b>Treatment Drug</b>	<b>Treatment % Tissue Spared</b>	<b>% Improvement from vehicle</b>
70.0	<b>Pargyline</b>	74.0	<b>5.7</b>
70.0	<b>Phenelzine</b>	72.4	<b>3.3</b>
70.0	<b>Hydralazine</b>	76.9	<b>9.8</b>

The percent improvement from vehicle calculated based upon the following equation:

$$100\% \times [1 - (\% \text{ tissue spared}_{\text{treatment}} / \% \text{ tissue spared}_{\text{vehicle}})].$$



### **Individual Coronal Section Percent Cortical Tissue Sparing (Fig. 4.14)**

For the CCI groups (vehicle, pargyline, phenelzine, hydralazine) the percent cortical tissue sparing (ipsilateral/contralateral) of each individual coronal sections (12 per animal) was compared. A two-way repeated measures ANOVA revealed a statistically significant effect across coronal section number (interaural level) ( $F[11,330] = 68.2, p < 0.0001$ ), but not treatment ( $F[3,30] = 1.386, p = 0.2661$ ) or interaction (section x treatment) ( $F[33,330] = 1.204, p = 0.2099$ ). Therefore, within each group there are significant differences in percent cortical tissue sparing between coronal section numbers (i.e. interaural levels), but within each corresponding coronal section number (i.e. interaural level) there are not significant differences between vehicle and drug groups ( $p > 0.05$ ), indicating lack of a neuroprotective drug effect which is consistent with the total cortical tissue sparing results (**Fig. 4.12**).

### **Qualitative Behavioral Observations of PZ group**

Based upon our previous experience with PZ [71, 72, 333, 334] as well extensive literature findings [74, 76, 206-208, 335] we did not expect PZ administration at the dosing paradigm chosen to result in adverse effects. Therefore, the current study was not designed to include quantitative analysis of behaviors such as hyperactivity, anxiety, stereotypy, etc. Although not measured directly, qualitative observations of the PZ group suggested an increase in locomotor activity (e.g. jumping off platform), stress (e.g. porphyrin secretion from eyes and nose), and stereotypy (e.g. rearing, head bobbing, etc. following PZ administration). In hindsight, inclusion of a more extensive battery of behavioral tests could have led to more thorough interpretation of the results.

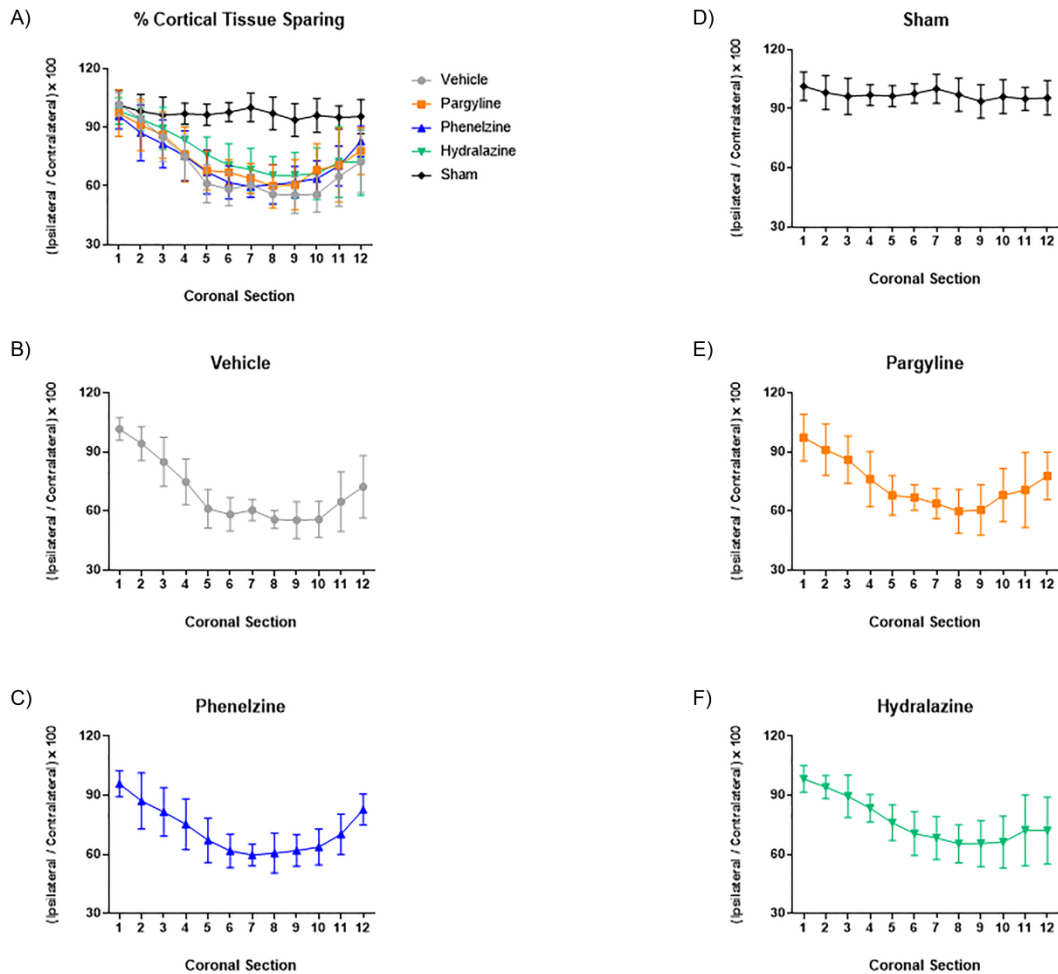


**Figure 4.14 Individual coronal section percent cortical tissue sparing post-CCI day 8.** Mean % cortical tissue sparing (ipsilateral/contralateral) for each coronal section (12 per animal) by group. Coronal sections are 40 $\mu$ m thick, 400 $\mu$ m apart, and were collected between approximately interaural level 8.20mm and 3.40mm Values =  $\pm$  standard deviation; **(A)** Overlay of all groups, **(B)** vehicle + CCI, **(C)** phenelzine + CCI, **(D)** sham, **(E)** pargyline + CCI, **(F)** hydralazine + CCI. n = 8-9 per group. Repeated measure two-way analysis of variance revealed a non-significant ( $p > 0.05$ ) treatment effect for CCI groups.

## **Discussion**

Overall, these results indicate that for the dosing paradigms utilized PZ (aldehyde scavenger, MAOI), PG (non-aldehyde scavenger, MAOI), and HZ (aldehyde scavenger, non-MAOI) (**Fig. 4.2**) led to little improvement of the outcomes measured. None of the drugs were able to improve CCI-induced deficits to reference memory (**Fig. 4.10**), or to significantly improve cortical tissue sparing following injury (**Fig. 4.12**). However, HZ, the non-MAOI aldehyde scavenger, improved cortical tissue the most, increasing the amount of tissue spared compared to vehicle by nearly 10% (**Table 4.1**). Of concern, PZ, lost a significant amount of weight compared to all other groups (**Fig. 4.11**), and was the only group that did not show significant improvement in platform latency/distance performance over the first four days of MWM (**Fig. 4.8**). It is possible that the PZ results seen here are at least partially explained by an MAO inhibition effect as evidenced by the significant elevation to NE and 5-HT seen in uninjured cortical tissue following administration of the same PZ dosing paradigm utilized for CCI experiments (**Fig. 4.5 and 4.6A**). However, at the dosage utilized other PZ non-aldehyde scavenging mechanisms of action or excessive aldehyde-scavenging could also be contributory factors.

### **Lipid Peroxidation and TBI Secondary Injury**

Although the current study does not include direct measurements of mitochondrial function or LP-derived neurotoxic aldehyde formation (e.g. 4-HNE, acrolein), both are central mediators of the TBI secondary injury cascade [1, 25, 51, 55, 332] and our previous work primarily focused on understanding the effects of PZ on mitochondria [71, 72, 333, 334]. Therefore, the synergistic role mitochondria and LP-derived neurotoxic aldehydes play in exacerbating TBI pathophysiology and initiating

downstream consequences such as neurodegeneration and neurologic impairment is detailed here for context. However, it should be noted that ROS and neurotoxic aldehydes can be derived from a variety of non-mitochondrial sources such as the metabolism of arachidonic acid by prostaglandin synthase or 5-lipoxygenase, or the activities of several oxidases including xanthine, polyamine, and spermine [1, 336].

Following TBI increases in intracellular calcium are taken up by mitochondria in an attempt to maintain homeostasis [25, 51]. However, one consequence of elevations in intra-mitochondrial calcium is increased generation of ROS/RNS species [51], such as superoxide ( $O_2^{\bullet-}$ ), nitric oxide ( $NO^{\bullet}$ ), and peroxynitrite (PN) [17]. Highly reactive PN-derived radicals are critical in initiating lipid peroxidation (LP). During LP, a hydrogen atom and its electron are extracted from membranous polyunsaturated fatty acids (PUFA) to form lipid ( $L^{\bullet}$ ) and lipid peroxy radicals ( $LOO^{\bullet}$ ) [1, 55]. LP self-propagates throughout adjacent PUFA, but is also catalyzed by factors such as the presence of iron or low pH which occur following TBI [1, 55]. LP terminates upon a scission reaction which produces carbonyl end products such as the neurotoxic aldehydes 4-hydroxynonenal (4-HNE) and 2-propenal (acrolein) [1, 55].

These neurotoxic aldehydes have multiple reactive sites, making it possible for them to covalently bind lysine, histidine, arginine and cysteine protein residues through both Schiff base and Michael addition reactions [1, 79, 81]. As a major site of PN formation, mitochondria are particularly susceptible to attack by LP-derived neurotoxic aldehydes. Following TBI, binding of LP-derived neurotoxic aldehydes to mitochondrial proteins further exacerbates TBI-induced impairment of mitochondrial bioenergetics and the ROS/RNS-LP-aldehyde cascade, which combined with high levels of intra-mitochondrial calcium leads to opening of the mitochondrial permeability transition pore (mPTP) [17, 51], causing cessation of ATP generation, release of cytochrome c and

other apoptotic proteins [51], and extrusion of mitochondrial-sequestered calcium back into the cytosol where it activates calcium-dependent proteases, such as calpain [51], leading to degradation of cytoskeletal proteins (e.g.  $\alpha$ II-spectrin) [106], neurodegeneration, neuronal cell death, and neurologic impairment [1, 55, 116, 332].

Overall, several studies have confirmed that mitochondrial dysfunction and LP peroxidation/formation of LP-derived aldehydes occur upstream of neurodegeneration and neurologic impairment [55, 56, 73] and that targeting mitochondrial dysfunction or lipid peroxidation can attenuate neurodegeneration and improve cognitive deficits [1, 25, 51, 55, 110, 122, 125, 303].

### **Aldehyde Scavengers and Neuroprotection**

LP-derived aldehydes such as the  $\alpha,\beta$ -unsaturated fatty acids, 4-HNE and acrolein, are strong electrophiles [260], and therefore can be scavenged by strong nucleophiles [260], including drugs that contain a hydrazine moiety (-NH-NH<sub>2</sub>). In fact, hydrazine (-NH-NH<sub>2</sub>) compounds have been demonstrated to be some of the most potent aldehyde scavengers available and are capable of scavenging both free aldehydes and binding aldehyde-protein conjugates, the latter of which prevents the formation of damaging cross-linking reactions [79, 258, 261].

Of the FDA-approved hydrazine (-NH-NH<sub>2</sub>) drugs, PZ and HZ have been the most studied in the context of brain and spinal cord injury. *In-vitro*, PZ has been found to improve mitochondrial function and decrease formation of mitochondria-aldehyde protein conjugates following exogenous administration of the neurotoxic aldehydes 4-HNE and acrolein [72]. Similarly, PZ attenuates retinal ganglion cell death following administration of the neurotoxic aldehyde 3-aminopropanal (3-MP) [76], and protects both neurons and glia from exogenous formaldehyde administration [311]. In experimental TBI, PZ has

been shown to improve mitochondrial function, decrease aldehyde load, attenuate cytoskeletal degradation, and improve cortical tissue sparing [71, 72, 333, 334]. Additionally, PZ improves survival of CA1 hippocampal neurons in ischemic-reperfusion injury [76]. Further, PZ has also been demonstrated to be neuroprotective in models of SCI, decreasing aldehyde load and pain hypersensitivity, attenuating motor dysfunction, and improving tissue and neuronal survival [74, 337].

Likewise, although the neuroprotective effects of HZ have not previously been evaluated in experimental TBI, *in-vitro* and *in-vivo* models of SCI and of exogenous acrolein administration demonstrate that HZ decreases aldehyde-load, attenuates mitochondrial dysfunction and free radical generation, restores antioxidant activity, improves tissue sparing and axonal function, and attenuates pain hypersensitivity and motor dysfunction [75, 88, 257, 270, 338].

### **Monoamines and Monoamine Oxidase (MAO)**

The neurotransmitters measured in the current study (**Fig. 4.5 – 4.7**), DA, NE, and 5-HT, are classified as monoamine neurotransmitters. DA and NE are catecholamines, sequentially synthesized from the amino acid tyrosine, whereas the non-catecholamine 5-HT is derived from tryptophan [151, 169]. The complexity, nuances, and interplay of the DA, NE, and 5-HT monoaminergic systems are beyond the scope of this study however; their general roles will be briefly reviewed here for context.

#### Dopamine

Within the nervous system DA is involved with a wide range of processes including movement, motivation, reward, addiction, memory, stress and mood [154]. Although the majority of DA is found within the striatum, DA is found throughout the brain [154]. For example, within the mesocorticolimbic system, DA neurons from the ventral

tegmental area project directly to the hippocampus and prefrontal cortex [153, 170]. Further, although the nigrostriatal pathway, predominately involved in movement regulation, consists of dopaminergic neurons projecting directly from the substantia nigra to the striatum, it is part of complex circuitry that includes input and output to the motor cortex, along tracts that pass through the thalamus [153]. As a catecholamine, in addition to binding DA receptors, DA can bind adrenergic receptors [154]. Clinically, DA can be used as a vasopressor to elevate cerebral perfusion pressure and mean arterial blood pressure following severe TBI [154].

### Norepinephrine

Within the brain NE neurons are concentrated in the locus coeruleus with widespread connections to areas including the cortex, limbic system, and thalamus, and it is involved in modulation of arousal, attention, mood, cognition and memory [150, 151]. As a catecholamine, NE, also known as the “flight or fight” neurotransmitter can bind adrenergic receptors and induce sympathetic responses such as vasoconstriction [154, 171]. As such, similar to DA, NE can be used as vasopressor in clinical TBI [154].

### Serotonin

Within the CNS, 5-HT neurons arise from the raphe nuclei and project extensively throughout most of the brain including the cortex, limbic system, and thalamus [151], modulating arousal, mood, cognition and memory [155]. Interestingly, the majority of 5-HT is found outside the CNS, within the gastrointestinal tract [155]. Additionally, 5-HT plays a role in platelet activation, vasodilation, and vasoconstriction [172].

### Monoamine Oxidase (MAO)

The enzyme monoamine oxidase (MAO) exists as two subtypes, MAO-A and MAO-B, both of which are located in the outer mitochondrial membrane. MAO contains a flavin group allowing it to participate in oxidative deamination reactions [186]. MAO is responsible for the metabolism of the monoamine neurotransmitters NE, 5-HT, and DA, measured within the current study, but additionally participates in the metabolism of epinephrine (EPI), several amino acids, and phenethylamine (PEA), a trace amine under physiologic conditions, but which is also an active metabolite of PZ [186, 189]. MAO-A and MAO-B have differing substrate affinities. For example, MAO-A is selective for NE and 5-HT, and the neurotransmitter EPI, whereas MAO-B is selective for PEA [186]. DA, on the other hand, is metabolized by both MAO-A and MAO-B [186]. However, the metabolism of DA by MAO differs between rodents and humans, with DA being predominately metabolized by MAO-A in rats and MAO-B in humans [186]. In the brain, monoamines are removed from the synaptic cleft by reuptake into pre-synaptic nerve terminals and glial cells [151]. In fact, the majority of MAO in the brain is located within the glial [190], with the MAO-B isoform predominating in glia as well as in serotonergic neurons and platelets [190].

Several additional enzymes are involved in monoamine metabolism such as the mitochondrial matrix protein aldehyde dehydrogenase (ALDH) and the cytosolic enzyme catechol-O-methyl transferase (COMT) [186]. Of note to this study is the involvement of COMT in the metabolism of DA to HVA which can take two paths. In one DA is first metabolized by MAO to the intermediate DOPAC, and then DOPAC is metabolized by COMT to HVA (DA → MAO → DOPAC → COMT → HVA). In the other DA is first metabolized by COMT to the intermediate 3-methoxytyramine (3-MT), and then 3-MT is metabolized by MAO to HVA (DA → COMT → 3-MT → MAO → HVA). These dual



pathways likely explain why the MAO inhibitory effects of PZ and PG are more apparent in regards to DOPAC tissue levels than HVA tissue levels (**Fig. 4.7**).

### **Choice of Experimental Design: Dosing Paradigms**

As lipid peroxidation and associated pathologies such as mitochondrial dysfunction and formation of LP-derived aldehydes peak 48h-72h following CCI [73], it follows that drug administration over the first 48h-72h may offer the best chance of neuroprotective success. Therefore, based on this assumption and previous studies demonstrating neuroprotective success with daily administration of PZ or HZ [72, 74, 75, 333], drugs were administered 15min, 24h, and 48h following injury.

Prior to this study neither PG nor HZ had been utilized in an experimental TBI study. Therefore, the HZ dosage chosen (5mg/kg/day, intraperitoneal) was based upon a dosage optimized for SCI by Shi and colleagues [74, 75]. Similarly, although our previous PZ studies showed protection with 10mg/kg/day subcutaneous PZ administration [72, 333], here we chose to administer PZ intraperitoneal at 15mg/kg/day [75], a dosage which was shown to be neuroprotective in SCI in a study which directly compared PZ to HZ [74]. In fact, subcutaneous PZ administration at 15mg/kg/day has also shown to be neuroprotective in a gerbil model of ischemic-reperfusion injury [76].

PG (15mg/kg/day, intraperitoneal) was administered at an equal concentration to PZ to parallel *ex-vivo* experiments in which the ability of PZ to protect isolated mitochondria from exogenous administration of 4-HNE and acrolein was compared to that of PG [72]. Similarly, equal concentrations of PG and PZ have been utilized *in-vivo* to study the effects of aldehyde scavenging on preventing vascular carbonyl stress and atherosclerosis [198]. PG is similarly structured to PZ. However, unlike PZ, PG does not contain the aldehyde-scavenging hydrazine moiety (-NH-NH<sub>2</sub>) (**Fig. 4.2**). Our previous

*ex-vivo* results indicated that while PZ protected isolated cortical mitochondria against exogenously administered aldehydes, an equivalent concentration of PG did not, confirming that the presence of the hydrazine moiety (-NH-NH<sub>2</sub>) and not steric hindrance is responsible for PZ's aldehyde scavenging properties [72]. Although the study did not likely allow for rigorous assessment of MAOI effects, as MAO substrates are largely absent from isolated mitochondria preparations [72], similar results were seen in an *in-vivo* study which demonstrated PZ, but not PG prevented formation of carbonyls and atherosclerotic plaques [198].

Although PZ and PG are both considered non-selective irreversible MAOIs, it must be noted that PZ is more selective toward MAO-A, whereas PG is more selective toward MAO- B [197], and both drugs have differing pharmacokinetics [189, 197, 208]. Therefore, although the choice was made to administer the two MAOIs, PG and PZ, in equivalent concentrations for the current study as an extension to previous work [72], results must be interpreted with caution as equal *in-vivo* concentrations of the two cannot be necessarily treated as equivalent in regards to their MAOI properties. In fact, this likely explains the HPLC data in which PZ administration leads to significant increases in NE and 5-HT, whereas PG administration at the same concentration does not (**Fig. 4.5 and 4.6A**).

#### **Choice of Experimental Design: Morris Water Maze**

Our previous PZ studies have focused on evaluating biochemical outcome measures 72h post-CCI, the peak of lipid peroxidation and mitochondrial dysfunction [72, 73, 333, 334]. Therefore, in order to correlate the current study with previous *in-vivo* PZ biochemical TBI studies, the current study began MWM testing at the early time point of 72h (3 days) post-CCI (**Fig. 4.4**). In theory, drugs capable of attenuating mitochondrial

dysfunction and preventing formation of LP-derived aldehydes such as PZ over the first 72h following injury [71, 72, 109, 333, 334] should also be able to attenuate downstream consequences such as neurodegeneration and neurologic impairment [1, 25, 51, 55, 110, 122, 125, 303]. Although based upon the literature, 72h (3 days) does appear to be an early point in which to begin cognitive behavioral testing, interventional improvements to TBI-induced cognitive deficits have been previously seen at this acute time period [141, 273]. Additionally, although the results of this study indicate that none of the drugs were able to improve CCI-induced deficits to reference memory (**Fig. 4.10**), all CCI groups, PZ excluded, were able to find the platform significantly faster as MWM acquisition trial days progressed (**Fig. 4.8**), indicating that following severe CCI the rats do have intact working memory at the acute 72h (3 days) post-CCI time point. However, it should be noted that sham animals took an average of 20s to find the platform on MWM day 4, which is longer than times reported in MWM studies that were conducted at later time points [125, 387] and may be the result of a residual anesthesia effect [388]. Similarly, although direct assessments of motor function were not conducted as part of this study (in order to avoid overloading the rats with too many behavioral tasks during the acute post-CCI period), the ability of rats to decrease their latency to platform (**Fig. 4.8**) and the lack of swim speed deficits in vehicle (**Fig. 4.9**) over the first four MWM days should indicate that if any CCI-induced motor or sensory deficits are present they are not interfering with MWM performance to a substantial degree.

In additional consideration to MWM performance, is the fact that monoamine neurotransmitters, such as NE, 5-HT, and DA, have important roles in cognitive and motor function [150, 151, 153-155]. Therefore, it is possible that MAO inhibition and the resulting increase in monoamine neurotransmitter levels, as was seen with PZ administration in the uninjured cortical tissue HPLC experiment (**Fig. 4.5 and 4.6A**),

could have had an effect on MWM performance absent injury or neuroprotective effects. For example, low-dose amphetamines are known to improve learning and memory, whereas high-dose amphetamines can be detrimental [339]. This is an interesting question which could have potentially been answered by adding additional cohorts of uninjured + drug or sham + drug groups to the study. However, several anti-depressants which modulate monoaminergic systems, including MAOIs, have been shown to have no ill effects on MWM performance in control animals [156-158]. Therefore, in the interest of reducing animal numbers and focusing specifically on protective effects (i.e. CCI + drug vs. CCI + vehicle), these extra cohorts were not included in the current study. However, it should be noted that upon further review of the literature the effect of acute PZ administration (15min – 2h prior to behavioral testing) on learning and memory seems to be mixed with some studies indicating impairment [159, 339] and some indicating improvement [340], with impairment seeming to be more likely to occur at higher PZ doses [159, 339] (*for further discussion see “The Effects of Phenelzine on Behavior” section*)

Although delaying the start of MWM testing beyond the acute time point chosen (3 days post-CCI, 24h following final drug administration) (**Fig. 4.4**) may have decreased the potential for MAOI-induced elevated monoamine levels to directly impact MWM performance, it is unlikely to have completely remitted theoretical effects because of the long lasting nature of irreversible MAOIs (e.g. PZ and PG). Whereas the plasma half-life of PZ is estimated to be anywhere from 30 minutes in rats to 11.5 hours in humans [74, 341], due to the fact that PZ and PG are irreversible MAOIs, their MAOI effects are much longer than their plasma-half lives would suggest and rely on MAO turnover rates. In rats, the half-life of MAO in healthy brain is 10-13 days [195]. In fact, both MAO isoforms remain significantly inhibited for at least a week following single PZ administration [342].

However, the effective recovery time for rat brain MAO may be lower, due to the fact that 65-80% of MAO inhibition is likely necessary to modulate monoamine neurotransmitter levels [186, 342]. Therefore, based upon previous studies of neurotransmitter levels in uninjured brain following PZ administration, the “wash out” period following single administration may range anywhere from 48h to greater than one week [205, 342]. Therefore, we concede that delaying the start of MWM beyond this timeframe may have resulted in a less confounding experimental design. However, considering that MAO is a mitochondrial enzyme [186], mitochondrial trafficking is impaired following TBI [19], and that mitochondrial dysfunction has been documented for weeks following TBI [22], MAO turnover may be much longer in injured brain, particularly in critical pre-synaptic nerve terminals, as regeneration of MAO within presynaptic nerve terminals requires trafficking of MAO and mitochondrion to the synapse [191]. Therefore, it is unknown the length of time MWM would have had to been delayed for direct MAOI/monoamine effects to completely “wash out” in order to conduct a cognitive assessment more isolative of neuroprotective effects. Further, as our research has focused on investigating PZ as a neuroprotectant for acute use in TBI [71, 72, 333, 334], and early and intensive neurorehabilitation following severe TBI is encouraged [343], the effects of PZ on behavior acutely following TBI are still important to discern.

Finally, in regard to the MWM protocol utilized here, on MWM day 5 during reference memory testing, following removal of the platform, platform crossings were only counted for 30s. Upon analysis of the latency to platform times during the MWM acquisition phase, only the sham group was on average able to find the platform in fewer than 30s on MWM day 4 (**Fig. 4.8**). Therefore, it unsurprising that during reference memory testing that there were no differences found between the vehicle and drug

groups (**Fig. 4.10**). In hindsight, allowing animals 60s to complete the reference memory task on day 5 of MWM would have represented a better experimental approach.

### **Phenelzine: A Comparison to Previous Neuroprotective CCI Studies**

The results of the current study indicate that 15mg/kg PZ administered intraperitoneal 15min, 24h, and 48h following severe CCI was unable to significantly improve injury-induced deficits to reference memory on post-CCI D7 (**Fig. 4.10**) or to improve cortical tissue sparing on post-CCI D8 (**Fig. 4.12**). These results differ from previous findings in which PZ was found to be protective in CCI [71, 72, 333, 334]. However, many of these prior PZ studies reported PZ improvement to more biochemical-type outcome measures such as mitochondrial function and protein-aldehyde conjugate formation at early time points ranging from 3h-72h [71, 72, 333, 334]. Although there is robust evidence in the literature that acute pharmacologic attenuation of mitochondrial dysfunction and lipid peroxidation can in turn lead to downstream behavioral and histologic improvements at later time points [1, 25, 51, 55, 110, 122, 125, 303], it is possible that while PZ can acutely (3h-72h) improve mitochondrial respiration and calcium-buffering capacity, and decrease formation of mitochondrial-aldehyde conjugates [71, 72, 333, 334], that such early biochemical protections do not translate to improvements in learning and memory or cortical tissue sparing. There is some evidence within the previous PZ studies to support this idea. For example, the ability of PZ to prevent cytoskeletal spectrin degradation or attenuate cellular wide protein-aldehyde formation, outcome measures that can also correlate with behavioral and histologic outcomes [56, 109, 110], but which are affected to a greater degree by mitochondrial-independent secondary injury mechanisms [1, 16, 59, 161], is more variable and less robust than it's mitochondrial specific effects [333, 334].

Additionally, it could also be the case that the protection provided by PZ acutely [71, 72, 333, 334] is not sustained out to more subacute time points. For example, in the current study, administration of PZ (15mg/kg, i.p., 15min, 24h, 48h post-CCI) was unable to improve cortical tissue sparing 8 days post-CCI (**Fig. 4.12**), whereas we had previously shown that subcutaneous (s.c.) administration of PZ (10mg/kg) 15min post-CCI followed by maintenance dosing (5mg/kg) every 12hr up to and including 60h, could significantly improve cortical tissue sparing 72h post-CCI [72]. Admittedly, 72h was an early time point for previous studies to conduct histologic analysis, as cortical contusions have been documented to continue to increase in volume for at least 28 days following experimental TBI [164]. However, because the primary targets of PZ (i.e. LP-derived neurotoxic aldehydes and aldehyde-damaged mitochondria) peak 48h-72h following injury before recovering 5-7 days post injury [73], it would be expected that a robust PZ protection of cortical tissue at 72h post-CCI [72] would maintain some effect at 8 days post-CCI.

Therefore, the inability of PZ to improve cortical tissue sparing here (**Fig. 4.12**) whereas it has been previously reported to do so at 72h [72], may be more likely due to methodological differences. For one, the current study included an early behavioral task, whereas the study by Cebak et al. did not [72]. Although other research groups have implemented water maze testing in rodents acutely following experimental TBI with no ill effects [141, 273], it is possible that the early use of MWM in this study could have led to an increase in neurodegeneration which expanded cortical lesion volumes. Although this study did not include any non-behavioral cohorts in which this question could have been analyzed directly, this is unlikely the case as the cortical lesion volumes observed here do not vary widely from those reported in similar studies in which MWM was not performed [122, 124, 227, 294]. Further, although clinical guidelines regarding the

optimal timing and structure of rehabilitation following severe TBI are still being developed [344], current evidence suggests that early and intensive neurorehabilitation following TBI promotes the best functional recovery [343].

The second major methodological difference between the current study and the 72h PZ histology study conducted by Cebak et al. [72] is the dosing paradigm. The current study represents an increase in total amount of PZ received over the first 48h, as well an increase in the amount of PZ received per bolus dose. Although our reasoning behind administering PZ over the first 48h-72h [72, 333] has been based on the idea that drug should be administered throughout the peak lipid peroxidation and mitochondrial dysfunctional periods [73], recent data from our lab indicates that lower dose PZ may actually offer better protection [334] than prolonged dosing [72, 333]. For example, PZ (10mg/kg, s.c.) administered 15min post-CCI with a second dose (5mg/kg, s.c.) given 12h post-injury is able to improve individual states of mitochondrial respiration [334], whereas 10mg/kg/day/3d subcutaneous continuous infusion of PZ or equivalent bolus dosing cannot [72, 333]. Similarly, an early PZ study showed that a single dose of PZ (10mg/kg) administered 15min following CCI can improve cortical tissue sparing 14 days post-injury [71].

Further, the current study was the first time in which PZ was administered intraperitoneal following experimental TBI, a route that results in more rapid drug absorption than subcutaneous administration [345]. Although intraperitoneal administration of PZ up to 60mg/kg has been reported safe under different conditions [74], it is unknown if this remains true in TBI. In fact, the majority of the MAO substrate, 5-HT, is found outside the CNS, within the gastrointestinal tract [155], as are naturally occurring trace amounts of tyramine, an amino acid known capable of inducing hypertensive crisis at extra-physiologic levels through both conversion to and



displacement of NE [346]. Therefore, it is possible that intraperitoneal administration of PZ following TBI had a greater effect on monoamines outside the CNS than subcutaneous administration, and the elevation of such monoamines had adverse effects.

### **Phenelzine as a Monoamine Oxidase Inhibitor**

As PZ is an irreversible non-selective MAOI, as well as an MAO substrate, it is possible that the decrease in protective effects seen here and with the higher PZ dosing paradigms [71, 72, 333, 334] is related to its MAOI effects. In fact, the PZ dosing paradigm utilized here, when evaluated in uninjured cortical tissue, shows significant MAO inhibition as measured by the decrease in 5-HT turnover to 5-HIAA (**Fig. 4.6C**) and DA turnover to DOPAC and/or HVA (**Fig. 4.7D-F**). In fact, not only does PZ result in MAO inhibition, but the MAO inhibition leads to a significant increase in NE (**Fig. 4.5**) and 5-HT (**Fig. 4.16A**). This is unsurprising given the fact that although classified as a non-selective MAO inhibitor, PZ is more selective toward MAO-A than MAO-B with a reported MAO-A: MAO-B selectivity ratio of 2:1 [197], and that both NE and 5-HT are selectively metabolized by MAO-A [186]. Interestingly, PZ did not affect overall DA tissue levels (**Fig. 4.7A**), possibly due to the lower affinity of PZ for MAO-B [197], the lower affinity of MAO-B for DA in rat [347], overall low tissue levels of DA in the cortex [348], or a compensatory-type effect as in addition to metabolism, monoamine turnover levels are affected by monoamine synthesis, release and re-uptake [349]. One consideration in regards to HPLC analysis is that it was conducted on cortical tissue samples which had not undergone saline perfusion. Therefore, neurotransmitters measurements, particularly that of 5-HT, a neurotransmitter which can be transported in platelets [172], are not necessarily specific to neuronal or glial compartments, however; in general the HPLC

data should be representative of an overall measure of drug-induced changes to monoamine turnover and monoamine and metabolite tissue levels.

### **The Effects of Phenzazine on Weight**

As the PZ dosing paradigm utilized for the current experiment was unable to attenuate CCI-induced memory impairment or enhance cortical tissue sparing (**Fig. 4.8, 4.10, 4.12**) and led to significant weight loss (**Fig. 4.11**), the decision was made to forego HPLC analysis of PZ effects on MAO inhibition and monoamine tissue levels following CCI. However, extrapolating from the effect the PZ dosing paradigm had on cortical tissue levels of NE (**Fig. 4.5**) and 5-HT (**Fig. 4.6A**) in uninjured tissue, it is possible similar elevations could explain the significant weight loss seen in PZ animals following CCI (**Fig. 4.11**). For example, catecholamines and 5-HT can induce weight loss through a variety of mechanisms ranging from increasing locomotor activity to decreasing appetite [350]. In fact, multiple PZ doses also led to weight loss in uninjured animals, albeit to a lesser degree (*see "Chapter Five"*). Similarly, non-PZ MAOIs have been shown to decrease weight gain and induce anorexia in a dose-dependent manner [158, 351]. Further, one of PZ's metabolites, phenethylamine (PEA) [189], itself an MAO substrate with amphetamine-like stimulatory effects [207], could have also contributed to the observed weight loss.

Additionally, it is possible that the weight loss experienced by the PZ group, as well as any associated anorexia or muscle wasting, could have been a factor in the poor performance of the PZ group during the first four days of MWM (**4.8**). However, if so, such factors did not seem to impair swim speed as compared to other CCI groups (**4.9**). Further, weight loss is unlikely to be a contributing factor in previous PZ studies which

found that acute administration of PZ can impair cognitive performance, particularly as dosage increases [159, 339].

### **The Effects of Phenelzine on Behavior**

Although PZ animals performed the worst during assessment of reference memory, it was not significantly different from other CCI groups. (**Fig. 4.10**) However, over the first four days of MWM (MWM D1-D4, post-CCI D3-76), the PZ group was the only group which showed no significant improvement in finding the platform between MWM D1 and subsequent MWM days (**Fig. 4.8**). Additionally, in regards to latency to platform, for the overall treatment effect across the first four days of MWM there was a trend toward PZ being significantly impaired as compared with vehicle ( $p = 0.07$ ). This suggests that PZ animals may have been struggling more with working memory than other groups, including vehicle. This is in contrast to several previous studies which have shown that use of anti-depressants either chronically or during MWM do not negatively affect working memory in naive rodents [156, 157], including such MAOI's as PG, deprenyl (MAO-B), and clorgyline (MAO-A) [158].

On the other hand, previous reports regarding the effects of acute PZ administration on cognition are variable. Low dose PZ (20mg/kg) administered 2h prior to training has been shown to improve Y-maze performance in rats [340]. However, 20mg/kg PZ administered 15min prior to training has also been shown to non-significantly impair T-maze performance in mice [339]. Similarly, administering PZ (15-30mg/kg) 2h prior to beginning MWM acquisition has been shown to impair reference memory [159], whereas delaying PZ administration until the start of reference memory (i.e. probe trial) tests does not, suggesting PZ may interfere with storage processing rather than retrieval [159]. Interestingly, the higher PZ dose used for those trials

(30mg/kg) also impaired the rate of MWM acquisition, while not abolishing learning completely, whereas the lower PZ dose (15mg/kg) did not [159]. Those findings are in line with the ones of the current study in which PZ was the only CCI group which did not show significant improvement throughout the MWM acquisition phase, although non-significant decreases in latency and distance were achieved (**Fig. 4.8**). Therefore, as previous studies have shown dose-dependent increases in cognitive impairment with PZ [339] it is possible that the MWM performance of the PZ+CCI group observed in the current study was due to the amount of PZ administered. However, an additional CCI-induced exacerbation of PZ effects due to injury-induced increases in monoamines or MAO inhibition cannot be ruled out (*see “Monoamines and TBI” section for further discussion*).

If PZ itself did contribute to cognitive impairment, there are several mechanisms of action in which it could have done so. For example, it is possible that PZ induced elevations to catecholamine levels (**Fig. 4.5**) and such elevated catecholamine levels induced cognitive impairment, as occurs with high dose amphetamines [339, 352]. Additionally, the PZ metabolite and MAO-substrate, PEA, [189] also has amphetamine-like properties [207]. Similarly, high levels of 5-HT (**Fig. 4.6A**), such as those that occur in serotonin syndrome, are capable of inducing cognitive dysfunction [346]. Further, the PZ metabolite, phenylethyldenehydrazine (PEH), can inhibit GABA-transaminase (GABA-T), leading to increased levels of GABA, a neurotransmitter that has also been implicated in cognitive impairment [159, 335, 342].

On the other hand, poor MWM performance is not always a reflection of cognitive impairment per se, but can instead be representative of sensorimotor dysfunction [147, 353]. On cursory inspection PZ animals do not appear to have motor deficits as their swim speed is not impaired (**Fig. 4.9**). In fact their swim speed is significantly increased

compared to sham (**Fig. 4.9**), an effect which has been previously demonstrated to occur following amphetamine or MAOI administration [158], and is usually contributed to an increase in monoamine levels. In fact, high catecholamine levels can induce motor dysfunction, including hyperactivity and “amphetamine-stereotyping” behaviors [352-355]. Similarly, high levels of 5-HT, as occur in serotonin syndrome, can induce motor dysfunctions characterized by restlessness, agitation, myoclonus, hyperreflexia, tremor, and ataxia [346, 354, 355]. Interestingly, previous studies have indicated that high (50mg/kg) – very high (80mg/kg) PZ doses can induce tremor and ataxia, respectively [207, 339]. Although sensorimotor function, locomotor activity, and “amphetamine-stereotypy” behaviors were not quantitatively assessed as part of this study, qualitative observations of the PZ group as a whole suggest increased “amphetamine-stereotypy” behavior (directly following PZ administration) as well as an increase in hyperactivity. In fact, PZ animals tended to have more difficulty remaining on (i.e. increases tendency to jump off) the MWM platform, which can confound the ability to interpret MWM results as memory deficits [147]. Therefore, it is possible PZ-induced sensorimotor effects, rather than PZ-induced cognitive impairment, contributed to the inability of the PZ group, in contrast to all other groups, to significantly improve their performance over the first four days of MWM.

In hindsight, inclusion of tests to quantitatively assess sensorimotor function, locomotor activity, or an alternative memory test would have further clarified the effects of PZ on behavior following CCI. In fact, PZ has been shown to have task-dependent effects on memory. For example, whereas high dose PZ impairs spatial memory in the MWM task, the same PZ dose enhances memory during the continuous multiple trial inhibitory avoidance (CMIA) task [159].

## **Phenelzine: A Comparison to Previous Neuroprotective SCI and Ischemic-Reperfusion Injury Studies**

Still, when taken in comparison to previous SCI and ischemic-reperfusion studies, which saw neuroprotection with 15mg/kg daily intraperitoneal PZ dosing paradigms and which extended out 7-14 days [74, 76], it is surprising that the PZ dosing paradigm (15mg/kg, i.p., 15min, 24h, 48h post-CCI) utilized in the current study was not only unable to enhance cortical tissue sparing (**Fig. 4.12**), but also had a negative effect on weight and behavior (**Fig. 4.8, 4.11, qualitative observation**). Contrarily, in SCI, intraperitoneal administration of PZ (15mg/kg/day/14d) beginning immediately following injury attenuates motor dysfunction and improves tissue sparing [74]. Similarly, subcutaneous administration of PZ (15mg/kg/day/7d) improves CA1 neuron survival in a gerbil modal of global ischemic-reperfusion injury [76].

It is possible this finding is due to differences in temporal assessments, species, or injury models. For example, although TBI and SCI share similar secondary injury characteristics [51, 55, 356], they are not equivalent models. Beyond structural differences, LP-derived aldehydes remain elevated longer in SCI than TBI [73, 338], brain and spinal cord mitochondria have different sensitivities to lipid peroxidation [29, 33] and inflammatory responses differ between TBI and SCI [356]. Further, pharmacotherapies do not always translate from one injury paradigm to the other. For instance, while acute methylprednisolone is a treatment option for SCI [55], its use is contraindicated in TBI [209].

Additionally, acrolein has been demonstrated to be extremely toxic to myelin due to its high protein and lipid content [357]. Given the anatomical differences between brain and spinal cord, attenuation of acrolein-induced myelin damage utilizing aldehyde-

scavengers, such as PZ, may lead to a more quantitatively observable behavioral effect in spinal cord than in brain. Moreover, in SCI, aldehyde-scavengers, including PZ, have a well demonstrated role in reducing pain hypersensitivity, which may help in attenuating other outcomes which have been assessed in SCI such as motor dysfunction, but which were not directly measured in the current study [74, 337, 338, 358, 359].

Further, PZ was recently identified as an agonist of the neuronal cell adhesion molecule L1 (L1CAM) [360], a compound which has been shown to promote axonal growth and re-myelination in the injured spinal cord [361]. In fact, in models of SCI PZ can decrease astrogliosis, enhance axonal growth and sprouting, and improve motor function in an L1CAM-dependent manner [361, 362]. Yet, the role L1CAM may have in recovery and regeneration following TBI is less well understood.

However, it is also possible that the PZ dosing paradigm utilized in the current study did have subtle neuroprotective effects which were not apparent upon cortical tissue sparing analysis (**Fig. 4.12**), but which may have been revealed by use of histological methods more sensitive to neurodegeneration, such as silver stain, or through analysis of specific regions, such as the hippocampus, as was done in the gerbil ischemic-reperfusion injury study [76]. However, given the overall PZ results for the current study, this is unlikely to be true and even less likely to be clinically relevant.

Yet, given the success of a similar dosing paradigm in other models of CNS injury, combined with the knowledge that intraperitoneal administration of PZ up to 60mg/kg has been reported to be safe in rodents following SCI [74], the PZ results obtained in the current study beg the following question: Is there something about TBI that causes a PZ dosing paradigm which is neuroprotective (or at the very least safe) in other models (e.g. SCI, ischemic-reperfusion, naïve), to become ineffective or even

detrimental following severe CCI? Is it possible that TBI itself leads to either an inhibition of monoamine oxidase or an increase in monoamine levels, effects which are then exacerbated by repetitive use of an irreversible MAO, such as PZ? Unfortunately, in general there is a paucity of information regarding acute monoamine dysfunction following TBI.

### **Monoamines and TBI**

Neurobehavioral sequelae following TBI are common and include dysregulation of cognition (e.g. attention, memory), mood (e.g. depression, anxiety), and emotion (e.g. aggression) [127]. Given the role the monoamines DA, NE, and 5-HT have in modulating these domains, sustained neurobehavioral impairments following TBI points to chronic dysregulation of monoamine neurotransmitter systems. In fact, pharmacologic agents, such as anti-depressants and stimulants, which modulate monoamine neurotransmitter systems, are often used to treat chronic TBI-induced neurobehavioral sequelae [127].

However, less is understood about acute effects to monoamine systems following TBI, with the majority of work being focused on DA systems [154, 170]. Although, we did not detect cortical elevations of DA, NE, or 5-HT in the pericontusional site over the first 24h following CCI (see “*Chapter Five*”), there is evidence that levels of DA, NE, and 5-HT become acutely elevated throughout various brain regions and systemically following TBI [154, 173, 174, 178, 182, 363-365].

Although acute administration of DA agonists (e.g. bromocriptine, amantadine, etc.) and 5-HT agonists (e.g. 8-OH-DPAT, buspirone, etc.) have shown great promise as neuroprotective agents in TBI, the administration of DA agonists is often delayed until 24h post-TBI [154, 170, 271], and therapeutic agonists are often receptor subtype specific. For example, bromocriptine is specific to the DA receptor subtype D2 [154],



amantadine doubles as an NMDA glutamate receptor antagonist [154], and 8-OH-DPAT and buspirone are specific to 5-HT<sub>1A</sub>, which is an inhibitory receptor [271]. Therefore, use of such agents, which target specific receptor subtypes, is not equivalent to increasing overall monoamine levels, as would be the case with the use of an MAOI, such as PZ.

Interestingly, following TBI, high catecholamine levels are associated with increased peripheral inflammation [366], cerebral edema [367], and poor outcome [181]. However, because catecholamine levels increase with activation of the sympathetic nervous system, as would occur following trauma, it is difficult to determine whether high catecholamine levels following TBI are an actual cause or rather an effect of injury severity [181]. Yet, early administration of NE in experimental TBI has been shown to increase pericontusional extracellular glutamate levels [368], and high dose NE leads to increases in systolic arterial blood pressure and intraparenchymal hemorrhage [369]. Further, acute administration of DA antagonists following experimental TBI has anti-excitotoxicity and neuroprotective effects [154].

Therefore, it is possible that in the current experiment, PZ-induced elevations to monoamines or PZ-enhancement of TBI-induced monoamine elevations [154, 173, 174, 178, 182, 363-365], led to exacerbation of dysfunction or even negated PZ aldehyde-scavenging protective effects, further impairing MWM performance (**Fig. 4.8**) and increasing weight loss (**Fig. 4.11**) compared to the CCI + vehicle group.

Extra-physiologic monoamines levels could have caused detrimental effects through a variety of mechanisms including direct catecholamine toxicity [170], vasoconstriction or thrombotic-induced ischemia [154, 171, 172, 182], or autoxidation generation of ROS/RNS [170, 194]. However, the latter scenario is unlikely, as even high

dose PZ has been shown to decrease markers of oxidative stress [72, 333]. Given the complexity, pervasiveness, and interconnectedness of the monoaminergic system, and the dearth of what is known regarding acute monoaminergic dysfunction in TBI, the complete answer of how PZ's MAOI mechanism of action effects TBI pathophysiology and outcome is likely complex. Further, as the current experiment did not directly measure MAO inhibition or monoamine tissue levels in PZ + CCI animals, the effects can only be hypothesized. As such, additional PZ mechanisms of action must also be considered.

### **Phenelzine: Other Possible Confounding Mechanisms of Action**

In general PZ has complicated pharmacokinetics. PZ is itself a MAO substrate with several active metabolites such as PEA and PEH [189]. As mentioned previously, PEA, also metabolized by MAO is an amphetamine-like metabolite that can produce stimulatory effects [207], and it is therefore possible that PEA, rather than more prevalent monoamine neurotransmitters such as DA, NE, and 5-HT, is responsible for PZ-induced weight loss (**Fig. 4.11**), working memory impairment (**Fig. 4.8**), and qualitative behavioral observations [352]. Additionally, the PZ metabolite, PEH, inhibits several important transaminases, including GABA transaminase (GABA-T), alanine transaminase (ALA-T), and ornithine transaminase (ORN-T) [169]. Although, GABA, ALA, and ORN levels were not measured as part of the current study, previous studies have shown a dose dependent increase in all three following PZ administration [342] [169, 335], and it is possible that inhibition of these transaminases following TBI could have negative consequences. For example, GABA-T is responsible for the conversion of the inhibitory neurotransmitter GABA, to succinic semi-aldehyde, which can be further oxidized to succinate [169], a substrate of the Krebs cycle and complex II of the ETC. Therefore, inhibition of GABA-T could lead to increases in GABA, which can

paradoxically cause excitotoxicity following neuronal injury through reversal of chloride channels [264], as well as decreases in ETC substrates during a time in which there is ongoing mitochondrial dysfunction and ATP depletion [22, 25, 51, 73]. Similarly, inhibiting ALA-T, the enzyme which catalyzes the reaction of alanine +  $\alpha$ -ketoglutarate to form glutamate + pyruvate, could also lead to decreased formation of Krebs cycle substrates. Further, ORN-T catalyzes the formation of glutamate, from the urea cycle product, ORN. However, inhibition of ORN-T could alternately lead to decarboxylation of ORN by ornithine decarboxylase (OCD), the result of which is formation of neurotoxic polyamines [169].

On the other hand, because PEA and PEH are metabolites of PZ metabolism by MAO, the effects of PZ metabolites, such as PEH, can be inhibited through pre-inhibition of MAO [169]. Therefore, the effect multiple PZ doses would have on GABA, ALA, and ORN levels, particularly in the context of TBI is unknown. However, PZ itself is also capable of inhibiting transaminases, as well as enzymes involved in the biosynthesis of neurotransmitters such as DA, 5-HT, and glutamate, as it can scavenge physiologically important carbonyls, such as the B<sub>6</sub>-derived cofactor, pyridoxal phosphate [78]. Furthermore, it is currently unknown how drug-aldehyde-protein ternary complexes are metabolized or what the longer-term consequences of ternary complex formation are [78]. In fact, evidence suggests that such complexes can be immunogenic [258]. Therefore, it is possible that *in-vivo* several PZ mechanisms of action could be interfering with its neuroprotective aldehyde-scavenging effects, particularly at higher doses.

### **Pargyline**

The results of the current study indicate that 15mg/kg PG administered intraperitoneal 15min, 24h, and 48h following severe CCI was unable to significantly

improve injury-induced deficits to reference memory on post-CCI D7 (**Fig. 4.10**) or to improve cortical tissue sparing on post-CCI D8 (**Fig. 4.12**). However, PG animals were able to significantly improve the time/distance it took to find the platform over the first four MWM days (**Fig. 4.8**), and did not lose a significant amount of weight following injury (**Fig. 4.11**).

In the literature PG is interchangeably referred to as a non-selective irreversible MAOI [191], and an MAO-B specific irreversible inhibitor [197], as the  $IC_{50}$  values of PG for MAO-A and MAO-B are 0.011522  $\mu\text{mol/L}$  and 0.00820  $\mu\text{mol/L}$ , respectively [202]. In fact, the  $ED_{50}$  for oral administration of PG gives a 6.6:1 selectivity ratio for MAO-B to MAO-A (1.4mg/kg for MAO-B, 9.3mg/kg for MAO-A) [197], whereas the  $ED_{50}$  for oral administration of PZ gives a 2:1 selectivity ratio of MAO-A to MAO-B (6mg/kg for MAO-A and 12mg/kg) [197]. The fact that PG is less selective for MAO-A, in conjunction with other pharmacokinetic differences between PG and PZ [189], likely explains why that for the dosing paradigms utilized in the current study, although both PG and PZ significantly inhibited MAO as measured by 5-HT and DA turnover (**Fig. 4.6C and 4.7D-F**), PG, unlike PZ, did not significantly raise tissue levels of the MAO-A substrates, NE (**Fig. 4.5**) or 5-HT (**Fig. 4.6A**).

These findings are in line with previous studies which directly compared the effects of PG and PZ on drug (e.g. nicotine, cocaine, ethanol) substitution and discrimination [205-208], processes thought to require both MAO-A and MAO-B inhibition [205-207]. Those studies found that PZ, administered at lower doses than PG, was able to enhance the discriminatory effects of nicotine [205] and nicotine-induced locomotor activity [206], whereas PG was not [205]. Further, although PZ and PG were both able to decrease cocaine and ethanol self-administration, PZ did so at lower doses and with prolonged effects [207, 208]. This data suggests that PG, at least when used at

a similar dosing concentration to PZ, has less of an effect than PZ on behavioral processes mediated by MAO inhibition. This knowledge, combined with the current study's HPLC data (**Fig. 4.5 – 4.7**), likely explains why the qualitative behavioral observations and negative effects such as weight loss (**Fig. 4.11**) and poor MWM acquisition performance (**Fig. 4.6**) that occurred in the PZ animals, was not seen in the PG group following CCI, despite both compounds being irreversible MAOIs. However, as with PZ, PG did significantly increase swim speed following CCI (**Fig 4.9**), suggesting that PG still possibly had some effect on elevating catecholamine levels following CCI [158]. Therefore, the absence of other confounding PZ mechanisms of action, such as formation of active metabolites or ternary drug-aldehyde-protein complexes (see *“Phenelzine: Other Possible Confounding Mechanisms of Action”* for further discussion) as factors in the behavioral differences between PG and PZ following CCI also cannot be ruled out.

As stated previously, PG was chosen as a comparison to PZ because it is similarly structured but lacks the aldehyde-scavenging hydrazine moiety (-NH-NH<sub>2</sub>) (**Fig. 4.2**), and that the dosing paradigms for the two were kept equivalent to parallel previous *ex-vivo* experiments [72]. However, we concede that choosing a non-hydrazine MAOI with more similar MAO-A to MAO-B affinity ratios, such as tranylcypromine [189, 197, 208], or altering PG concentrations to better reflect PZ MOAI affinities or other pharmacokinetics may have offered more clear insight into the effects of MAOI following TBI.

Due to PG's lack of an aldehyde-scavenging hydrazine (-NH-NH<sub>2</sub>) moiety it was not surprising that PG was unable to improve behavioral deficits or cortical tissue sparing following CCI (**Fig 4.8, 4.10, 4.12**). However, it should be noted that some studies have demonstrated MAOIs to have neuroprotective effects. For example, MAO

substrates such as DA and tyramine (an MAO substrate incapable of undergoing autoxidation) have been shown to induce mitochondrial dysfunction, an effect which can be attenuated by administration of a variety of irreversible MAOIs, including PG [193]. Similarly, *in-vitro*, MAOIs can prevent mitochondrial-dependent apoptosis following serum withdrawal [275]. Although these results may seem to contradict our previous findings that PG is unable to protect mitochondria from exogenous administration of the toxic aldehydes 4-HNE and acrolein *ex-vivo* [72], the differences are likely explained by the isolative nature of the mitochondrial preparation technique in which monoamine substrates or other molecules such as those involved in apoptotic signaling are likely absent. As such, although not included as part of this study, evaluating the effects of *in-vivo* administration of PG following CCI on mitochondrial function, as we have previously done with PZ [71, 72, 333, 334] could have yielded interesting results.

Further, several irreversible MAOIs have demonstrated *in-vivo* neuroprotection in models of stroke [272], TBI [273], and aging [279]. However, many of these studies suggest that the neuroprotective effects of MAOIs are independent of MAO inhibition [274, 275], and are instead possibly due to the presence of an *N*-propargyl moiety, a structure shared by several demonstratively neuroprotective MAOIs, including deprenyl (selegiline), clorgyline, rasagiline, and importantly, PG [192, 201, 276-278]. Hypotheses regarding the mechanisms of action in which *N*-propargyl compounds may exert their neuroprotective effects are vast and include modulation of apoptotic proteins and protein kinase C (PKC), upregulation of antioxidants and growth factors, or direct targeting of the mPTP [192, 274-276, 278, 279].

Therefore, even though PG did not demonstrate protective effects following CCI in the current experiment, and other studies have demonstrated that PG can actually exacerbate DA neurotoxicity [194], it is possible that under different experimental

parameters, such as an alternative dosing paradigm, that PG could demonstrate acute neuroprotective effects following CCI, possibly due to the presence of an *N*-propargyl moiety. On the other hand, it should be noted that in addition to possible MAOI effects (see “*Monoamines and TBI*” section for further discussion), PG has several properties which could instead either negate protective effects or exacerbate dysfunction. Although the latter is unlikely the case as out of all three drugs, PG performed most similarly to vehicle (**Fig. 4.8 – 4.12**).

First, PG is metabolized by the liver enzyme CYP2E1 to the toxic aldehyde, propionaldehyde, which has similar effects to acrolein and can induce hepatocyte toxicity, lipid peroxidation, and glutathione (GSH) depletion [370]. Interestingly, CYP2E1, itself a producer of ROS during substrate metabolism, is found in rat brain at 25% the levels of that in the liver and is highly expressed within rat brain mitochondria [371]. Although PG appears to be non-toxic to rat brain mitochondria when exogenously applied *ex-vivo* [72], it is unknown what role CYP2E1 and its potential products have in the metabolism of PG, particularly multiple doses of PG, following CCI.

Second, although developed and classified as an MAOI, PG was more frequently used clinically as an anti-hypertensive [203]. Although this sounds counterintuitive given the known risk of hypertensive crisis that can be induced by combining MAOIs with ingestion of tyramine-rich foods [191], its anti-hypertensive properties are thought to be due to MAOI-induced increases in NE and its action on inhibitory  $\alpha_2$ -adrenergic receptors of the brainstem and periphery [204]. Although only slight and non-significant changes in NE tissue level were seen following multiple PG administration in uninjured animals (**Fig. 4.5**), and previous studies have not detected blood pressure changes in Sprague-Dawley rats over a 24h period following intravenous PG (10mg/kg) administration [204], as blood pressure was not measured during the current study, it is

unknown what effect PG has on blood pressure following CCI, an experimental model of TBI which can induce hypotension acutely following impact [372]. In fact, it is known that hypotension can exacerbate dysfunction following experimental TBI [373, 374]. Interestingly, given the proposed mechanism of action regarding PG's anti-hypertensive effects, it is possible that as a drug class all MAOIs, and therefore PZ, could have anti-hypertensive effects. In fact low blood pressure is an uncommon side effect of PZ [198, 341]. Further, the third drug used in this study, HZ, also has potential anti-hypertensive effects [268] (*see "Hydralazine" section for further discussion*). On the other hand, blood pressure monitoring following drug administration could have revealed the opposite effect, as MAOI-induced catecholamine elevations can elicit increases in blood pressure [346]. Admittedly, including blood pressure measurements as part of the current study may have revealed important physiologic changes subsequent to CCI + drug administration.

### **Hydralazine**

The results of the current study indicate that 5mg/kg HZ administered intraperitoneal 15min, 24h, and 48h following severe CCI was unable to significantly improve injury-induced deficits to reference memory on post-CCI D7 (**Fig. 4.10**). However, HZ animals were able to significantly improve the time/distance it took to find the platform over the first four MWM days (**Fig. 4.8**), and did not lose a significant amount of weight following injury (**Fig. 4.11**). Although HZ was unable to significantly decrease cortical degeneration on post-CCI D8 (**Fig. 4.12**), of the three drugs tested, HZ did lead to the greatest amount of cortical tissue spared, improving the amount of cortical tissue sparing seen in the vehicle group by nearly 10% (**Table 4.1**). As this was the first time HZ was investigated in the context of TBI, it is possible that choosing an alternative HZ dosing paradigm could have enhanced protective effects.



For example, the plasma half-life of HZ is only 60 minutes [74, 78]. Therefore, theoretically more frequent doses of HZ could have led to enhanced protection. However, that is not the case in SCI, where intraperitoneal dosing of 5mg/kg HZ every 24h has been shown to be neuroprotective, improving motor function, increasing tissue sparing, and decreasing pain hypersensitivity [74, 75, 338, 358]. In fact, as HZ can exert its effects as an aldehyde-scavenger by binding protein-bound aldehydes and preventing damaging cross-linking reactions [79, 262], its neuroprotective aldehyde-scavenging effects are likely prolonged beyond its short plasma half-life. However, additional neuroprotective mechanisms of action for HZ have also been recently proposed. For example, HZ has been shown capable of activating Nrf2 (nuclear factor erythroid 2-related factor), a transcription factor which activates antioxidant genes following neuronal injury [375], which would also act in prolonging its neuroprotective effects.

Unfortunately, the HZ dosing paradigm utilized in the current study did not translate well from SCI to TBI. As discussed previously, this is not entirely surprising as the SCI and CCI injury models are not necessarily equivalent. In fact, it is possible that additional, non-aldehyde-scavenging HZ mechanisms of actions are more confounding in TBI than they are in SCI.

First, like PZ and PG, HZ has MAOI properties [258, 269], likely due to the presence of its hydrazine moiety (-NH-NH<sub>2</sub>), which is known to participate in one mechanism of MAO inhibition [199]. Specifically, HZ has been demonstrated to reversibly inhibit MAO-A and MAO-B, with a slight preference for MAO-A [269]. Such a property likely explains the results shown in **Fig. 4.6C** in which HZ causes a slight but significant decrease in 5-HT turnover in uninjured cortex, as well as the slight but significant increase in swim speed (**Fig. 4.9**) seen in HZ animals following CCI, which was similar to that seen with the MAOIs PG and PZ. And although inhibiting MAO along

with scavenging acrolein may synergistically attenuate pain hypersensitivity in SCI [74, 338], as discussed previously, modulation of MAO following TBI may have unintended negative consequences (see “*Monoamines and TBI*” section for further discussion).

More concerning, however, is the fact that HZ is an anti-hypertensive, clinically used to treat emergent and essential hypertension [268]. The anti-hypertensive properties of HZ are due to its ability to act as an arteriolar vasodilator. Although the exact mechanism of action remains unclear, it has been hypothesized to be due to activation of guanylate cyclase, inhibition of sarcoplasmic reticulum calcium release, or increased conductance of calcium-dependent  $K^+$  channels [258]. Although intraperitoneal doses of HZ ranging from 5mg/kg - 25mg/kg have been reported not to induce changes to systolic blood pressure in rats [270], because CCI can acutely induce hypotension [372], and as mentioned previously blood pressures were not measured as part of the current study, it is currently unknown whether HZ induced hypotension under the current experimental conditions. However, if under the current experimental conditions HZ did induce hypotension and as a consequence cerebral hypoperfusion occurred, it could explain the differences between the results seen here and those seen in previous SCI studies [74, 75, 338, 358], as any protective aldehyde-scavenging effects could have been partially negated by the consequences of cerebral hypoperfusion. In fact decreases in cerebral perfusion pressure have been shown to exacerbate functional deficits and cortical lesion volumes [373, 374]. Admittedly, including blood pressure measurements, as well as measures of aldehyde load, either by tissue staining or evaluation of urine metabolites such as 3-HPMA (N-acetyl-S-3-hydroxypropylcysteine) [270], could have potentially helped to interpret the current study's results in regards to HZ's aldehyde-scavenging properties versus its anti-hypertensive effects.

## Clinical Translation of PZ, HZ, and Other Aldehyde Scavengers

The ultimate goal in evaluating neuroprotective agents in experimental TBI is to translate their use into the human TBI population. Therefore, selecting study compounds which are FDA-approved for other indications and which could be potentially repurposed for use in TBI often offers a faster and more cost-effective approach than development of novel agents. Of the hydrazine (-NH-NH<sub>2</sub>) aldehyde scavenging drugs available, three are currently FDA-approved and in clinical use, including PZ, HZ, and the anti-tuberculosis agent isoniazid, which itself has some MAOI properties [198, 376].

As MAOIs were designed to target the CNS, along with concerns that an anti-hypertensive like HZ would be dangerous for use clinically in TBI, our lab originally selected PZ for its studies into the protective effects of aldehyde scavengers following TBI [71, 72, 333, 334]. Despite previous studies by our lab and other groups demonstrating PZ to be neuroprotective in experimental models of CNS injury [71, 72, 74-76, 333, 334, 361, 362], unfortunately the PZ dosing paradigm utilized in the current study (15mg/kg, i.p., 15min, 24h, 48h post-CCI) was unable to provide protective effects in regards to reference memory (**Fig. 4.10**) or cortical degeneration (**Fig. 4.12**), while also inducing significant weight loss (**Fig. 4.11**) and impairing MWM acquisition performance (**Fig. 4.8**). As discussed previously, it is becoming clearer that lower doses of PZ may offer better protection [71, 334], possibly due to several PZ mechanisms of action which may confound neuroprotective effects as dosage increases, including its MAOI properties (**Fig. 4.5 – 4.7**). As such, it may be possible to optimize PZ for neuroprotection in experimental TBI using low or single dosing paradigms. However, as an MAOI, even conservative dosing paradigm may still prove impractical for clinical translation.

For example, in rats a single dose of PZ has been shown capable of inhibiting MAO and increasing monoamine levels for at least a week following administration [205, 342]. However, the half-life of MAO in healthy human brain is reported to be as much as 30 days [196], three times that in the rat [195]. Further, it is currently unknown what effect TBI has on the turnover of MAO in human brain, suggesting that even a single dose of PZ could have either prolonged effects or unintended negative consequences in TBI patients. For example, although in general there is little known about the monoaminergic system acutely following TBI, high catecholamine levels have been shown to correlate with poor outcome [181], and therefore, administration of PZ acutely in clinical TBI, even at low doses, may represent a risk in regards to modulating the monoaminergic system in a way that leads to direct catecholamine toxicity [170], or catecholamine-induced vasoconstrictive or ischemic events [154, 171, 172, 182].

Additionally, clinical administration of PZ would likely be restricted to patients not receiving vasopressors (e.g. NE or DA) as part of their clinical treatment, and contraindicated for use in patients taking serotonin modulating drug such as SSRIs (serotonin-reuptake inhibitors) or SNRIs (serotonin-norepinephrine-reuptake inhibitors) [346], a medical history unlikely to be known at the time of acute clinical treatment given the severe nature TBI. Of additional concern in regards to clinical translation of PZ is that anti-depressants can lower seizure threshold [265], a complication for which TBI patients are already at increased risk [209], although of all the anti-depressant drug classes, MAOIs are at the least risk to do so [265]. Therefore, use of PZ could increase the risk of post-traumatic seizure in TBI patients.

Similarly, although HZ was unable to provide significant protection in the current study (**Fig. 4.8, 4.10, 4.12**), it has shown extensive promise as a neuroprotective agent in experimental SCI [74, 75]. Yet, even if a HZ dosing paradigm for protection in

experimental TBI could be optimized, its anti-hypertensive properties also likely make it impractical for clinical translation. In fact, anti-hypertensives would be contraindicated for use in clinical TBI, as maintaining systolic blood pressure is important for decreasing mortality and improving outcome [209], particularly in patients in which autoregulation is impaired [377].

However, despite the likely difficulty in clinical translation that PZ and HZ would face in order to be used in TBI, and despite the poor performance of the chosen PZ and HZ dosing paradigms in the current study in regards to the outcome measures evaluated, there is a preponderance of evidence that hydrazine (-NH-NH<sub>2</sub>) compounds such as PZ and HZ can provide protection *in-vitro* and *in-vivo* under a variety of injury paradigms [71, 72, 74-76, 88, 257, 270, 311, 333, 334, 337, 338]. Therefore, in our opinion it is still too early to abandon pursuit of aldehyde scavengers as therapeutic agents in TBI.

However, there is a need for new hydrazine compounds (-NH-NH<sub>2</sub>) to be developed, such as ones with less complicated pharmacokinetics that do not result in potentially confounding off target effects such as MAO inhibition or hypotension. Although it should be noted that the hydrazine moiety (-NH-NH<sub>2</sub>) is purported to interact with MAO to cause inhibition [199], a variety of hydrazine (-NH-NH<sub>2</sub>) containing compounds have been shown to have differing levels of inhibitor activity [199, 378], therefore, development of an aldehyde-scavenging hydrazine (-NH-NH<sub>2</sub>) compound with no MAOI effects should theoretically be possible. Alternatively, although not as potent as the hydrazine (-NH-NH<sub>2</sub>) compounds, additional aldehyde-scavenging moieties exist including cysteines, histidines, and pyridines, and could also serve as the basis for further development [79].

## **Conclusion**

In conclusion, utilizing a severe CCI model of TBI in 3mo male Sprague-Dawley rats, intraperitoneal administration (15min, 24h, 48h post-CCI) of the drugs PG (15mg/kg, MAOI, non-aldehyde scavenger), PZ (15mg/kg, MAOI, aldehyde scavenger), and HZ (5mg/kg, non-MAOI, aldehyde scavenger) were unable to attenuate reference memory deficits (D7 post-CCI) (**Fig. 4.10**) or improve cortical tissue sparing (D8 post-CCI) (**Fig. 4.12**) following injury. However, although non-significant, HZ led to the most improvement to cortical tissue sparing (**Table 4.1**). Of concern, following CCI PZ animals lost a significant amount of weight (**Fig. 4.11**), and their MWM acquisition performance did not significantly improve across time (D3-6 post-CCI) (**Fig. 4.8**), possibly due to PZ-induced high monoamine levels as was seen in uninjured cortical tissue utilizing the same PZ dosing paradigm (**Fig. 4.5 – 4.7**). Similarly, qualitative behaviors observed in the PZ group following CCI may have also been suggestive of elevated monoamine levels. However, the effects of other PZ mechanism of actions, such as inhibition of GABA-T or formation of PEA, cannot be ruled out as factors effecting outcome. Admittedly, this study had several limitations that make precise data interpretation difficult. Namely, MAO inhibition and monoamine levels were not evaluated following CCI + drug administration, MWM testing began very early following CCI and final drug administration, blood pressure was not monitored, and quantitative behavioral testing was limited to one task. Although the precise reasons the aldehyde-scavengers PZ and HZ were unable to provide significant protection in the current study cannot be identified with certainty, the dosing paradigm and experimental parameters utilized are likely contributory factors, as a number of previous studies have shown that the aldehyde-scavengers PZ and HZ are indeed protective under different conditions (e.g. lower doses, SCI, mitochondrial bioenergetics, etc.). However, given the fact that PZ is a non-

selective irreversible MAOI with complicated pharmacokinetics and active metabolites and HZ is an anti-hypertensive, clinical translation of either drug for use in TBI patients may prove challenging. Therefore, we urge the development of aldehyde-scavenging drugs that do not contain confounding mechanisms of action such as irreversible MAO inhibition or hypotension, and for such compounds to be used in future investigations of aldehyde-scavenging as a means of neuroprotection in experimental TBI.

### **Acknowledgments**

This work was supported by NIH-NINDS 5R01 NS083405 & 5R01 NS084857. Jacqueline R. Kulbe is currently supported by NIH-NINDS NRSA NS096876. We would like to thank Ms. Linda Simmerman for assistance in scanning of histology slides, Ms. Deann Hopkins for assistance in setting up of behavioral experiments, and Dr. Rachel Hill for some assistance in animal handling.

## **CHAPTER FIVE:**

### **Supplementary Data: Comparative Effects of Phenzelzine, Hydralazine, and Pargyline on Learning and Memory and Cortical Tissue Sparing Following Experimental Traumatic Brain Injury**

#### **Introduction**

The data presented here is an extension of the work presented in “*Chapter 4: Comparative Effects of Phenzelzine, Hydralazine, and Pargyline on Learning and Memory and Cortical Tissue Sparing Following Experimental Traumatic Brain Injury*”. High Performance Liquid Chromatography (HPLC) is utilized to analyze the tissue levels of monoamines, metabolites, and turnover ratios in order to assess monoamine oxidase (MAO) inhibition in uninjured cortical tissue following a single dose of phenzelzine (PZ), pargyline (PG), or hydralazine (HZ). Additionally, HPLC is utilized to analyze the tissue levels of monoamines, metabolites, and turnover ratios in the penumbra of cortical tissue in order to assess MAO inhibition and metabolite tissue levels 3h, 12h, and 24h following a severe controlled cortical impact injury (CCI). Further, percent weight loss for uninjured animals following two doses of PZ, PG, or HZ is presented.



## **Methods**

Please see “*Chapter Four: Comparative Effects of Phenelzine, Hydralazine, and Pargyline on Learning and Memory and Cortical Tissue Sparing Following Experimental Traumatic Brain Injury*” for detailed methods regarding animals, HPLC tissue collection, HPLC, CCI, choice of drug concentration, statistical analysis, etc.

### **Experimental Design: 24h HPLC Monoamine and Metabolite Analysis (Fig. 5.1)**

In order to assess MAO inhibition 24h following single drug administration HPLC was used to evaluate monoamine and metabolite tissue levels and turnover ratios in uninjured cortex. Uninjured animals (n = 6 animals per group) were administered an intraperitoneal (i.p.) dose of saline, PZ (15 mg/kg), HZ (5 mg/kg) or PG (15 mg/kg) [72, 74]. Animals were euthanized 24h following drug administration and cortical tissue punches were collected for HPLC analysis.

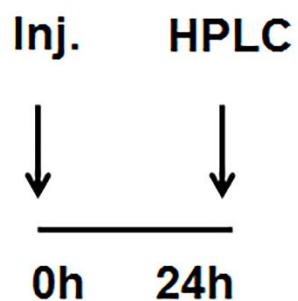


**Figure 5.1 Monoamine and metabolite 24h HPLC experimental design.** Uninjured rats received intraperitoneal injections of vehicle (saline), pargyline (15mg/kg), phenelzine (15mg/kg), or hydralazine (5mg/kg) at 0h. Animals were euthanized and cortical tissue was collected for HPLC analysis 24h following injection.

### **Experimental Design: CCI Time Course HPLC Monoamine and Metabolite Analysis (Fig. 5.2)**

HPLC was utilized to assess MAO inhibition and monoamine neurotransmitter tissue levels following severe CCI. Animals received a severe CCI (n = 6 per time point) or sham surgery (n = 6). At 3h, 12h, and 24h post-CCI 3mm cortical tissue punches were collected from the penumbra region lateral to the epicenter of injury and sent for HPLC analysis. Sham tissue was collected 12h post-surgery.

### **Percent Weight Loss in Uninjured Rats Following PG, PZ, or HZ Administration**

Animals were weighed daily prior to each drug administration for the uninjured 72h HPLC experiments (**Fig. 4.3**). However, a final weight was not measured at the 72h time point prior to euthanasia. Therefore, percent weight loss is calculated between day zero (prior to drug administration) and day two following intraperitoneal administration of saline, PG (15mg/kg), PZ (15mg/kg), or HZ (5mg/kg) on day zero and day one.

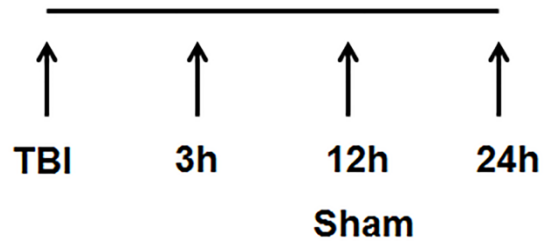


**Figure 5.2 Monoamine and metabolite CCI time course experimental design.** Rats received severe a CCI (TBI). Cortical punches were collected from penumbral tissue lateral to the injury epicenter at 3h, 12h, and 24h following injury. Sham tissue was collected 12h following sham surgery. Tissue was sent for HPLC analysis.

## Results

### **24h Single Dose PG, PZ, or HZ: HPLC Monoamine and Metabolite Tissue Levels and Turnover Ratios in Uninjured Cortical Tissue (Fig. 5.3 – 5.5)**

For norepinephrine (NE), a single saline sample was identified as an outlier (Grubb's) and excluded ( $G = 2.009$ ,  $Y = 6$ ). For NE, a one-way ANOVA revealed a statistically significant effect across all groups ( $F[3,19] = 15.74$ ,  $p < 0.0001$ ). However, Brown-Forsythe revealed an inequality of variance ( $p = 0.0002$ ). Therefore, Kruskal-Wallis was used in lieu of a one-way ANOVA. KW revealed a significant effect across all groups ( $H[3, n = 23] = 15.33$ ,  $p = 0.0016$ ). *Post-hoc* testing (Dunn's) revealed that compared with saline, NE (ng/g) was significantly increased in PZ ( $p < 0.05$ ) and PG ( $p < 0.05$ ), and that compared with HZ, NE (ng/g) was significantly increased in PZ ( $p < 0.05$ ) (**Fig. 5.3**). Thus, PZ and PG result in an increase in NE.

For the analysis of 5-HT and 5-HT metabolites, during 5-HIAA analysis, a single PZ sample was identified as an outlier (Grubb's) and excluded ( $G = 1.903$ ,  $Y = 6$ ). In order to maintain consistency and be able to calculate the 5-HIAA/5-HT ratio, this PZ animal was excluded from the entire 5-HT data set.

For serotonin (5-HT), a one-way ANOVA revealed a statistically significant effect across all groups ( $F[3,19] = 28.13$ ,  $p < 0.0001$ ). *Post-hoc* testing (Tukey's) revealed that compared with saline, 5-HT (ng/g) was significantly increased in PZ ( $p < 0.0001$ ) and PG ( $p < 0.01$ ), and that compared with HZ, 5-HT (ng/g) was significantly increased in PZ ( $p < 0.0001$ ) and PG ( $p < 0.05$ ), and that PZ and PG were significantly different from each other ( $p < 0.01$ ) (**Fig. 5.4A**). Thus, PZ and PG result in an increase in 5-HT. However, the increase in 5-HT is greater with PZ.

### Norepinephrine 24h

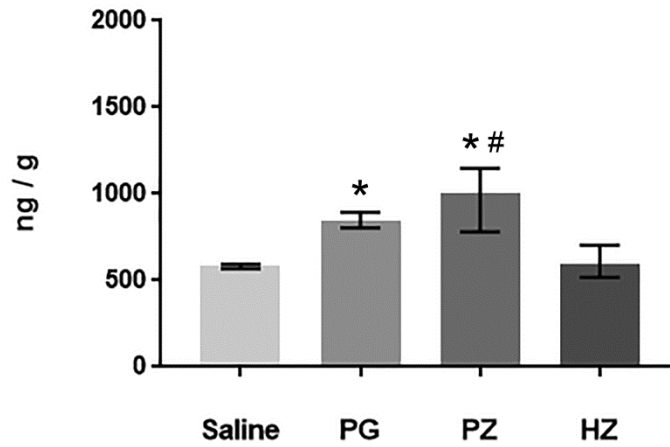


**Figure 5.3 Tissue Level (ng/g) of norepinephrine (NE) in 24h uninjured cortex.** NE measured via HPLC 24h following single intraperitoneal injection of saline, pargyline (PG), phenzazine (PZ) or hydralazine (HZ). Values= median  $\pm$  interquartile range; Kruskal-Wallis followed by Dunn *post hoc*; \* $p < 0.05$  compared with saline; # $p < 0.05$  compared with HZ;  $n = 5-6$  per group.

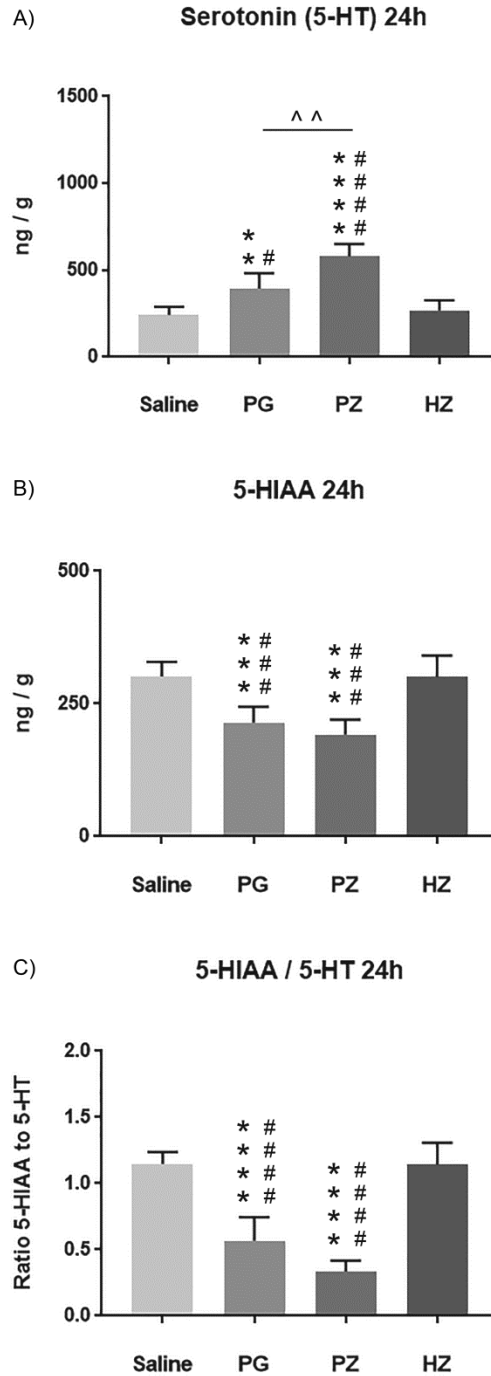


**Figure 5.4 Tissue Level (ng/g) of serotonin (5-HT) and metabolites in 24h uninjured cortex. (A) 5-HT, (B) the 5-HT metabolite 5-hydroxyindoleacetic acid (5-HIAA), (C) and the turnover ratio (5-HIAA / 5-HT) in uninjured cortex as measured via HPLC 24h following single intraperitoneal injection of saline, pargyline (PG), phenelzine (PG) or hydralazine (HZ). Values = mean  $\pm$  standard deviation; one-way analysis of variance followed by Tukey *post hoc*; \*\* $p < 0.01$ , \*\*\* $p < 0.001$ , \*\*\*\* $p < 0.0001$  compared with saline; # $p < 0.05$ , ### $p < 0.001$ , #### $p < 0.0001$  compared with HZ;  $\wedge p < 0.01$ ,  $n = 5-6$  per group.**

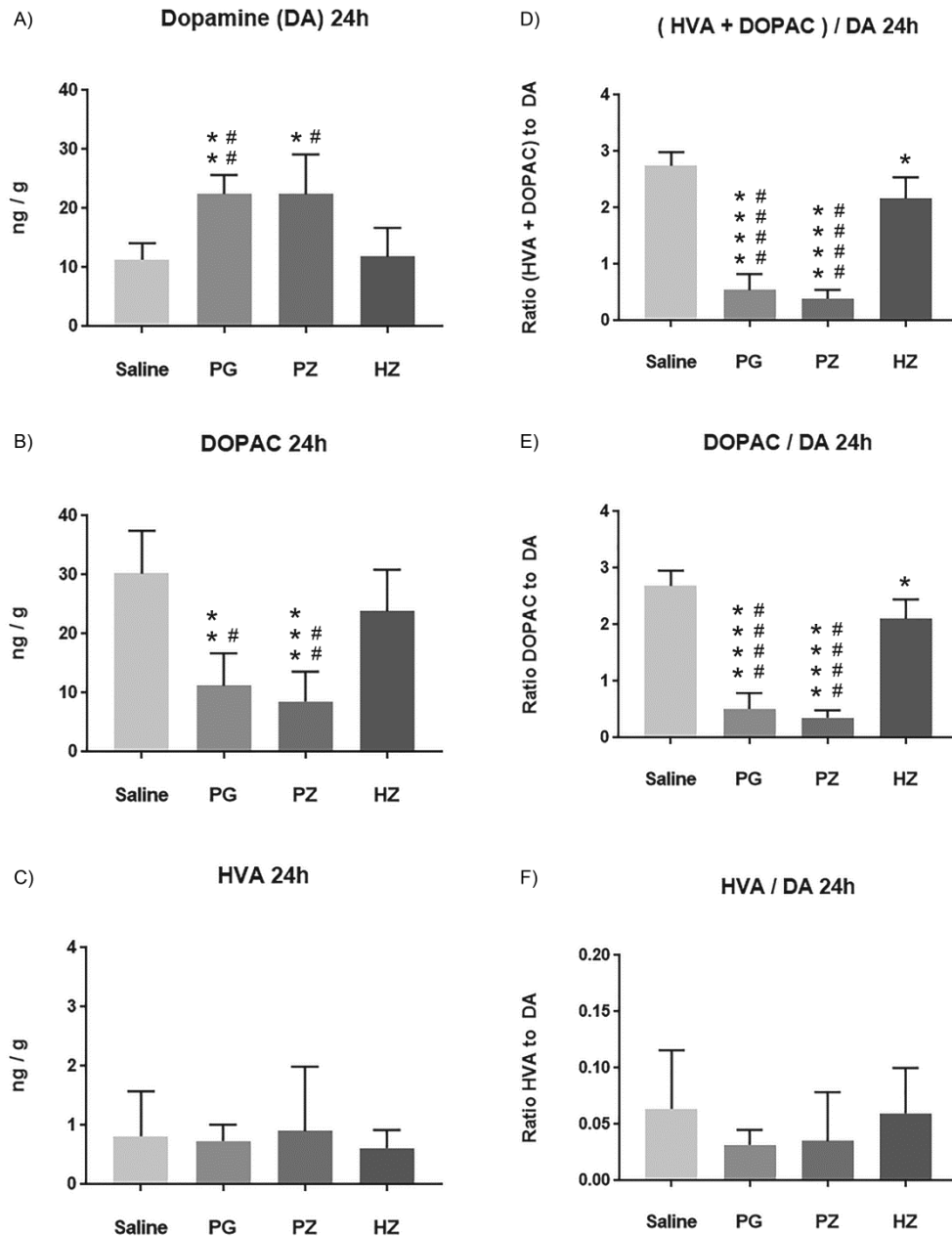


**Figure 5.5 Tissue Level (ng/g) of dopamine (DA) and metabolites in 24h uninjured cortex. (A) DA, (B) the DA metabolite 3,4 5-dihydroxyphenylacetic acid (DOPAC), (C) the DA metabolite homovanillic acid (HVA), and the DA turnover ratios (D) (DOPAC + HVA / DA, (E) DOPAC / DA, and (F) HVA / DA in uninjured cortex as measured via HPLC 24h following single intraperitoneal injection of saline, pargyline (PG), phenelzine (PG) or hydralazine (HZ). Values = mean  $\pm$  standard deviation; one-way analysis of variance followed by Tukey *post hoc*; \* $p < 0.05$ , \*\* $p < 0.01$ , \*\*\* $p < 0.001$ , \*\*\*\* $p < 0.0001$  compared to saline; # $p < 0.05$ , ## $p < 0.01$ , #### $p < 0.0001$  compared to HZ;  $n = 4-6$  per group.**



For 5-hydroxyindoleacetic acid (5-HIAA), a one-way ANOVA revealed a statistically significant effect across all groups ( $F[3,19] = 17.74$ ,  $p < 0.0001$ ). *Post-hoc* testing (Tukey's) revealed that compared with saline, 5-HIAA (ng/g) was significantly decreased in PZ ( $p < 0.001$ ) and PG ( $p < 0.001$ ), and that compared with HZ, 5-HIAA (ng/g) was significantly decreased in PZ ( $p < 0.001$ ) and PG ( $p < 0.001$ )(**Fig. 5.4B**). Thus, both PZ and PG result in a decrease in the 5-HT metabolite, 5-HIAA.

For the ratio 5-HIAA / 5-HT, a one-way ANOVA revealed a statistically significant effect across all groups ( $F[3,18] = 46.37$ ,  $p < 0.0001$ ). *Post-hoc* testing (Tukey's) revealed that compared with saline, the ratio 5-HIAA / 5-HT was significantly decreased in PZ ( $p < 0.0001$ ) and PG ( $p < 0.0001$ ), and that compared with HZ, the ratio 5-HIAA / 5-HT was significantly decreased in PZ ( $p < 0.0001$ ) and PG ( $p < 0.0001$ )(**Fig. 5.4C**). Thus, PZ and PG result in a decrease in 5-HT turnover to 5-HIAA (i.e. increase in monoamine oxidase inhibition).

Prior to statistical analysis, due to undetectable HVA levels, two animals were removed from the PZ group for all analysis of DA and DA metabolites. Additionally, during HVA statistical analysis, a saline sample ( $G = 1.995$ ,  $Y = 6$ ) and PG sample ( $G = 2.2027$ ,  $Y = 6$ ) were identified as an outliers (Grubb's) and excluded. In order to maintain consistency and be able to calculate DA metabolite/DA turnover ratios, these animals were further excluded from the entire DA data set.

For dopamine (DA), a one-way ANOVA revealed a statistically significant effect across all groups ( $F[3,16] = 9.424$ ),  $p = 0.0008$ ). *Post-hoc* testing (Tukey's) revealed that compared with saline, dopamine (ng/g) was significantly increased in PZ ( $p < 0.05$ ) and PG ( $p < 0.01$ ), and that compared with HZ, dopamine (ng/g) was significantly increased in PZ ( $p < 0.05$ ) and PG ( $p < 0.01$ )(**Fig. 5.5A**). Thus, PZ and PG result in an increase in DA.

For 3,4-dihydroxyphenylacetic acid (DOPAC), a one-way ANOVA revealed a statistically significant effect across all groups ( $F[3,16] = 12.17, p = 0.0002$ ). *Post-hoc* testing (Tukey's) revealed that compared with saline, DOPAC (ng/g) was significantly decreased in PZ ( $p < 0.001$ ) and PG ( $p < 0.01$ ), and that compared with HZ, DOPAC (ng/g) was significantly decreased in PZ ( $p < 0.01$ ) and PG ( $p < 0.05$ )(**Fig. 5.5B**). Thus, PZ and PG result in a decrease in the DA metabolite, DOPAC.

For homovanillic acid (HVA), a one-way ANOVA did not reveal a statistically significant effect across all groups ( $F[3,16] = 0.1774, p = 0.9101$ )(**Fig. 5.5C**). Thus, PZ, PG, nor HZ affected HVA levels.

For the ratio (HVA + DOPAC) / DA, a one-way ANOVA revealed a statistically significant effect across all groups ( $F[3,16] = 80.58, p < 0.0001$ ). *Post-hoc* testing (Tukey's) revealed that compared with saline, the ratio (HVA + DOPAC) / DA was significantly decreased in PZ ( $p < 0.0001$ ), HZ ( $p < 0.05$ ) and PG ( $p < 0.0001$ ), and that compared with HZ, the ratio (HVA + DOPAC) / DA was significantly decreased in PZ ( $p < 0.0001$ ) and PG ( $p < 0.0001$ ) (**Fig. 5.5D**). Thus, PZ, PG, and HZ result in a decrease in DA turnover to HVA+DOPAC (i.e. increase in monoamine oxidase inhibition). However, PZ and PG do so to a greater degree.

For the ratio DOPAC / DA, a one-way ANOVA revealed a statistically significant effect across all groups ( $F[3,16] = 83.17, p < 0.0001$ ). *Post-hoc* testing (Tukey's) revealed that compared with saline, DOPAC / DA was significantly decreased in PZ ( $p < 0.0001$ ), HZ ( $p < 0.05$ ), and PG ( $p < 0.0001$ ), and that compared with HZ, DOPAC / DA was significantly decreased in PZ ( $p < 0.0001$ ) and PG ( $p < 0.0001$ )(**Fig. 5.5E**). Thus, PZ, PG, and HZ result in a decrease in DA turnover to DOPAC (i.e. increase in monoamine oxidase inhibition). However, PZ and PG do so to a greater degree.

For the ratio HVA / DA, a one-way ANOVA did not reveal a statistically significant effect across all groups ( $F[3,16] = 0.8669$ ,  $p = 0.4785$ )(**Fig. 5.5F**). Thus, PZ, PG, nor HZ affected DA turnover to HVA.

#### **CCI Time Course HPLC Monoamine and Metabolite Tissue Levels and Turnover Ratios in Penumbral Cortical Tissue (Fig. 5.6 – 5.8)**

For NE, a one-way ANOVA revealed a statistically significant effect across all groups ( $F[3,20] = 31.91$ ,  $p < 0.0001$ ). However, Brown-Forsythe revealed an inequality of variance ( $p = 0.0152$ ). Therefore, Kruskal-Wallis was used in lieu of a one-way ANOVA. KW revealed a significant effect across all groups ( $H[3, n = 24] = 18.63$ ,  $p = 0.0003$ ). *Post-hoc* testing (Dunn's) revealed that compared with sham NE (ng/g) was significantly decreased at 3h ( $p < 0.05$ ) and 24h ( $p < 0.001$ ) post-injury (**Fig. 5.6**). Thus, following CCI NE is decreased at 3h and 24h.

For 5-HT, a one-way ANOVA revealed a statistically significant effect across all groups ( $F[3,20] = 21.29$ ,  $p < 0.0001$ ). However, Brown-Forsythe revealed an inequality of variance ( $p = 0.0324$ ). Therefore, Kruskal-Wallis was used in lieu of a one-way ANOVA. KW revealed a significant effect across all groups ( $H[3, n = 24] = 15.65$ ,  $p = 0.0013$ ). *Post-hoc* testing (Dunn's) revealed that compared with sham 5-HT (ng/g) was significantly decreased at 3h ( $p < 0.05$ ) and 24h ( $p < 0.01$ ) post-injury (**Fig. 5.7A**). Thus, following CCI 5-HT is decreased at 3h and 24h.

## Norepinephrine

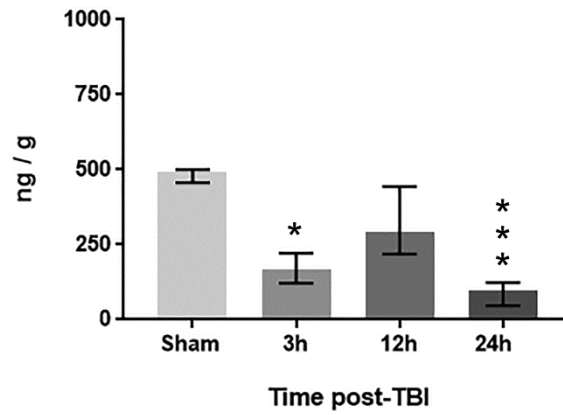


**Figure 5.6 Tissue Level (ng/g) of norepinephrine (NE) in penumbral cortical tissue** measured via HPLC 3h, 12h, and 24h following severe CCI. Values= median  $\pm$  interquartile range; Kruskal-Wallis followed by Dunn *post hoc*; \* $p < 0.05$  \*\*\* $p < 0.00$  compared with sham;  $n = 6$  per group.

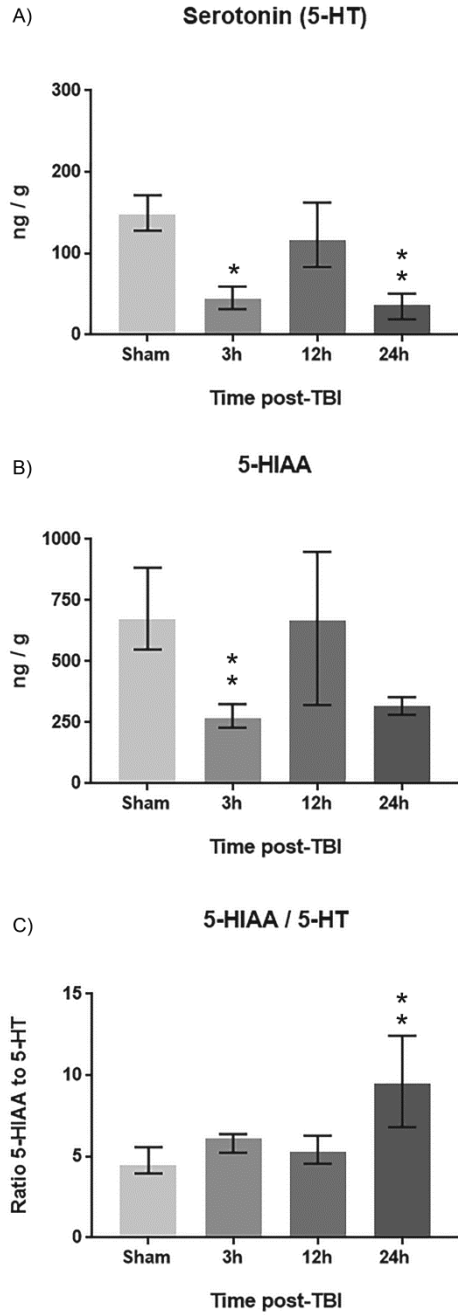


**Figure 5.7 Tissue Level (ng/g) of serotonin (5-HT) and metabolites in penumbral cortical tissue** measured via HPLC 3h, 12h, and 24h following severe CCI **(A)** 5-HT, **(B)** the 5-HT metabolite 5-hydroxyindoleacetic acid (5-HIAA), **(C)** and the turnover ratio (5-HIAA / 5-HT). Values= median  $\pm$  interquartile range; Kruskal-Wallis followed by Dunn *post hoc*; \* $p < 0.05$ , \*\* $p < 0.01$  compared with sham;  $n = 5-6$  per group.

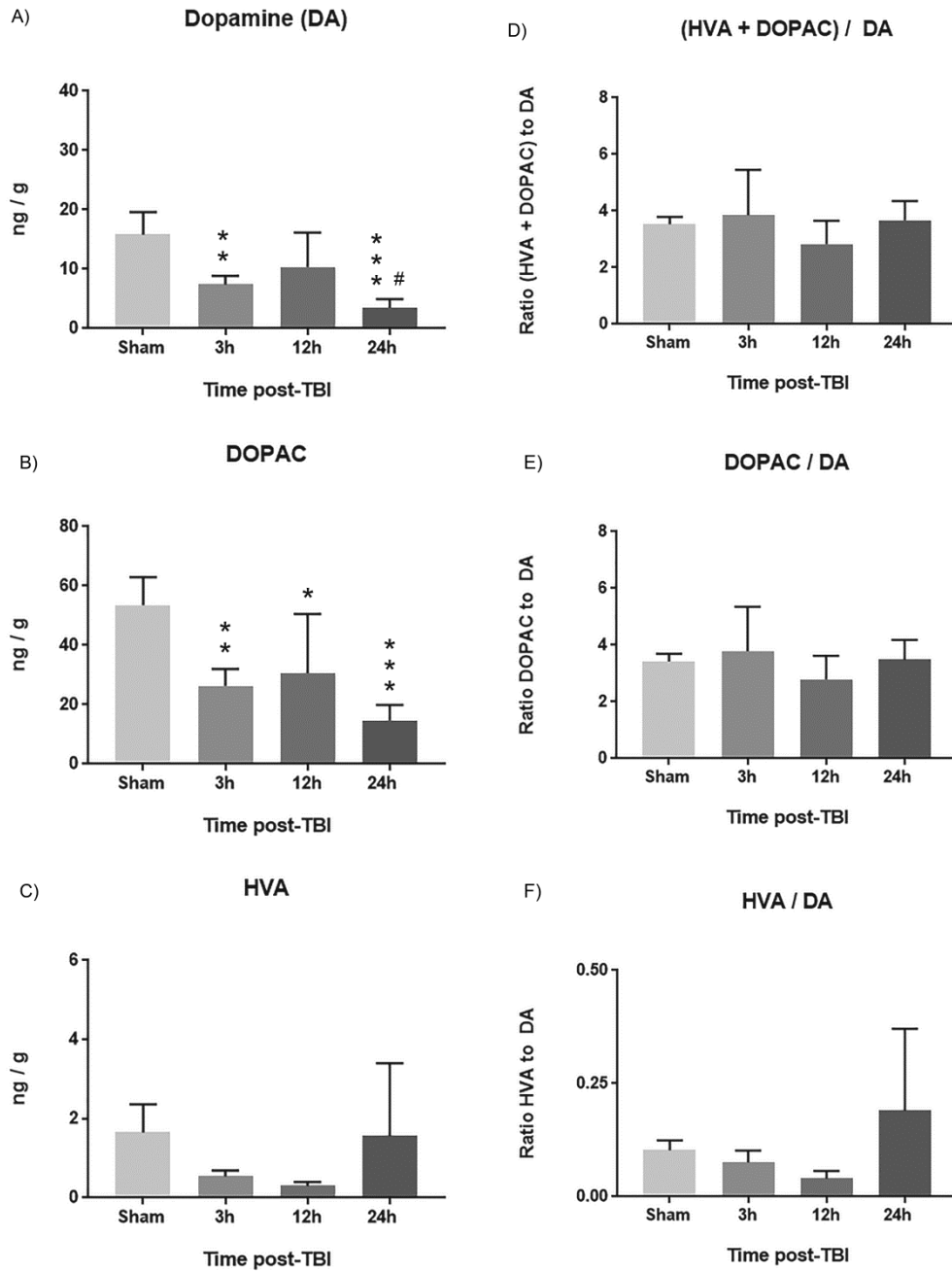


**Figure 5.8 Tissue Level (ng/g) of dopamine (DA) and metabolites in penumbral cortical tissue** measured via HPLC 3h, 12h, and 24h following severe CCI **(A)** DA, **(B)** the DA metabolite 3,4 5-dihydroxyphenylacetic acid (DOPAC), **(C)** the DA metabolite homovanillic acid (HVA), and the DA turnover ratios **(D)** (DOPAC + HVA) / DA, **(E)** DOPAC / DA, and **(F)** HVA / DA. Values = mean  $\pm$  standard deviation; one-way analysis of variance followed by Tukey *post hoc*; \* $p < 0.05$ , \*\* $p < 0.01$ , \*\*\* $p < 0.001$  compared with sham; # $p < 0.05$  compared with 12h;  $n = 3-5$  per group.

For 5-HIAA, a one-way ANOVA revealed a statistically significant effect across all groups ( $F[3,20] = 8.059$ ,  $p = 0.001$ ). However, Brown-Forsythe revealed an inequality of variance ( $p = 0.0001$ ). Therefore, Kruskal-Wallis was used in lieu of a one-way ANOVA. KW revealed a significant effect across all groups ( $H[3, n = 24] = 13.98$ ,  $p = 0.0029$ ). *Post-hoc* testing (Dunn's) revealed that compared with sham 5-HIAA (ng/g) was significantly decreased 3h ( $p < 0.01$ ) (**Fig. 5.7B**) post-injury. Thus, following CCI the 5-HT metabolite 5-HIAA is decreased at 3h.

For the ratio 5-HIAA / 5-HT, a single 3h sample was identified as an outlier (Grubb's) and excluded ( $G = 1.922$ ,  $Y = 6$ ). For the ratio 5-HIAA / 5-HT, a one-way ANOVA revealed a statistically significant effect across all groups ( $F[3,19] = 6.91$ ,  $p = 0.0025$ ). However, Brown-Forsythe revealed an inequality of variance ( $p = 0.0365$ ). Therefore, Kruskal-Wallis was used in lieu of a one-way ANOVA. KW revealed a significant effect across all groups ( $H[3, n = 23] = 11.76$ ,  $p = 0.0082$ ). *Post-hoc* testing (Dunn's) revealed that the 5-HIAA / 5-HT at 24h was significantly increased compared with sham ( $p < 0.01$ )(**Fig. 5.7C**). Thus, following CCI there is an increase in the 5-HT turnover to 5-HIAA at 24h.

Prior to statistical analysis, due to undetectable HVA levels, one animal was removed from the 3h group and two animals were removed from the 12h group for all analysis of DA and DA metabolites. Additionally, during DA statistical analysis, a sham sample ( $G = 1.908$ ,  $Y = 6$ ) and 24h sample ( $G = 2.009$ ,  $Y = 6$ ) were identified as outliers (Grubb's) and excluded. In order to maintain consistency and be able to calculate DA metabolite/DA turnover ratios, these animals were further excluded from the entire DA data set. During HVA statistical analysis, a sham sample ( $G = 1.759$ ,  $Y = 5$ ) and a 12h sample ( $G = 1.653$ ,  $Y = 4$ ) were identified as outliers (Grubb's) and excluded. In order to

maintain consistency and be able to calculate DA metabolite/DA turnover ratios, these animals were further excluded from the entire DA data set.

For DA, a one-way ANOVA revealed a statistically significant effect across all groups ( $F[3,13] = 12.01$ ,  $p = 0.0005$ ). *Post-hoc* testing (Tukey's) revealed that compared with sham DA (ng/g) was significantly decreased at 3h ( $p < 0.01$ ) and 24h ( $p < 0.001$ ) post-injury. Additionally, DA (ng/g) was significantly decreased at 24h ( $p < 0.05$ ) compared with 12h post-injury (**Fig. 5.8A**). Thus, following CCI DA is decreased at 3h and 24h.

For DOPAC, a one-way ANOVA revealed a statistically significant effect across all groups ( $F[3,13] = 11.5$ ,  $p = 0.0006$ ). *Post-hoc* testing (Tukey's) revealed that compared to sham DOPAC (ng/g) was significantly decreased at 3h ( $p < 0.01$ ), 12h ( $p < 0.05$ ), and 24h ( $p < 0.001$ ) post-injury (**Fig. 5.8B**). Thus, following CCI the DA metabolite DOPAC is decreased at 3h, 12h, and 24h.

For HVA, a one-way ANOVA did not reveal a statistically significant effect across all groups ( $F[3,13] = 1.633$ ,  $p = 0.2300$ ) (**Fig. 5.8C**). Thus, the DA metabolite HVA remains unchanged following CCI.

For the ratio (HVA + DOPAC) / DA, a single 24h sample was identified as an outlier (Grubb's) and excluded ( $G = 1.771$ ,  $Y = 5$ ). For the ratio (HVA + DOPAC) / DA, a one-way ANOVA did not reveal a statistically significant effect across all groups ( $F[3,12] = 0.6453$ ,  $p = 0.6006$ ) (**Fig 5.8D**). Thus, the turnover of DA to HVA+DOPAC remains unchanged following CCI.

For the ratio DOPAC / DA, a single 24h sample was identified as an outlier (Grubb's) and excluded ( $G = 1.754$ ,  $Y = 5$ ). For the ratio DOPAC / DA, a one-way ANOVA did not reveal a statistically significant effect across all groups ( $F[3,12] =$



0.5785,  $p = 0.6402$ ) (**Fig. 5.8E**). Thus, the turnover of DA to DOPAC remains unchanged following CCI.

For the ratio HVA / DA, a single 24h sample was identified as an outlier (Grubb's) and excluded ( $G = 1.768$ ,  $Y = 5$ ). For the ratio HVA / DA, a one-way ANOVA did not reveal a statistically significant effect across all groups. ( $F[3,12] = 1.1782$ ,  $p = 0.2040$ ) (**Fig. 5.8F**). Thus, the turnover of DA to HVA remains unchanged following CCI.

### **Percent Weight Loss in Uninjured Rats Following PG, PZ, or HZ Administration (HPLC Experiments) (Fig. 5.9)**

For the 72h triple dose HPLC monoamine and metabolite uninjured cortical tissue experiment a final weight for animals was taken at time 48h following intraperitoneal administration of saline, PG, PZ, or PG at time 0h and 24h for a total to two injections (**Fig. 4.3**). Animals were not weighed at the time of euthanasia (72h) and therefore had not received the third/final injection (48h) at the time of final weigh-in. For percent weight loss in uninjured rats between D0 (before first injection) and D2 (after second injection), a one-way ANOVA revealed a statistically significant effect across all groups ( $F[3, 20] = 5.157$ ,  $p = 0.0084$ ). *Post-hoc* testing (Tukey's) revealed that compared to the saline group ( $p < 0.01$ ) and the PG group ( $p < 0.05$ ), PZ lost a significant amount of weight.

Thus indicating that intraperitoneal administration of PZ (15mg/kg) at 0h and 24h leads to significant weight loss at 48h in uninjured animals.

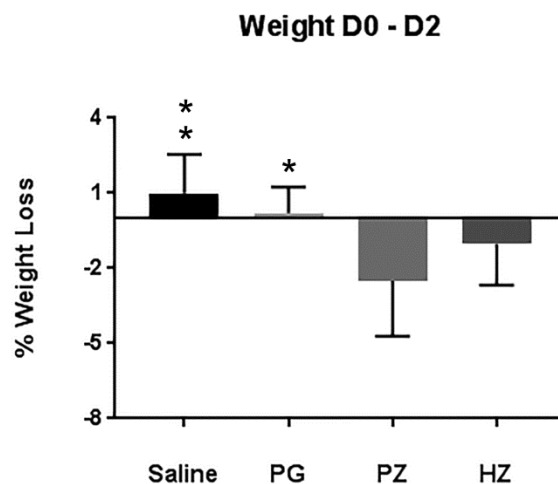


**Figure 5.9 Percent weight loss in uninjured animals for 72h HPLC experiment.** Percent weight loss in uninjured rats between D0 (before first injection) and D2 (after second injection). Animals were not weighed following third/final injection prior to euthanasia. Values mean  $\pm$  standard deviation; one-way analysis of variance followed by Tukey *post hoc*; \* $p < 0.05$ , \*\*  $p < 0.01$  compared with PZ; Saline, PG = pargyline, PZ = phenelzine, HZ = hydralazine;  $n = 6$  per group.

## Discussion and Conclusion

### **24h Single Dose PG, PZ, or HZ: HPLC Monoamine and Metabolite Tissue Levels and Turnover Ratios in Uninjured Cortical Tissue**

Overall these results indicate that 24h following a single intraperitoneal injection of the MAOIs PG (15mg/kg) and PZ (15mg/kg) there is significant MAO inhibition in uninjured cortical tissue as evidenced by the significant decrease in both 5-HT turnover (**Fig 5.4C**) and DA turnover (**Fig 5.5D-F**), as well as the significant increase in the tissue level of the MAO substrate NE (**Fig 5.3**). Additionally, the non-MAO HZ (5 mg/kg) also led to a significant decrease in DA turnover (**Fig. 5.5D-F**), likely due to a MAO effect as the significant decrease in DA turnover is seen in the ratios that contain the MAO product DOPAC (**Fig. 5.5D-E**). Interestingly, this is different than what was seen following the triple dosing HPLC experiments (**Fig. 4.3**), in which HZ led to a significant decrease in 5-HT turnover (**Fig. 4.6C**). However, it is likely still explained by the fact that HZ has previously been demonstrated to have reversible MAO inhibitory effects with a preference toward MAO-A [269]. As stated previously, NE and 5-HT are selectively metabolized by MAO, and although DA can be metabolized by either MAO isoform, the majority of DA in rats is metabolized by MAO-A [186].

There are several other important differences found between the single and triple dosing paradigms in regard to monoamine and metabolite tissue levels. First, continuing with DA, the 24h single injection dosing paradigm (**Fig 5.1**) led to a significant increase in DA tissue level (**Fig 5.5A**), whereas the 72h triple injection dosing paradigm (**Fig. 4.7A**) did not, despite having a significant effect on DA turnover (**Fig. 4.7D-F**). It is unknown why this is, but as stated previously, the results obtained in **Fig. 4.7A** may be

due to some type of compensatory effect [349], which was not affected by the single dose administrations (**Fig 5.5A**).

Further, although direct statistical comparisons were not done, three doses of PZ or PG (**Fig 4.3**) caused more monoamine oxidase inhibition than single doses (**Fig. 5.1**). For example, in regards to NE a single dose of PG or PZ led to a mean ( $\pm$  standard deviation) tissue level (ng/g) of  $852.90 \pm 57.23$  and  $980.10 \pm 186.30$ , respectively, whereas three doses of PG or PZ led to a mean ( $\pm$  standard deviation) tissue level (ng/g) of  $940.2 \pm 90.58$  and  $1155 \pm 242.9$ , respectively. In regards to 5-HT, a single dose of PG or PZ led to a mean ( $\pm$  standard deviation) tissue level (ng/g) of  $394.10 \pm 87.92$  and  $580.60 \pm 69.98$ , respectively, whereas three doses of PG or PZ led to a mean tissue level of  $499.20 \pm 49.01$  and  $855.00 \pm 180.00$ , respectively. In regards to 5-HT turnover, a single dose of PG or PZ led to a mean ( $\pm$  standard deviation) turnover ratio of  $0.57 \pm 0.18$  and  $0.34 \pm 0.08$ , respectively, whereas three doses of PG or PZ led to a mean ( $\pm$  standard deviation) turnover ratio of  $0.28 \pm 0.03$  and  $0.13 \pm 0.04$ , respectively. Further, this effect is most evidenced in the (DOPAC + HVA) / DA turnover ratios in which a single dose of PG or PZ led to a mean ( $\pm$  standard deviation) turnover ratio of  $0.54 \pm 0.29$  and  $0.39 \pm 0.16$ , respectively, whereas three doses of PG or PZ led to a mean ( $\pm$  standard deviation) turnover ratio of  $0.053 \pm 0.013$  and  $0.035 \pm 0.002$ , respectively. In fact, the change in DA turnover ratios were so great between the single and triple dosing paradigms that the scale of the x-axis in the triple dosing paradigm (**Fig. 4.7D-F**) had to be decreased by a factor of 4 from the scale of the x-axis for the single dosing paradigm (**Fig. 5.5D-F**). However, it should be noted that this was also true for the saline and HZ groups as well (**Fig. 4.7 and Fig. 5.5**). Therefore, it is possible that the very large change in DA turnover seen between the single dosing paradigm (**Fig. 4.7D-F**) and triple dosing paradigm (**Fig. 4.7D-F**) may be due to a technical or collection issue between

HPLC experiments or due to the total number of injections given (1 vs 3), as stress has been shown to increase endogenous inhibition of monoamine oxidase [379]. However, the latter may not be the case because the effect of saline on NE (**Fig. 4.5 and Fig. 5.3**) and 5-HT (**Fig. 4.6 and Fig. 5.4**) do not widely differ between the single and triple dosing paradigms.

### **CCI Time Course HPLC Monoamine and Metabolite Tissue Levels and Turnover Ratios in Penumbra Cortical Tissue**

As discussed in “*Chapter Four*” the PZ dosing paradigm utilized in the current study had previously been shown to be not only safe but beneficial in non-CCI models such as SCI and ischemic-reperfusion injury [74, 76]. However, as shown in “*Chapter Four*”, for the current study the PZ dosing paradigm utilized was not only unable to improve reference memory (**Fig. 4.10**) or cortical tissue sparing (**Fig. 4.12**), but it also led to significant weight loss (**Fig. 4.11**), qualitative behavioral concerns, and PZ animals were unable to make significant improvements during the MWM acquisition phase (**Fig. 4.8**). One possible explanation for these findings is that after severe CCI monoamine levels are significantly elevated or monoamine oxidase is significantly inhibited, and that administration of PZ after injury, particularly multiple doses of PZ, is exacerbating these effects, leading to negative consequences. Therefore, we hypothesized that over the first 24h following CCI monoamine tissue levels would be significantly elevated and monoamine turnover ratios would be significantly decreased.

However, the results indicate the contrary. In fact, at 3h and 24h after severe CCI the monoamines NE (**Fig. 5.6**), 5-HT (**Fig. 5.7A**), and DA (**Fig. 5.8A**), are significantly decreased compared with sham. Interestingly, there was not a significant difference in any of the neurotransmitter tissue levels between sham and the 12h post-CCI time point.

This is similar to other post-CCI processes such as mitochondrial dysfunction which increase 3h after CCI before recovering and then beginning to decline again at 24h [73]. However, it should be noted that all sham tissue was collected at the midway time point of 12h (**Fig. 5.2**). It is therefore possible that technical or tissue collection issues could have also influenced these results.

In regards to monoamine turnover (i.e. MAO inhibition), the only significant change from sham was seen at 24h in which there was an increase in 5-HT turnover to 5-HIAA (**Fig. 5.7C**). However, as both a significant decrease in tissue level of 5-HT (**Fig. 5.7A**) and a non-significant decrease in tissue level of the 5-HT metabolite, 5-HIAA (**Fig. 5.7B**) were also seen at this time point the increase in the 5-HIAA / 5-HT ratio is likely due to the larger of the two decreases being seen in the denominator (5-HT). Although it is possible the significant increase seen in the 5-HIAA / 5-HT ratio 24h post-CCI is in fact due to an decrease in MAO inhibition, the more likely explanation is that due to injury 5-HT has been depleted or serotonergic neurons have degenerated in the penumbral area analyzed, whereas the metabolite 5-HIAA has not been removed to a such a degree. Additionally, it should be noted that 5-HT may come from other sources, such as platelet activation. However, platelets only contain MAO-B [380], whereas MAO-A selectively metabolizes 5-HT [186], so platelets should not be a large source of the 5-HT metabolite 5-HIAA.

Although our data did not indicate any CCI-induced monoamine elevations, it should be noted that this study was limited to analysis of the penumbral tissue directly lateral to the epicenter of injury. It is possible that other brain regions would have shown increases either in monoamine tissue levels or MAO inhibition as previous studies have demonstrated that tissue levels of monoamines vary after experimental TBI depending region [154, 173, 174, 178, 182, 363-365]. It is also possible that increases in tissue

levels of monoamines or MAO inhibition occur at later time points still relevant to our CCI + drug studies (**Fig. 4.4**), such as 48h-72h post-CCI. However, we forewent conducting experiments at these later time points based upon the results obtained over the first 24h (**Fig. 5.6-5.8**).

#### **Percent Weight Loss in Uninjured Rats Following PG, PZ, or HZ Administration (HPLC Experiments)**

Overall the results indicate that in uninjured animals two doses of PZ led to a significant amount of weight loss compared with both saline and PG. Although HZ also led to weight loss, it was not significant (**Fig. 5.9**). This is similar to what was seen in CCI, in which three doses of PZ led to a significant amount of weight loss following MWM compared with all other groups including sham, vehicle (saline), PG and HZ (**Fig. 4.11**). As stated previously in regard to PZ it is possible that the weight loss seen in the current experiment was due to an increase in monoamine levels (**Fig. 4.5 and 4.6A**), as monoamines are capable of inducing weight loss through a variety of mechanisms [350], an effect which has been previously seen with non-PZ MAOIs [158, 351]. However, as weight loss was not observed in the other MAOI group, PG, it is possible that PZ causes weight loss through another mechanism, such as formation of the metabolite, phenethylamine (PEA) [189], itself an MAO substrate with amphetamine-like stimulatory effects [207].

## **CHAPTER SIX:**

### **Final Discussion and Concluding Remarks**

#### **Summary of Results and Conclusions**

TBI represents a significant health crisis in the United States and worldwide. However, currently there are no FDA-approved pharmacological agents capable of attenuating the devastating neurologic consequences that occur after TBI [1]. As central mediators of the TBI secondary injury cascade, mitochondria and LP-derived neurotoxic aldehydes, such as 4-HNE and acrolein, make promising therapeutic targets (**Fig 1.2**). In fact, CsA, an FDA-approved immunosuppressant capable of inhibiting the mPTP has been shown to be neuroprotective in experimental TBI [110, 122-124, 135, 136, 223-227]. Additionally, PZ, an FDA-approved non-selective irreversible MAOI-class antidepressant has also been shown to be neuroprotective in experimental TBI due to the presence of a hydrazine (-NH-NH<sub>2</sub>) moiety allowing for the scavenging of LP-derived neurotoxic aldehydes [71, 72, 334].

Due to the complex pathophysiology that occurs following TBI it is imperative that robust neuroprotective drugs be developed. It is possible that robust neuroprotection could be achieved through effective targeting of vulnerable mitochondrial subpopulations, such as synaptic mitochondria, the combining of two partially neuroprotective drugs, or through use of single agents which have dually protective mechanisms of action. Therefore, the overall goal of this dissertation was to further examine the neuroprotective efficacy of the mPTP inhibitor CsA and the LP-derived neurotoxic aldehyde scavenger PZ using a severe CCI model in 3-month old male Sprague-Dawley rats. Specifically, we evaluate 1) the protective effects of CsA on isolated synaptic and non-synaptic mitochondria, 2) the ability of a novel 72h



subcutaneous continuous infusion of PZ combined with CsA to improve mitochondrial respiration, attenuate mitochondria-aldehyde conjugate formation, and prevent cytoskeletal spectrin degradation compared to monotherapy, and 3) the effects of PZ (MAOI, aldehyde scavenger) on learning and memory and cortical tissue sparing following CCI compared to the effects of PG (MAOI, non-aldehyde scavenger) and HZ (non-MAOI, aldehyde scavenger).

### **Synaptic Mitochondria Sustain More Damage than Non-Synaptic Mitochondria after Traumatic Brain Injury and are Protected by Cyclosporine A**

In order to test the hypothesis that CsA has a differential protective effect on isolated synaptic and non-synaptic mitochondrial bioenergetics following experimental TBI, 3mo male Sprague-Dawley rats were administered an intraperitoneal dose of CsA (20mg/kg) 15min after a severe controlled cortical impact injury (2.2mm), cortical synaptic and non-synaptic mitochondria were isolated 24h post-CCI, and respiratory rates were measured using a Clark-type oxygen electrode.

Results indicate that 24h after severe CCI synaptic mitochondria are more damaged than non-synaptic mitochondria, particularly in regard to RCR (**Fig. 2.4**). In fact, statistical analysis revealed a significant interaction between injury and population for this measure, indicating that synaptic mitochondria are indeed more susceptible to injury. There are several possibilities for why synaptic mitochondria are more vulnerable to injury than non-synaptic mitochondria, including increased susceptibility to calcium-induced permeability transition due to high cyclophilin D content [38], increased exposure to oxidative damage [37, 38], and decreased respiratory chain activity and subunit content [296]. Further, non-synaptic mitochondria can tolerate larger impairments to respiratory complex activity before ATP production is significantly

decreased [35]. Impressively, these results also indicate that the more significantly damaged synaptic mitochondria are protected by intraperitoneal administration of CsA (20mg/kg) 15min post-CCI (**Fig. 2.1 – 2.6**). In fact, significant protection is achieved for respiratory states II (**Fig. 2.1**), III (**Fig. 2.2**), V(II) (**Fig. 2.6**), and the RCR (**Fig. 2.4**). Additionally, CsA improved non-synaptic respiration (**Fig. 2.1 – 2.6**). However, the improvements were non-significant likely due to the fact non-synaptic mitochondria are less severely damaged 24h after severe CCI (**Fig. 2.4**) [322].

This was the first study to investigate the effects of CsA on isolated and purified synaptic and non-synaptic mitochondria after experimental TBI and the results are important for several reasons. First, synaptic mitochondria represent a more purely neuronal population [37-39], have been implicated in neuronal and synaptic degeneration absent overt cell death [37, 48, 49], and are essential for proper neurotransmission and synaptic plasticity [44-46]. Therefore, it is critically important that synaptic mitochondrial function be protected after TBI. Yet, synaptic mitochondria are more vulnerable to damage after experimental TBI [41, 322] and previous studies in SCI have demonstrated that synaptic mitochondria often respond less favorably to pharmaceutical intervention than their non-synaptic counterparts [50]. As such, the ability of a previously optimized CsA dose [225, 294] to significantly protect the more vulnerable synaptic mitochondria population after experimental TBI, despite high cyclophilin D concentrations (i.e. CsA binding partner) [37], strengthens the growing body of evidence that CsA is protective in TBI and that its clinical translation should be pursued.

In fact, several clinical trials have shown that CsA is safe for use in patients with severe TBI with a trend toward improved outcomes [234, 235]. Unfortunately, due a biphasic dose-response curve [227] and concerns over the toxicity of cremophor, the

vehicle in which the currently available commercial preparation of CsA (Sandimmune®) is provided, [381, 382], larger CsA clinical trials have not been conducted. Although concerns over cremophor toxicity may be overblown and limited to chronic or *in-vitro* administrations [300-302], recently a novel cremophor-free lipid emulsion CsA preparation (NeuroSTAT®) was shown to be neuroprotective in a porcine model of TBI [381] as well to be bioequivalent to Sandimmune®. Therefore, future clinical trials investigating the neuroprotective effects of the non-cremophor CsA preparation NeuroSTAT® are planned [383].

As future clinical trials investigating the neuroprotective effects of CsA in TBI are likely to use non-cremophor preparations of CsA, the use of cremophor-CsA in the current study does represent a limitation and future experimental TBI studies of CsA may want to consider alternately using non-cremophor CsA. This study was additionally limited by several other factors such as the inability to further separate non-synaptic mitochondria into neuronal and non-neuronal cell types. Previous studies have demonstrated that mitochondria isolated from cultured neurons and glia have differing properties [38, 296]. Therefore, it is likely that in regards to synaptic mitochondria, the results of this study were influenced both by cell type (neuronal) and subcellular location (pre-synaptic). As techniques to isolate mitochondria from various cell types improve, future studies could offer insight into the differential properties of synaptic neuronal vs non-synaptic neuronal vs non-neuronal mitochondrial populations following experimental TBI, as well as their response to CsA. Additionally, this study was limited to one outcome measure (i.e. respiration), time point (i.e. 24h post-CCI), and dosing paradigm (20mg/kg CsA i.p. 15min post-CCI). Utilization of additional outcome measures such as calcium buffering capacity, enzyme activity, or formation of aldehyde-mitochondrial conjugates could have offered more specific insight into the differential effects of CCI and CsA on

synaptic and non-synaptic mitochondrial function. Further, evaluation of synaptic and non-synaptic mitochondrial function at a later time point, such as 48h, in which non-synaptic mitochondria have sustained further damaged [322], may have shown CsA to have an enhanced protective effect on the non-synaptic mitochondrial population. Last, delaying CsA administration beyond 15min post-CCI may have revealed that synaptic and non-synaptic mitochondria have different therapeutic windows, an effect which has been previously seen in SCI [50], and one which may explain the finding that although CsA remains neuroprotective when administration is delayed 8h, it is most effective when administered within 3h of TBI [122].

### **Continuous Infusion of Phenezine, Cyclosporine A, or Their Combination: Evaluation of Mitochondrial Bioenergetics, Oxidative Damage, and Cytoskeletal Degradation Following Severe Controlled Cortical Impact Traumatic Brain Injury in Rats**

To date all monotherapy clinical trials for TBI have failed [1]. Based upon the complex secondary injury cascade that occurs following TBI combinational therapies may offer more complete neuroprotection after injury than single agent therapies [213]. Therefore, the purpose of this study was to test the hypothesis that a 72h subcutaneous continuous infusion of PZ combined with CsA would improve mitochondrial respiration, attenuate formation of LP-derived aldehyde mitochondrial protein conjugates, and maintain cytoskeletal integrity following experimental TBI to a greater degree than monotherapy. Following a severe controlled cortical impact injury (2.2mm) in 3mo male Sprague-Dawley rats, subcutaneous osmotic pumps containing PZ (10mg/kg/day/3d), CsA (10mg/kg/day/3d), or PZ + CsA were implanted. Animals also received loading doses of PZ (10mg/kg s.c.), CsA (20mg/kg i.p.), or PZ + CsA 15min post-CCI (**Table 3.1**). At 72h post-injury cortical mitochondria (total) respiratory rates were assessed

using a Clark-type oxygen electrode and cortical mitochondria (total) bound 4-HNE and acrolein were assessed using Western blot. Additionally, Western blot was used to assess cortical tissue for 145kD (calpain-only) and 150kD (calpain/caspase 3)  $\alpha$ -spectrin breakdown as a marker for cytoskeletal integrity. Further, Western blot of spectrin breakdown products was used to compare a 72h subcutaneous continuous infusion PZ dosing paradigm to a dosing paradigm in which bolus PZ doses were administered every 12h over the first 72h following CCI (**Table 3.2**).

Our results (**Table 3.3**) indicate that a 72h subcutaneous continuous infusion of PZ (10 mg/kg subcutaneous loading dose 15 min post-injury + 10 mg/kg/day subcutaneous infusion of PZ for 3 days) maintained mitochondrial RCR and cytoskeletal integrity, and decreased binding of 4-HNE and acrolein to mitochondrial proteins 72h following severe CCI. In fact, continuous infusion of PZ was able to maintain cytoskeletal integrity, whereas 12hr intermittent dosing of PZ was not (10 mg/kg PZ subcutaneous loading dose 15 min post-injury + 5 mg/kg PZ subcutaneous maintenance bolus every 12h up to and including 60h) was not. Additionally, continuous infusion of CsA (20 mg/kg CsA intraperitoneal loading dose 15 min post-injury + 10 mg/kg/day subcutaneous infusion of CsA for 3 days) decreased binding of 4-HNE and acrolein to mitochondrial proteins. Although the combination of PZ + CsA was able to maintain cytoskeletal integrity, it did so to a similar degree as PZ alone, suggestive of a purely PZ effect, and was unable to attenuate other outcome measures. In fact, once combined the protective effect PZ and CsA individually had on formation of mitochondrial bound 4-HNE and acrolein was lost.

Although enhanced protection was not seen with the combination PZ + CsA and the protection that was seen with each individual therapy was limited, it should be noted that this study had several limitations. First, only one dosing paradigm was investigated.

This study was designed to combine an optimized CsA dosing paradigm [122] with a PZ dosing paradigm previously demonstrated to be neuroprotective in experimental TBI [72]. However, the results were similar to previous combinational therapy studies in which utilization of drug doses optimized for monotherapy did not result in enhanced protection once combined [280]. A better approach likely would have been to either combine sub-therapeutic doses of PZ and CsA or to conduct a dose-response of the combined therapy.

Second, the study was limited to one time point (i.e. 72h post-CCI) and only a few biochemical outcome measures (i.e. total mitochondrial respiration, mitochondria-aldehyde conjugate formation, spectrin degradation). It is possible that a greater degree of neuroprotection was achieved with the dosing paradigms utilized, but that such neuroprotection was not seen in the specific outcome measures evaluated. For example, as the CsA dosing paradigm utilized has previously been shown to improve cortical tissue sparing [225, 294], it is possible that the same dosing paradigm did have a protective effect on mitochondrial respiration, but that the effect was masked in the total mitochondrial preparations (synaptic and non-synaptic mitochondria) because CsA has a greater effect on synaptic mitochondria than non-synaptic mitochondria (**Fig. 2.1 – 2.6**) [309], but at 72h post-injury synaptic mitochondria make up a minority of the mitochondrial population [121, 128, 321]. On the other hand, the inability of CsA to improve mitochondrial respiration makes sense physiologically as CsA inhibition of the mPTP allows mitochondria to sequester calcium, causing the mitochondrial membrane potential to decrease and respiration to slow. Although neither of these scenarios may be the case, as continuous infusion of CsA was also unable to prevent cytoskeletal  $\alpha$ -spectrin degradation (**Fig. 3.5**). However, it should be noted that pharmacologic-dependent neurologic improvements have been documented absent attenuation of

spectrin degradation [132]. Further, based upon the preponderance of studies demonstrating CsA to be protective in experimental TBI, including its effects on synaptic mitochondria (**Fig. 2.1 – 2.6**) [309], we do not believe the absence of protective effects seen here preclude its future development as a translational therapy for TBI.

Similar to CsA, it is possible that the mitochondria isolation technique utilized has also masked PZ protective effects to individual states of mitochondria respiration. For example, PZ binds mitochondrial aldehyde-protein conjugates [79, 262], but it is unknown what effect this has on post-injury mitochondrial dynamics, such as fission, fusion and mitophagy. It is possible that binding of PZ to mitochondria which are beyond saving is preventing these mitochondria from being degraded by normal post-injury processes and at the same time significantly improving the bioenergetics of the less damaged mitochondria. The unusual presence of these considerably damaged mitochondria in the mitochondria preps could mask improvements to individual states of mitochondrial respiration. Additionally in that regard, if aldehyde-scavengers are going to be pursued as therapeutic agents for TBI it will be important for future studies to investigate their effects on post-injury homeostatic mechanisms such as mitochondrial dynamics, mitophagy, and protein degradation. Also of note is the possibility that the significant decrease seen in aldehyde-mitochondrial conjugates following PZ administration (**Fig. 3.4**) is due to the inability of the 4-HNE and acrolein antibodies to recognize ternary drug-aldehyde-protein complexes. However, this is likely not the case as the continuous PZ dosing paradigm did demonstrate partial protective effects as evidence by the maintenance of RCR (**Fig. 3.3**) and cytoskeletal integrity (**Fig. 3.5**).

Additionally, this study may have been complicated by the choice of drug combination. For example, CsA and PZ both physically bind mitochondria [79, 218, 258], which may have resulted in too many non-physiologic interactions for mitochondria,

particularly damaged mitochondria, to handle (**Fig. 3.9**). Additionally, CsA has a biphasic dose-response curve [294] and is metabolized by cyp3A4 [246], an enzyme which can be inhibited by PZ [266, 267]. In fact, although CsA has been previously identified as a good candidate for combination drug therapies [213], because it is metabolized by cyp3A4 [246], has a biphasic dose-response curve [294], and is a calcineurin inhibiting immunosuppressant [316], the number and types of drugs it could be safely combined with may be severely limited. In fact, a previous experimental TBI study which combined CsA with the antibiotic minocycline resulted in a 100% lethality rate [215, 283]. Therefore, clinical translation of CsA for use in TBI may hold the most promise if its use is restricted to that of a monotherapy agent. Similarly, given the complicated pharmacokinetics of PZ, an irreversible MAOI and MAO substrate, with several active metabolites [169, 189], PZ also may not represent the optimal choice for combinational drug therapy.

However, several combinational therapy experimental designs do exist that avoid the above complications. First, two drugs that are mechanistically complementary but spatially distinct could be combined. For example, a blood brain barrier penetrable drug could be combined with tirilazad, as tirilazad's primary effects are localized to the vasculature [1, 256]. Second, although the use of FDA-approved drugs such as CsA and PZ potentially makes clinical translation for TBI easier, faster, and cheaper than the use of experimental agents, combining drugs with less complicated mechanisms of action, such as the non-immunosuppressive mPTP inhibitor, NIM811, or a pure aldehyde-scavenger, may limit confounding factors and offer a more straightforward approach. Finally, a drug could be combined with a non-pharmacological therapy such as stem cell administration or environmental enrichment. In fact, such pharmacologic + non-



pharmacologic combinational designs seem to have a higher success rate than purely pharmacologic combinational approaches [215, 280].

### **Comparative Effects of Phenelzine, Hydralazine, and Pargyline on Learning and Memory and Cortical Tissue Sparing Following Experimental Traumatic Brain Injury**

Several studies have indicated that PZ can offer protection in experimental brain injury [71, 72, 76, 333, 334]. However, in order for PZ to be further developed for use in clinical TBI, the effect its MAOI properties have on TBI pathophysiology must be considered. Therefore, this study was designed to test the hypothesis that PZ, a LP-derived neurotoxic aldehyde scavenger and MAOI, and hydralazine (HZ), an LP-derived neurotoxic aldehyde scavenger non-MAOI would improve cognitive function and cortical tissue sparing following experimental TBI, whereas pargyline (PG), a MAOI non-aldehyde scavenger would not. Following severe controlled cortical impact injury (2.0mm), 3mo male Sprague-Dawley rats received an intraperitoneal dose of PZ (15mg/kg), HZ (5mg/kg), or PG (15mg/kg) at 15min, 24h, and 48h following injury. Morris water maze testing was conducted on day 3 – day 7 post-CCI and cortical tissue sparing was analyzed on post-CCI day 8. Additionally, the effects of the PZ, HZ, and PG dosing paradigms on tissue levels of monoamines and metabolites were evaluated via HPLC in uninjured cortical tissue as a surrogate marker of MAO inhibition.

This was not only the first study to evaluate the effects of PG and HZ in experimental TBI, but it was also the first study to assess the behavioral effects of PZ in experimental TBI. Contrary to the hypothesis, the results indicate that PZ (15mg/kg, MAOI, aldehyde scavenger) and HZ (5mg/kg, non-MAOI, aldehyde scavenger), as well as PG (15mg/kg, MAOI, non-aldehyde scavenger), were unable to attenuate reference

memory deficits (D7 post-CCI) (**Fig. 4.10**) or improve cortical tissue sparing (D8 post-CCI) (**Fig. 4.12**) when administered intraperitoneal 15min, 24h, and 48h after a severe CCI (2.0mm) in 3mo male Sprague-Dawley rats. However, although non-significant, HZ led to the most improvement to cortical tissue sparing (**Table 4.1**). Of concern, following CCI PZ animals lost a significant amount of weight (**Fig. 4.11**), and their MWM acquisition performance did not significantly improve across time (D3-6 post-CCI), possibly indicating deficits to working memory, (**Fig. 4.8**), and perhaps being caused by PZ-induced high monoamine tissue levels as was seen in uninjured cortical tissue (i.e. NE, 5-HT) utilizing the same PZ dosing paradigm (**Fig. 4.5 – 4.7**). Similarly, qualitative behaviors observed in the PZ group following CCI may have also been suggestive of elevated monoamine levels. However, the effects of excessive aldehyde scavenging or other PZ mechanisms of actions, such as inhibition of GABA-T or formation of PEA, cannot be ruled out as factors effecting outcome.

There are several possible reasons for why, contrary to the original hypothesis, the hydrazine (-NH-NH<sub>2</sub>) containing aldehyde scavengers PZ and HZ were unable to provide significant protection in the current study. In regards to PZ, it is possible that at higher doses additional PZ mechanisms of action (MAO inhibition, GABA-T inhibition, PEA formation, etc.) or excessive aldehyde scavenging are detrimental and negate protective effects. It does seem that in the context of experimental TBI, lower doses of PZ may be more protective as they have been shown to improve cortical tissue sparing [71] and individual states of mitochondrial respiration [334], whereas higher PZ doses do not (**Fig. 3.2 and Fig. 4.12**) [333]. However, this dose effect may also be outcome specific as continuous infusion of PZ is able to maintain cytoskeletal integrity better than bolus dosing (**Table 3.4**) [333, 334]. Although a different PZ dosing paradigm may have resulted in better outcomes, inclusion of additional experiments, such as HPLC analysis

of CCI + PZ tissue, measurement of GABA levels, and additional quantitative behavioral testing may also have led to a greater understanding of the effects PZ's non-aldehyde scavenging mechanisms of action are having after TBI. Additionally, although a PG concentration equal to that of PZ was utilized as an extension of previous *ex-vivo* studies [72], because equal concentrations of PG and PZ are not necessarily pharmacologically equivalent, specifically in regards to MAO inhibition [189], choosing an alternate PG dosing concentration or a different MAOI for comparison to PZ may have led to a better understanding of MAO effects on TBI pathophysiology.

Similarly, in regards to HZ, as this was the first study to evaluate HZ in experimental TBI, it is possible than an alternate dosing paradigm would have led to different results. It may be that the HZ dosing paradigm utilized was too low to achieve significant aldehyde scavenging and protective effects. Alternately, it is possible that as an anti-hypertensive [268], the concentration of HZ utilized induced hypotension and negated any protective effects. Admittedly, this study would have been strengthened by the inclusion of blood pressure measurements after drug administration.

On the other hand, it is possible that the PZ and HZ dosing paradigms utilized can provide protection, but that such protection was not observed in the single early behavioral task or in the single histological method analyzed. It is possible that delay of behavioral analysis, use of alternative behavioral tasks, or inclusion of additional histological methods may have yielded different results.

Although it is unfortunate that the hydrazine (-NH-NH<sub>2</sub>) containing aldehyde scavengers, PZ and HZ, were unable to provide significant protection in the current study, both have shown extensive promise as neuroprotective agents in previous experimental studies of CNS injury [71, 72, 74-76, 333, 334, 361, 362]. Therefore,

aldehyde scavengers likely still offer a valid approach to neuroprotection after TBI and their development should continue to be pursued. However, based upon the results obtained in the current study, the PZ dosing paradigm has clearly not been optimized. Although the limitations of the current study make it impossible to say for sure if the effects of PZs MAOI mechanism of action are detrimental following TBI, the weight loss (**Fig. 4.11**), MWM acquisition performance (**Fig. 4.8**), qualitative behavioral observations, and uninjured HPLC data (**Fig. 4.5 – 4.7**) are concerning and suggestive of an MAOI effect. These observations, combined with the knowledge that MAOIs can lower seizure threshold [265], PZ is both an irreversible MAO inhibitor and substrate with complicated pharmacokinetics and several active metabolites [189], may make clinical translation of PZ for use in human TBI difficult even if dosing paradigms are optimized in experimental rodent models. Similarly, HZ's antihypertensive properties may limit its clinical translation. Therefore, if hydrazine (-NH-NH<sub>2</sub>) containing aldehyde scavengers are going to be further pursued as neuroprotective agents for TBI, it may be beneficial for future studies to develop hydrazine (-NH-NH<sub>2</sub>) compounds which lack confounding off target mechanisms of action.

Further, it is interesting that the PZ dosing paradigm utilized in the current study was not only unable to provide protection but also resulted in significant weight loss (**Fig. 4.11**) and negative behavioral effects (**Fig. 4.8, qualitative observation**), whereas similar dosing paradigms were safe and beneficial in other models of CNS injury such as SCI and ischemic-reperfusion [74-76]. One hypothesis for this is that PZ exacerbated severe CCI-induced monoamine elevations or monoamine oxidase inhibition. Although HPLC analysis of penumbral tissue did not show elevated monoamine levels post-CCI (**Fig. 5.6 – 5.8**), previous studies have found elevated monoamine levels after TBI depending on time point and brain region [154, 173, 174, 178, 182, 363-365]. However,

there is a dearth of information regarding the monoaminergic system acutely after TBI. Additionally, despite the central role mitochondria have in TBI and the known damage to mitochondrial function that occurs after TBI, little is known about the function of the mitochondrial enzyme, MAO, following injury. In fact, in general, controversy exists as to whether monoamines and monoamine oxidase inhibition are neuroprotective or toxic [154, 170, 181, 193, 194]. Therefore, such topics may be interesting areas of investigation for future TBI studies to pursue.

## **APPENDIX: Abbreviations**

2-propenal: acrolein

2,4-DNP: 2,4-dinitrophenol

3-HPMA: N-acetyl-S-3-hydroxypropylcysteine

3-MP: 3-aminopropanal

3-MT: 3-methoxytyramine

3-NT: 3-nitrotyrosine

4-HNE: 4-hydroxynonenal

5-HIAA: 5-hydroxyindolacetic acid

5-HT: 5-hydroxytryptamine (i.e. serotonin)

ADP: adenosine diphosphate

AIF: apoptosis inducing factor

ALA-T: alanine transaminase

ALDH: aldehyde dehydrogenase

ANT: adenine nucleotide translocase

ANOVA: analysis of variance

APP: amyloid precursor protein

ARE: antioxidant responsive element

ATP: adenosine triphosphate

CCI: controlled cortical impact traumatic brain injury

CHI: closed head traumatic brain injury

CMIA: continuous multiple trial inhibitory avoidance task

CNS: central nervous system

CO<sub>2</sub>: carbon dioxide

CO<sup>\*-</sup><sub>3</sub>: carbonate radical

COMT: catechol-O-methyl transferase

CsA: cyclosporine A

CSF: cerebral spinal fluid

CT: computerized tomography

CyD: cyclophilin D

DA: dopamine

DHBA: dihydroxybenzylamine

DOPAC: 3,4-dihydroxyphenylacetic acid

eNOS: endothelial nitric oxide synthase

EPI: epinephrine

ER: endoplasmic reticulum

ETC: electron transport chain

FAD<sup>+</sup> / FADH<sub>2</sub>: flavin adenine dinucleotide

FCCP: carbonyl cyanide-p-trifluoromethoxyphenylhydrazone

FDA: Federal Drug Administration

Fe<sup>2+</sup>: ferrous iron

Fe<sup>3+</sup>: ferric iron

FPI: fluid percussion traumatic brain injury

GABA: gamma-aminobutyric acid

GABA-T: GABA transaminase

GCEE: gamma-glutamylcysteine ethyl ester

GCS: Glasgow coma scale

GPx: glutathione peroxidase

GSH: glutathione

GST: glutathione-S-transferase

H<sub>2</sub>O<sub>2</sub>: hydrogen peroxide

HPLC: high performance liquid chromatography

HO-1: heme oxygenase-1

HVA: homovanillic acid

HZ: hydralazine

iNOS: inducible nitric oxide synthase

i.p.: intraperitoneal

K<sup>+</sup>: potassium cation

L•: lipid radical

L1CAM: neuronal cell adhesion molecule L1

LOO•: lipid peroxy radical

LP: lipid peroxidation

MAO: monoamine oxidase

MAOI: monoamine oxidase inhibitor

MAP: microtubule associated protein

Mito: mitochondria

Mn-SOD: mitochondrial superoxide dismutase 2 (i.e. manganese superoxide dismutase)

mPT: mitochondrial permeability transition

mPTP: mitochondria permeability transition pore

MR: magnetic resonance

mtNOS: mitochondrial nitric oxide synthase

MWM: Morris water maze

NAC: n-acetylcysteine

NACA: n-acetylcysteine amide

NAD<sup>+</sup> / NADH: nicotinamide adenine dinucleotide

NAD(P)H: nicotinamide adenine dinucleotide phosphate

NE: norepinephrine



NH-NH<sub>2</sub>: hydrazine moiety

NIH: National Institutes of Health

NIM811: n-methyl-4-isoleucine cyclosporine

NMDA: n-methyl-D-aspartic acid

nNOS: neuronal nitric oxide synthase

NO•: nitric oxide radical

NO<sub>2</sub>•: nitrogen dioxide oxide radical

NOS: nitric oxide synthase

NqO1: NAD(P)H quinone oxidoreductase 1

Nrf2: nuclear factor (erythroid-derived 2)

NS: non-synaptic

O<sub>2</sub>: molecular oxygen

O<sub>2</sub>•<sup>-</sup>: superoxide radical

OCD: ornithine decarboxylase

OH•: hydroxyl radical

OH<sup>-</sup>: hydroxyl anion

ONOO<sup>-</sup>: peroxyxynitrite anion

ONOOCO<sub>2</sub><sup>-</sup>: nitrosperoxocarbonate

ONOOH: peroxyxynitrous acid

ORN-T: ornithine transaminase

P<sub>i</sub>: inorganic phosphate

PBS: phosphate buffered saline

PEA: phenethylamine

PEG-SOD: polyethylene glycol superoxide dismutase

PEH: phenylethyldenehydrazine

PFA: paraformaldehyde

PG: pargyline  
PKC: protein kinase C  
PN: peroxy nitrite  
psi: pounds per square inch  
PUFA: polyunsaturated fatty acid  
PZ: phenelzine  
RCR: respiratory control ratio  
ROS: reactive oxygen species  
RNS: reactive nitrogen species  
SBDP: spectrin breakdown products  
s.c.: subcutaneous  
SCI: spinal cord injury  
SNK: Student-Newman-Keuls  
SNRI: serotonin-norepinephrine-reuptake inhibitor  
SOD: superoxide dismutase  
SSRI: selective serotonin reuptake inhibitor  
Syn: synaptic  
TCA: tricarboxylic acid cycle (i.e. citric acid cycle, Krebs cycle)  
TBI: traumatic brain injury  
TBS: tris-buffered saline  
TBST: tris-buffered saline with tween  
VDAC: voltage-dependent anion channel  
WD: weight drop traumatic brain injury

## REFERENCES

1. Hall, E.D., R.A. Vaishnav, and A.G. Mustafa, *Antioxidant therapies for traumatic brain injury*. Neurotherapeutics, 2010. **7**(1): p. 51-61.
2. Taylor, C.A., et al., *Traumatic Brain Injury-Related Emergency Department Visits, Hospitalizations, and Deaths - United States, 2007 and 2013*. MMWR Serveill Summ, 2017. **66**(No. SS-9): p. 1-16.
3. Holm, L., et al., *Summary of the WHO Collaborating Centre for Neurotrauma Task Force on Mild Traumatic Brain Injury*. J Rehabil Med, 2005. **37**(3): p. 137-41.
4. Jordan, B.D., *The clinical spectrum of sport-related traumatic brain injury*. Nat Rev Neurol, 2013. **9**(4): p. 222-30.
5. Marion, D.W., et al., *Proceedings of the military mTBI Diagnostics Workshop, St. Pete Beach, August 2010*. J Neurotrauma, 2011. **28**(4): p. 517-26.
6. Langlois, J.A., W. Rutland-Brown, and M.M. Wald, *The epidemiology and impact of traumatic brain injury: a brief overview*. J Head Trauma Rehabil, 2006. **21**(5): p. 375-8.
7. Faul M, X.L., Wald MM, Coronado VG, *Traumatic Brain Injury in the United States: Emergency Department Visits, Hospitalizations and Deaths 2002 – 2006*. Atlanta (GA): Centers for Disease Control and Prevention, National Center for Injury Prevention and Control,; 2010.
8. Teasdale, G., et al., *The Glasgow Coma Scale at 40 years: standing the test of time*. Lancet Neurol, 2014. **13**(8): p. 844-54.
9. Saatman, K.E., et al., *Classification of traumatic brain injury for targeted therapies*. J Neurotrauma, 2008. **25**(7): p. 719-38.
10. Coronado, V.G., McGuire, L.C., Faul, M.F., Sugerman, D.E., Pearson, W.S., *Traumatic Brain Injury Epidemiology and Public Health Issues*, in *Brain Injury Medicine: Principles and Practice*, N.D. Zasler, Katz, D.I., Zafonte, R.D. , Editor. 2012, Demos Medical Publishing New York, N.Y. p. 84-100.
11. Finkelstein, E.A., P.S. Corso, and T.R. Miller, *The Incidence and Economic Burden of Injuries in the United States*. Oxford University Press: New York, N.Y., 2006.
12. Thurman, D.J., et al., *Traumatic brain injury in the United States: A public health perspective*. J Head Trauma Rehabil, 1999. **14**(6): p. 602-15.
13. Selassie, A.W., et al., *Incidence of long-term disability following traumatic brain injury hospitalization, United States, 2003*. J Head Trauma Rehabil, 2008. **23**(2): p. 123-31.

14. Maas, A.I., N. Stocchetti, and R. Bullock, *Moderate and severe traumatic brain injury in adults*. *Lancet Neurol*, 2008. **7**(8): p. 728-41.
15. McAllister, T.W., *Neurobiological consequences of traumatic brain injury*. *Dialogues Clin Neurosci*, 2011. **13**(3): p. 287-300.
16. Weber, J.T., *Altered calcium signaling following traumatic brain injury*. *Front Pharmacol*, 2012. **3**: p. 60.
17. Hall, E.D., et al., *Lipid peroxidation in brain or spinal cord mitochondria after injury*. *J Bioenerg Biomembr*, 2015.
18. Burda, J.E., A.M. Bernstein, and M.V. Sofroniew, *Astrocyte roles in traumatic brain injury*. *Exp Neurol*, 2016. **275 Pt 3**: p. 305-15.
19. Kulbe, J.R. and E.D. Hall, *Chronic traumatic encephalopathy-integration of canonical traumatic brain injury secondary injury mechanisms with tau pathology*. *Prog Neurobiol*, 2017. **158**: p. 15-44.
20. Rizzuto, R., P. Bernardi, and T. Pozzan, *Mitochondria as all-round players of the calcium game*. *J Physiol*, 2000. **529 Pt 1**: p. 37-47.
21. Rizzuto, R., et al., *Mitochondria as biosensors of calcium microdomains*. *Cell Calcium*, 1999. **26**(5): p. 193-9.
22. Xiong, Y., et al., *Mitochondrial dysfunction and calcium perturbation induced by traumatic brain injury*. *J Neurotrauma*, 1997. **14**(1): p. 23-34.
23. Fiskum, G., *Mitochondrial participation in ischemic and traumatic neural cell death*. *J Neurotrauma*, 2000. **17**(10): p. 843-55.
24. Lifshitz, J., et al., *Structural and functional damage sustained by mitochondria after traumatic brain injury in the rat: evidence for differentially sensitive populations in the cortex and hippocampus*. *J Cereb Blood Flow Metab*, 2003. **23**(2): p. 219-31.
25. Yonutas, H.M., H.J. Vekaria, and P.G. Sullivan, *Mitochondrial specific therapeutic targets following brain injury*. *Brain Res*, 2016. **1640**(Pt A): p. 77-93.
26. Vos, M., E. Lauwers, and P. Verstreken, *Synaptic mitochondria in synaptic transmission and organization of vesicle pools in health and disease*. *Front Synaptic Neurosci*, 2010. **2**: p. 139.
27. Prins, M., et al., *The pathophysiology of traumatic brain injury at a glance*. *Dis Model Mech*, 2013. **6**(6): p. 1307-15.
28. Nicholls, D.G. and M.W. Ward, *Mitochondrial membrane potential and neuronal glutamate excitotoxicity: mortality and millivolts*. *Trends Neurosci*, 2000. **23**(4): p. 166-74.

29. Vaishnav, R.A., et al., *Lipid peroxidation-derived reactive aldehydes directly and differentially impair spinal cord and brain mitochondrial function*. J Neurotrauma, 2010. **27**(7): p. 1311-20.
30. Brand, M.D. and D.G. Nicholls, *Assessing mitochondrial dysfunction in cells*. Biochem J, 2011. **435**(2): p. 297-312.
31. Nicholls, D.G., *Mitochondrial ion circuits*. Essays Biochem, 2010. **47**: p. 25-35.
32. Eliseev, R.A., et al., *Role of cyclophilin D in the resistance of brain mitochondria to the permeability transition*. Neurobiol Aging, 2007. **28**(10): p. 1532-42.
33. Yonutas, H.M., J.D. Pandya, and P.G. Sullivan, *Changes in mitochondrial bioenergetics in the brain versus spinal cord become more apparent with age*. J Bioenerg Biomembr, 2014.
34. Battino, M., et al., *Structural and functional aspects of the respiratory chain of synaptic and nonsynaptic mitochondria derived from selected brain regions*. J Bioenerg Biomembr, 1991. **23**(2): p. 345-63.
35. Davey, G.P., L. Canevari, and J.B. Clark, *Threshold effects in synaptosomal and nonsynaptic mitochondria from hippocampal CA1 and paramedian neocortex brain regions*. J Neurochem, 1997. **69**(6): p. 2564-70.
36. Brustovetsky, N., et al., *Increased susceptibility of striatal mitochondria to calcium-induced permeability transition*. J Neurosci, 2003. **23**(12): p. 4858-67.
37. Brown, M.R., P.G. Sullivan, and J.W. Geddes, *Synaptic mitochondria are more susceptible to Ca<sup>2+</sup>-overload than nonsynaptic mitochondria*. J Biol Chem, 2006. **281**(17): p. 11658-68.
38. Naga, K.K., P.G. Sullivan, and J.W. Geddes, *High cyclophilin D content of synaptic mitochondria results in increased vulnerability to permeability transition*. J Neurosci, 2007. **27**(28): p. 7469-75.
39. Hazelton, J.L., et al., *Cyclophilin D is expressed predominantly in mitochondria of gamma-aminobutyric acidergic interneurons*. J Neurosci Res, 2009. **87**(5): p. 1250-9.
40. Kristian, T., et al., *Heterogeneity of the calcium-induced permeability transition in isolated non-synaptic brain mitochondria*. J Neurochem, 2002. **83**(6): p. 1297-308.
41. Gilmer, L.K., et al., *Age-related mitochondrial changes after traumatic brain injury*. J Neurotrauma, 2010. **27**(5): p. 939-50.
42. Gilmer, L.K., et al., *Age-related changes in mitochondrial respiration and oxidative damage in the cerebral cortex of the Fischer 344 rat*. Mech Ageing Dev, 2010. **131**(2): p. 133-43.

43. Stauch, K.L., P.R. Purnell, and H.S. Fox, *Quantitative proteomics of synaptic and nonsynaptic mitochondria: insights for synaptic mitochondrial vulnerability*. J Proteome Res, 2014. **13**(5): p. 2620-36.
44. Sheng, Z.H. and Q. Cai, *Mitochondrial transport in neurons: impact on synaptic homeostasis and neurodegeneration*. Nat Rev Neurosci, 2012. **13**(2): p. 77-93.
45. Cheng, A., Y. Hou, and M.P. Mattson, *Mitochondria and neuroplasticity*. ASN Neuro, 2010. **2**(5): p. e00045.
46. MacAskill, A.F., T.A. Atkin, and J.T. Kittler, *Mitochondrial trafficking and the provision of energy and calcium buffering at excitatory synapses*. Eur J Neurosci, 2010. **32**(2): p. 231-40.
47. Sullivan, P.G., et al., *Traumatic brain injury alters synaptic homeostasis: implications for impaired mitochondrial and transport function*. J Neurotrauma, 1998. **15**(10): p. 789-98.
48. Mattson, M.P., J.N. Keller, and J.G. Begley, *Evidence for synaptic apoptosis*. Exp Neurol, 1998. **153**(1): p. 35-48.
49. Ikegami, K. and T. Koike, *Non-apoptotic neurite degeneration in apoptotic neuronal death: pivotal role of mitochondrial function in neurites*. Neuroscience, 2003. **122**(3): p. 617-26.
50. Patel, S.P., et al., *Differential effects of the mitochondrial uncoupling agent, 2,4-dinitrophenol, or the nitroxide antioxidant, Tempol, on synaptic or nonsynaptic mitochondria after spinal cord injury*. J Neurosci Res, 2009. **87**(1): p. 130-40.
51. Sullivan, P.G., et al., *Mitochondrial permeability transition in CNS trauma: cause or effect of neuronal cell death?* J Neurosci Res, 2005. **79**(1-2): p. 231-9.
52. Pandya, J.D., V.N. Nukala, and P.G. Sullivan, *Concentration dependent effect of calcium on brain mitochondrial bioenergetics and oxidative stress parameters*. Front Neuroenergetics, 2013. **5**: p. 10.
53. Bringold, U., P. Ghafourifar, and C. Richter, *Peroxynitrite formed by mitochondrial NO synthase promotes mitochondrial Ca<sup>2+</sup> release*. Free Radic Biol Med, 2000. **29**(3-4): p. 343-8.
54. Radi, R., et al., *Peroxynitrite reactions and formation in mitochondria*. Free Radic Biol Med, 2002. **33**(11): p. 1451-64.
55. Bains, M. and E.D. Hall, *Antioxidant therapies in traumatic brain and spinal cord injury*. Biochim Biophys Acta, 2012. **1822**(5): p. 675-84.
56. Deng, Y., et al., *Temporal relationship of peroxynitrite-induced oxidative damage, calpain-mediated cytoskeletal degradation and neurodegeneration after traumatic brain injury*. Exp Neurol, 2007. **205**(1): p. 154-65.

57. Hall, E.D., et al., *Peroxynitrite-mediated protein nitration and lipid peroxidation in a mouse model of traumatic brain injury*. J Neurotrauma, 2004. **21**(1): p. 9-20.
58. Singh, I.N., P.G. Sullivan, and E.D. Hall, *Peroxynitrite-mediated oxidative damage to brain mitochondria: Protective effects of peroxynitrite scavengers*. J Neurosci Res, 2007. **85**(10): p. 2216-23.
59. Hall, E.D., J.A. Wang, and D.M. Miller, *Relationship of nitric oxide synthase induction to peroxynitrite-mediated oxidative damage during the first week after experimental traumatic brain injury*. Exp Neurol, 2012. **238**(2): p. 176-82.
60. Hansson, M.J., et al., *Calcium-induced generation of reactive oxygen species in brain mitochondria is mediated by permeability transition*. Free Radic Biol Med, 2008. **45**(3): p. 284-94.
61. Sousa, S.C., et al., *Ca<sup>2+</sup>-induced oxidative stress in brain mitochondria treated with the respiratory chain inhibitor rotenone*. FEBS Lett, 2003. **543**(1-3): p. 179-83.
62. Starkov, A.A., B.M. Polster, and G. Fiskum, *Regulation of hydrogen peroxide production by brain mitochondria by calcium and Bax*. J Neurochem, 2002. **83**(1): p. 220-8.
63. Gyulxhandanyan, A.V. and P.S. Pennefather, *Shift in the localization of sites of hydrogen peroxide production in brain mitochondria by mitochondrial stress*. J Neurochem, 2004. **90**(2): p. 405-21.
64. Adibhatla, R.M. and J.F. Hatcher, *Lipid oxidation and peroxidation in CNS health and disease: from molecular mechanisms to therapeutic opportunities*. Antioxid Redox Signal, 2010. **12**(1): p. 125-69.
65. Turrens, J.F., *Mitochondrial formation of reactive oxygen species*. J Physiol, 2003. **552**(Pt 2): p. 335-44.
66. Ruzskiewicz, J. and J. Albrecht, *Changes in the mitochondrial antioxidant systems in neurodegenerative diseases and acute brain disorders*. Neurochem Int, 2015. **88**: p. 66-72.
67. James, A.M., R.A. Smith, and M.P. Murphy, *Antioxidant and prooxidant properties of mitochondrial Coenzyme Q*. Arch Biochem Biophys, 2004. **423**(1): p. 47-56.
68. Bayir, H., et al., *Selective early cardiolipin peroxidation after traumatic brain injury: an oxidative lipidomics analysis*. Ann Neurol, 2007. **62**(2): p. 154-69.
69. Mustafa, A.G., et al., *Mitochondrial protection after traumatic brain injury by scavenging lipid peroxyl radicals*. J Neurochem, 2010. **114**(1): p. 271-80.
70. Mustafa, A.G., et al., *Pharmacological inhibition of lipid peroxidation attenuates calpain-mediated cytoskeletal degradation after traumatic brain injury*. J Neurochem, 2011. **117**(3): p. 579-88.

71. Singh, I.N., et al., *Phenelzine mitochondrial functional preservation and neuroprotection after traumatic brain injury related to scavenging of the lipid peroxidation-derived aldehyde 4-hydroxy-2-nonenal*. J Cereb Blood Flow Metab, 2013. **33**(4): p. 593-9.
72. Cebak, J.E., et al., *Phenelzine protects brain mitochondrial function in vitro and in vivo following traumatic brain injury by scavenging the reactive carbonyls 4-hydroxynonenal and acrolein leading to cortical histological neuroprotection* J Neurotrauma, 2016.
73. Hill, R.L., et al., *Time courses of post-injury mitochondrial oxidative damage and respiratory dysfunction and neuronal cytoskeletal degradation in a rat model of focal traumatic brain injury*. Neurochem Int, 2017.
74. Chen, Z., et al., *Mitigation of sensory and motor deficits by acrolein scavenger phenelzine in a rat model of spinal cord contusive injury*. J Neurochem, 2016. **138**(2): p. 328-38.
75. Park, J., et al., *Neuroprotective role of hydralazine in rat spinal cord injury-attenuation of acrolein-mediated damage*. J Neurochem, 2014. **129**(2): p. 339-49.
76. Wood, P.L., et al., *Aldehyde load in ischemia-reperfusion brain injury: neuroprotection by neutralization of reactive aldehydes with phenelzine*. Brain Res, 2006. **1122**(1): p. 184-90.
77. Shi, R., T. Rickett, and W. Sun, *Acrolein-mediated injury in nervous system trauma and diseases*. Mol Nutr Food Res, 2011. **55**(9): p. 1320-31.
78. Burcham, P.C., *Potentialities and pitfalls accompanying chemico-pharmacological strategies against endogenous electrophiles and carbonyl stress*. Chem Res Toxicol, 2008. **21**(4): p. 779-86.
79. Aldini, G., et al., *Intervention strategies to inhibit protein carbonylation by lipoxidation-derived reactive carbonyls*. Med Res Rev, 2007. **27**(6): p. 817-68.
80. Fritz, K.S. and D.R. Petersen, *An overview of the chemistry and biology of reactive aldehydes*. Free Radic Biol Med, 2013. **59**: p. 85-91.
81. LoPachin, R.M., D.S. Barber, and T. Gavin, *Molecular mechanisms of the conjugated alpha,beta-unsaturated carbonyl derivatives: relevance to neurotoxicity and neurodegenerative diseases*. Toxicol Sci, 2008. **104**(2): p. 235-49.
82. Siems, W. and T. Grune, *Intracellular metabolism of 4-hydroxynonenal*. Mol Aspects Med, 2003. **24**(4-5): p. 167-75.
83. Levine, R.L., *Carbonyl modified proteins in cellular regulation, aging, and disease*. Free Radic Biol Med, 2002. **32**(9): p. 790-6.



84. Pocernich, C.B. and D.A. Butterfield, *Acrolein inhibits NADH-linked mitochondrial enzyme activity: implications for Alzheimer's disease*. Neurotox Res, 2003. **5**(7): p. 515-20.
85. Moghe, A., et al., *Molecular mechanisms of acrolein toxicity: relevance to human disease*. Toxicol Sci, 2015. **143**(2): p. 242-55.
86. Luo, J., J.P. Robinson, and R. Shi, *Acrolein-induced cell death in PC12 cells: role of mitochondria-mediated oxidative stress*. Neurochem Int, 2005. **47**(7): p. 449-57.
87. Lovell, M.A., C. Xie, and W.R. Markesbery, *Acrolein is increased in Alzheimer's disease brain and is toxic to primary hippocampal cultures*. Neurobiol Aging, 2001. **22**(2): p. 187-94.
88. Hamann, K., et al., *Critical role of acrolein in secondary injury following ex vivo spinal cord trauma*. J Neurochem, 2008. **107**(3): p. 712-21.
89. Kruman, I., et al., *Evidence that 4-hydroxynonenal mediates oxidative stress-induced neuronal apoptosis*. J Neurosci, 1997. **17**(13): p. 5089-100.
90. Mello, C.F., et al., *Acrolein induces selective protein carbonylation in synaptosomes*. Neuroscience, 2007. **147**(3): p. 674-9.
91. Perluigi, M., et al., *Redox proteomics identification of 4-hydroxynonenal-modified brain proteins in Alzheimer's disease: Role of lipid peroxidation in Alzheimer's disease pathogenesis*. Proteomics Clin Appl, 2009. **3**(6): p. 682-693.
92. Hortigon-Vinagre, M.P., et al., *Inhibition by 4-hydroxynonenal (HNE) of Ca<sup>2+</sup> transport by SERCA1a: low concentrations of HNE open protein-mediated leaks in the membrane*. Free Radic Biol Med, 2011. **50**(2): p. 323-36.
93. Keller, J.N., et al., *4-Hydroxynonenal, an aldehydic product of membrane lipid peroxidation, impairs glutamate transport and mitochondrial function in synaptosomes*. Neuroscience, 1997. **80**(3): p. 685-96.
94. Lovell, M.A., M.A. Bradley, and S.X. Fister, *4-Hydroxyhexenal (HHE) impairs glutamate transport in astrocyte cultures*. J Alzheimers Dis, 2012. **32**(1): p. 139-46.
95. Lovell, M.A., C. Xie, and W.R. Markesbery, *Acrolein, a product of lipid peroxidation, inhibits glucose and glutamate uptake in primary neuronal cultures*. Free Radic Biol Med, 2000. **29**(8): p. 714-20.
96. Mattson, M.P., et al., *4-Hydroxynonenal, a product of lipid peroxidation, inhibits dephosphorylation of the microtubule-associated protein tau*. Neuroreport, 1997. **8**(9-10): p. 2275-81.
97. Miller, D.M., et al., *Administration of the Nrf2-ARE activators sulforaphane and carnosic acid attenuates 4-hydroxy-2-nonenal-induced mitochondrial dysfunction ex vivo*. Free Radic Biol Med, 2013. **57**: p. 1-9.

98. Picklo, M.J., et al., *4-Hydroxy-2(E)-nonenal inhibits CNS mitochondrial respiration at multiple sites*. J Neurochem, 1999. **72**(4): p. 1617-24.
99. Picklo, M.J. and T.J. Montine, *Acrolein inhibits respiration in isolated brain mitochondria*. Biochim Biophys Acta, 2001. **1535**(2): p. 145-52.
100. Packer, M.A. and M.P. Murphy, *Peroxynitrite formed by simultaneous nitric oxide and superoxide generation causes cyclosporin-A-sensitive mitochondrial calcium efflux and depolarisation*. Eur J Biochem, 1995. **234**(1): p. 231-9.
101. Luo, J. and R. Shi, *Acrolein induces oxidative stress in brain mitochondria*. Neurochem Int, 2005. **46**(3): p. 243-52.
102. Luo, J. and R. Shi, *Acrolein induces axolemmal disruption, oxidative stress, and mitochondrial impairment in spinal cord tissue*. Neurochem Int, 2004. **44**(7): p. 475-86.
103. Halestrap, A.P., *What is the mitochondrial permeability transition pore?* J Mol Cell Cardiol, 2009. **46**(6): p. 821-31.
104. Galluzzi, L., K. Blomgren, and G. Kroemer, *Mitochondrial membrane permeabilization in neuronal injury*. Nat Rev Neurosci, 2009. **10**(7): p. 481-94.
105. Kinnally, K.W., et al., *Is mPTP the gatekeeper for necrosis, apoptosis, or both?* Biochim Biophys Acta, 2011. **1813**(4): p. 616-22.
106. Wang, K.K., *Calpain and caspase: can you tell the difference?* Trends Neurosci, 2000. **23**(1): p. 20-6.
107. Machnicka, B., et al., *Spectrins: a structural platform for stabilization and activation of membrane channels, receptors and transporters*. Biochim Biophys Acta, 2014. **1838**(2): p. 620-34.
108. Saatman, K.E., et al., *Prolonged calpain-mediated spectrin breakdown occurs regionally following experimental brain injury in the rat*. J Neuropathol Exp Neurol, 1996. **55**(7): p. 850-60.
109. Deng-Bryant, Y., et al., *Neuroprotective effects of tempol, a catalytic scavenger of peroxynitrite-derived free radicals, in a mouse traumatic brain injury model*. J Cereb Blood Flow Metab, 2008. **28**(6): p. 1114-26.
110. Mbye, L.H., et al., *Comparative neuroprotective effects of cyclosporin A and NIM811, a nonimmunosuppressive cyclosporin A analog, following traumatic brain injury*. J Cereb Blood Flow Metab, 2009. **29**(1): p. 87-97.
111. Miller, D.M., et al., *Temporal and spatial dynamics of nrf2-antioxidant response elements mediated gene targets in cortex and hippocampus after controlled cortical impact traumatic brain injury in mice*. J Neurotrauma, 2014. **31**(13): p. 1194-201.

112. Bains, M., et al., *Pharmacological analysis of the cortical neuronal cytoskeletal protective efficacy of the calpain inhibitor SNJ-1945 in a mouse traumatic brain injury model*. J Neurochem, 2013. **125**(1): p. 125-32.
113. Miller, D.M., et al., *Nrf2-ARE activator carnosic acid decreases mitochondrial dysfunction, oxidative damage and neuronal cytoskeletal degradation following traumatic brain injury in mice*. Exp Neurol, 2014. **264C**: p. 103-110.
114. Springer, J.E., *Apoptotic cell death following traumatic injury to the central nervous system*. J Biochem Mol Biol, 2002. **35**(1): p. 94-105.
115. Pike, B.R., et al., *Accumulation of non-erythroid alpha II-spectrin and calpain-cleaved alpha II-spectrin breakdown products in cerebrospinal fluid after traumatic brain injury in rats*. J Neurochem, 2001. **78**(6): p. 1297-306.
116. Kampf, A., et al., *Mechanisms of calpain proteolysis following traumatic brain injury: implications for pathology and therapy: implications for pathology and therapy: a review and update*. J Neurotrauma, 1997. **14**(3): p. 121-34.
117. Colley, B.S., L.L. Phillips, and T.M. Reeves, *The effects of cyclosporin-A on axonal conduction deficits following traumatic brain injury in adult rats*. Exp Neurol, 2010. **224**(1): p. 241-51.
118. Kilinc, D., G. Gallo, and K.A. Barbee, *Mechanically-induced membrane poration causes axonal beading and localized cytoskeletal damage*. Exp Neurol, 2008. **212**(2): p. 422-30.
119. Albeni, B.C., et al., *Cyclosporin ameliorates traumatic brain-injury-induced alterations of hippocampal synaptic plasticity*. Exp Neurol, 2000. **162**(2): p. 385-9.
120. Youle, R.J. and A.M. van der Bliek, *Mitochondrial fission, fusion, and stress*. Science, 2012. **337**(6098): p. 1062-5.
121. Hall, E.D., et al., *Evolution of post-traumatic neurodegeneration after controlled cortical impact traumatic brain injury in mice and rats as assessed by the de Olmos silver and fluorojade staining methods*. J Neurotrauma, 2008. **25**(3): p. 235-47.
122. Sullivan, P.G., A.H. Sebastian, and E.D. Hall, *Therapeutic window analysis of the neuroprotective effects of cyclosporine A after traumatic brain injury*. J Neurotrauma, 2011. **28**(2): p. 311-8.
123. Readnower, R.D., et al., *Post-injury administration of the mitochondrial permeability transition pore inhibitor, NIM811, is neuroprotective and improves cognition after traumatic brain injury in rats*. J Neurotrauma, 2011. **28**(9): p. 1845-53.
124. Scheff, S.W. and P.G. Sullivan, *Cyclosporin A significantly ameliorates cortical damage following experimental traumatic brain injury in rodents*. J Neurotrauma, 1999. **16**(9): p. 783-92.

125. Pandya, J.D., et al., *Post-Injury Administration of Mitochondrial Uncouplers Increases Tissue Sparing and Improves Behavioral Outcome following Traumatic Brain Injury in Rodents*. J Neurotrauma, 2007. **24**(5): p. 798-811.
126. Pandya, J.D., et al., *N-acetylcysteine amide confers neuroprotection, improves bioenergetics and behavioral outcome following TBI*. Exp Neurol, 2014. **257**: p. 106-13.
127. Group, N.G.W., et al., *Guidelines for the pharmacologic treatment of neurobehavioral sequelae of traumatic brain injury*. J Neurotrauma, 2006. **23**(10): p. 1468-501.
128. Hall, E.D., et al., *Spatial and temporal characteristics of neurodegeneration after controlled cortical impact in mice: more than a focal brain injury*. J Neurotrauma, 2005. **22**(2): p. 252-65.
129. Johnson, V.E., et al., *Inflammation and white matter degeneration persist for years after a single traumatic brain injury*. Brain, 2013. **136**(Pt 1): p. 28-42.
130. McKee, A.C. and M.E. Robinson, *Military-related traumatic brain injury and neurodegeneration*. Alzheimers Dement, 2014. **10**(3 Suppl): p. S242-53.
131. Sharp, D.J., G. Scott, and R. Leech, *Network dysfunction after traumatic brain injury*. Nat Rev Neurol, 2014. **10**(3): p. 156-66.
132. Saatman, K.E., et al., *Behavioral efficacy of posttraumatic calpain inhibition is not accompanied by reduced spectrin proteolysis, cortical lesion, or apoptosis*. J Cereb Blood Flow Metab, 2000. **20**(1): p. 66-73.
133. Saatman, K.E., et al., *Calpain inhibitor AK295 attenuates motor and cognitive deficits following experimental brain injury in the rat*. Proc Natl Acad Sci U S A, 1996. **93**(8): p. 3428-33.
134. Watson, W.D., et al., *Impaired cortical mitochondrial function following TBI precedes behavioral changes*. Front Neuroenergetics, 2013. **5**: p. 12.
135. Alessandri, B., et al., *Cyclosporin A improves brain tissue oxygen consumption and learning/memory performance after lateral fluid percussion injury in rats*. J Neurotrauma, 2002. **19**(7): p. 829-41.
136. Riess, P., et al., *Effects of chronic, post-injury Cyclosporin A administration on motor and sensorimotor function following severe, experimental traumatic brain injury*. Restor Neurol Neurosci, 2001. **18**(1): p. 1-8.
137. Long, D.A., et al., *Deferoxamine improves spatial memory performance following experimental brain injury in rats*. Brain Res, 1996. **717**(1-2): p. 109-17.
138. Dash, P.K., et al., *Sulforaphane improves cognitive function administered following traumatic brain injury*. Neurosci Lett, 2009. **460**(2): p. 103-7.

139. Davis, L.M., et al., *Fasting is neuroprotective following traumatic brain injury*. J Neurosci Res, 2008. **86**(8): p. 1812-22.
140. Guseva, M.V., et al., *Dietary choline supplementation improves behavioral, histological, and neurochemical outcomes in a rat model of traumatic brain injury*. J Neurotrauma, 2008. **25**(8): p. 975-83.
141. Sikoglu, E.M., et al., *Enhancement in cognitive function recovery by granulocyte-colony stimulating factor in a rodent model of traumatic brain injury*. Behav Brain Res, 2014. **259**: p. 354-6.
142. de Castro, M.R.T., et al., *Previous physical exercise alters the hepatic profile of oxidative-inflammatory status and limits the secondary brain damage induced by severe traumatic brain injury in rats*. J Physiol, 2017. **595**(17): p. 6023-6044.
143. Chen, H., et al., *Moderate traumatic brain injury is linked to acute behaviour deficits and long term mitochondrial alterations*. Clin Exp Pharmacol Physiol, 2016. **43**(11): p. 1107-1114.
144. Naim, M.Y., et al., *Folic acid enhances early functional recovery in a piglet model of pediatric head injury*. Dev Neurosci, 2010. **32**(5-6): p. 466-79.
145. Peterson, T.C., et al., *A behavioral and histological comparison of fluid percussion injury and controlled cortical impact injury to the rat sensorimotor cortex*. Behav Brain Res, 2015. **294**: p. 254-63.
146. D'Hooge, R. and P.P. De Deyn, *Applications of the Morris water maze in the study of learning and memory*. Brain Res Brain Res Rev, 2001. **36**(1): p. 60-90.
147. Vorhees, C.V. and M.T. Williams, *Morris water maze: procedures for assessing spatial and related forms of learning and memory*. Nat Protoc, 2006. **1**(2): p. 848-58.
148. Guillery, R.W., *Anatomical evidence concerning the role of the thalamus in corticocortical communication: a brief review*. J Anat, 1995. **187 ( Pt 3)**: p. 583-92.
149. de Bourbon-Teles, J., et al., *Thalamic control of human attention driven by memory and learning*. Curr Biol, 2014. **24**(9): p. 993-9.
150. Moret, C. and M. Briley, *The importance of norepinephrine in depression*. Neuropsychiatr Dis Treat, 2011. **7**(Suppl 1): p. 9-13.
151. Purves D, A.G., Fitzpatrick D, et al., *The Biogenic Amines*, in *Neuroscience*, A.G. Purves D, Fitzpatrick D, et al., Editor. 2001, Sinauer Associates: Sunderland (MA).
152. Bondi, C.O., et al., *Old dog, new tricks: the attentional set-shifting test as a novel cognitive behavioral task after controlled cortical impact injury*. J Neurotrauma, 2014. **31**(10): p. 926-37.

153. Kwon, H.G. and S.H. Jang, *Differences in neural connectivity between the substantia nigra and ventral tegmental area in the human brain*. Front Hum Neurosci, 2014. **8**: p. 41.
154. Osier, N.D. and C.E. Dixon, *Catecholaminergic based therapies for functional recovery after TBI*. Brain Res, 2016. **1640**(Pt A): p. 15-35.
155. Charnay, Y. and L. Leger, *Brain serotonergic circuitries*. Dialogues Clin Neurosci, 2010. **12**(4): p. 471-87.
156. Misrani, A., et al., *Differential effects of citalopram on sleep-deprivation-induced depressive-like behavior and memory impairments in mice*. Prog Neuropsychopharmacol Biol Psychiatry, 2019. **88**: p. 102-111.
157. McAllister, B.B., et al., *The effects of chronic fluoxetine treatment following injury of medial frontal cortex in mice*. Behav Brain Res, 2015. **290**: p. 102-16.
158. Barbelivien, A., et al., *Inhibition of MAO-A activity enhances behavioural activity of rats assessed using water maze and open arena tasks*. Pharmacol Toxicol, 2001. **88**(6): p. 304-12.
159. Parent, M.B., M.K. Habib, and G.B. Baker, *Task-dependent effects of the antidepressant/antipanic drug phenelzine on memory*. Psychopharmacology (Berl), 1999. **142**(3): p. 280-8.
160. Bolton Hall, A.N., et al., *Repeated Closed Head Injury in Mice Results in Sustained Motor and Memory Deficits and Chronic Cellular Changes*. PLoS One, 2016. **11**(7): p. e0159442.
161. Hall, E.D., et al., *Generation and detection of hydroxyl radical following experimental head injury*. Ann N Y Acad Sci, 1994. **738**: p. 15-24.
162. Smith, S.L., et al., *Direct measurement of hydroxyl radicals, lipid peroxidation, and blood-brain barrier disruption following unilateral cortical impact head injury in the rat*. J Neurotrauma, 1994. **11**(4): p. 393-404.
163. Singh, I.N., et al., *Time course of post-traumatic mitochondrial oxidative damage and dysfunction in a mouse model of focal traumatic brain injury: implications for neuroprotective therapy*. J Cereb Blood Flow Metab, 2006. **26**(11): p. 1407-18.
164. Chen, S., J.D. Pickard, and N.G. Harris, *Time course of cellular pathology after controlled cortical impact injury*. Exp Neurol, 2003. **182**(1): p. 87-102.
165. Tyurin, V.A., et al., *Oxidative stress following traumatic brain injury in rats: quantitation of biomarkers and detection of free radical intermediates*. J Neurochem, 2000. **75**(5): p. 2178-89.
166. Ansari, M.A., K.N. Roberts, and S.W. Scheff, *Oxidative stress and modification of synaptic proteins in hippocampus after traumatic brain injury*. Free Radic Biol Med, 2008. **45**(4): p. 443-52.

167. Xiong, Y., A. Mahmood, and M. Chopp, *Animal models of traumatic brain injury*. Nat Rev Neurosci, 2013. **14**(2): p. 128-42.
168. Ojo, J.O., B.C. Mouzon, and F. Crawford, *Repetitive head trauma, chronic traumatic encephalopathy and tau: Challenges in translating from mice to men*. Exp Neurol, 2016. **275 Pt 3**: p. 389-404.
169. MacKenzie, E.M., et al., *Phenelzine causes an increase in brain ornithine that is prevented by prior monoamine oxidase inhibition*. Neurochem Res, 2008. **33**(3): p. 430-6.
170. Bales, J.W., et al., *Targeting Dopamine in Acute Traumatic Brain Injury*. Open Drug Discov J, 2010. **2**: p. 119-128.
171. McCorry, L.K., *Physiology of the autonomic nervous system*. Am J Pharm Educ, 2007. **71**(4): p. 78.
172. Vanhoutte, P.M., *Cardiovascular effects of serotonin*. J Cardiovasc Pharmacol, 1987. **10 Suppl 3**: p. S8-11.
173. Massucci, J.L., et al., *Time dependent alterations in dopamine tissue levels and metabolism after experimental traumatic brain injury in rats*. Neurosci Lett, 2004. **372**(1-2): p. 127-31.
174. McIntosh, T.K., T. Yu, and T.A. Gennarelli, *Alterations in regional brain catecholamine concentrations after experimental brain injury in the rat*. J Neurochem, 1994. **63**(4): p. 1426-33.
175. Yan, H.Q., et al., *Traumatic brain injury reduces dopamine transporter protein expression in the rat frontal cortex*. Neuroreport, 2002. **13**(15): p. 1899-901.
176. Yan, H.Q., et al., *Tyrosine hydroxylase, but not dopamine beta-hydroxylase, is increased in rat frontal cortex after traumatic brain injury*. Neuroreport, 2001. **12**(11): p. 2323-7.
177. Chen, Y.H., et al., *Impact of Traumatic Brain Injury on Dopaminergic Transmission*. Cell Transplant, 2017. **26**(7): p. 1156-1168.
178. Levin, B.E., et al., *Widespread and lateralization effects of acute traumatic brain injury on norepinephrine turnover in the rat brain*. Brain Res, 1995. **674**(2): p. 307-13.
179. Kawa, L., et al., *Neurotransmitter Systems in a Mild Blast Traumatic Brain Injury Model: Catecholamines and Serotonin*. J Neurotrauma, 2015. **32**(16): p. 1190-9.
180. Woolf, P.D., et al., *The predictive value of catecholamines in assessing outcome in traumatic brain injury*. J Neurosurg, 1987. **66**(6): p. 875-82.
181. Rizoli, S.B., et al., *Catecholamines as outcome markers in isolated traumatic brain injury: the COMA-TBI study*. Crit Care, 2017. **21**(1): p. 37.

182. Busto, R., et al., *Extracellular release of serotonin following fluid-percussion brain injury in rats*. J Neurotrauma, 1997. **14**(1): p. 35-42.
183. Mustafa, G., et al., *Mild closed head traumatic brain injury-induced changes in monoamine neurotransmitters in the trigeminal subnuclei of a rat model: mechanisms underlying orofacial allodynia and headache*. Neural Regen Res, 2017. **12**(6): p. 981-986.
184. Abe, K., et al., *Traumatic brain injury decreases serotonin transporter expression in the rat cerebrum*. Neurol Res, 2016. **38**(4): p. 358-63.
185. Kajstura, T.J., S.E. Dougherty, and D.J. Linden, *Serotonin axons in the neocortex of the adult female mouse regrow after traumatic brain injury*. J Neurosci Res, 2018. **96**(4): p. 512-526.
186. Bortolato, M.S.J.C., *Behavior Outcomes of Monoamine Oxidase Deficiency: Preclinical and Clinical Evidence*, in *Monoamine Oxidases and their Inhibitors* M.R. Youdim, P., Editor. 2011, Elsevier Science.
187. Hall, M., B. Hoffer, and G. Gerhardt, *Rapid and sensitive determination of catecholamines in small tissue sample by HPLC coupled with dual electrode coulometric electrochemical detection*. LCGC, 1989. **7**: p. 259-65.
188. Fernandez, E., et al., *Monoamine metabolism and behavioral responses to ethanol in mitochondrial aldehyde dehydrogenase knockout mice*. Alcohol Clin Exp Res, 2006. **30**(10): p. 1650-8.
189. Baker, G.B. and R.T. Coutts, *Metabolism of monoamine oxidase inhibitors*. Prog Neuropsychopharmacol Biol Psychiatry, 1989. **13**(3-4): p. 395-403.
190. Ramsay, R.R. and K.F. Tipton, *Assessment of Enzyme Inhibition: A Review with Examples from the Development of Monoamine Oxidase and Cholinesterase Inhibitory Drugs*. Molecules, 2017. **22**(7).
191. Finberg, J.P., *Update on the pharmacology of selective inhibitors of MAO-A and MAO-B: focus on modulation of CNS monoamine neurotransmitter release*. Pharmacol Ther, 2014. **143**(2): p. 133-52.
192. Al-Nuaimi, S.K., E.M. Mackenzie, and G.B. Baker, *Monoamine oxidase inhibitors and neuroprotection: a review*. Am J Ther, 2012. **19**(6): p. 436-48.
193. Cohen, G. and N. Kesler, *Monoamine oxidase and mitochondrial respiration*. J Neurochem, 1999. **73**(6): p. 2310-5.
194. Ben-Shachar, D., R. Zuk, and Y. Glinka, *Dopamine neurotoxicity: inhibition of mitochondrial respiration*. J Neurochem, 1995. **64**(2): p. 718-23.
195. Neff, N.H. and C. Goidis, *Neuronal monoamine oxidase: specific enzyme types and their rates of formation*. Adv Biochem Psychopharmacol, 1972. **5**: p. 307-23.



196. Arnett, C.D., et al., *Turnover of brain monoamine oxidase measured in vivo by positron emission tomography using L-[11C]deprenyl*. J Neurochem, 1987. **49**(2): p. 522-7.
197. Curet, O., et al., *Preclinical profile of befloxatone, a new reversible MAO-A inhibitor*. J Affect Disord, 1998. **51**(3): p. 287-303.
198. Galvani, S., et al., *Carbonyl scavenger and antiatherogenic effects of hydrazine derivatives*. Free Radic Biol Med, 2008. **45**(10): p. 1457-67.
199. Binda, C., et al., *Structural and mechanistic studies of arylalkylhydrazine inhibition of human monoamine oxidases A and B*. Biochemistry, 2008. **47**(20): p. 5616-25.
200. Di Pietro, O., et al., *Design, synthesis and biological evaluation of N-methyl-N-[(1,2,3-triazol-4-yl)alkyl]propargylamines as novel monoamine oxidase B inhibitors*. Bioorg Med Chem, 2016. **24**(20): p. 4835-4854.
201. Ling, L., et al., *Synthesis of N-propargylphenelzine and analogues as neuroprotective agents*. Bioorg Med Chem Lett, 2001. **11**(20): p. 2715-7.
202. Murphy, D.L., et al., *Differential trace amine alterations in individuals receiving acetylenic inhibitors of MAO-A (clorgyline) or MAO-B (selegiline and pargyline)*. J Neural Transm Suppl, 1998. **52**: p. 39-48.
203. Miller, M.H., L.M. Roberts, and C.H. Fellner, *A Study of the Antidepressant Effects of Pargyline*. Am J Psychiatry, 1964. **120**: p. 897-9.
204. Fuentes, J.A., A. Ordaz, and N.H. Neff, *Central mediation of the antihypertensive effect of pargyline in spontaneously hypertensive rats*. Eur J Pharmacol, 1979. **57**(1): p. 21-7.
205. Wooters, T.E. and M.T. Bardo, *The monoamine oxidase inhibitor phenelzine enhances the discriminative stimulus effect of nicotine in rats*. Behav Pharmacol, 2007. **18**(7): p. 601-8.
206. Villegier, A.S., et al., *Monoamine oxidase inhibitors allow locomotor and rewarding responses to nicotine*. Neuropsychopharmacology, 2006. **31**(8): p. 1704-13.
207. Gatch, M.B., et al., *Effects of monoamine oxidase inhibitors on cocaine discrimination in rats*. Behav Pharmacol, 2006. **17**(2): p. 151-9.
208. Cohen, C., et al., *Reduction of oral ethanol self-administration in rats by monoamine oxidase inhibitors*. Pharmacol Biochem Behav, 1999. **64**(3): p. 535-9.
209. Carney, N., et al., *Guidelines for the Management of Severe Traumatic Brain Injury, Fourth Edition*. Neurosurgery, 2016.

210. Skolnick, B.E., et al., *A clinical trial of progesterone for severe traumatic brain injury*. N Engl J Med, 2014. **371**(26): p. 2467-76.
211. Narayan, R.K., et al., *Clinical trials in head injury*. J Neurotrauma, 2002. **19**(5): p. 503-57.
212. Menon, D.K. and A.I. Maas, *Traumatic brain injury in 2014. Progress, failures and new approaches for TBI research*. Nat Rev Neurol, 2015. **11**(2): p. 71-2.
213. Margulies, S., R. Hicks, and L. Combination Therapies for Traumatic Brain Injury Workshop, *Combination therapies for traumatic brain injury: prospective considerations*. J Neurotrauma, 2009. **26**(6): p. 925-39.
214. Maas, A.I., et al., *Re-orientation of clinical research in traumatic brain injury: report of an international workshop on comparative effectiveness research*. J Neurotrauma, 2012. **29**(1): p. 32-46.
215. Kline, A.E., et al., *Combination therapies for neurobehavioral and cognitive recovery after experimental traumatic brain injury: Is more better?* Prog Neurobiol, 2016. **142**: p. 45-67.
216. Wang, K.K., et al., *Neuroprotection targets after traumatic brain injury*. Curr Opin Neurol, 2006. **19**(6): p. 514-9.
217. Liu, Y. and X.J. Chen, *Adenine nucleotide translocase, mitochondrial stress, and degenerative cell death*. Oxid Med Cell Longev, 2013. **2013**: p. 146860.
218. Nicolli, A., et al., *Interactions of cyclophilin with the mitochondrial inner membrane and regulation of the permeability transition pore, and cyclosporin A-sensitive channel*. J Biol Chem, 1996. **271**(4): p. 2185-92.
219. Baines, C.P., et al., *Loss of cyclophilin D reveals a critical role for mitochondrial permeability transition in cell death*. Nature, 2005. **434**(7033): p. 658-62.
220. Halestrap, A.P. and A.M. Davidson, *Inhibition of Ca<sup>2+</sup>(+)-induced large-amplitude swelling of liver and heart mitochondria by cyclosporin is probably caused by the inhibitor binding to mitochondrial-matrix peptidyl-prolyl cis-trans isomerase and preventing it interacting with the adenine nucleotide translocase*. Biochem J, 1990. **268**(1): p. 153-60.
221. Begley, D.J., et al., *Permeability of the blood-brain barrier to the immunosuppressive cyclic peptide cyclosporin A*. J Neurochem, 1990. **55**(4): p. 1222-30.
222. Baldwin, S.A., et al., *Blood-brain barrier breach following cortical contusion in the rat*. J Neurosurg, 1996. **85**(3): p. 476-81.
223. Okonkwo, D.O. and J.T. Povlishock, *An intrathecal bolus of cyclosporin A before injury preserves mitochondrial integrity and attenuates axonal disruption in traumatic brain injury*. J Cereb Blood Flow Metab, 1999. **19**(4): p. 443-51.

224. Okonkwo, D.O., et al., *Cyclosporin A limits calcium-induced axonal damage following traumatic brain injury*. Neuroreport, 1999. **10**(2): p. 353-8.
225. Sullivan, P.G., M.B. Thompson, and S.W. Scheff, *Cyclosporin A attenuates acute mitochondrial dysfunction following traumatic brain injury*. Exp Neurol, 1999. **160**(1): p. 226-34.
226. Mbye, L.H., et al., *Attenuation of acute mitochondrial dysfunction after traumatic brain injury in mice by NIM811, a non-immunosuppressive cyclosporin A analog*. Exp Neurol, 2008. **209**(1): p. 243-53.
227. Sullivan, P.G., M. Thompson, and S.W. Scheff, *Continuous infusion of cyclosporin A postinjury significantly ameliorates cortical damage following traumatic brain injury*. Exp Neurol, 2000. **161**(2): p. 631-7.
228. Fujita, M., et al., *The combination of either tempol or FK506 with delayed hypothermia: implications for traumatically induced microvascular and axonal protection*. J Neurotrauma, 2011. **28**(7): p. 1209-18.
229. Kaminska, B., K. Gaweda-Walerych, and M. Zawadzka, *Molecular mechanisms of neuroprotective action of immunosuppressants--facts and hypotheses*. J Cell Mol Med, 2004. **8**(1): p. 45-58.
230. Marmarou, C.R. and J.T. Povlishock, *Administration of the immunophilin ligand FK506 differentially attenuates neurofilament compaction and impaired axonal transport in injured axons following diffuse traumatic brain injury*. Exp Neurol, 2006. **197**(2): p. 353-62.
231. Oda, Y., et al., *Combinational therapy using hypothermia and the immunophilin ligand FK506 to target altered pial arteriolar reactivity, axonal damage, and blood-brain barrier dysfunction after traumatic brain injury in rat*. J Cereb Blood Flow Metab, 2011. **31**(4): p. 1143-54.
232. Singleton, R.H., et al., *The immunophilin ligand FK506 attenuates axonal injury in an impact-acceleration model of traumatic brain injury*. J Neurotrauma, 2001. **18**(6): p. 607-14.
233. Zawadzka, M., et al., *Early steps of microglial activation are directly affected by neuroprotectant FK506 in both in vitro inflammation and in rat model of stroke*. J Mol Med (Berl), 2012. **90**(12): p. 1459-71.
234. Hatton, J., et al., *Dosing and safety of cyclosporine in patients with severe brain injury*. J Neurosurg, 2008. **109**(4): p. 699-707.
235. Mazzeo, A.T., et al., *Safety and tolerability of cyclosporin a in severe traumatic brain injury patients: results from a prospective randomized trial*. J Neurotrauma, 2009. **26**(12): p. 2195-206.
236. Tsuji, A., et al., *Restricted transport of cyclosporin A across the blood-brain barrier by a multidrug transporter, P-glycoprotein*. Biochem Pharmacol, 1993. **46**(6): p. 1096-9.

237. Famiglio, L., et al., *Central nervous system toxicity of cyclosporine in a rat model*. *Transplantation*, 1989. **48**(2): p. 316-21.
238. Walker, R.W. and J.A. Brochstein, *Neurologic complications of immunosuppressive agents*. *Neurol Clin*, 1988. **6**(2): p. 261-78.
239. Wijdicks, E.F., R.H. Wiesner, and R.A. Krom, *Neurotoxicity in liver transplant recipients with cyclosporine immunosuppression*. *Neurology*, 1995. **45**(11): p. 1962-4.
240. de Groen, P.C., et al., *Central nervous system toxicity after liver transplantation. The role of cyclosporine and cholesterol*. *N Engl J Med*, 1987. **317**(14): p. 861-6.
241. Dixon, C.E., et al., *Cyclosporine Treatment in Traumatic Brain Injury: Operation Brain Trauma Therapy*. *J Neurotrauma*, 2015.
242. Berden, J.H., et al., *Severe central-nervous-system toxicity associated with cyclosporin*. *Lancet*, 1985. **1**(8422): p. 219-20.
243. Hughes, R.L., *Cyclosporine-related central nervous system toxicity in cardiac transplantation*. *N Engl J Med*, 1990. **323**(6): p. 420-1.
244. Reece, D.E., et al., *Neurologic complications in allogeneic bone marrow transplant patients receiving cyclosporin*. *Bone Marrow Transplant*, 1991. **8**(5): p. 393-401.
245. Gelderblom, H., et al., *Cremophor EL: the drawbacks and advantages of vehicle selection for drug formulation*. *Eur J Cancer*, 2001. **37**(13): p. 1590-8.
246. Vanhove, T., P. Annaert, and D.R. Kuypers, *Clinical determinants of calcineurin inhibitor disposition: a mechanistic review*. *Drug Metab Rev*, 2016. **48**(1): p. 88-112.
247. Mattiasson, G. and P.G. Sullivan, *The emerging functions of UCP2 in health, disease, and therapeutics*. *Antioxid Redox Signal*, 2006. **8**(1-2): p. 1-38.
248. Pandya, J.D., J.R. Pauly, and P.G. Sullivan, *The optimal dosage and window of opportunity to maintain mitochondrial homeostasis following traumatic brain injury using the uncoupler FCCP*. *Exp Neurol*, 2009. **218**(2): p. 381-9.
249. Greco, T., et al., *Ketogenic diet decreases oxidative stress and improves mitochondrial respiratory complex activity*. *J Cereb Blood Flow Metab*, 2015.
250. Sullivan, P.G., et al., *The ketogenic diet increases mitochondrial uncoupling protein levels and activity*. *Ann Neurol*, 2004. **55**(4): p. 576-80.
251. Xiong, Y., et al., *Prevention of mitochondrial dysfunction in post-traumatic mouse brain by superoxide dismutase*. *J Neurochem*, 2005. **95**(3): p. 732-44.
252. Chen, G., et al., *Role of the Nrf2-ARE pathway in early brain injury after experimental subarachnoid hemorrhage*. *J Neurosci Res*, 2011. **89**(4): p. 515-23.

253. Reed, T.T., et al., *Proteomic identification of nitrated brain proteins in traumatic brain-injured rats treated postinjury with gamma-glutamylcysteine ethyl ester: insights into the role of elevation of glutathione as a potential therapeutic strategy for traumatic brain injury*. J Neurosci Res, 2009. **87**(2): p. 408-17.
254. Xiong, Y., P.L. Peterson, and C.P. Lee, *Effect of N-acetylcysteine on mitochondrial function following traumatic brain injury in rats*. J Neurotrauma, 1999. **16**(11): p. 1067-82.
255. Lok, J., et al., *gamma-glutamylcysteine ethyl ester protects cerebral endothelial cells during injury and decreases blood-brain barrier permeability after experimental brain trauma*. J Neurochem, 2011. **118**(2): p. 248-55.
256. Hall, E.D., *Inhibition of lipid peroxidation in central nervous system trauma and ischemia*. J Neurol Sci, 1995. **134 Suppl**: p. 79-83.
257. Hamann, K., et al., *Hydralazine inhibits compression and acrolein-mediated injuries in ex vivo spinal cord*. J Neurochem, 2008. **104**(3): p. 708-18.
258. Burcham, P.C., et al., *Protein adduct-trapping by hydrazinophthalazine drugs: mechanisms of cytoprotection against acrolein-mediated toxicity*. Mol Pharmacol, 2004. **65**(3): p. 655-64.
259. LoPachin, R.M., et al., *Molecular mechanisms of 4-hydroxy-2-nonenal and acrolein toxicity: nucleophilic targets and adduct formation*. Chem Res Toxicol, 2009. **22**(9): p. 1499-508.
260. Lopachin, R.M., et al., *Application of the Hard and Soft, Acids and Bases (HSAB) theory to toxicant--target interactions*. Chem Res Toxicol, 2012. **25**(2): p. 239-51.
261. Burcham, P.C., et al., *Aldehyde-sequestering drugs: tools for studying protein damage by lipid peroxidation products*. Toxicology, 2002. **181-182**: p. 229-36.
262. Burcham, P.C. and S.M. Pyke, *Hydralazine inhibits rapid acrolein-induced protein oligomerization: role of aldehyde scavenging and adduct trapping in cross-link blocking and cytoprotection*. Mol Pharmacol, 2006. **69**(3): p. 1056-65.
263. Baker, G.B., et al., *Metabolism of monoamine oxidase inhibitors*. Cell Mol Neurobiol, 1999. **19**(3): p. 411-26.
264. van den Pol, A.N., K. Obrietan, and G. Chen, *Excitatory actions of GABA after neuronal trauma*. J Neurosci, 1996. **16**(13): p. 4283-92.
265. Alldredge, B.K., *Seizure risk associated with psychotropic drugs: clinical and pharmacokinetic considerations*. Neurology, 1999. **53**(5 Suppl 2): p. S68-75.
266. Gillman, P.K., *Advances pertaining to the pharmacology and interactions of irreversible nonselective monoamine oxidase inhibitors*. J Clin Psychopharmacol, 2011. **31**(1): p. 66-74.

267. Polasek, T.M., et al., *An evaluation of potential mechanism-based inactivation of human drug metabolizing cytochromes P450 by monoamine oxidase inhibitors, including isoniazid*. Br J Clin Pharmacol, 2006. **61**(5): p. 570-84.
268. Herman, L.L. and S.S. Bhimji, *Hydralazine*, in *StatPearls*. 2017: Treasure Island (FL).
269. Lyles, G.A., J. Garcia-Rodriguez, and B.A. Callingham, *Inhibitory actions of hydralazine upon monoamine oxidizing enzymes in the rat*. Biochem Pharmacol, 1983. **32**(17): p. 2515-21.
270. Zheng, L., et al., *Determination of urine 3-HPMA, a stable acrolein metabolite in a rat model of spinal cord injury*. J Neurotrauma, 2013. **30**(15): p. 1334-41.
271. Cheng, J.P., et al., *5-hydroxytryptamine1A (5-HT1A) receptor agonists: A decade of empirical evidence supports their use as an efficacious therapeutic strategy for brain trauma*. Brain Res, 2016. **1640**(Pt A): p. 5-14.
272. Damsma, G., et al., *Effects of transient forebrain ischemia and pargyline on extracellular concentrations of dopamine, serotonin, and their metabolites in the rat striatum as determined by in vivo microdialysis*. J Neurochem, 1990. **54**(3): p. 801-8.
273. Huang, W., et al., *Neuroprotective effect of rasagiline, a selective monoamine oxidase-B inhibitor, against closed head injury in the mouse*. Eur J Pharmacol, 1999. **366**(2-3): p. 127-35.
274. Tatton, W.G., et al., *(-)-Deprenyl reduces neuronal apoptosis and facilitates neuronal outgrowth by altering protein synthesis without inhibiting monoamine oxidase*. J Neural Transm Suppl, 1996. **48**: p. 45-59.
275. Wadia, J.S., et al., *Mitochondrial membrane potential and nuclear changes in apoptosis caused by serum and nerve growth factor withdrawal: time course and modification by (-)-deprenyl*. J Neurosci, 1998. **18**(3): p. 932-47.
276. Youdim, M.B., D. Edmondson, and K.F. Tipton, *The therapeutic potential of monoamine oxidase inhibitors*. Nat Rev Neurosci, 2006. **7**(4): p. 295-309.
277. Maruyama, W. and M. Naoi, *Neuroprotection by (-)-deprenyl and related compounds*. Mech Ageing Dev, 1999. **111**(2-3): p. 189-200.
278. Song, M.S., et al., *An update on amine oxidase inhibitors: multifaceted drugs*. Prog Neuropsychopharmacol Biol Psychiatry, 2013. **44**: p. 118-24.
279. Kiray, M., et al., *Deprenyl and the relationship between its effects on spatial memory, oxidant stress and hippocampal neurons in aged male rats*. Physiol Res, 2006. **55**(2): p. 205-12.
280. Margulies, S., et al., *Combination Therapies for Traumatic Brain Injury: Retrospective Considerations*. J Neurotrauma, 2016. **33**(1): p. 101-12.

281. Sullivan, P.G., et al., *Dietary supplement creatine protects against traumatic brain injury*. *Ann Neurol*, 2000. **48**(5): p. 723-9.
282. Dunkerson, J., et al., *Combining enriched environment and induced pluripotent stem cell therapy results in improved cognitive and motor function following traumatic brain injury*. *Restor Neurol Neurosci*, 2014. **32**(5): p. 675-87.
283. Abdel Baki, S.G., et al., *Minocycline synergizes with N-acetylcysteine and improves cognition and memory following traumatic brain injury in rats*. *PLoS One*, 2010. **5**(8): p. e12490.
284. Faden, A.I., et al., *The role of excitatory amino acids and NMDA receptors in traumatic brain injury*. *Science*, 1989. **244**(4906): p. 798-800.
285. Gilmer, L.K., et al., *Early mitochondrial dysfunction after cortical contusion injury*. *J Neurotrauma*, 2009. **26**(8): p. 1271-80.
286. Buki, A., et al., *The role of calpain-mediated spectrin proteolysis in traumatically induced axonal injury*. *J Neuropathol Exp Neurol*, 1999. **58**(4): p. 365-75.
287. Lifshitz, J., et al., *Mitochondrial damage and dysfunction in traumatic brain injury*. *Mitochondrion*, 2004. **4**(5-6): p. 705-13.
288. Raghupathi, R., *Cell death mechanisms following traumatic brain injury*. *Brain Pathol*, 2004. **14**(2): p. 215-22.
289. Xiong, Y., et al., *Mitochondrial dysfunction after experimental traumatic brain injury: combined efficacy of SNX-111 and U-101033E*. *J Neurotrauma*, 1998. **15**(7): p. 531-44.
290. Bernardi, P., *The permeability transition pore. Control points of a cyclosporin A-sensitive mitochondrial channel involved in cell death*. *Biochim Biophys Acta*, 1996. **1275**(1-2): p. 5-9.
291. Prins, M.L., L.S. Fujima, and D.A. Hovda, *Age-dependent reduction of cortical contusion volume by ketones after traumatic brain injury*. *J Neurosci Res*, 2005. **82**(3): p. 413-20.
292. Kilbaugh, T.J., et al., *Cyclosporin A preserves mitochondrial function after traumatic brain injury in the immature rat and piglet*. *J Neurotrauma*, 2011. **28**(5): p. 763-74.
293. Azevedo, F.A., et al., *Equal numbers of neuronal and nonneuronal cells make the human brain an isometrically scaled-up primate brain*. *J Comp Neurol*, 2009. **513**(5): p. 532-41.
294. Sullivan, P.G., et al., *Dose-response curve and optimal dosing regimen of cyclosporin A after traumatic brain injury in rats*. *Neuroscience*, 2000. **101**(2): p. 289-95.

295. Brown, M.R., et al., *Nitrogen disruption of synaptoneurosome: an alternative method to isolate brain mitochondria*. J Neurosci Methods, 2004. **137**(2): p. 299-303.
296. Kristian, T., et al., *Isolation of mitochondria with high respiratory control from primary cultures of neurons and astrocytes using nitrogen cavitation*. J Neurosci Methods, 2006. **152**(1-2): p. 136-43.
297. Waldmeier, P.C., et al., *Inhibition of the mitochondrial permeability transition by the nonimmunosuppressive cyclosporin derivative NIM811*. Mol Pharmacol, 2002. **62**(1): p. 22-9.
298. Okonkwo, D.O., et al., *Dose-response of cyclosporin A in attenuating traumatic axonal injury in rat*. Neuroreport, 2003. **14**(3): p. 463-6.
299. Signoretti, S., et al., *The protective effect of cyclosporin A upon N-acetylaspartate and mitochondrial dysfunction following experimental diffuse traumatic brain injury*. J Neurotrauma, 2004. **21**(9): p. 1154-67.
300. Sanchez, H., et al., *Immunosuppressive treatment affects cardiac and skeletal muscle mitochondria by the toxic effect of vehicle*. J Mol Cell Cardiol, 2000. **32**(2): p. 323-31.
301. Sanchez, H., et al., *Effect of cyclosporin A and its vehicle on cardiac and skeletal muscle mitochondria: relationship to efficacy of the respiratory chain*. Br J Pharmacol, 2001. **133**(6): p. 781-8.
302. Nassberger, L., *Effect of cyclosporin A and different vehicles on ATP production in mitochondria isolated from the rat kidney cortex*. Pharmacol Toxicol, 1990. **67**(2): p. 147-50.
303. Sauerbeck, A., et al., *Pioglitazone attenuates mitochondrial dysfunction, cognitive impairment, cortical tissue loss, and inflammation following traumatic brain injury*. Exp Neurol, 2011. **227**(1): p. 128-35.
304. Lai, J.C. and J.B. Clark, *Preparation and properties of mitochondria derived from synaptosomes*. Biochem J, 1976. **154**(2): p. 423-32.
305. Opii, W.O., et al., *Proteomic identification of oxidized mitochondrial proteins following experimental traumatic brain injury*. J Neurotrauma, 2007. **24**(5): p. 772-89.
306. Robertson, C.L., M. Saraswati, and G. Fiskum, *Mitochondrial dysfunction early after traumatic brain injury in immature rats*. J Neurochem, 2007. **101**(5): p. 1248-57.
307. Brand, M.D., et al., *Mitochondrial superoxide: production, biological effects, and activation of uncoupling proteins*. Free Radic Biol Med, 2004. **37**(6): p. 755-67.
308. Radi, R., *Peroxynitrite reactions and diffusion in biology*. Chem Res Toxicol, 1998. **11**(7): p. 720-1.



309. Kulbe, J.R., et al., *Synaptic Mitochondria Sustain More Damage Than Non-Synaptic Mitochondria Following Traumatic Brain Injury and Are Protected by Cyclosporine A*. J Neurotrauma, 2016.
310. Xiong, Y., I.N. Singh, and E.D. Hall, *Tempol protection of spinal cord mitochondria from peroxynitrite-induced oxidative damage*. Free Radic Res, 2009. **43**(6): p. 604-12.
311. Song, M.S., et al., *The antidepressant phenelzine protects neurons and astrocytes against formaldehyde-induced toxicity*. J Neurochem, 2010. **114**(5): p. 1405-13.
312. Burcham, P.C., P.G. Kerr, and F. Fontaine, *The antihypertensive hydralazine is an efficient scavenger of acrolein*. Redox Rep, 2000. **5**(1): p. 47-9.
313. McEwen, M.L., P.G. Sullivan, and J.E. Springer, *Pretreatment with the cyclosporin derivative, NIM811, improves the function of synaptic mitochondria following spinal cord contusion in rats*. J Neurotrauma, 2007. **24**(4): p. 613-24.
314. Osier, N.D. and C.E. Dixon, *The Controlled Cortical Impact Model: Applications, Considerations for Researchers, and Future Directions*. Front Neurol, 2016. **7**: p. 134.
315. Xiong, Y., et al., *Amelioration of mitochondrial function by a novel antioxidant U-101033E following traumatic brain injury in rats*. J Neurotrauma, 1997. **14**(12): p. 907-17.
316. Liu, J., et al., *Calcineurin is a common target of cyclophilin-cyclosporin A and FKBP-FK506 complexes*. Cell, 1991. **66**(4): p. 807-15.
317. Basso, E., et al., *Properties of the permeability transition pore in mitochondria devoid of Cyclophilin D*. J Biol Chem, 2005. **280**(19): p. 18558-61.
318. Brustovetsky, N. and J.M. Dubinsky, *Limitations of cyclosporin A inhibition of the permeability transition in CNS mitochondria*. J Neurosci, 2000. **20**(22): p. 8229-37.
319. Chinopoulos, C., A.A. Starkov, and G. Fiskum, *Cyclosporin A-insensitive permeability transition in brain mitochondria: inhibition by 2-aminoethoxydiphenyl borate*. J Biol Chem, 2003. **278**(30): p. 27382-9.
320. Garcia, N., et al., *On the opening of an insensitive cyclosporin A non-specific pore by phenylarsine plus mersalyl*. Cell Biochem Biophys, 2007. **49**(2): p. 84-90.
321. McKee, C.A. and J.R. Lukens, *Emerging Roles for the Immune System in Traumatic Brain Injury*. Front Immunol, 2016. **7**: p. 556.
322. Hill, R.L., et al., *Synaptic Mitochondria are More Susceptible to Traumatic Brain Injury-induced Oxidative Damage and Respiratory Dysfunction than Non-synaptic Mitochondria*. Neuroscience, 2018. **386**: p. 265-283.

323. Gizatullina, Z.Z., et al., *Effects of cyclosporine A and its immunosuppressive or non-immunosuppressive derivatives [D-Ser]8-CsA and Cs9 on mitochondria from different brain regions*. Mitochondrion, 2011. **11**(3): p. 421-9.
324. Furman, J.L., et al., *Blockade of Astrocytic Calcineurin/NFAT Signaling Helps to Normalize Hippocampal Synaptic Function and Plasticity in a Rat Model of Traumatic Brain Injury*. J Neurosci, 2016. **36**(5): p. 1502-15.
325. Panter, S.S., J.M. Braugher, and E.D. Hall, *Dextran-coupled deferoxamine improves outcome in a murine model of head injury*. J Neurotrauma, 1992. **9**(1): p. 47-53.
326. Kristal, B.S., B.K. Park, and B.P. Yu, *4-Hydroxyhexenal is a potent inducer of the mitochondrial permeability transition*. J Biol Chem, 1996. **271**(11): p. 6033-8.
327. Edmondson, D.E., et al., *Molecular and mechanistic properties of the membrane-bound mitochondrial monoamine oxidases*. Biochemistry, 2009. **48**(20): p. 4220-30.
328. Kobori, N., B. Hu, and P.K. Dash, *Altered adrenergic receptor signaling following traumatic brain injury contributes to working memory dysfunction*. Neuroscience, 2011. **172**: p. 293-302.
329. Prakash, R. and S.T. Carmichael, *Blood-brain barrier breakdown and neovascularization processes after stroke and traumatic brain injury*. Curr Opin Neurol, 2015. **28**(6): p. 556-64.
330. Matveychuk, D., et al., *Elevation of rat brain tyrosine levels by phenelzine is mediated by its active metabolite beta-phenylethylidenehydrazine*. Prog Neuropsychopharmacol Biol Psychiatry, 2014. **53**: p. 67-73.
331. Hamann, K. and R. Shi, *Acrolein scavenging: a potential novel mechanism of attenuating oxidative stress following spinal cord injury*. J Neurochem, 2009. **111**(6): p. 1348-56.
332. Hall, E.D., et al., *Newer pharmacological approaches for antioxidant neuroprotection in traumatic brain injury*. Neuropharmacology, 2019. **145**(Pt B): p. 247-258.
333. Kulbe, J.R., et al., *Continuous Infusion of Phenelzine, Cyclosporine a or the Combination: Evaluation of Mitochondrial Bioenergetics, Oxidative Damage and Cytoskeletal Degradation Following Severe Controlled Cortical Impact Traumatic Brain Injury in Rats*. J Neurotrauma, 2018.
334. Hill, R.L., et al., *The Effects of Phenelzine Administration of Mitochondrial Function, Calcium Handling and Cytoskeletal Degradation Following Experimental Traumatic Brain Injury*. J Neurotrauma, 2018.
335. Paslawski, T., et al., *The antidepressant drug phenelzine produces antianxiety effects in the plus-maze and increases in rat brain GABA*. Psychopharmacology (Berl), 1996. **127**(1): p. 19-24.

336. Wood, P.L., M.A. Khan, and J.R. Moskal, *The concept of "aldehyde load" in neurodegenerative mechanisms: cytotoxicity of the polyamine degradation products hydrogen peroxide, acrolein, 3-aminopropanal, 3-acetamidopropanal and 4-aminobutanal in a retinal ganglion cell line*. Brain Res, 2007. **1145**: p. 150-6.
337. Lin, Y., et al., *Acrolein Contributes to the Neuropathic Pain and Neuron Damage after Ischemic-Reperfusion Spinal Cord Injury*. Neuroscience, 2018. **384**: p. 120-130.
338. Due, M.R., et al., *Acrolein involvement in sensory and behavioral hypersensitivity following spinal cord injury in the rat*. J Neurochem, 2014. **128**(5): p. 776-786.
339. Latz, A., et al., *Maze learning after the administration of antidepressant drugs*. J Pharmacol Exp Ther, 1967. **156**(1): p. 76-84.
340. Simpson, S.M., et al., *The antidepressant phenelzine enhances memory in the double Y-maze and increases GABA levels in the hippocampus and frontal cortex of rats*. Pharmacol Biochem Behav, 2012. **102**(1): p. 109-17.
341. Pfizer. *Nardil: Phenelzine sulfate tablets* 2009 [cited 2019; Available from: [https://www.pfizer.com/files/products/uspi\\_nardil.pdf](https://www.pfizer.com/files/products/uspi_nardil.pdf)].
342. Parent, M.B., M.K. Habib, and G.B. Baker, *Time-dependent changes in brain monoamine oxidase activity and in brain levels of monoamines and amino acids following acute administration of the antidepressant/antipanic drug phenelzine*. Biochem Pharmacol, 2000. **59**(10): p. 1253-63.
343. Konigs, M., et al., *Effects of Timing and Intensity of Neurorehabilitation on Functional Outcome After Traumatic Brain Injury: A Systematic Review and Meta-Analysis*. Arch Phys Med Rehabil, 2018. **99**(6): p. 1149-1159 e1.
344. INESS-ONF. *Clinical Practice Guideline for the Rehabilitation of Adults with Moderate to Severe TBI*. 2015 [cited 2019; Available from: <https://braininjuryguidelines.org/modtosevere/>].
345. Turner, P.V., et al., *Administration of substances to laboratory animals: routes of administration and factors to consider*. J Am Assoc Lab Anim Sci, 2011. **50**(5): p. 600-13.
346. Flockhart, D.A., *Dietary restrictions and drug interactions with monoamine oxidase inhibitors: an update*. J Clin Psychiatry, 2012. **73 Suppl 1**: p. 17-24.
347. Fowler, C.J. and M.S. Benedetti, *The metabolism of dopamine by both forms of monoamine oxidase in the rat brain and its inhibition by cimoxatone*. J Neurochem, 1983. **40**(6): p. 1534-41.
348. Versteeg, D.H., et al., *Regional concentrations of noradrenaline and dopamine in rat brain*. Brain Res, 1976. **113**(3): p. 563-74.

349. Best, J.A., H.F. Nijhout, and M.C. Reed, *Homeostatic mechanisms in dopamine synthesis and release: a mathematical model*. Theor Biol Med Model, 2009. **6**: p. 21.
350. Adan, R.A., *Mechanisms underlying current and future anti-obesity drugs*. Trends Neurosci, 2013. **36**(2): p. 133-40.
351. Willis, G.L. and G.C. Smith, *Anorexic properties of three monoamine oxidase inhibitors*. Pharmacol Biochem Behav, 1982. **17**(6): p. 1135-9.
352. Wood, S., et al., *Psychostimulants and cognition: a continuum of behavioral and cognitive activation*. Pharmacol Rev, 2014. **66**(1): p. 193-221.
353. McNamara, R.K. and R.W. Skelton, *The neuropharmacological and neurochemical basis of place learning in the Morris water maze*. Brain Res Brain Res Rev, 1993. **18**(1): p. 33-49.
354. Villegier, A.S., et al., *Irreversible blockade of monoamine oxidases reveals the critical role of 5-HT transmission in locomotor response induced by nicotine in mice*. Eur J Neurosci, 2006. **24**(5): p. 1359-65.
355. Geyer, M.A., *Serotonergic functions in arousal and motor activity*. Behav Brain Res, 1996. **73**(1-2): p. 31-5.
356. Zhang, B. and J.C. Gensel, *Is neuroinflammation in the injured spinal cord different than in the brain? Examining intrinsic differences between the brain and spinal cord*. Exp Neurol, 2014. **258**: p. 112-20.
357. Shi, R., J.C. Page, and M. Tully, *Molecular mechanisms of acrolein-mediated myelin destruction in CNS trauma and disease*. Free Radic Res, 2015. **49**(7): p. 888-95.
358. Park, J., et al., *Acrolein contributes to TRPA1 up-regulation in peripheral and central sensory hypersensitivity following spinal cord injury*. J Neurochem, 2015. **135**(5): p. 987-97.
359. Butler, B., G. Acosta, and R. Shi, *Exogenous Acrolein intensifies sensory hypersensitivity after spinal cord injury in rat*. J Neurol Sci, 2017. **379**: p. 29-35.
360. Kataria, H., et al., *Small Molecule Agonists of Cell Adhesion Molecule L1 Mimic L1 Functions In Vivo*. Mol Neurobiol, 2016. **53**(7): p. 4461-83.
361. Li, R., S. Sahu, and M. Schachner, *Phenelzine, a cell adhesion molecule L1 mimetic small organic compound, promotes functional recovery and axonal regrowth in spinal cord-injured zebrafish*. Pharmacol Biochem Behav, 2018. **171**: p. 30-38.
362. Li, R., S. Sahu, and M. Schachner, *Phenelzine, a small organic compound mimicking the functions of cell adhesion molecule L1, promotes functional recovery after mouse spinal cord injury*. Restor Neurol Neurosci, 2018. **36**(4): p. 469-483.

363. Dunn-Meynell, A.A., M. Hassanain, and B.E. Levin, *Norepinephrine and traumatic brain injury: a possible role in post-traumatic edema*. Brain Res, 1998. **800**(2): p. 245-52.
364. Huger, F. and G. Patrick, *Effect of concussive head injury on central catecholamine levels and synthesis rates in rat brain regions*. J Neurochem, 1979. **33**(1): p. 89-95.
365. Bales, J.W., et al., *Persistent cognitive dysfunction after traumatic brain injury: A dopamine hypothesis*. Neurosci Biobehav Rev, 2009. **33**(7): p. 981-1003.
366. Di Battista, A.P., et al., *Inflammatory cytokine and chemokine profiles are associated with patient outcome and the hyperadrenergic state following acute brain injury*. J Neuroinflammation, 2016. **13**: p. 40.
367. Chen, W., et al., *Early stage alterations of catecholamine and adrenocorticotrophic hormone levels in posttraumatic acute diffuse brain swelling*. Brain Res Bull, 2017. **130**: p. 47-52.
368. Kroppenstedt, S.N., et al., *Influence of norepinephrine and dopamine on cortical perfusion, EEG activity, extracellular glutamate, and brain edema in rats after controlled cortical impact injury*. J Neurotrauma, 2002. **19**(11): p. 1421-32.
369. Van Landeghem, F.K., et al., *Differential concentration-dependent effects of prolonged norepinephrine infusion on intraparenchymal hemorrhage and cortical contusion in brain-injured rats*. J Neurotrauma, 2003. **20**(12): p. 1327-37.
370. Moridani, M.Y., et al., *Cytochrome P450 2E1 metabolically activates propargyl alcohol: propionaldehyde-induced hepatocyte cytotoxicity*. Chem Biol Interact, 2001. **130-132**(1-3): p. 931-42.
371. Garcia-Suastegui, W.A., et al., *The Role of CYP2E1 in the Drug Metabolism or Bioactivation in the Brain*. Oxid Med Cell Longev, 2017. **2017**: p. 4680732.
372. Dixon, C.E., et al., *A controlled cortical impact model of traumatic brain injury in the rat*. J Neurosci Methods, 1991. **39**(3): p. 253-62.
373. Hemerka, J.N., et al., *Severe brief pressure-controlled hemorrhagic shock after traumatic brain injury exacerbates functional deficits and long-term neuropathological damage in mice*. J Neurotrauma, 2012. **29**(12): p. 2192-208.
374. Kroppenstedt, S.N., et al., *Effect of cerebral perfusion pressure on contusion volume following impact injury*. J Neurosurg, 1999. **90**(3): p. 520-6.
375. Dehghan, E., et al., *Hydralazine induces stress resistance and extends C. elegans lifespan by activating the NRF2/SKN-1 signalling pathway*. Nat Commun, 2017. **8**(1): p. 2223.
376. DiMartini, A., *Isoniazid, tricyclics and the "cheese reaction"*. Int Clin Psychopharmacol, 1995. **10**(3): p. 197-8.

377. Rangel-Castilla, L., et al., *Cerebral pressure autoregulation in traumatic brain injury*. Neurosurg Focus, 2008. **25**(4): p. E7.
378. Dar, A., et al., *Inhibition of monoamine oxidase-A activity in rat brain by synthetic hydrazines: structure-activity relationship (SAR)*. J Enzyme Inhib Med Chem, 2005. **20**(3): p. 269-74.
379. Bhattacharya, S.K., et al., *Stress causes an increase in endogenous monoamine oxidase inhibitor (tribulin) in rat brain*. Neurosci Lett, 1988. **92**(2): p. 218-21.
380. Zhou, G., et al., *Platelet monoamine oxidase B and plasma beta-phenylethylamine in Parkinson's disease*. J Neurol Neurosurg Psychiatry, 2001. **70**(2): p. 229-31.
381. Karlsson, M., et al., *Neuroprotective Effects of Cyclosporine in a Porcine Pre-Clinical Trial of Focal Traumatic Brain Injury*. J Neurotrauma, 2018.
382. Ehinger, K.H., et al., *Bioequivalence and tolerability assessment of a novel intravenous ciclosporin lipid emulsion compared to branded ciclosporin in Cremophor (R) EL*. Clin Drug Investig, 2013. **33**(1): p. 25-34.
383. Pharmaceutical, N. *TBI\_presentation* 2017 October 23, 2017 [cited 2019; Available from: [http://www.neurovive.com/wp-content/uploads/2017/10/TBI\\_presentation\\_23Oct\\_-2017\\_for-the-webpage.pdf](http://www.neurovive.com/wp-content/uploads/2017/10/TBI_presentation_23Oct_-2017_for-the-webpage.pdf)].
384. Kochanek, P.M., et al., *Approach to Modeling, Therapy Evaluation, Drug Selection, and Biomarker Assessments for a Multicenter Pre-Clinical Drug Screening Consortium for Acute Therapies in Severe Traumatic Brain Injury: Operation Brain Trauma Therapy*. J Neurotrauma, 2016. **33**(6): 513-22.
385. Mehlman, M.J., *Cognition-enhancing drugs*. Milbank Q, 2004. **82**(3): 483-506.
386. Terry, A.V., Jr, *Spatial Navigation (Water Maze) Tasks*, in *Methods of Behavior Analysis in Neuroscience*, J.J. Buccafusco, Ed. 2009: Boca Raton (FL).
387. Kelso, M.L., et al., *Melatonin and minocycline for combinational therapy to improve functional and histopathological functional deficits following traumatic brain injury*. Neurosci Lett, 2011. **488**(1): 60-4.
388. Su, D., et al., *Isoflurane-induced spatial memory impairment in mice is prevented by the acetylcholinesterase inhibitor donepezil*. PloS One, 2011. **6**(11): e27632.

## VITA

Jacqueline Renee Kulbe

### Education

University of Kentucky College of Medicine, Lexington, KY

Clinical and Translational Sciences Certificate 2018

Doctor of Philosophy 2014 – Present

Department of Neuroscience  
Spinal Cord and Brain Injury Research Center

Doctor of Medicine 2012 – Present

Promoted with High Distinction (2012 – 2013)  
Promoted with High Distinction (2013 – 2014)

University of Denver, Denver, CO 2004

Bachelor of Science in Biology  
Magna cum laude, Phi Beta Kappa  
Minors in chemistry and mathematics

### Research Experience

Graduate Research Assistant (with Dr. Edward Hall) 2015 – Present  
University of Kentucky College of Medicine, Lexington, KY  
Department of Neuroscience, Spinal Cord & Brain Injury Research Center

MD/PhD Student Research Rotation (with Dr. James Geddes) 2014  
University of Kentucky College of Medicine, Lexington, KY  
Department of Neuroscience, Spinal Cord & Brain Injury Research Center

MD/PhD Student Summer Research Rotation (with Dr. Patrick Sullivan) 2012  
University of Kentucky College of Medicine, Lexington, KY  
Department of Neuroscience, Spinal Cord & Brain Injury Research Center

Professional Research Assistant (with Dr. K. Ulrich Bayer) 2007 – 2011  
University of Colorado Denver School of Medicine, Denver, CO  
Department of Pharmacology

Biological Research Technician (with Dr. Kim Heidenreich) 2005 – 2006  
University of Colorado Denver School of Medicine, Denver, CO  
Department of Pharmacology

## **Publications**

Hill RL, **Kulbe JR**, Singh IN, Wang JA, Hall ED. Synaptic mitochondria are more susceptible to traumatic brain injury-induced oxidative damage and respiratory dysfunction than non-synaptic mitochondria. *Neuroscience* 386:265-283 (2018)

**Kulbe JR**, Singh IN, Wang JA, Cebak JE, Hall ED. Continuous infusion of phenelzine, cyclosporine A, or their combination: evaluation of mitochondrial respiration, oxidative damage, and spectrin degradation following severe controlled cortical impact injury. *J Neurotrauma* 35(11): 1280 - 1293 (2018)

**Kulbe JR** and Hall ED. Chronic traumatic encephalopathy-integration of canonical traumatic brain injury secondary injury mechanisms with tau pathology. *Prog Neurobiol* 158: 15-44 (2017) *Review*

**Kulbe JR**, Hill RL, Singh IN, Wang JA, Hall ED. Synaptic mitochondria sustain more damage than non-synaptic mitochondria following traumatic brain injury and are protected by cyclosporine A. *J Neurotrauma* 34(7): 1291-1301 (2017)

Cebak JE, Singh IN, Wang JA, Hill RL, **Kulbe JR**, Hall ED. Carbonyl scavenging as an antioxidant neuroprotective strategy for acute traumatic brain injury, in *New Therapeutics for Traumatic Brain Injury: Prevention of Secondary Brain Damage and Enhancement of Repair and Regeneration*, Heidenreich KA (ed.), Academic Press (2016) *Book chapter*

**Kulbe JR** and Geddes JW. Current status of fluid biomarkers in mild traumatic brain injury. *Exp Neurol* 375:334-352 (2016) *Review*

Barcomb K, Buard I, Coultrap SJ, **Kulbe JR**, O'Leary H, Benke TA, Bayer KU. Autonomous CaMKII requires further stimulation by Ca<sup>2+</sup>/calmodulin for enhancing synaptic strength. *FASEB J* 28: 3810-9 (2014)

**Kulbe JR**, Mulcahy Levy JM, Coultrap SJ, Thorburn A, Bayern KU. Excitotoxic glutamate insults block autophagic flux in hippocampal neurons. *Brain Res* 1542: 12-19 (2014)

Coultrap SJ, Buard I, **Kulbe JR**, Dell'Acqua ML, Bayer KU. CaMKII autonomy is substrate-dependent and further stimulated by Ca<sup>2+</sup>/calmodulin. *J Biol Chem* 285: 17930-17937 (2010)

## **Acknowledgements**

Coultrap SJ, Bayer KU. Nitric oxide induces Ca<sup>2+</sup>-independent activity of the Ca<sup>2+</sup>/calmodulin-dependent protein kinase II (CaMKII). *J Biol Chem* 289: 19458-19465 (2014)



Coultrap SJ, Barcomb K, Bayer KU. A significant but rather mild contribution of T286 autophosphorylation to Ca<sup>2+</sup>/CaM-stimulated CaMKII activity. PLoS One 7: e37176 (2012)

O'Leary H, Liu WH, Rorabaugh JM, Coultrap SJ, Bayer KU. Nucleotides and phosphorylation bi-directionally modulate Ca<sup>2+</sup>/calmodulin-dependent protein kinase II (CaMKII) binding to the N-methyl-D-aspartate (NMDA) receptor subunit GluN2B. J Biol Chem 286: 31272-31281 (2011)

Coultrap SJ, Bayer KU. Improving a natural CaMKII inhibitor by random and rational design. PLoS One 6: e25245 (2011)

### **National Posters and Abstracts**

**Kulbe JR**, Dunkerson JA, Huettl PF, Wang JA, Smith R, and Hall ED *“Phenelzine, pargyline, and hydralazine: the effects of lipid-peroxidation-derived aldehyde scavenging and monoamine oxidase inhibition on learning and memory and cortical tissue sparing following experimental TBI”* Poster presented at 45<sup>th</sup> Annual Eastern-Atlantic Student Research Forum, Miami, FL (2019).

**Kulbe JR**, Singh IN, Dunkerson JA, Wang JA, Huettl PF, Hill RL, Smith R, and Hall ED *“Neuroprotective Strategies following experimental traumatic brain injury: inhibition of permeability transition, lipid-peroxidation derived aldehyde scavenging, and monoamine oxidase inhibition”* Poster presented at 48<sup>th</sup> Annual Society for Neuroscience Meeting, San Diego, CA (2018). Program No. 567.02. 2018 Neuroscience Meeting Planner. San Diego, CA: Society for Neuroscience, 2018. Online.

**Kulbe JR**, Singh IN, Dunkerson JA, Wang JA, Cebak JE, Hill RL, Smith R, Huettl PF, and Hall ED *“A pharmacologic neuroprotective approach to experimental TBI: targeting mitochondria & lipid peroxidation-derived aldehydes”* Poster presented at 3<sup>rd</sup> Joint Symposium of the International and National Neurotrauma Societies, Toronto, Canada (2018). Journal of Neurotrauma: 35: PS1.04.182 (2018)

**Kulbe JR**, Singh IN, Dunkerson JA, Wang JA, Cebak JE, Hill RL, Smith R, Huettl PF, and Hall ED *“A pharmacologic neuroprotective approach to severe traumatic brain injury: targeting mitochondria and lipid peroxidation”* Poster presented at AAP/ASCI/APSA 2018 Joint Meeting, Chicago, IL (2018)

**Kulbe JR**, Singh IN, Cebak JE, Wang JA, and Hall ED *“Neuroprotective strategies following severe controlled impact traumatic brain injury: lipid peroxidation-derived neurotoxic aldehyde scavenging and inhibition of mitochondrial permeability transition”* Poster at 47<sup>th</sup> Annual Society for Neuroscience Meeting, Washington, DC (2017). Program No. 395.19. 2017 Neuroscience Meeting Planner. Washington, DC: Society for Neuroscience, 2017. Online.

**Kulbe JR**, Singh IN, Cebak JE, Wang JA, and Hall ED “*Neuroprotective evaluation of the combination phenelzine and cyclosporine A following severe controlled cortical impact traumatic brain injury*” Poster presented at 35<sup>th</sup> Annual National Neurotrauma Symposium, Snowbird, UT (2017). Journal of Neurotrauma: 34: A-1-A-164 (2017)

Hill RL, Singh IN, Wang JA, **Kulbe JR**, Hall ED “*Phenelzine administration following traumatic brain injury improves synaptic and non-synaptic mitochondrial respiratory function*” Poster at 35<sup>th</sup> Annual National Neurotrauma Symposium, Snowbird, UT (2017). Journal of Neurotrauma: 34: A-1-A-164 (2017)

**Kulbe JR**, Singh IN, Wang JA, and Hall ED “*Evaluation of the combinational therapy cyclosporine A and phenelzine on protection of mitochondria following severe controlled cortical impact injury*” Poster presented at AAP/ASCI/APSA 2017 Joint Meeting, Chicago, IL (2017)

**Kulbe JR**, Hill RL, Singh IN, Wang JA, and Hall ED “*Cyclosporine A protects synaptic and non-synaptic mitochondria following severe controlled cortical impact injury in rats*” Poster presented at 34<sup>th</sup> Annual National Neurotrauma Symposium, Lexington, KY (2016). Journal of Neurotrauma: 33(13): A-1-A-139 (2016)

Hill RL, Singh IN, Wang JA, **Kulbe JR**, and Hall ED “*Differing time courses of synaptic & non-synaptic mitochondrial dysfunction & oxidative damage following TBI in young adult males*” Poster at 34<sup>th</sup> Annual National Neurotrauma Symposium, Lexington, KY (2016). Journal of Neurotrauma: 33(13): A-1-A-139 (2016)

**Kulbe JR**, Hill RL, Singh IN, Wang JA, and Hall ED “*Temporal profile of non-synaptic and synaptic mitochondrial bioenergetics following severe controlled cortical impact traumatic brain injury in rats*” Poster presented at 3<sup>rd</sup> Annual Molecular Psychiatry Meeting, San Francisco, CA (2015)

### **Regional, Local, Institutional Posters and Abstracts**

**Kulbe JR**, Dunkerson JA, Huettl PF, Wang JA, Smith R, and Hall ED “*Phenelzine, pargyline, and hydralazine: the effects of lipid-peroxidation-derived aldehyde scavenging and monoamine oxidase inhibition on learning and memory and cortical tissue sparing following experimental TBI*” Poster presented at 14<sup>th</sup> Annual Center for Clinical and Translational Sciences Spring Conference, Lexington, KY (2019)

**Kulbe JR**, Singh IN, Dunkerson JA, Wang JA, Hill RL, Smith R, Huettl PF, and Hall ED “*Neuroprotective strategies following experimental traumatic brain injury: inhibition of mitochondrial permeability transition, lipid peroxidation-derived aldehyde formation, and monoamine oxidase*” Poster presented at University of Kentucky Department of Neurology Resident and Trainee Research Day, Lexington, KY (2018)

**Kulbe JR**, Singh IN, Dunkerson JA, Wang JA, Hill RL, Smith R, Huettl PF, and Hall ED *“Neuroprotective strategies following severe controlled impact traumatic brain injury: lipid peroxidation-derived neurotoxic aldehyde scavenging and inhibition of mitochondrial permeability transition”* Poster presented at 24<sup>th</sup> Annual KSCHIRT Symposium, Lexington, KY (2018)

**Kulbe JR**, Singh IN, Dunkerson JA, Wang JA, Hill RL, Smith R, Huettl PF, and Hall ED *“Neuroprotective strategies following severe controlled impact traumatic brain injury: lipid peroxidation-derived neurotoxic aldehyde scavenging and inhibition of mitochondrial permeability transition”* Poster presented at 13<sup>th</sup> Annual Center for Clinical and Translational Sciences Spring Conference, Lexington, KY (2018)

**Kulbe JR**, Singh IN, Wang JA, and Hall ED *“Neuroprotective evaluation of the combination phenelzine and cyclosporine A following severe controlled cortical impact traumatic brain injury”* Poster presented at 23<sup>rd</sup> Annual KSCHIRT Symposium, Louisville, KY (2017)

**Kulbe JR**, Singh IN, Wang JA, and Hall ED *“Evaluation of the combinational therapy cyclosporine A and phenelzine on protection of mitochondrial respiratory function following severe controlled cortical impact injury in rats”* Poster presented at 12<sup>th</sup> Annual Center for Clinical and Translational Sciences Spring Conference, Lexington, KY (2017)

**Kulbe JR**, Hill RL, Singh IN, Wang JA, and Hall ED *“Cyclosporine A protects synaptic and non-synaptic mitochondria following severe controlled cortical impact injury in rats”* Poster at Kentucky Neuroscience Institute Clinical-Translational Research Symposium, Lexington, KY (2016)

**Kulbe JR**, Hill RL, Singh IN, Wang JA, and Hall ED *“Cyclosporine A protects synaptic and non-synaptic mitochondrial bioenergetics 24h following severe controlled cortical impact injury”* Poster presented at 31<sup>st</sup> Annual Bluegrass Society for Neuroscience Spring Neuroscience Research Day, Lexington, KY (2016)

**Kulbe JR**, Hill RL, Singh IN, Wang JA, and Hall ED *“Cyclosporine A protects synaptic and non-synaptic mitochondria and attenuates calpain-mediated cytoskeletal degradation 24h following severe controlled cortical impact traumatic brain injury in rats”* Poster presented at University of Kentucky AOA Groves Memorial MD/PhD Student Research Day, Lexington, KY (2016)

**Kulbe JR** and Geddes JW *“Identification of novel serum biomarkers for mild traumatic brain injury using phage display”* Poster presented at University of Kentucky AOA Groves Memorial MD/PhD Student Research Day, Lexington, KY (2015)

**Kulbe JR**, Mulcahy Levy JM, Coultrap SJ, Thorburn A, and Bayer KU “*Excitotoxic glutamate insults block autophagic flux in hippocampal neurons*” Poster presented at University of Kentucky AOA Groves Memorial MD/PhD Student Research Day, Lexington, KY (2014)

**Kulbe JR**, Mulcahy Levy JM, Coultrap SJ, Thorburn A, and Bayer KU “*Excitotoxic glutamate insults block autophagic flux in hippocampal neurons*” Poster presented at University of Kentucky AOA Groves Memorial MD/PhD Student Research Day, Lexington, KY (2013)

### **Oral Conference Presentations**

“A pharmacologic neuroprotective approach to experimental TBI: targeting mitochondria & lipid peroxidation-derived aldehydes” 3<sup>rd</sup> Annual Neuroscience Clinical-Translational Research Symposium, Lexington, KY (2018)

“Multi-Mechanistic Attenuation of Mitochondrial Dysfunction and Lipid Peroxidation Following Experimental Traumatic Brain Injury” 13<sup>th</sup> Annual Center for Clinical and Translational Sciences Spring Conference, Lexington, KY (2018)

“Continuous Infusion of Phenyelzine, Cyclosporine A, or the Combination: Evaluation of Mitochondrial Bioenergetics, Oxidative Damage, and Cytoskeletal Degradation Following Severe Cortical Impact Traumatic Brain Injury in Rats” 2<sup>nd</sup> Annual University of Michigan Massey TBI Summit Invited Mentee Research Presentation, Ann Arbor, MI (2017)

“Cyclosporine A Protects Synaptic Mitochondria Following TBI”, NIMH MD/PhD Student Conference Data Blitz, San Francisco, CA (2015)

### **Oral Department Presentations**

“Multi-Mechanistic Attenuation of Mitochondrial Dysfunction and Lipid Peroxidation Following Experimental Traumatic Brain Injury” Center for Clinical and Translational Sciences Seminar, University of Kentucky, Lexington, KY (2018)

“Neuroprotective Evaluation of 72h Subcutaneous Continuous Infusion of Phenyelzine, Cyclosporine A, and the Combination Following Severe Controlled Cortical Impact Injury” Department of Neuroscience Seminar, University of Kentucky, Lexington, KY (2017)

“Cyclosporine A Improves Synaptic and Non-Synaptic Mitochondrial Respiration following TBI”, Department of Neuroscience Seminar, University of Kentucky, Lexington, KY (2016)

“Identification of Novel Serum Biomarkers for Mild Traumatic Brain Injury Using Phage Display”, Center for Clinical and Translational Sciences Seminar, University of Kentucky, Lexington, KY (2015)

### **Journal Club Presentations**

Journal Club Paper Presentation: “*Cyclic head rotations produce modest brain injury in infant piglets (Coats et al. 2016)*”, University of Kentucky Spinal Cord and Brain Injury Research Center Journal Club, Lexington, KY (2016)

Journal Club Paper Presentation: “*Neurobehavioral, neuropathological and biochemical profiles in a novel mouse model of co-morbid post-traumatic stress disorder and mild traumatic brain injury (Ojo et al. 2014)*”, University of Kentucky Spinal Cord and Brain Injury Research Center Journal Club, Lexington, KY (2016)

### **Course Lectures**

“Chronic traumatic encephalopathy-integration of canonical traumatic brain injury 22018secondary injury mechanisms with tau pathology” 2018  
ANA 605 / PGY605 *Neurobiology of CNS Injury and Repair*, University of Kentucky

“Programmed Cell Death Mechanisms: Role in CNS Injury” 2016, 2018  
ANA 605 / PGY605 *Neurobiology of CNS Injury and Repair*, University of Kentucky

### **Funding**

NIH F30 (NINDS) NRSA pre-doctoral Fellowship (F30NS096876) 07/2016 – Present  
“Multi-mechanistic protection of mitochondria following traumatic brain injury”

### **Honors & Awards**

P.E.O. Scholar Award 2019  
Merit-based scholarship awarded for scholarly excellence, academic achievement, & worthwhile career goals by the International Chapter of the P.E.O.

University of Kentucky Graduate School Incentive Award 2018  
Awarded for receipt of a nationally competitive fellowship, i.e. NRSA F30

Society for Neuroscience Trainee Professional Development Award 2018  
Awarded to attend the 2018 Society for Neuroscience Annual Meeting, San Diego, CA

University of Kentucky Graduate School Travel Award Awarded to attend the 3 <sup>rd</sup> Joint Symposium of the International and National Neurotrauma Societies, Toronto, Canada	2018
2 <sup>nd</sup> Annual University of Michigan Massey TBI Summit Invited Mentee Invited mentee, Ann Arbor, MI	2017
EMBO-FEBS Lecture Course “Mitochondria in Life, Death, and Disease” Selected attendee, Brindisi, Italy	2017
National Neurotrauma Symposium Sensor Travel Grant Award Awarded to attend the “ <i>Environmental Sensor Use for Quantifying Neural Exposure to Inertial and Blast Forces</i> ” Pre-Meeting Workshop, 35 <sup>th</sup> Annual National Neurotrauma Symposium, Snowbird, UT	2017
University of Kentucky Graduate School Travel Award Awarded to attend the 2017 AAP/ASCI/APSA Joint Meeting, Chicago, IL	2017
University of Kentucky Graduate School Incentive Award Awarded for receipt of a nationally competitive fellowship, i.e. NRSA F30	2016
AUPN/NINDS Travel Award Awarded to attend the Combining Clinical and Research Careers in Neuroscience Symposium, Washington, DC	2016
Kentucky Spinal Cord and Head Injury Research Trust (KSCHIRT) Travel Award Awarded to attend the 34 <sup>th</sup> Annual National Neurotrauma Symposium, Lexington, KY	2016
NIMH Travel Award Awarded to attend the NIMH MD/PhD Student Conference & 3 <sup>rd</sup> Annual Molecular Psychiatry Meeting, San Francisco, CA	2015
University of Kentucky College of Medicine (M1 and M2)	
Promoted with High Distinction	2013 – 2014
Promoted with High Distinction	2012 – 2013
Highest Academic Achievement: Behavioral Basis of Medicine	2013
Distinguished Portfolio Award: Introduction to Clinical Medicine I	2013

Undergraduate 2001 – 2004  
Magna cum laude  
Phi Beta Kappa  
Alpha Epsilon Delta and Golden Key National Honor Societies  
Dean's List, National Dean's List and Hornbeck Scholar  
Outstanding Student Achievement, Department of Chemistry

### **Service**

*Ad hoc* reviewer, *Headache: The Journal of Head and Face Pain*

University of Kentucky MD-PhD Internal Advisory Committee 2015 – 2017

### **Teaching Assistantship**

Neuroscience Department Proctor  
*Principles of Human Anatomy* 2018 – 2019  
*Anatomy and Physiology for Nursing* 2016 – 2017  
*Principles of Human Anatomy* 2014 – 2015

Neuroscience Department Teaching Assistant  
*Anatomy and Physiology for Nursing* 2015 – 2016

### **Membership**

Society for Neuroscience  
American Physician Scientist Association  
National Neurotrauma Society  
Women in Neurotrauma Research  
Bluegrass Chapter of the Society for Neuroscience  
American Medical Student Association